Angewandte Chemie
Eine Zeitschrift der Gesellschaft Deutscher Chemiker

Supporting Information

Nocathioamides, Uncovered by a Tunable Metabologenomic Approach, Define a Novel Class of Chimeric Lanthipeptides

*Hamada Saad, Saefuddin Aziz, Matthias Gehringer, Markus Kramer, Jan Straetener, Anne Berscheid, Heike Brötz-Oesterhelt, and Harald Gross**

anie_202102571_sm_miscellaneous_information.pdf

Author Contributions

H.S. Conceptualization: Lead; Gene cluster analysis: Lead; Methodology & HRMS analysis: Lead; Structural elucidation: Lead; Writing: Original draft: Lead; Writing: Review & Editing: Lead

S.A. Experimental: Preliminary bioassays: Supporting

M.G. Experimental: Chemical transformations and computer modeling: Lead

M.K. Experimental: (special) NMR measurements: Lead; Review & Editing: Supporting

J.S. Experimental: Antibacterial and cytotoxicity assays: Lead

A.B. Experimental: Antifungal assays: Lead

H.B.O Funding acquisition: Lead; Methodology & Antimicrobial tests: Lead; Writing: Review & Editing: Supporting

H.G. Funding acquisition: Lead; Conceptualization: Supporting; Gene cluster analysis: Supporting; Structural elucidation: Supporting; Writing: Review & Editing: Lead

Table of Contents

3. Supplemental References

1. Experimental Procedures

1.1 General experimental procedures

Solvents employed were all HPLC grade. Chemical reagents and standards were purchased from Sigma Aldrich unless indicated otherwise. The isotopically labeled substrates [($^{15}NH_4$)$_2$SO$_4$, L-leucine (D10, 98%), and L-proline (D7, 97-98%)] were purchased from Cambridge Isotope Laboratories. Optical rotation values were measured on a Jasco P-2000 polarimeter, using a 3.5 mm × 10 mm cylindrical quartz cell. UV spectra were recorded on a PerkinElmer Lambda 25 UV/vis spectrometer. Infrared spectra were obtained by employing a Jasco FT/IR 4200 spectrometer, interfaced with a MIRacle ATR device (ZnSe crystal).

For Liquid Chromatography/High-resolution Electron Spray Ionization Mass Spectrometry (LC/HRESI-MSMS) measurements, an Ultimate 3000 HPLC (Thermo Fisher Scientific) system united with MaXis-4G instrument (Bruker Daltonics, Bremen, Germany) was used. The developed HPLC-method was (0.1% FA in H_2O as solvent A and MeOH as solvent B), a gradient of 10% B to 100% B in 40 min ending with 100% B for an additional 15 min, with a flow rate of 0.3 ml/min, 5 µl injection volume and UV detector (UV/VIS) wavelength monitoring at 210, 254, 280 and 360 nm. Integrating Phenomenex Luna Omega polar C18 (3 µm, 150 x 3 mm) column enabled the separation with MS acquisition range of *m/z* 50-1800. A capillary voltage of 4500 V, nebulizer gas pressure (nitrogen) of 2 (1.6) bar, ion source temperature of 200 °C, the dry gas flow of 9 l/min source temperature, and spectral rates of 3 Hz for MS^1 and 10 Hz for MSMS were used. For MS/MS fragmentation, the 10 most intense ions per MS^1 were chosen for subsequent collision-induced dissociation (CID) with the stepped recommended CID energies.[1] For the mass calibration, sodium formate was directly infused before each sample measurement.

Vacuum liquid chromatography (VLC) was accomplished using the reversed-phase (RP) C18 column (dimensions: 10×5 cm; material: Macherey-Nagel Polygoprep 50–60 C18 RP silica gel) whereas size exclusion chromatography was done using a Sephadex LH-20 (GE Healthcare) manually packed in a column (dimension: 3 × 32 cm) running under the atmospheric pressure.

HPLC profiling was carried out using a system consisting of Waters 1525 Binary Pump with a 7725i Rheodyne injection port, a Kromega Solvent Degasser, Waters 2998 Photodiode Array Detector, and a Luna Omega polar C18 (5 µm, 250 × 4.6 mm, Phenomenex). ACN (solvent A) and H_2O + 0.1% TFA (solvent B) were used for the gradient elution of the analytes with a steady flow rate of 0.5 ml/min with an injection volume of 7 µl. For the main separation and purification, the same previous RP-HPLC setup was recalled using a Phenomenex Kinetex EVO C18 column (5 µm, 4.6×250 mm); 1 ml/min flow rate, and UV monitoring at 211, 250 and 280 nm.

1.2 NMR spectroscopy

1D and 2D NMR spectra were measured on a Bruker Avance III HD spectrometer (400, 100 and 40.6 MHz for ^{1}H, ^{13}C and ^{15}N NMR, respectively) at 297 K using a 5 mm SMART probe head. The NMR spectra were recorded in (d_4-CH_3OH, d_3-CH_3OH, d_6-DMSO) processed with TopSpin 3.5 and MestReNova 12.0.4 and calibrated to the residual solvent signals ($\delta_{H/C}$ 3.31/49.15 => d_4-CH_3OH, d_3-CH_3OH & $\delta_{H/C}$ 2.50/39.51=> d_6-DMSO). Mixing times were 80 ms for TOCSY and 300 ms for NOESY spectra. Band-Selective constant time HMBC spectra were recorded to dissect the peptide carbonyl region better.
Further d_3-CH_3OH datasets were attained from Bruker Avance III HDX spectrometer (700, 176 and 71 MHz for ^{1}H, ^{13}C and ^{15}N NMR, respectively) equipped with a 5 mm Prodigy TCI CryoProbe head. Mixing times were 80 ms for TOCSY and 300, 500 ms for NOESY spectra. For both spectrometers, ^{15}N unreferenced chemical shifts were reported in ppm (spectrometer default values). All NMR raw data have been deposited in an OA repository (http://doi.org/10.5281/zenodo.4661802).

1.3 Mass spectrometry data processing and molecular networking

Mass spectral data were analyzed using Compass Data Analysis 4.4 (Bruker Daltonik), while MetaboScape 3.0 (Bruker Daltonik) was consulted for molecular features selection. Raw data files were imported into MetaboScape 3.0 for the entire data treatment and pre-processing in which T-ReX 3D (Time aligned Region Complete eXtraction) algorithm is integrated for retention time alignment with an automatic detection to decompose fragments, isotopes, and adducts intrinsic to the same compound into one single feature. All the harvested ions were categorized as a bucket table with their corresponding retention times, measured m/z, molecular weights, detected ions, and their intensity within the sample. The Bucket table was prepared with an intensity threshold ($1e^4$) for the positive measurement with a minimum peak length 3 for the retention time range of interest from 15 to 30 min possessing a mass range *m/z* 150 - 1600 Da.

Metaboscape bucketing parameters were as follow:

Intensity threshold [counts]	10000.0
Minimum peak length [spectra]	3
Minimum peak length (recursive) [spectra]	1
Minimum # Features for Extraction	1
Presence of features in minimum # of analyses	1
Lock mass calibration	false
Mass calibration	true
Primary Ion	$[M+H]^+$
Seed Ions	$[M+Na]^+$, $[2M+H]^+$, $[2M+Na]^+$, $[M+2H]^{2+}$, $[M+H+Na]^{2+}$
Common Ions	$[M-H_2O+H]^+$, $[M+H_2O+H]^+$, $[2M+H_2O+H]^+$, $[2M-H_2O+H]^+$
EIC correlation	0.8
Mass range: Start [m/z]	150.0
Mass range: End [m/z]	1600.0
Retention time range: Start [min]	15.0
Retention time range: End [min]	30.0
Perform MS/MS import	true
Group by collision energy	true
MS/MS import method	average

The features list of the pre-processed retention time range was exported from MetaboScape as a single MGF file which was in turn uploaded to the GNPS online platform where Feature-Based Molecular Network (FBMN) was created. The precursor ion mass tolerance was set to 0.03 Da and a MS/MS fragment ion tolerance of 0.03 Da. A network was then created where edges were filtered to have a cosine score above 0.70 and more than 5 matched peaks. Further, edges between two nodes were kept in the network if and only if each of the nodes appeared in each other's respective top 10 most similar nodes. Finally, the maximum size of a molecular family was set to 100, and the lowest-scoring edges were removed from molecular families until the molecular family size was below this threshold. Cytoscape 3.5.1 was used for molecular network visualization.[2]

GNPS job URL: https://gnps.ucsd.edu/ProteoSAFe/status.jsp?task=450f6e9825bd4accb5fe353d4e4ebe42

1.4 Bacterial strains

Nocardia terpenica IFM 0406 was attained from the Medical Mycology Research Center (MMRC) culture collection, Chiba University, Chiba, Japan, while *N. terpenica* IFM 0706 (DSM 44935) was purchased from the DSMZ (German collection of microorganisms and cell cultures).[3]

1.5 Isotopic labeling experiments

N. terpenica IFM 0406 was revived on Brain Heart Infusion (BHI) broth agar plates (2%) incubated at 37 °C for three successive days observed by the growth of colonies. Using fresh spores of IFM 0406, triplicates of seed cultures were prepared in BHI broth media (80 ml) in 250 ml baffled Erlenmeyer flasks at 37 °C with 150 rpm for four consecutive days.

0.4 ml of the grown preculture was used to inoculate 50 ml of the production medium consisting of glucose 0.5%, glycerol 2%, soluble starch 2.0%, Pharmamedia 1.5%, yeast extract 0.3%,[4] in a 250 ml Erlenmeyer baffled flask at 37 °C with 150 rpm for five days to a final concentration of 2 mM of the corresponding labeled amino acid. After 5-6 days, the supernatant was freed from cells by centrifugation and extracted twice with 50 ml of n-BuOH. The organic phases were combined, dried *in vacuo*, dissolved in MeOH and submitted to LC/HRESI-MSMS.

1.6 Large scale fermentation, extraction scheme, and (sub)fractionation

Nocardia terpenica IFM 0406 was grown adopting both Ikeda's *et al.* nutrients recipe and Chen's *et al.* cultivation parameters up to twenty liters (22 L).[4,5]

Following large scale cultivation, cultures were centrifuged twice in a Thermo Scientific Heraeus Multifuge 4KR centrifuge at 4000 g at 4 °C for 30 min to discard the cells. Subsequently, using n-BuOH (1:1), the supernatant (SN) was extracted twice. Under reduced pressure, the n-BuOH extract was evaporated affording the crude extract (Bu SN extract), which was resuspended in methanol followed by centrifugation to get rid of debris prior to LC/MS analysis, HPLC profiling, and VLC. Fractionation of the Bu SN extract was accomplished through a VLC system by stepwise elution of H_2O mixed with methanol controlled by vacuum with a decreased polarity fashion, shifting from 100% H_2O to pure methanol in ten fractions (750 ml per fraction).

The prioritized VLC fraction (70% MeOH VLC) was redissolved in a mixture of MeOH:H_2O (40:60) to be further sub-fractionated over a Sephadex LH-20 open column with a gradual elution starting with 100% H_2O and ending with 100% MeOH delivering eight subfractions.

1.7 Isolation of nocathioamides (A, B)

The subfractions A and B, arising from Sephadex LH-20, were further purified by RP-HPLC with a polar gradient for 23 min using the formerly described HPLC setup equipped with a Phenomenex Kinetex EVO C18 column (5µm, 4.6×250 mm); 1 ml/min flow rate, and UV monitoring at 211, 250 and 280 nm. An additional round of purification was completed with a shorter run time, which resulted in pure nocathioamide A (**1**) (25 mg) and nocathioamide B (**2**) (12 mg).

1.8 Biological assays

The antibacterial assays and the determination of the cytotoxicity were performed as previously described.[5] For MIC testing of *Mycobacterium smegmatis*, instead of cation-adjusted Müller Hinton medium, Middlebrook 7H9 broth was used.

The minimal inhibitory concentration (MIC) of **1** and **2** against different *Candida* clinical isolates was determined by broth microdilution using the direct colony suspension method with an inoculum of 0.5-2.5 x 10^5 CFU/ml, according to the recommendations of the European Committee on Antimicrobial Susceptibility Testing (EUCAST).[6] Caspofungin was used as reference antifungal agent. MIC testing was performed in sterile 96-well microdilution plates using MOPS-buffered RPMI 1640 medium supplemented with glucose to a final concentration of 2%, pH 7.0. MICs were read after incubation of the microplates at 37°C for 24-48 h.

Results and Discussion

The gene cluster coding for nocathioamides has been deposited in the Minimum Information about a Biosynthetic Gene Cluster (MIBiG) repository[7] under accession number BGC0002120.
Protein homology analysis found in the nocathioamide biosynthetic gene cluster (*nta* BGC) employing the web-based tool RODEO and a manual BlastP search.[8]
The manual BlastP search was limited to records that exclude the species ´*Nocardia terpenica* (taxid:455432)´; listed are the top 1-3 hits. The protein hits, which represent the products of the *nta* BGC in the bacterium *Longimycelium tulufanense* CGMCC 4.5737 are indicated in orange.

		Automated RODEO Analysis					Manual BlastP Analysis	
Protein	Nucleotide Accession Nr. IFM 0706[a] IFM 0406[b]	Protein Accession Nr. IFM 0706 IFM 0406	Length [aa]	PFAM hits (TIGRFam hits)	Description	E-value	Protein hits (Protein ID)	Identity/ Similarity [% / %]
Orf-1	HPY32_RS36330 AWN90_28350	NQE92403.1 KZM72695.1	231 210	PF00440	Bacterial regulatory proteins, tetR family	3.20E-17	TetR/AcrR family transcriptional regulator (WP_139175378.1) TetR/AcrR family transcriptional regulator (WP_068369163.1) TetR family transcriptional regulator (WP_162141431.1)	37/52 34/54 40/63
NtaJ	HPY32_RS36335 AWN90_28345	NQE92404.1 KZM72694.1	614 592	PF02624 (TIGR03604, TIGR03882)	YcaO cyclodehydratase, ATP-ad Mg^{2+}-binding	6.10E-73	TOMM precursor leader peptide-binding protein (WP_189056215.1) TOMM precursor leader peptide-binding protein (WP_090933850.1) TOMM precursor leader peptide-binding protein (WP_071803308.1)	48/62 42/54 37/51
NatI	HPY32_RS36340 AWN90_28340	NQE92405.1 KZM72693.1	617 630	TIGR03693	Ocin_ThiF_like: putative thiazole-containing bacteriocin maturation protein	3.30E-23	hypothetical protein (WP_189056217.1) hypothetical protein (WP_100559871.1) hypothetical protein (WP_107412486.1)	37/52 31/43 31/44
		The RRE domain, fused to NtaI, is indicated in green (AA 9-91 of NatI) MDRDHKLDLRRPVLRAGVRATPTPEGIALEGPSELRITLQGPEVRDVLVWLVSQFDGVTGANEIMGRLDED RRSLAERIIVALDRYGIIRDRARDRSHSLTAHELDCHAGEIAQIARHRESPEQRFDDFRSTPMVLIGSVHAVSP VVRLALDSGLRRLRVLVPGGMSCEPGDLARCADVRIIDAGAPGIETIRPLLAEFPVVVHVCTAHSADLLRRLD RLCWEERKYLVPAVVLGDQAWIGPVGLPGHEWTRWAAFWQRHRTTVPEQPRHSDPTLVQLELVANHLLLL WFRRITGIEQARAPDVVHLEFGELRSRKRTVAPHPHGLPRSPETSTEVAAKIGALSDAEPLIEHDFYRSIRRYI DERVGIFADIRAARTDPLPLQVAEVVVTDPLKSYRAQHVPVIVRGAGPDMLRARLDALRRACELYAYLVVDP QRLHTADGTPAFLEFMPDEWAAGRLWGMSLGTGQPCTVRAGDAFPHLVSGPTATTPVGVASGNTFCEAV ERALIDQCASHAITSAETEQSPLDLWSLELRGIGSHYRNLLRLSGETVHAVRFTHELAPPVVRLSNSTVGDLY STGRSLGEAIGHGIEQLLLHRQCQRLSPPESPCPPVGHRIGQPAPGPRTSGASTLGRRLVDRLTRRGLHPV AVTLDHDPVLSRLHPFVVRVLVLPDAAEGPGTCW						
NatH	HPY32_RS36345 AWN90_28335	NQE92406.1 KZM72692.1	424 424	PF13527 PF13530 PF17668	Acetyltransferase (GNAT) domain Sterol carrier protein domain Acetyltransferase (GNAT) domain	2.80E-23 1.10E-19 3.80E-13	GNAT family N-acetyltransferase (WP_189056219.1) GNAT family N-acetyltransferase (PZN46310.1) GNAT family N-acetyltransferase (WP_124440951.1)	55/68 43/54 42/56
NatG	HPY32_RS36350 AWN90_28330	NQE92407.1 KZM72691.1	286 286	PF14028	Lantibiotic biosynthesis dehydratase C-terminus	4.30E-30	thiopeptide-type bacteriocin biosynthesis protein (WP_189056204.1) thiopeptide-type bacteriocin biosynthesis protein (WP_131736176.1) thiopeptide-type bacteriocin biosynthesis protein (WP_099929903.1)	70/80 49/58 48/55
NtaF	HPY32_RS36355 AWN90_28325	NQE92408.1 KZM72690.1	830 796	PF04738	Lantibiotic dehydratase, N-terminus	5.30E-19	lantibiotic dehydratase (WP_189056202.1) hypothetical protein GCM10012275_19850 (GGM48992.1) lantibiotic dehydratase (WP_189056221.1)	66/76 49/59 49/59
NtaE	HPY32_RS36360 AWN90_28320	NQE92409.1 KZM72689.1	512 512	PF00881 (TIGR03605)	SagB: SagB-type dehydrogenase domain	5.00E-41	SagB family peptide dehydrogenase (WP_189056200.1) SagB-type dehydrogenase domain (KPI02545.1) SagB family peptide dehydrogenase (WP_020665156.1)	60/70 44/57 44/56
NtaD	HPY32_RS36365 AWN90_28315	NQE92410.1 KZM72688.1	193 193	PF01738 PF12697	Dienelactone hydrolase family Alpha/beta hydrolase family	2.60E-12 2.40E-07	α/β fold hydrolase (WP_189056198.1) hypothetical protein GCM10012275_19730 (GGM48884.1) dienelactone hydrolase family protein (WP_131968989.1)	72/80 72/80 48/60
NtaC	HPY32_RS36370 AWN90_28310	NQE92411.1 KZM72687.1	377 365	PF01135 (TIGR04188, TIGR04364)	Methyltransferase	3.20E-38	hypothetical protein (WP_189056196.1) methyltransferase domain-containing protein (WP_189060694.1) methyltransferase domain-containing protein (WP_102918215.1)	62/77 38/52 37/49

NtaB	HPY32_RS36375 AWN90_28305	NQE92412.1 KZM72686.1	421 414	PF05147	Lanthionine synthetase C-like protein	1.90E-51	hypothetical protein (WP_189056194.1) lanthionine synthetase C family protein (RLU79699.1) lanthionine synthetase C family protein (WP_189782898.1)	62/74 35/47 35/48
NtaA	HPY32_RS36380 not annotated	NQE92413.1 not annotated	51		----------	---------	hypothetical protein (WP_189056192.1)	78/86
NtaK	HPY32_RS36385 AWN90_28300	NQE92414.1 KZM72685.1	426 394	PF07812	TfuA-like protein	2.80E-32	hypothetical protein (WP_189056190.1) hypothetical protein GCM10012275_19690 (GGM48852.1) hypothetical protein (WP_063274436.1)	66/76 66/76 48/63
NtaL	HPY32_RS36390 AWN90_28295	NQE92415.1 KZM72684.1	391 391	PF02624 (TIGR00702)	YcaO cyclodehydratase, ATP-ad Mg^{2}+-binding	7.90E-58	YcaO-like family protein (WP_189056188.1) YcaO-like family protein (WP_063274437.1) hypothetical protein (MQT02134.1)	70/83 52/70 54/67
NtaM	HPY32_RS36395 AWN90_28290	NQE92416.1 KZM72683.1	394 368	PF00067	cytochrome P450	5.20E-37	cytochrome P450 (WP_189056186.1) cytochrome P450 (GGM48838.1) cytochrome P450 (WP_189060646.1)	69/78 70/79 53/65
NtaN	HPY32_RS36400 AWN90_28285	NQE92417.1 KZM73943.1	155 155	PF00583 PF13508 PF13673	Acetyltransferase (GNAT) family Acetyltransferase (GNAT) domain Acetyltransferase (GNAT) domain	2.00E-10 2.10E-07 1.30E-05	GNAT family N-acetyltransferase (WP_150404808.1) GNAT family N-acetyltransferase (WP_067538111.1) GNAT family N-acetyltransferase (WP_169813135.1)	75/84 78/83 69/83
Orf+1	HPY32_RS36405 AWN90_28280	NQE92418.1 KZM72682.1	230 230	PF13419 PF00702 PF13242	Haloacid dehalogenase-like hydrolase haloacid dehalogenase-like hydrolase HAD-hyrolase-like	2.20E-08 3.40E-08 2.80E-05	haloacid dehalogenase type II (WP_165257141.1) haloacid dehalogenase type II (WP_201875758.1) haloacid dehalogenase type II (WP_190052985.1)	83/91 81/87 81/87
Orf+2	HPY32_RS36410 AWN90_28275	NQE92419.1 KZM72681.1	190 190	PF07336 PF11706	Putative stress-induced transcription regulator CGNR zinc finger	4.70E-17 4.20E-16	ABATE domain-containing protein (WP_165257307.1) ABATE domain-containing protein (WP_042153133.1) ABATE domain-containing protein (WP_027942564.1)	90/92 88/91 85/90
Orf+3	HPY32_RS36415 AWN90_28270	Not annotated KZM72680.1	29 64	PF00248	Aldo/keto reductase family	5.60E-06	aldo/keto reductase (WP_185941606.1) aldo/keto reductase (WP_192776860.1) aldo/keto reductase (GFE07022.1)	100/100 100/100 97/100
Orf+4	HPY32_RS36420 AWN90_28265	NQE92420.1 KZM72679.1	465 465	PF01425	Amidase	6.50E-105	amidase (WP_173868031.1) amidase (WP_073766127.1) amidase (NEW71157.1)	66/74 65/72 67/76
Orf+5	HPY32_RS36425 AWN90_28260	NQE92421.1 KZM72678.1	192 192	PF16859 PF00440	Tetracyclin repressor-like, C-terminal domain Bacterial regulatory proteins, tetR family	1.70E-14 5.20E-09	TetR/AcrR family transcriptional regulator (WP_092550168.1) TetR/AcrR family transcriptional regulator (WP_188675544.1) TetR family transcriptional regulator (GGF20957.1)	58/76 57/73 57/73
Orf+6	HPY32_RS36430 AWN90_28255	NQE92422.1 KZM72677.1	284 284	PF00126 PF03466	Bacterial regulatory helix-turn-helix protein, lysR family LysR substrate binding domain	2.20E-20 9.20E-18	transcriptional regulator, LysR family (CDR16212.1) LysR family transcriptional regulator (WP_020873917.1) LysR family transcriptional regulator (WP_040020027.1)	87/91 87/91 84/90

Table S1. Putative functions of proteins from the *nta* BGC based on the web-based tool RODEO and a manual BlastP search.
[a]The *nta* BGC of strain IFM 0706 is located on contig 5 of the genome (Accession: NZ_JABMCZ010000005.1).
[b]The *nta* BGC of strain IFM 0406 is located on contig 15 of the genome (Accession: LWGR01000007.1).

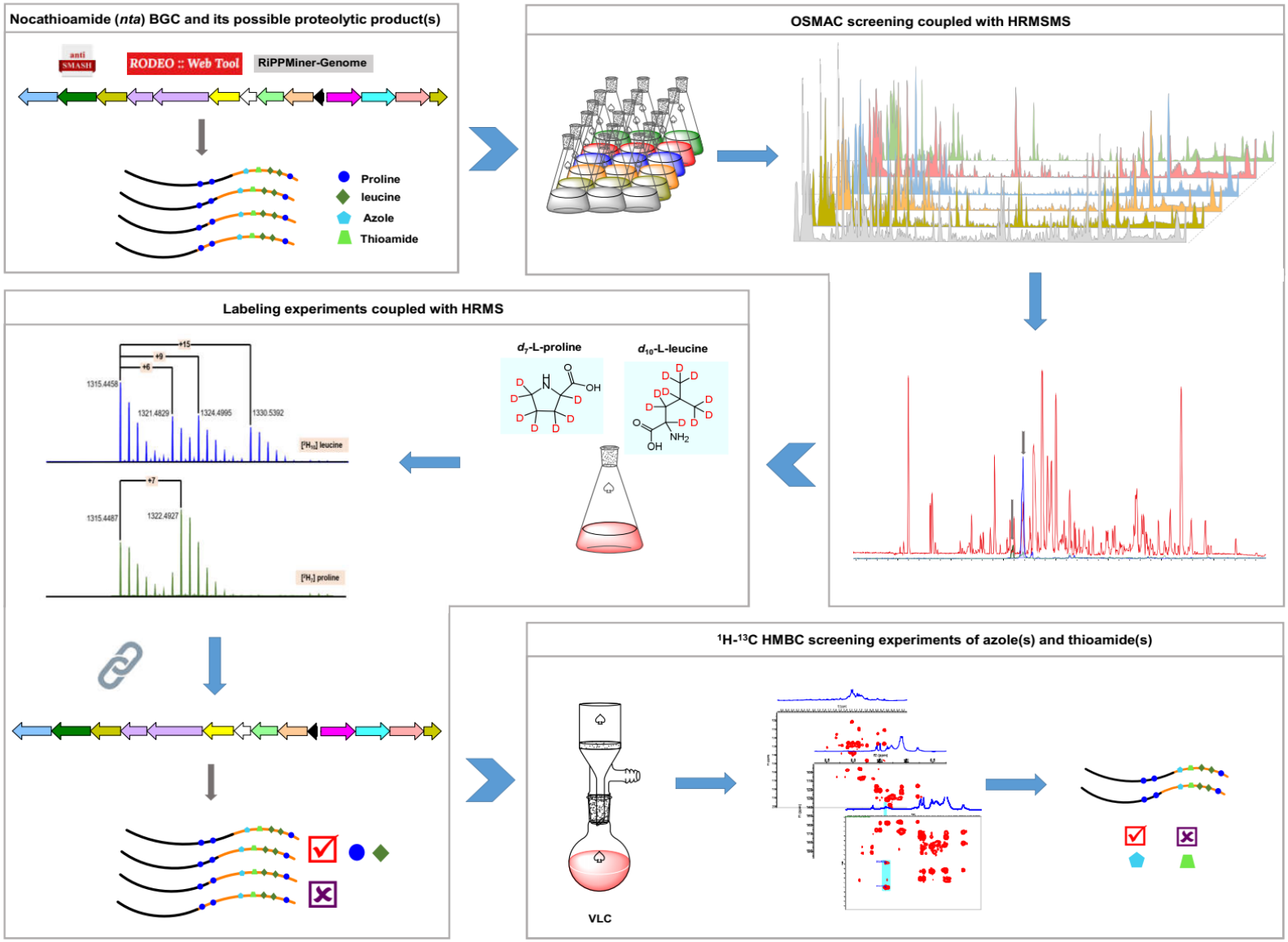

Figure S1. Overview of the adopted metabologenomic strategy for the discovery of nocathioamides

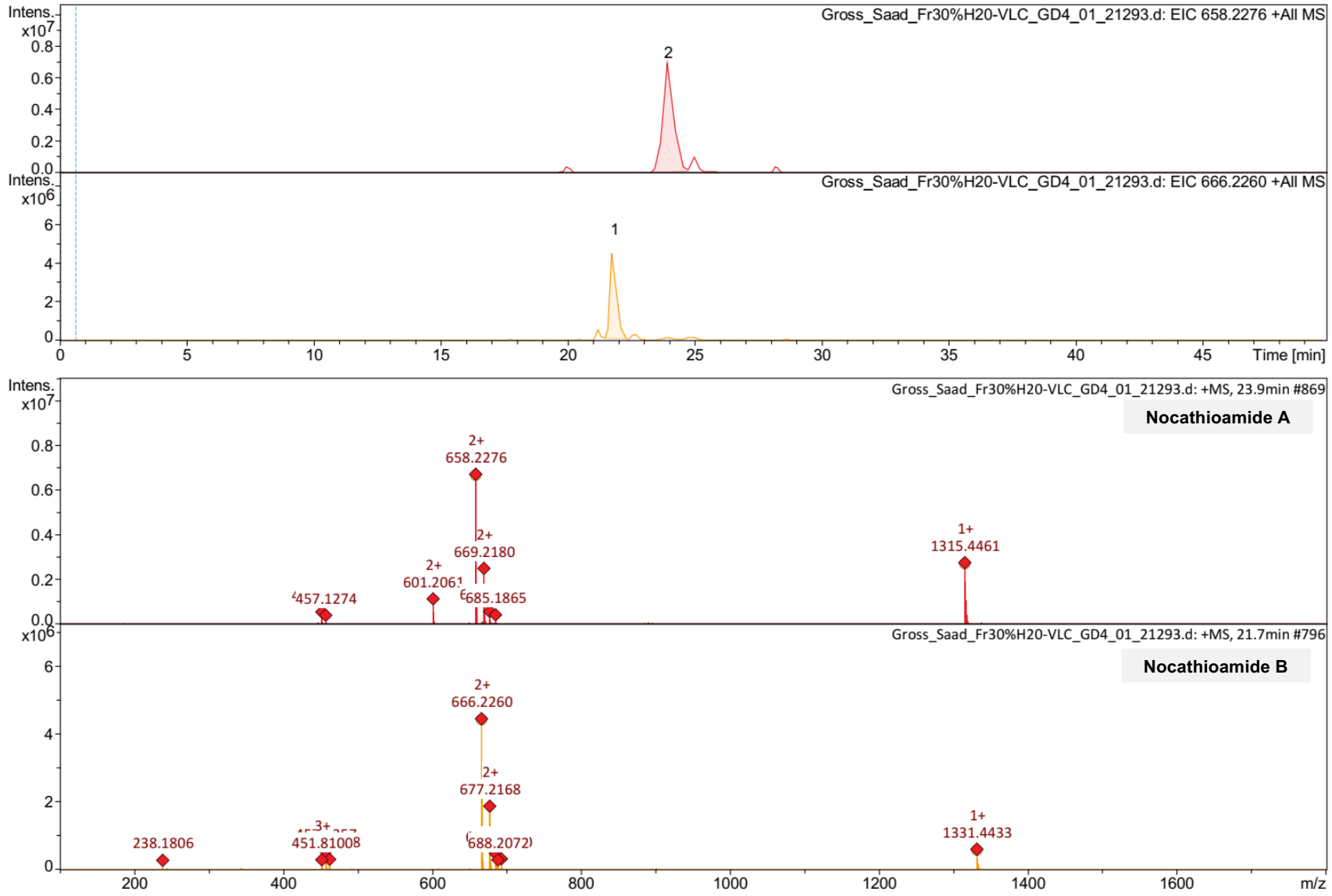

Figure S2. Extracted ion chromatograms (EICs) and MS^1 of nocathioamide A (**1**) (1315 Da $[M+H]^+$) and B (**2**) (1331 Da $[M+H]^+$)

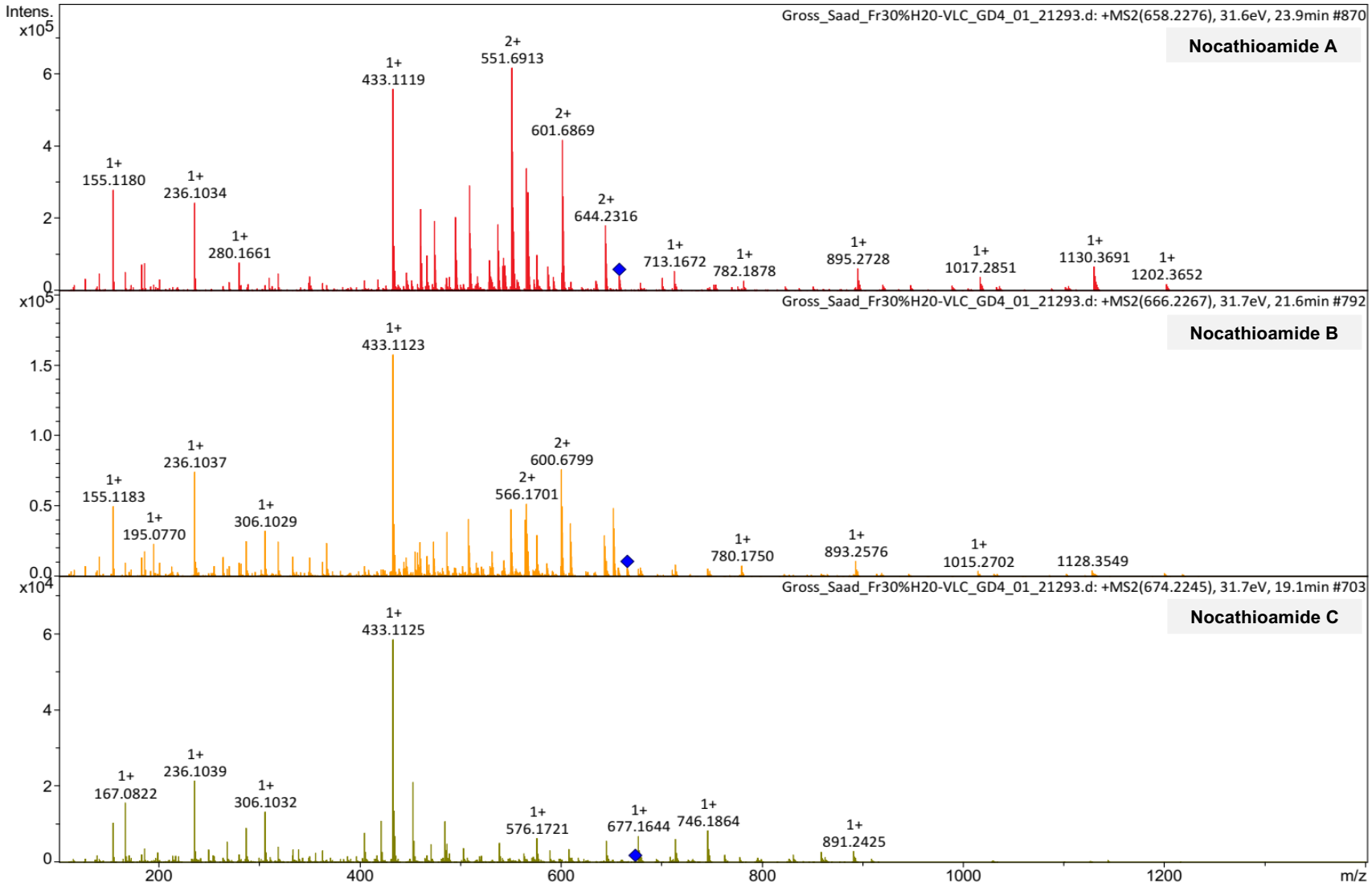

Figure S2A. Comparative $[M+2H]^{2+}$ MS^2 of nocathioamide A, B, and C (**1**-**3**) (658, 666, and 674 Da)

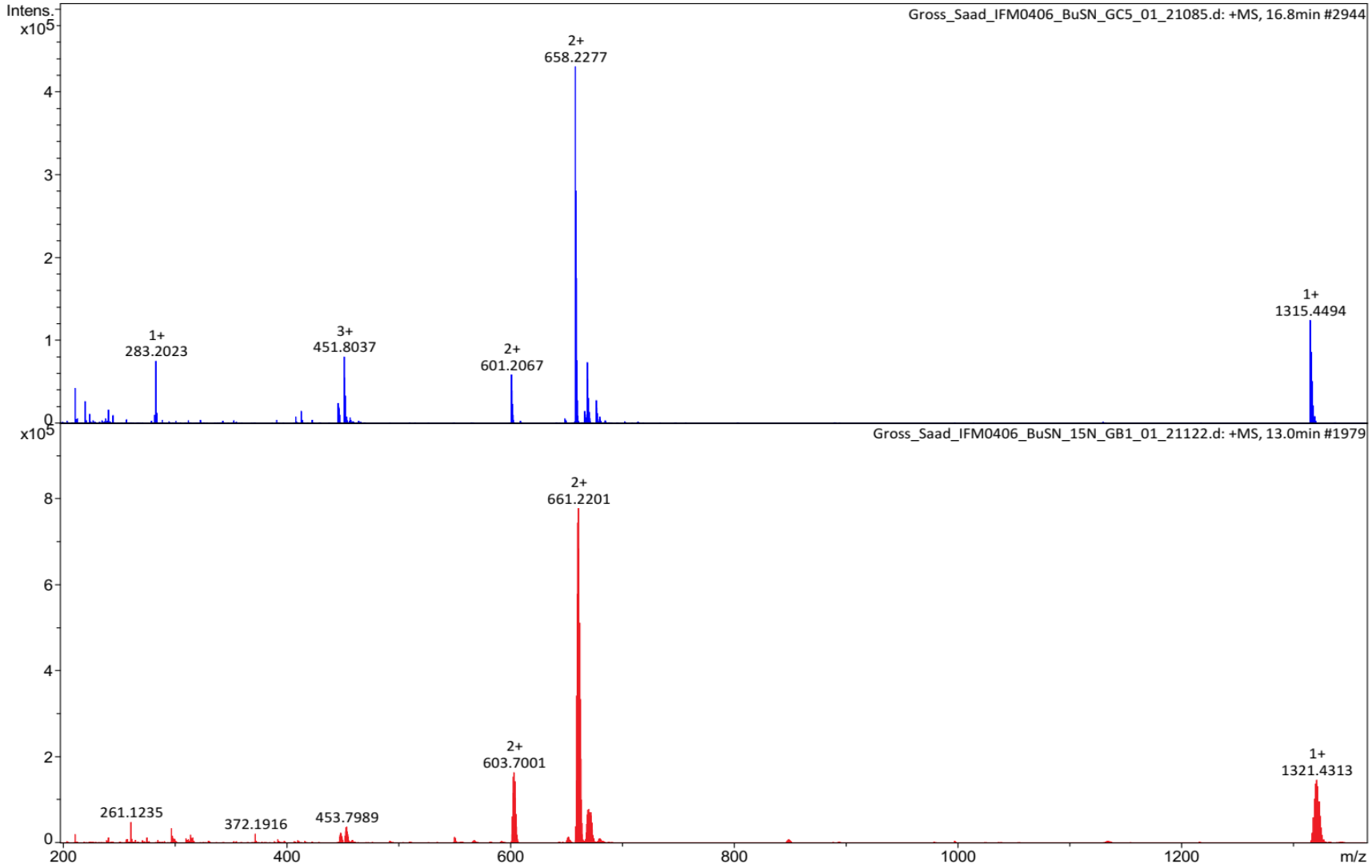

Figure S3. Comparative MS^1 of nocathioamide A (**1**) (1315 Da $[M+H]^+$, 658 Da $[M+2H]^{2+}$) and its ^{15}N-based version

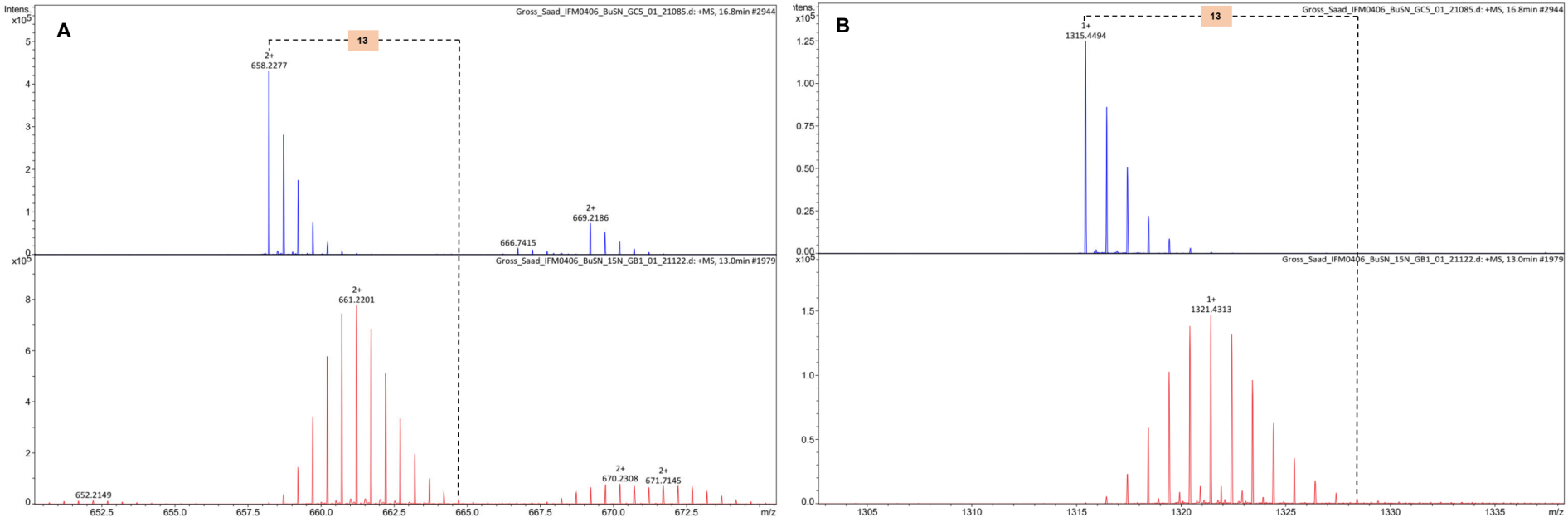

Figure S3A. Enlarged doubly ($[M+2H]^{2+}$, panel A) and singly ($[M+H]^{+}$, panel B) charged ions of nocathioamide A (**1**) and its ^{15}N-based version

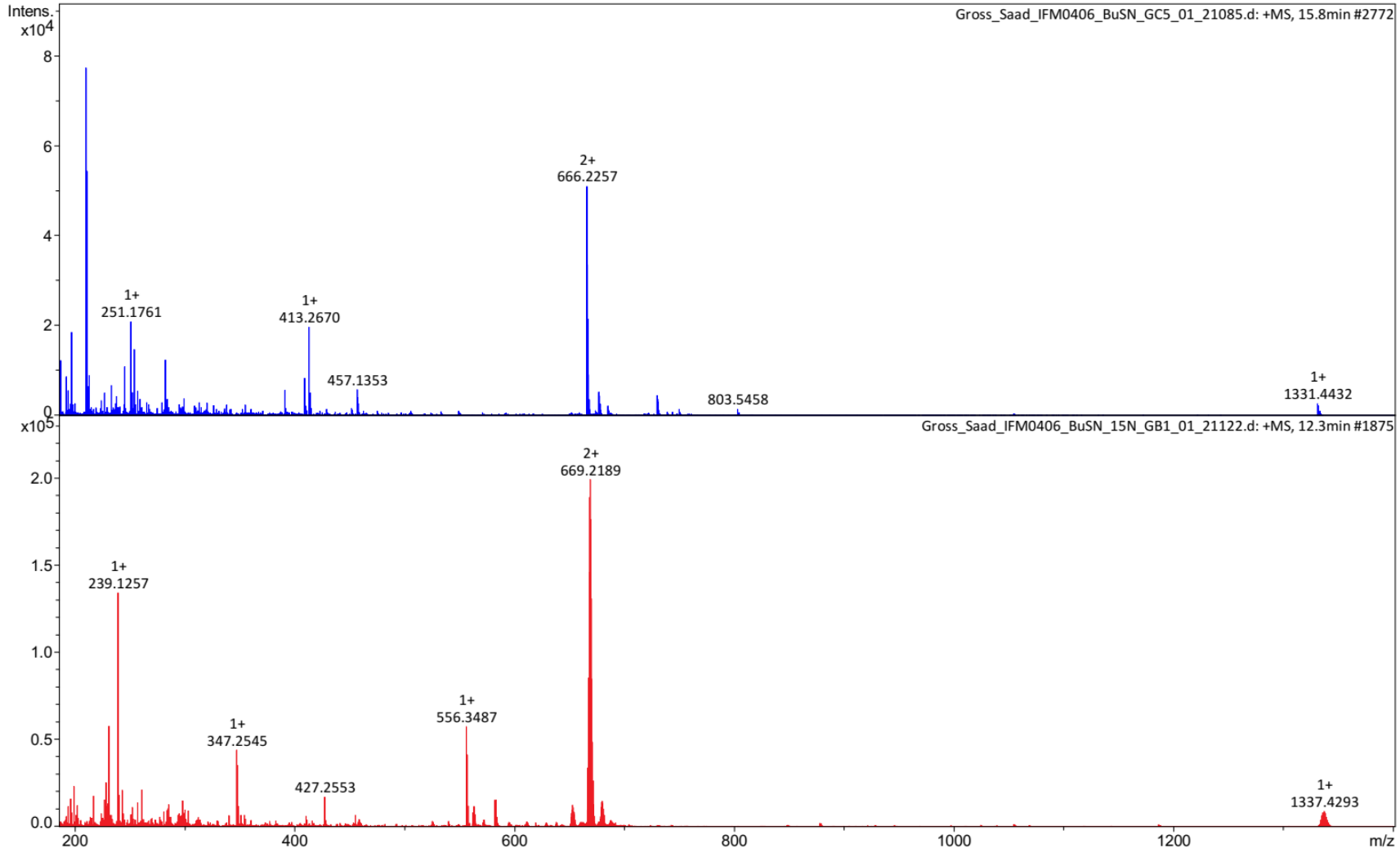

Figure S4. Comparative MS[1] of nocathioamide B (**2**) (1331 Da $[M+H]^+$, 666 Da $[M+2H]^{2+}$) and its ^{15}N-based version

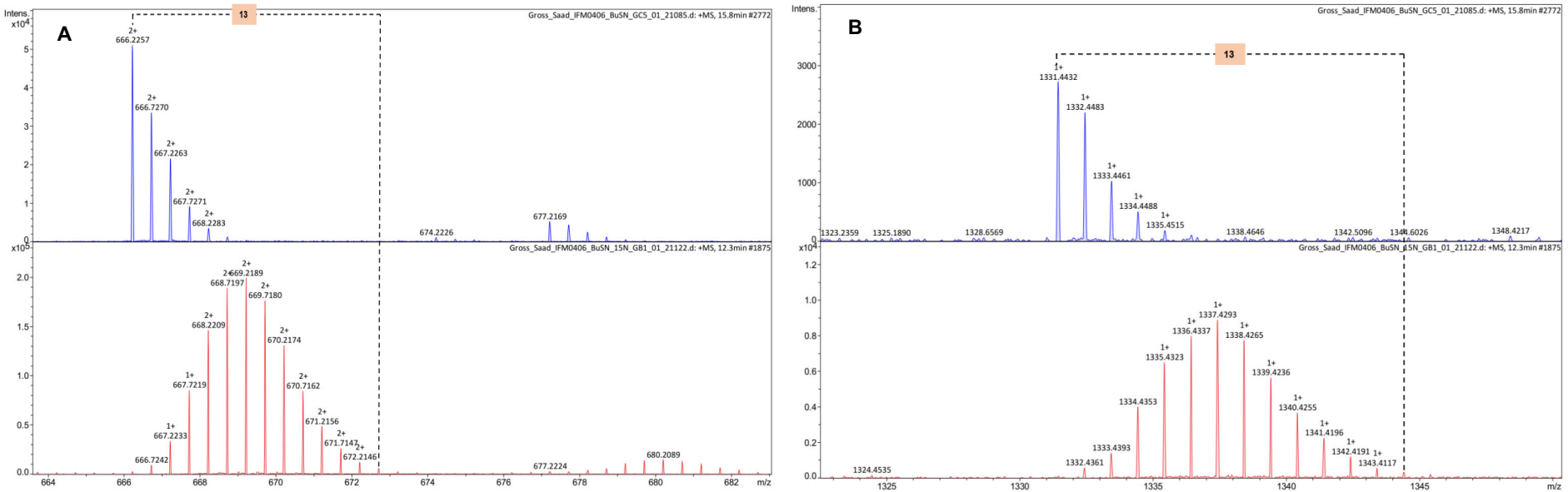

Figure S4A. Enlarged doubly ($[M+2H]^{2+}$, panel A) and singly ($[M+H]^{+}$, panel B) charged ions of nocathioamide B (**2**) and its ^{15}N-based version

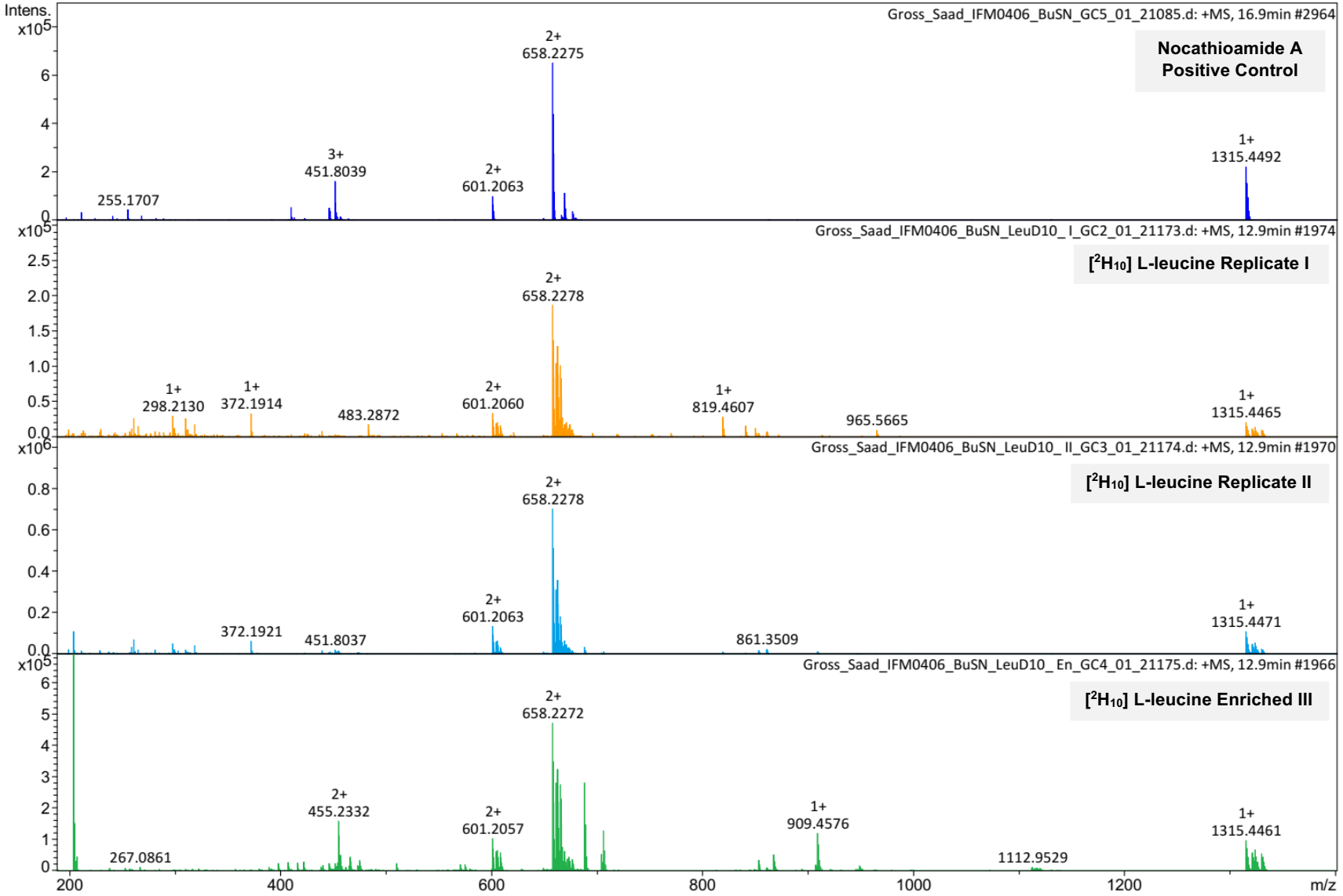

Figure S5. Comparative MS[1] of nocathioamide A (**1**) and its ([$^2H_{10}$] L-leucine)-based version

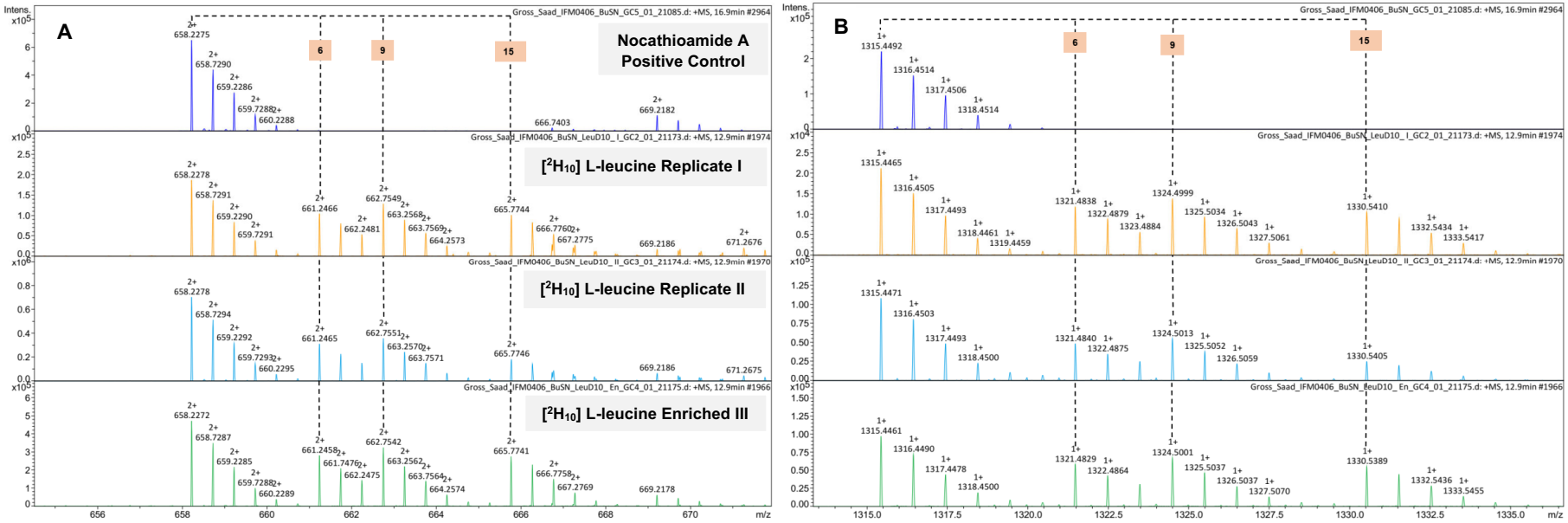

Figure S5A. Enlarged doubly ([M+2H]$^{2+}$, panel A) and singly ([M+H]$^{+}$, panel B) charged ions of nocathioamide A (**1**) and its ([$^{2}H_{10}$] L-leucine)-based version

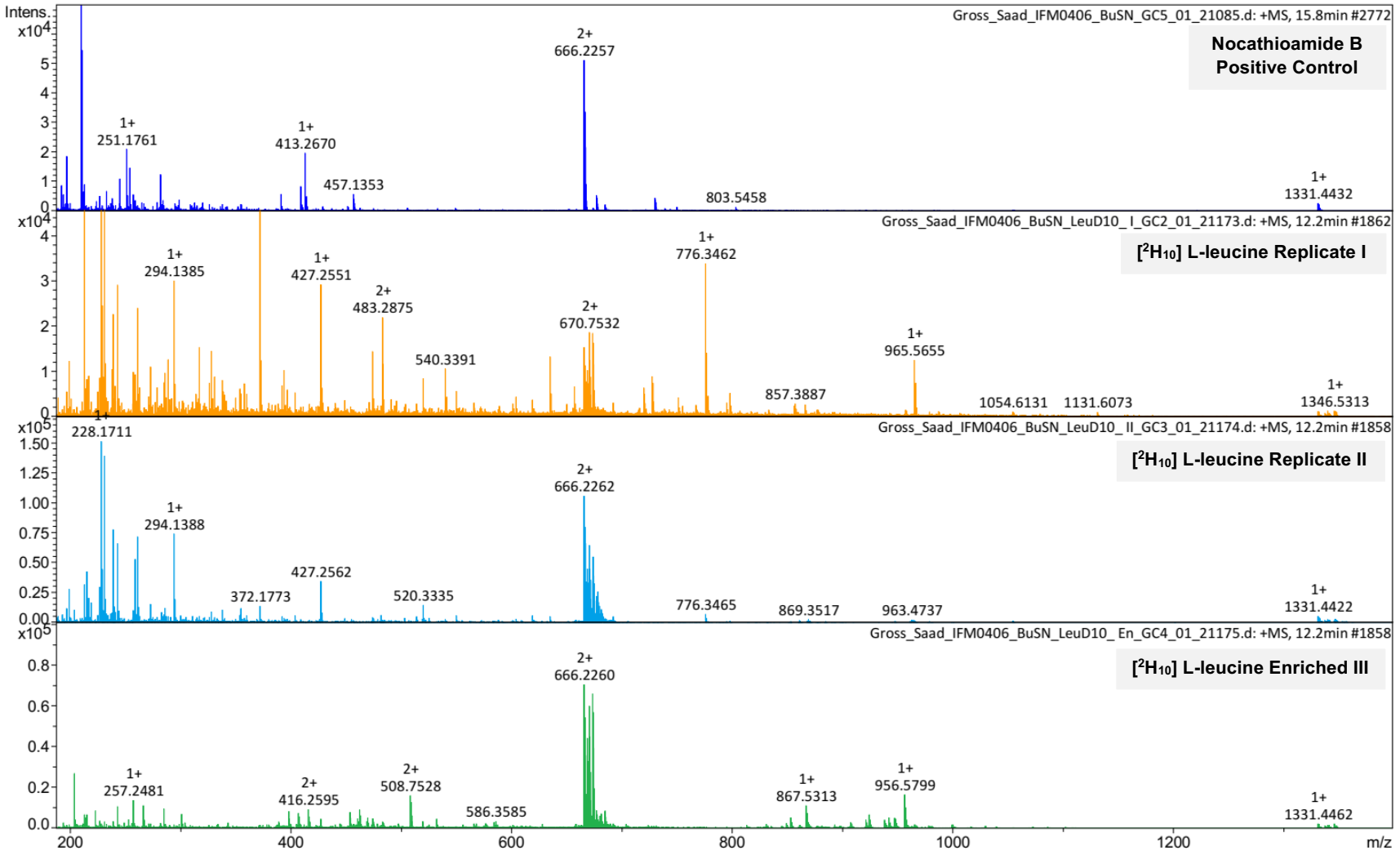

Figure S6. Comparative MS[1] of nocathioamide B (**2**) and its ([$^2H_{10}$] L-leucine)-based version

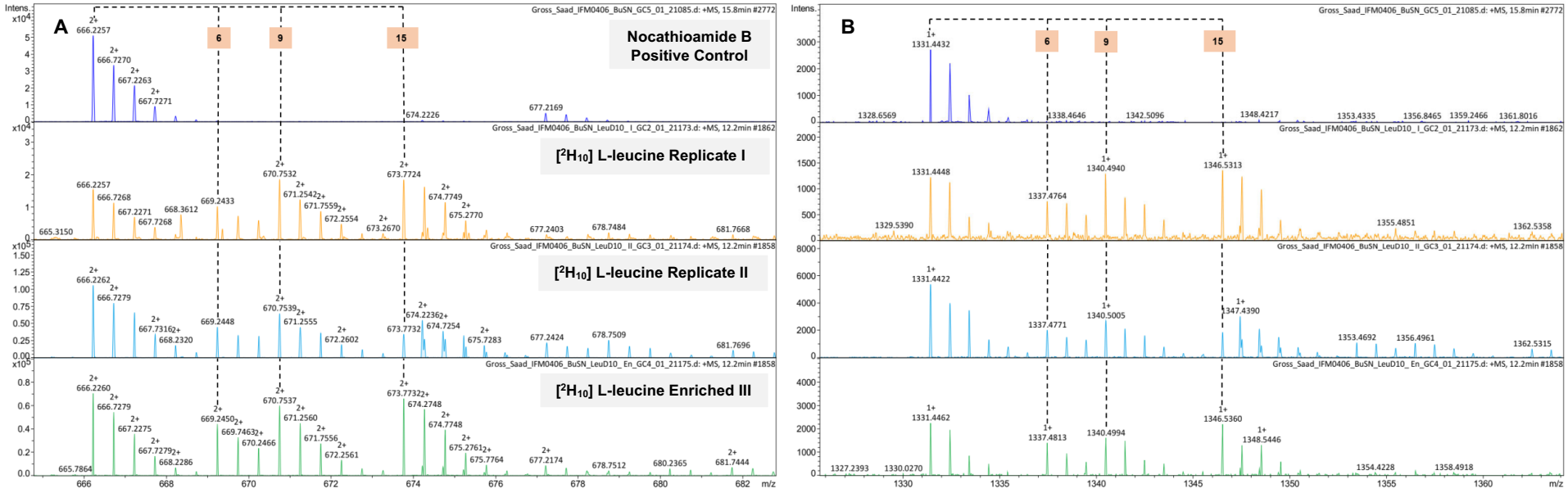

Figure S6A. Enlarged doubly ($[M+2H]^{2+}$, panel A) and singly ($[M+H]^{+}$, panel B) charged ions of nocathioamide B (**2**) and its ($[^2H_{10}]$ L-leucine)-based version

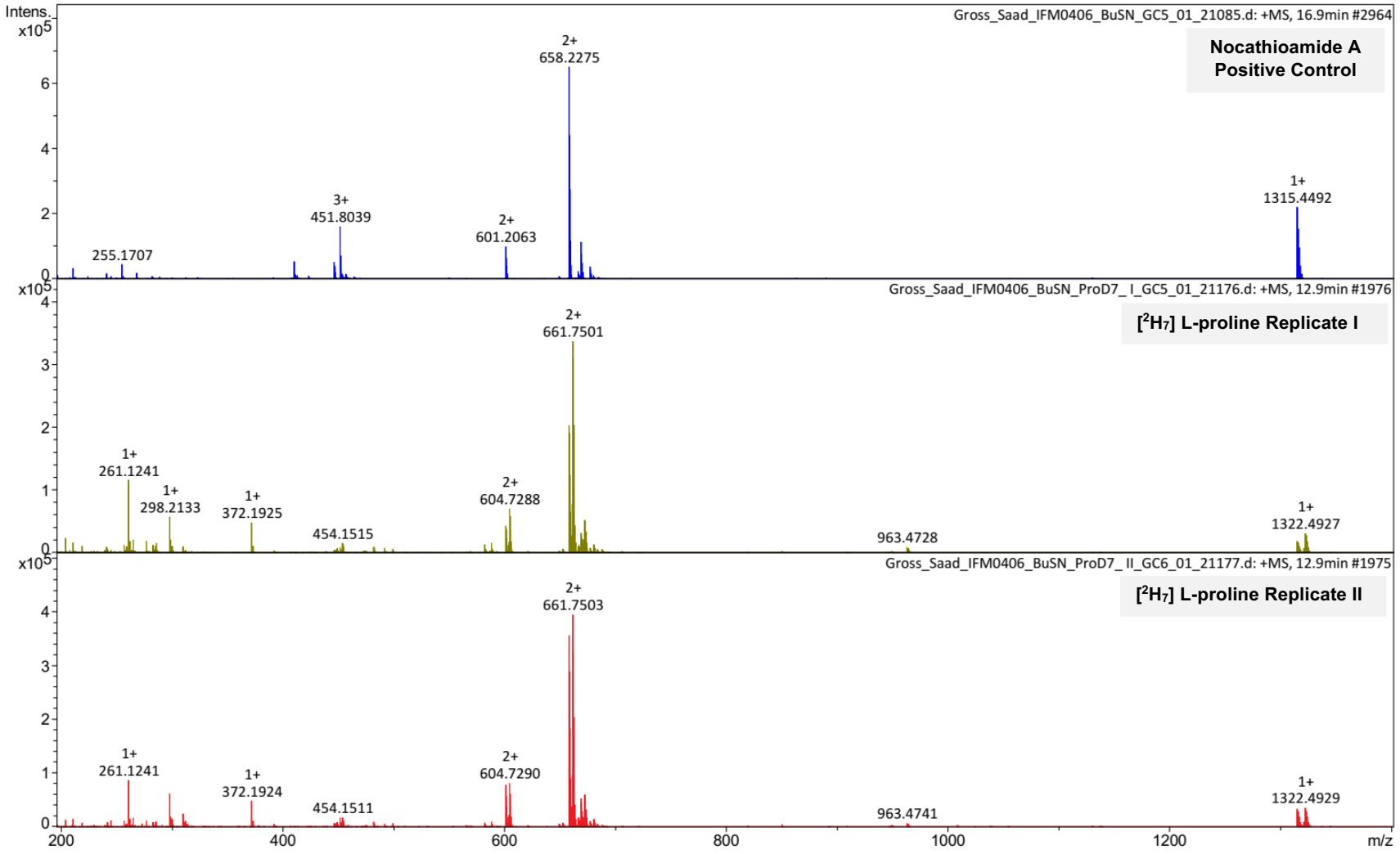

Figure S7. Comparative MS[1] of nocathioamide A (**1**) and its ([$^2H_7$] L-proline)-based version

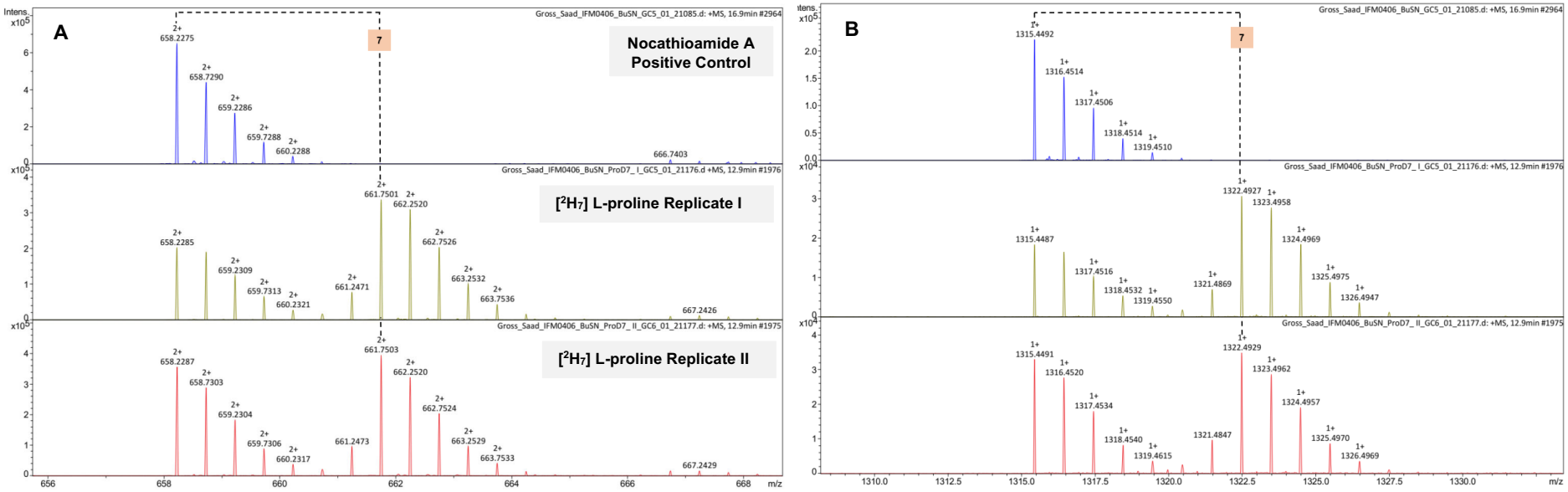

Figure S7A. Enlarged doubly ($[M+2H]^{2+}$, panel A) and singly ($[M+H]^{+}$, panel B) charged ions of nocathioamide A (**1**) and its ($[^2H_7]$ L-proline)-based version

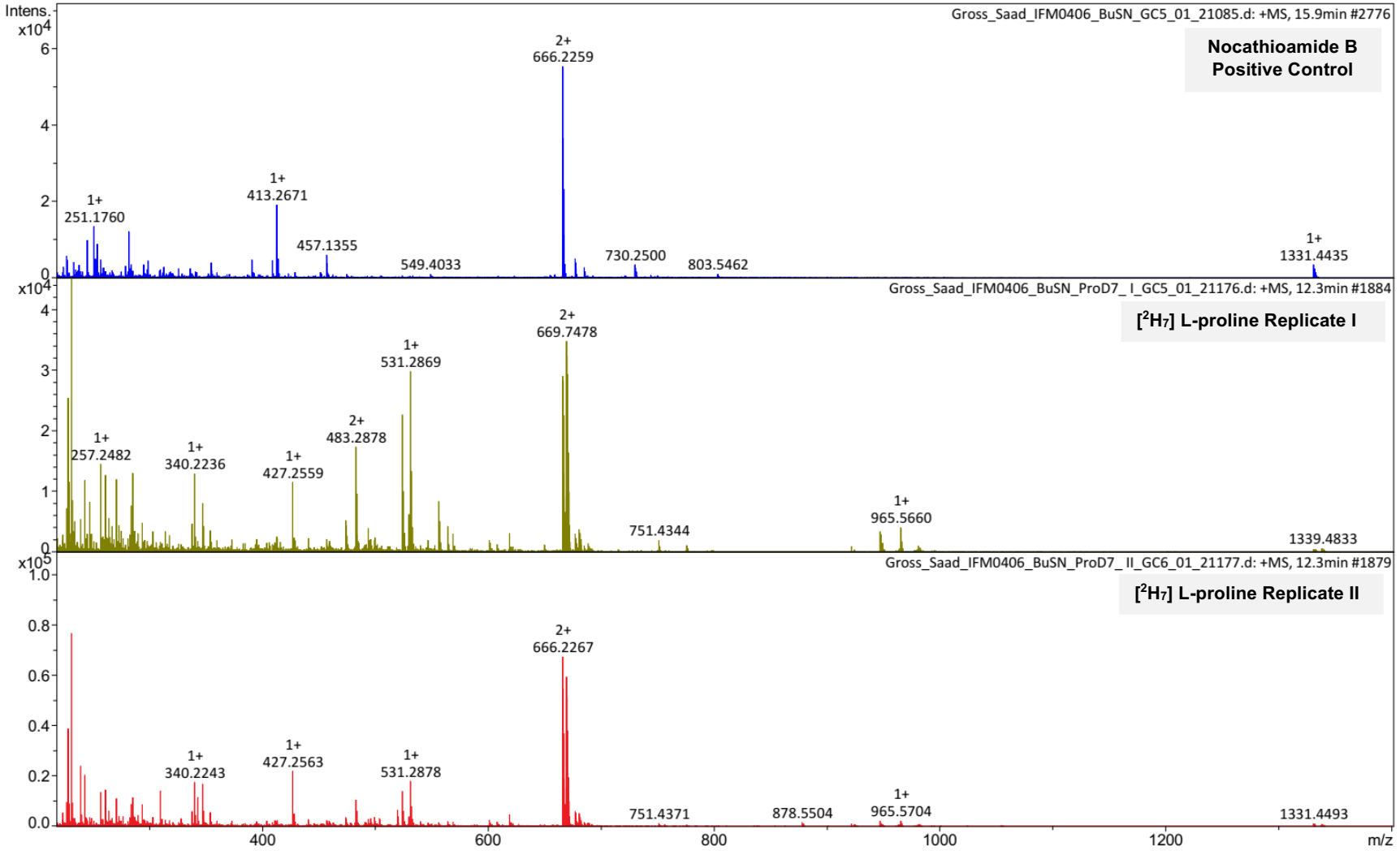

Figure S8. Comparative MS[1] of nocathioamide B (**2**) and its ([$^2H_7$] L-proline)-based version

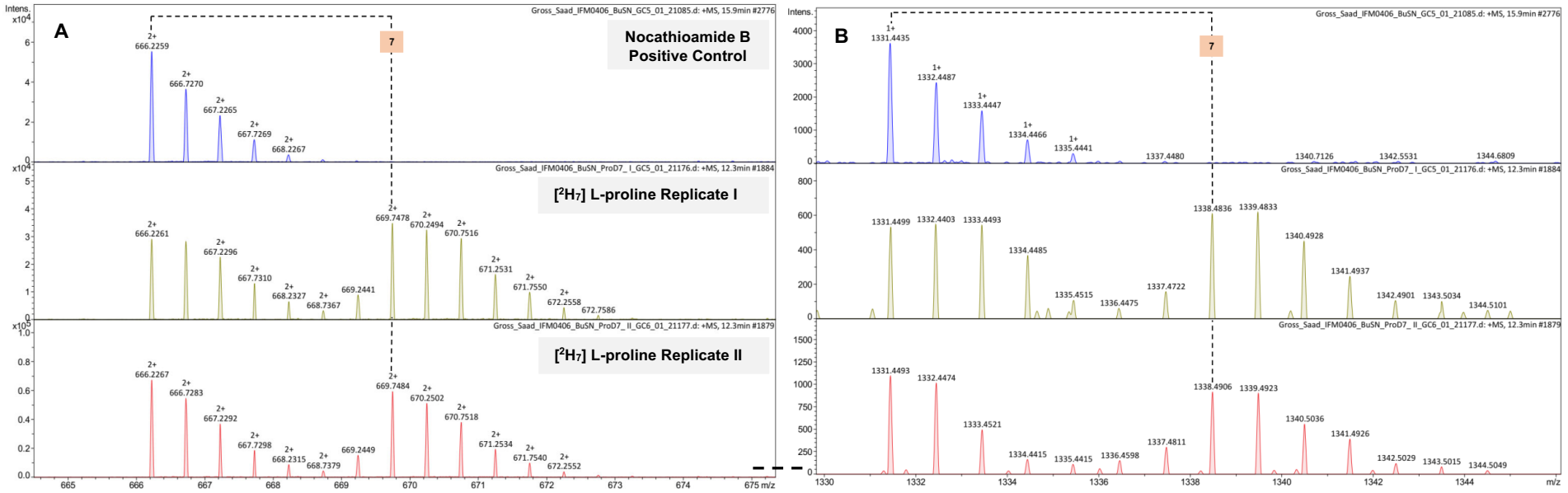

Figure S8A. Enlarged doubly ($[M+2H]^{2+}$, panel A) and singly ($[M+H]^{+}$, panel B) charged ions of nocathioamide B (**2**) and its ($[^2H_7]$ L-proline)-based version

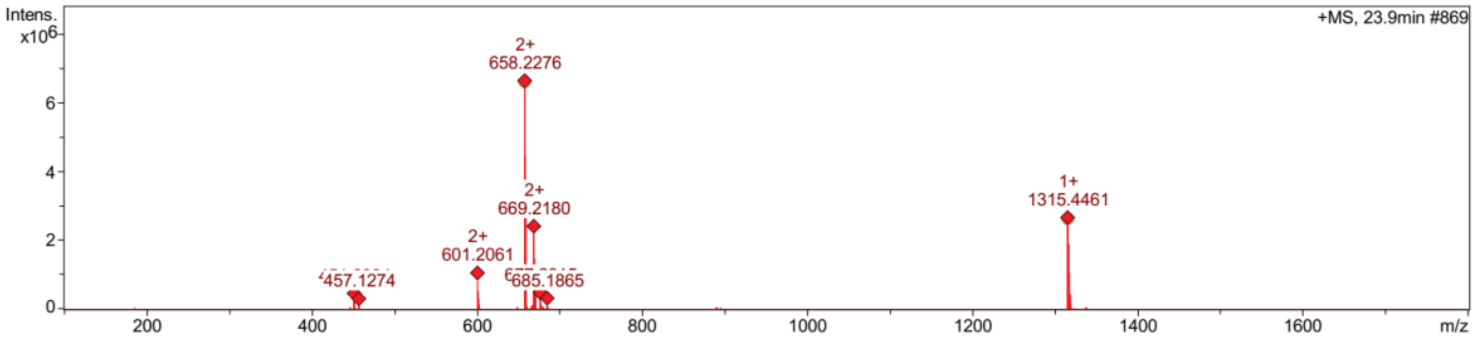

Meas. m/z	#	Ion Formula	m/z	err [ppm]	Mean err [ppm]	rdb	N-Rule	eÂ¯ Conf	mSigma	Std I
658.2276	1	C55H76N14O18S3	658.2307	4.7	5.0	26.0	ok	even	10.9	11.1
	2	C54H76N16O15S4	658.2274	-0.3	-0.5	26.0	ok	even	11.6	14.2
	3	C54H64N26O9S3	658.2250	-3.9	-4.0	37.0	ok	even	13.8	15.3
	4	C53H80N12O19S4	658.2267	-1.3	-1.4	21.0	ok	even	13.8	15.3
	5	C53H68N22O13S3	658.2244	-4.9	-4.9	32.0	ok	even	14.2	15.6
	6	C53H64N28O8S3	658.2307	4.7	4.5	37.0	ok	even	14.9	17.0
	7	C55H80N8O23S3	658.2244	-4.9	-4.4	21.0	ok	even	15.9	14.1
	8	C55H72N20O11S4	658.2281	0.7	0.5	31.0	ok	even	17.1	17.6
	9	C54H80N10O22S3	658.2300	3.7	4.1	21.0	ok	even	18.6	16.9
	10	C54H84N4O27S3	658.2237	-5.9	-5.3	16.0	ok	even	25.2	22.0
	11	C53H84N6O26S3	658.2293	2.6	3.1	16.0	ok	even	27.8	24.6
	12	C55H64N24O12S2	658.2283	1.1	1.6	37.0	ok	even	32.7	39.5
	13	C54H68N20O16S2	658.2276	0.1	0.7	32.0	ok	even	35.1	41.4
	14	C53H72N16O20S2	658.2270	-0.9	-0.2	27.0	ok	even	39.9	44.9
	15	C55H84N2O30S2	658.2270	-0.9	0.3	16.0	ok	even	41.3	42.9
1315.4461	1	C52H63N30O5S4	1315.4475	1.0	0.8	37.0	ok	even	24.7	23.8
	2	C54H63N26O9S3	1315.4428	-2.5	-2.2	37.0	ok	even	25.4	20.1
	3	C55H71N20O11S4	1315.4489	2.1	2.2	31.0	ok	even	27.8	28.9
	4	C51H67N26O9S4	1315.4462	0.0	-0.1	32.0	ok	even	33.2	29.6
	5	C54H75N16O15S4	1315.4475	1.0	1.3	26.0	ok	even	35.0	33.4
	6	C55H63N24O12S2	1315.4493	2.4	3.3	37.0	ok	even	40.2	38.7
	7	C50H71N22O13S4	1315.4448	-1.0	-1.0	27.0	ok	even	42.4	36.5
	8	C53H79N12O19S4	1315.4462	0.0	0.3	21.0	ok	even	43.4	39.3
	9	C54H67N20O16S2	1315.4480	1.4	2.4	32.0	ok	even	48.9	45.5
	10	C52H83N8O23S4	1315.4448	-1.0	-0.6	16.0	ok	even	52.5	46.2
	11	C51H59N30O10S2	1315.4466	0.4	1.0	38.0	ok	even	53.2	51.8
	12	C53H71N16O20S2	1315.4466	0.4	1.5	27.0	ok	even	58.0	53.0
	13	C50H75N16O20S3	1315.4500	3.0	3.5	22.0	ok	even	58.0	48.5
	14	C50H63N26O14S2	1315.4453	-0.6	0.1	33.0	ok	even	61.8	58.9
	15	C51H87N4O27S4	1315.4435	-2.0	-1.5	11.0	ok	even	61.9	54.0
	16	C55H83N2O30S2	1315.4467	0.4	2.0	16.0	ok	even	64.0	56.3
	17	C52H87N2O30S3	1315.4500	3.0	3.9	11.0	ok	even	66.3	55.7
	18	C52H75N12O24S2	1315.4453	-0.6	0.6	22.0	ok	even	67.2	61.1
	19	C50H91O31S4	1315.4422	-3.0	-2.4	6.0	ok	even	71.5	62.2
	20	C51H79N8O28S2	1315.4440	-1.6	-0.3	17.0	ok	even	76.5	69.7
	21	C50H83N4O32S2	1315.4426	-2.7	-1.2	12.0	ok	even	85.9	78.6

Figure S9. MS^1 and molecular formula prediction of nocathioamide A (**1**)

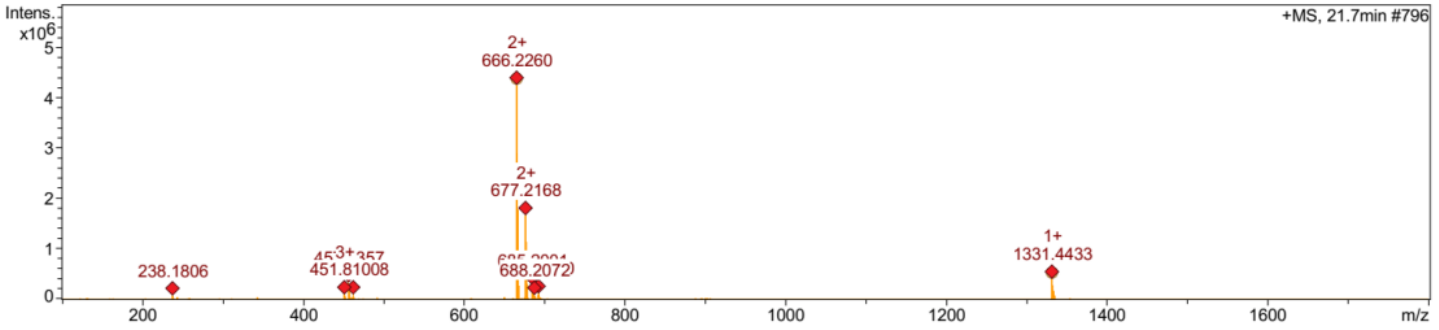

Meas. m/z	#	Ion Formula	m/z	err [ppm]	Mean err [ppm]	rdb	N-Rule	eÅ¯ Conf	mSigma	Std I
666.2260	1	C55H76N14O19S3	666.2281	3.2	3.4	26.0	ok	even	8.2	9.4
	2	C52H80N14O19S4	666.2298	5.7	5.5	21.0	ok	even	10.5	12.3
	3	C53H80N12O20S4	666.2242	-2.7	-2.9	21.0	ok	even	11.6	13.9
	4	C54H80N10O23S3	666.2274	2.2	2.5	21.0	ok	even	12.5	12.5
	5	C52H68N24O13S3	666.2274	2.1	2.0	32.0	ok	even	14.1	16.7
	6	C54H76N16O16S4	666.2249	-1.7	-2.0	26.0	ok	even	14.7	15.9
	7	C52H84N8O24S4	666.2235	-3.7	-3.8	16.0	ok	even	16.3	16.9
	8	C53H64N28O9S3	666.2281	3.2	2.9	37.0	ok	even	16.7	18.1
	9	C54H64N26O10S3	666.2225	-5.3	-5.4	37.0	ok	even	16.8	17.2
	10	C52H64N30O6S4	666.2248	-1.7	-2.4	37.0	ok	even	18.5	16.1
	11	C54H92O29S4	666.2298	5.7	5.9	10.0	ok	even	19.8	21.4
	12	C53H84N6O27S3	666.2268	1.2	1.6	16.0	ok	even	21.2	19.4
	13	C55H72N20O12S4	666.2255	-0.7	-1.1	31.0	ok	even	22.7	21.1
	14	C52H88N2O31S3	666.2261	0.1	0.7	11.0	ok	even	30.6	27.8
	15	C55H64N24O13S2	666.2258	-0.4	0.0	37.0	ok	even	32.0	39.1
	16	C54H68N20O17S2	666.2251	-1.4	-0.9	32.0	ok	even	32.4	39.8
	17	C53H72N16O21S2	666.2244	-2.4	-1.7	27.0	ok	even	35.7	42.3
	18	C55H84N2O31S2	666.2244	-2.4	-1.3	16.0	ok	even	35.8	39.1
	19	C52H72N18O20S2	666.2300	6.0	6.6	27.0	ok	even	38.2	45.1
	20	C54H84N4O30S2	666.2300	6.0	7.1	16.0	ok	even	38.5	42.1
	21	C52H76N12O25S2	666.2238	-3.4	-2.6	22.0	ok	even	41.1	46.4
	22	C53H88O34S2	666.2294	5.0	6.2	11.0	ok	even	45.8	48.2
1331.4433	1	C51H67N26O10S4	1331.4411	-1.7	-2.0	32.0	ok	even	8.5	9.2
	2	C52H63N30O6S4	1331.4424	-0.7	-1.0	37.0	ok	even	8.9	9.6
	3	C54H75N16O16S4	1331.4424	-0.7	-0.6	26.0	ok	even	13.2	15.4
	4	C55H71N20O12S4	1331.4438	0.3	0.3	31.0	ok	even	14.9	16.5
	5	C50H71N22O14S4	1331.4397	-2.7	-2.9	27.0	ok	even	16.6	14.9
	6	C53H79N12O20S4	1331.4411	-1.7	-1.5	21.0	ok	even	18.5	18.7
	7	C51H71N20O17S3	1331.4463	2.2	2.5	27.0	ok	even	26.8	25.2
	8	C52H83N8O24S4	1331.4398	-2.7	-2.4	16.0	ok	even	26.8	24.7
	9	C55H63N24O13S2	1331.4442	0.7	1.4	37.0	ok	even	32.2	38.6
	10	C53H83N6O27S3	1331.4463	2.2	3.0	16.0	ok	even	32.6	28.3
	11	C50H75N16O21S3	1331.4449	1.2	1.6	22.0	ok	even	35.8	32.7
	12	C54H67N20O17S2	1331.4429	-0.3	0.5	32.0	ok	even	36.2	41.4
	13	C51H59N30O11S2	1331.4416	-1.3	-0.9	38.0	ok	even	42.1	49.3
	14	C53H71N16O21S2	1331.4416	-1.3	-0.4	27.0	ok	even	42.2	45.9
	15	C52H87N2O31S3	1331.4449	1.2	2.1	11.0	ok	even	42.4	37.1
	16	C55H83N2O31S2	1331.4416	-1.3	0.1	16.0	ok	even	44.8	44.9
	17	C50H63N26O15S2	1331.4402	-2.4	-1.8	33.0	ok	even	47.6	53.4
	18	C52H75N12O25S2	1331.4402	-2.3	-1.3	22.0	ok	even	49.4	51.6

Figure S10. MS^1 and molecular formula prediction of nocathioamide B (**2**)

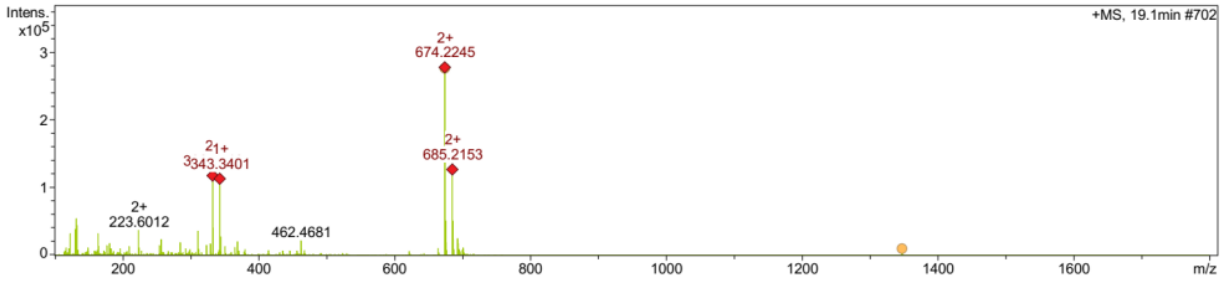

Meas. m/z	#	Ion Formula	m/z	err [ppm]	Mean err [ppm]	rdb	N-Rule	eÂ¯ Conf	mSigma	Std I
674.2245	1	C52H80N14O20S4	674.2273	4.1	3.9	21.0	ok	even	5.1	5.2
	2	C53H80N12O21S4	674.2216	-4.2	-4.4	21.0	ok	even	6.0	6.4
	3	C51H68N26O11S4	674.2216	-4.2	-4.8	32.0	ok	even	8.9	7.3
	4	C53H76N18O16S4	674.2279	5.1	4.8	26.0	ok	even	9.2	7.7
	5	C55H88N4O26S4	674.2279	5.1	5.2	15.0	ok	even	10.1	11.0
	6	C52H84N8O25S4	674.2210	-5.2	-5.3	16.0	ok	even	11.9	11.1
	7	C54H76N16O17S4	674.2223	-3.2	-3.5	26.0	ok	even	11.9	10.3
	8	C51H84N10O24S4	674.2266	3.2	3.0	16.0	ok	even	13.3	12.0
	9	C55H76N14O20S3	674.2256	1.6	1.8	26.0	ok	even	14.3	17.5
	10	C54H92O30S4	674.2273	4.2	4.3	10.0	ok	even	14.8	14.6
	11	C54H80N10O24S3	674.2249	0.7	0.9	21.0	ok	even	16.3	19.0
	12	C51H64N32O6S4	674.2279	5.1	4.3	37.0	ok	even	16.8	13.7
	13	C52H64N30O7S4	674.2223	-3.2	-3.9	37.0	ok	even	19.0	15.1
	14	C52H68N24O14S3	674.2249	0.6	0.5	32.0	ok	even	20.0	24.7
	15	C55H72N20O13S4	674.2230	-2.2	-2.6	31.0	ok	even	21.5	17.4
	16	C51H72N20O18S3	674.2242	-0.3	-0.4	27.0	ok	even	22.2	26.4
	17	C53H64N28O10S3	674.2256	1.6	1.4	37.0	ok	even	22.6	25.8
	18	C53H84N6O28S3	674.2242	-0.3	0.0	16.0	ok	even	23.0	24.0
	19	C52H88N2O32S3	674.2236	-1.3	-0.9	11.0	ok	even	31.5	30.8
	20	C55H80N8O27S2	674.2282	5.5	6.4	21.0	ok	even	36.9	44.4
	21	C54H68N20O18S2	674.2225	-2.8	-2.4	32.0	ok	even	38.0	47.5
	22	C55H64N24O14S2	674.2232	-1.9	-1.5	37.0	ok	even	38.0	47.0
	23	C55H84N2O32S2	674.2219	-3.8	-2.8	16.0	ok	even	39.4	45.3
	24	C53H68N22O17S2	674.2282	5.5	5.9	32.0	ok	even	40.0	49.9
	25	C53H72N16O22S2	674.2219	-3.8	-3.2	27.0	ok	even	40.4	49.4
	26	C54H84N4O31S2	674.2275	4.5	5.5	16.0	ok	even	41.9	48.3
	27	C52H72N18O21S2	674.2275	4.5	5.0	27.0	ok	even	42.8	52.2
	28	C51H60N30O12S2	674.2219	-3.8	-3.7	38.0	ok	even	44.0	55.4
	29	C52H76N12O26S2	674.2212	-4.8	-4.1	22.0	ok	even	44.9	52.9
	30	C51H76N14O25S2	674.2268	3.5	4.1	22.0	ok	even	47.4	55.8
	31	C53H88O35S2	674.2268	3.5	4.6	11.0	ok	even	48.4	53.5
	32	C51H80N8O30S2	674.2205	-5.8	-5.0	17.0	ok	even	50.8	57.7
1347.4373	1	C53H71N16O22S2	1347.4366	0.6	1.7	27.0	ok	even	12.6	14.5
	2	C55H83N2O32S2	1347.4365	-0.6	-1.3	16.0	ok	even	13.9	13.3
	3	C54H67N20O18S2	1347.4378	0.4	-0.9	32.0	ok	even	14.4	15.7
	4	C53H83N6O28S3	1347.4412	2.9	1.3	16.0	ok	even	16.0	20.0
	5	C52H75N12O26S2	1347.4351	-1.6	-2.5	22.0	ok	even	17.6	18.4
	6	C55H63N24O14S2	1347.4392	1.4	-0.1	37.0	ok	even	21.4	20.9
	7	C52H87N2O32S3	1347.4399	1.9	0.5	11.0	ok	even	21.8	23.8
	8	C51H79N8O30S2	1347.4338	-2.6	-3.3	17.0	ok	even	25.7	25.5
	9	C50H63N26O16S2	1347.4351	-1.6	-1.7	33.0	ok	even	54.6	67.5
	10	C51H59N30O12S2	1347.4365	-0.6	-1.1	38.0	ok	even	55.9	68.9
	11	C50H75N16O22S3	1347.4398	1.9	0.9	22.0	ok	even	64.5	83.6
	12	C51H71N20O18S3	1347.4412	2.9	1.6	27.0	ok	even	65.5	84.9
	13	C50H71N22O15S4	1347.4347	-2.0	-2.3	27.0	ok	even	79.7	103.2
	14	C51H87N4O29S4	1347.4333	-3.0	-2.8	11.0	ok	even	80.9	106.0
	15	C52H83N8O25S4	1347.4347	-2.0	-2.1	16.0	ok	even	82.0	107.1
	16	C51H67N26O11S4	1347.4360	-1.0	-1.6	32.0	ok	even	83.1	105.6
	17	C53H79N12O21S4	1347.4360	-1.0	-1.4	21.0	ok	even	84.4	108.9
	18	C52H63N30O7S4	1347.4373	0.0	-0.9	37.0	ok	even	87.7	108.6
	19	C54H75N16O17S4	1347.4373	0.0	-0.7	26.0	ok	even	87.9	111.3
	20	C55H71N20O13S4	1347.4387	1.0	0.0	31.0	ok	even	92.6	114.3

Figure S11. MS^1 and molecular formula prediction of nocathioamide C (**3**)

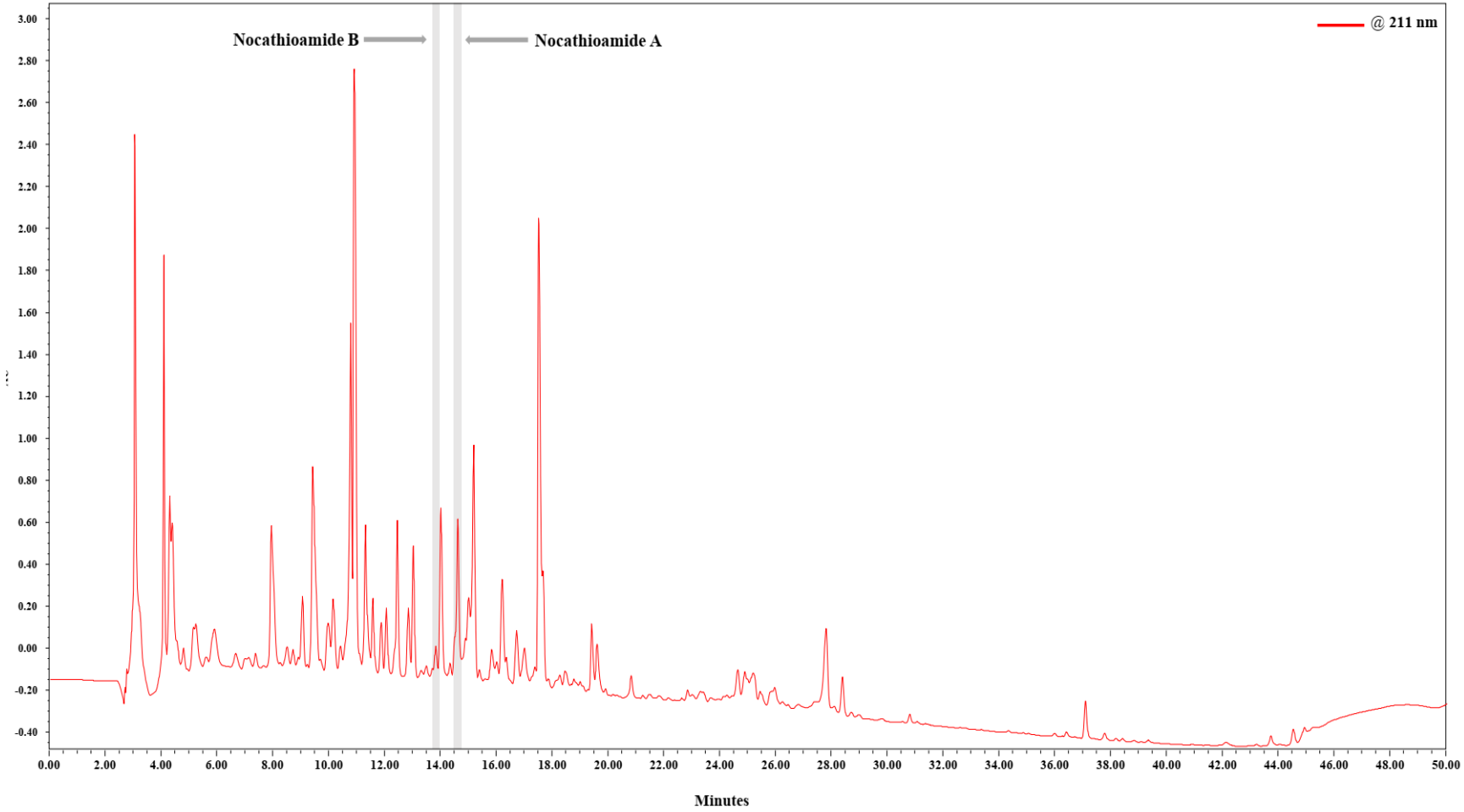

Figure S12. HPLC profile of the *n*-butanol extract of cell-free supernatant of IFM 0406

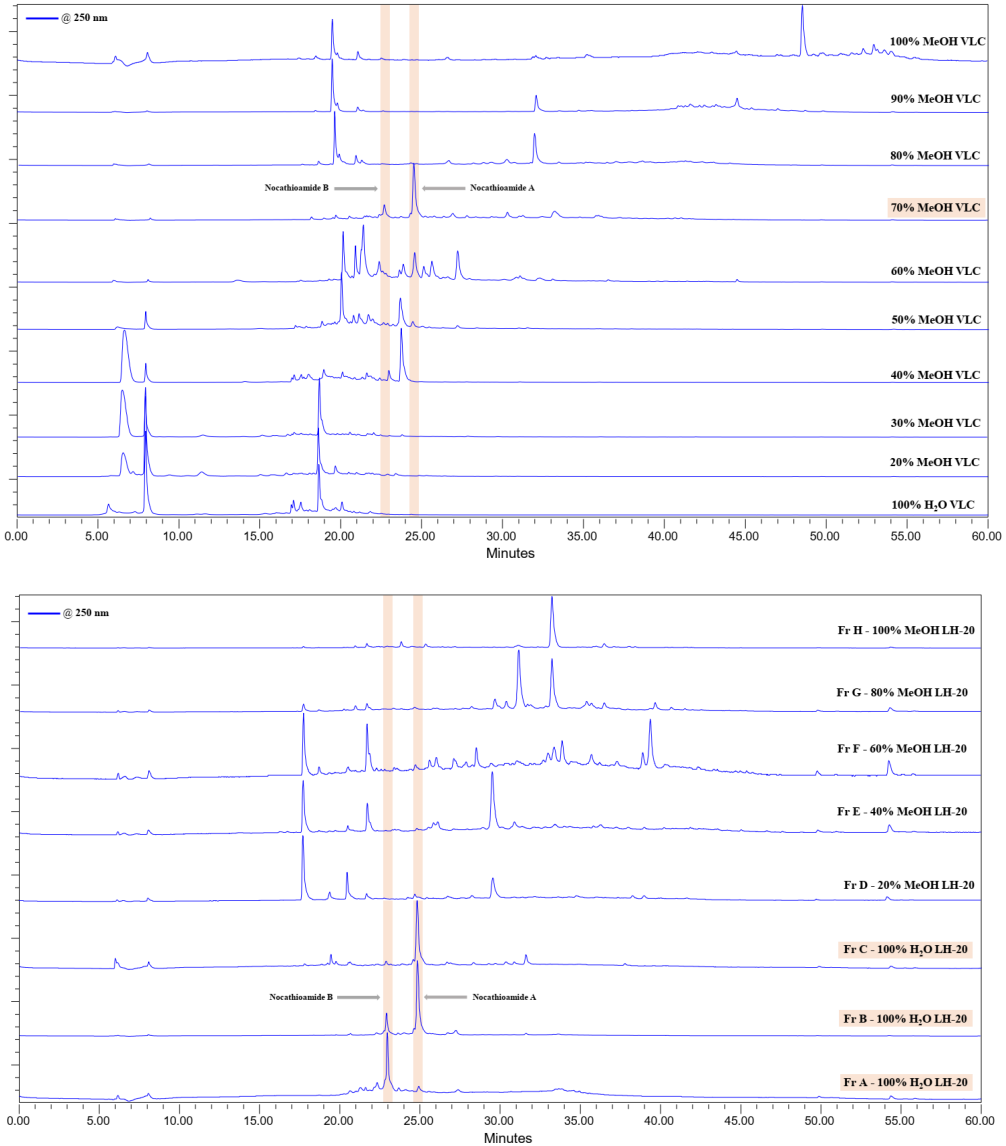

Figure S13. HPLC profiles of VLC fractions of the *n*-butanol extract (Upper) & HPLC profiles of Sephadex LH-20 subfractions of 70% MeOH VLC fraction (Bottom)

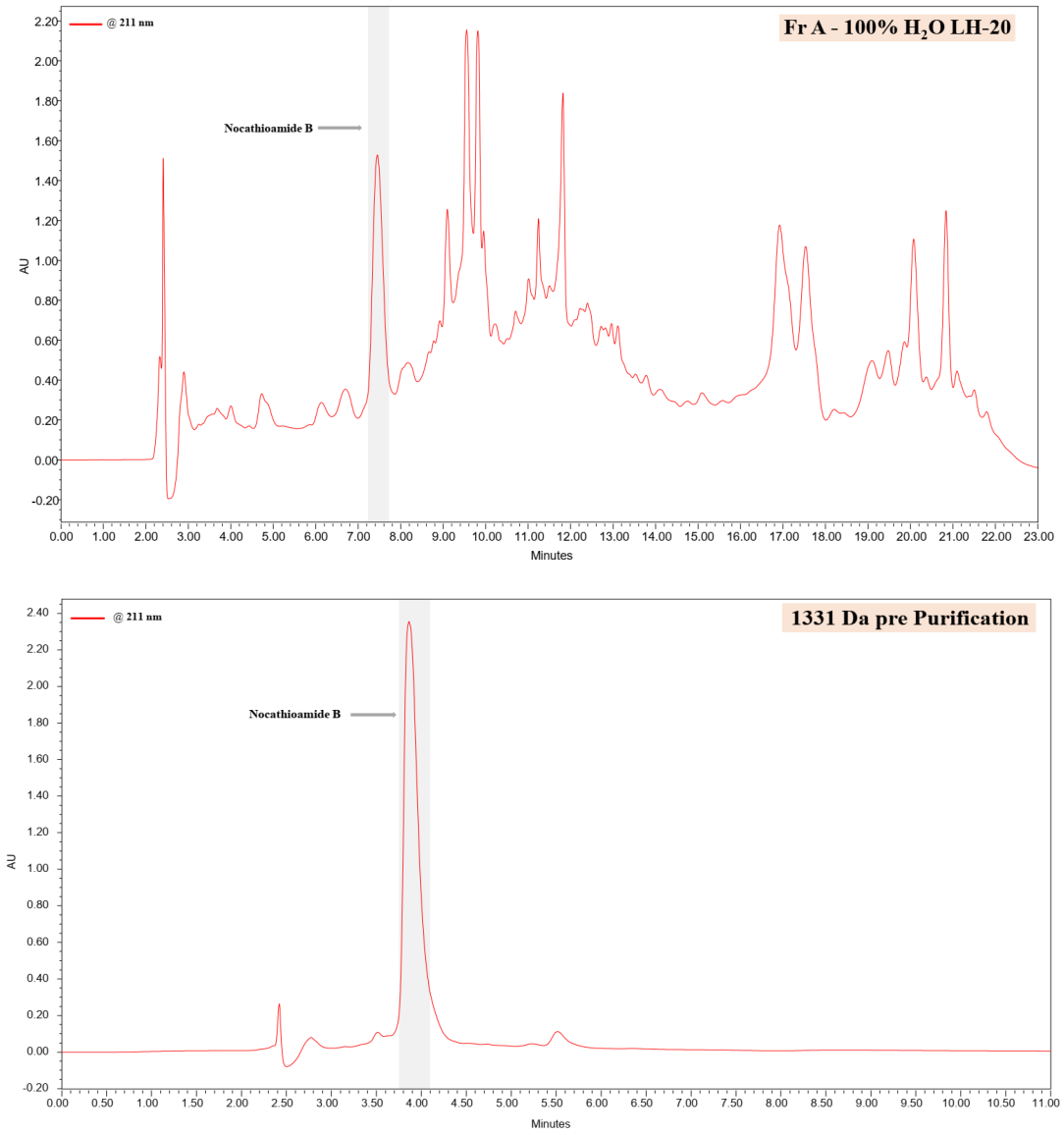

Figure S14. HPLC profile of fraction A-100% H_2O LH-20 (Upper) & HPLC profile of prepurified nocathioamide B (**2**) (Bottom)

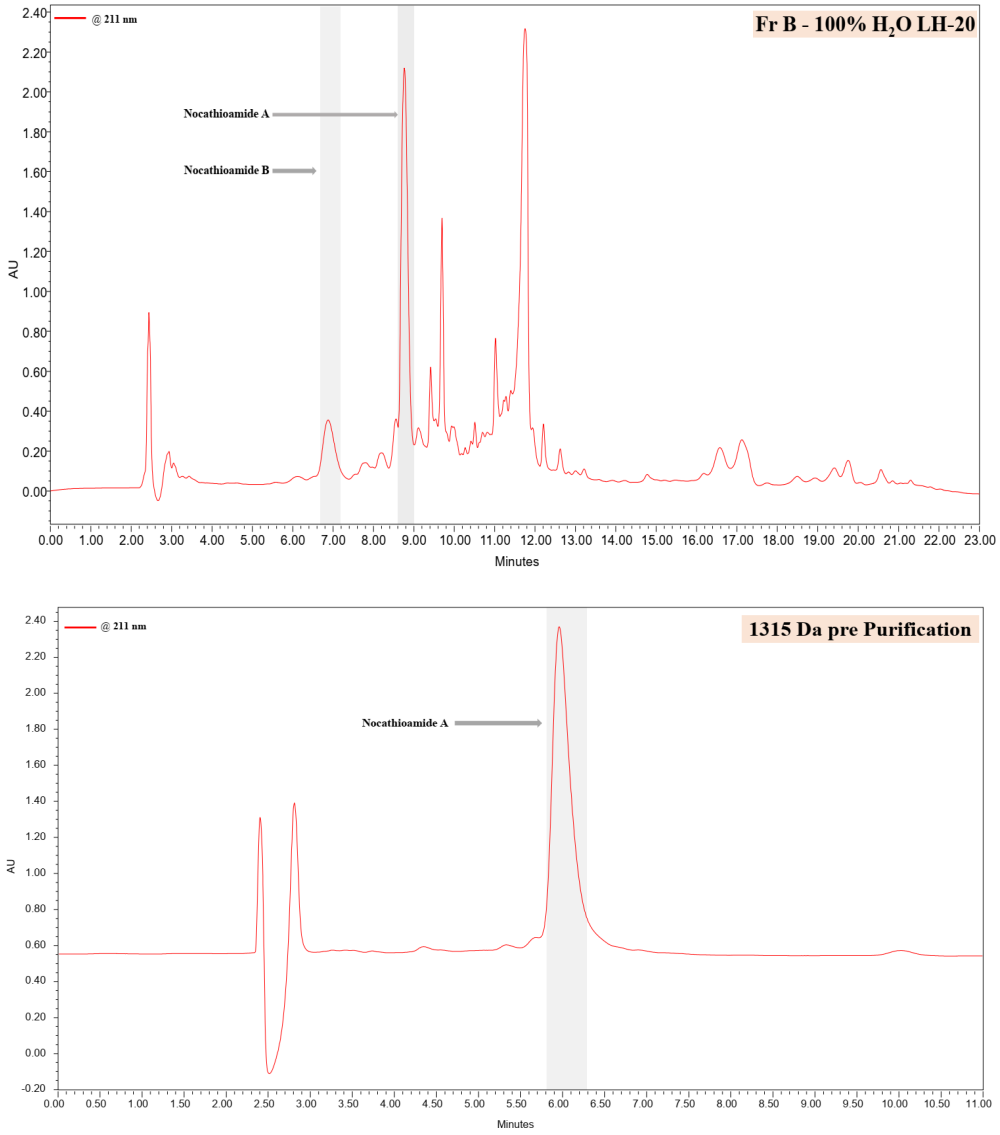

Figure S15. HPLC profile of fraction B-100% H_2O LH-20 (Upper figure) & HPLC profile of prepurified nocathioamide A (**1**) (Bottom figure)

Structural elucidation: NMR spectroscopy

In combination with extensive NMR analyses, the suggested elemental compositions of nocathioamide A (**1**) possessing *m/z* 1315 $[M+H]^+$ and 658 $[M+2H]^{2+}$ was expected to be $C_{54}H_{74}N_{16}O_{15}S_4$ with 26 degrees of unsaturation (RDB) with no matched hits to any known naturally occurring compound from any natural resource.

Expectedly, ^{13}C-NMR spectra in the differently used solvents (d_4-, d_3-CH_3OH) exhibited a greater number of signals due to the inseparable minor conformer(s), which were also observed in the LC/MS (Figure S2) and HPLC (Figure S15) profiles. Additionally, careful inspection of the 1D and 2D NMR data unveiled a pairing phenomenon of almost all signals emphasizing a mixture of conformers. The observation of multiple doubly charged species as 658 $[M+2H]^{2+}$, 669 $[M+H+Na]^{2+}$, 677 $[M+H+K]^{2+}$ (Figure S2) with a large number of exchangeable amide NH protons (δ_H 6.5-10.5) and carbonyl carbons (δ_C 160-185) from 1D NMR (Figures S38-39) aligned with the postulated peptide nature.

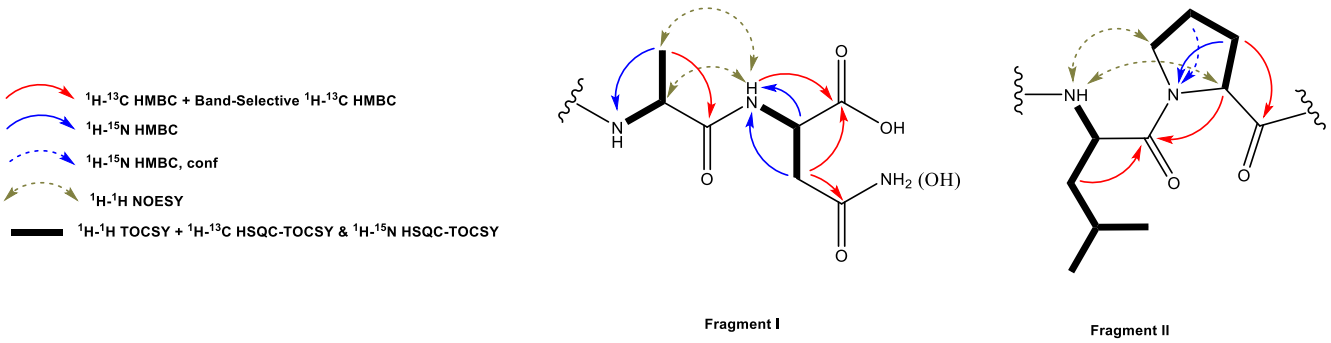

Figure S16. Structural fragments **I**, and **II**

Analyzing various 2D (^{1}H-^{1}H, ^{1}H-^{13}C and ^{1}H-^{15}N) NMR experiments (COSY, TOCSY, NOESY, HSQC, HSQC-TOCSY, HMBC) instantly resulted in the assignment of four proteogenic amino acid residues encompassing leucine (**Leu**), proline (**Pro**), alanine (**Ala-12**), and asparagine/aspartic acid (**Asn**/**Asp** due to the initial inabilities to allocate the δ_H of either -$CONH_2$ or –COOH, respectively). Exploiting HMBC and NOESY correlations, the connectivity between these readily discovered spin systems were directly established, offering a pair of fragments (**I**, and **II**), each consisting of two-stitched residues (Figure S16).

The distinctive olefinic CH_2 [$\delta_{H/C}$ 5.35/111.63 ppm in d_3-CH_3OH (700/176 MHz)] and its characteristic downfield NH_2 signal [$\delta_{H/N}$ 10.05/127.35 ppm in d_3-CH_3OH (700/71 MHz)] in tandem with the correlations from HMBC and NOESY experiments could unequivocally outline extended fragment **II** with an extra unit in the form of 2,3-didehydroalanine (**Dha**) (Figure S17A).

The clearly found singlets and their conformers in the aliphatic and aromatic regions [δ_H (2.02–2.04 & 7.30–8.90) ppm in d_4-CH_3OH (400 MHz)] aided in constructing fragment **III** with the help of the derived data mostly from ^{1}H-^{13}C and ^{1}H-^{15}N HMBC experiments (Figures S39, and S48). It started with a terminal acetyl group (**Ac**) linked to an alanine residue (**Ala-1**) which was in turn found to be connected to the thiazole moiety (**Thz**). Guided by the unique **Thz** resonances of 3-CH ($\delta_{H/C}$ 8.16/126.66 ppm in d_4-CH_3OH), and –N= (δ_N 305.60 ppm in d_3-CH_3OH) in joint with the ^{1}H-^{13}C and ^{1}H-^{15}N HMBC couplings,[9] **Thz** unit was completely assigned to be in in a direct fusion with **Ala-1** (Figure S17B).

Analogously, histidine (**His**) was deciphered from its characteristic imidazole signals ($\delta_{5H/C}$ 7.48/119.05, $\delta_{6H/C}$ 8.86/135.23, δ_{5N} 175.04, and δ_{6N} 191.59 ppm in d_4-CH_3OH). The inter-residue NOESY proved its occurrence to be in a direct linkage with **Thz** unit. Moreover, the ^{1}H-^{13}C HMBC exhibited several cross-peaks around δ_C 206 - 209 ppm corresponding to an intensely relaxed signal in the 1D ^{13}C-NMR spectrum (Figures S29, 39, 53), which were identified as couplings between the 2-CH (αH), and 3-CH_2 (βH) of histidine with the genetically expected thioamide tailoring that typically resonates around (200–210 ppm).[10] Thus, **His** was selectively posttranslationally modified into thio-histidine portraying fragment **III** (Figure S17B).

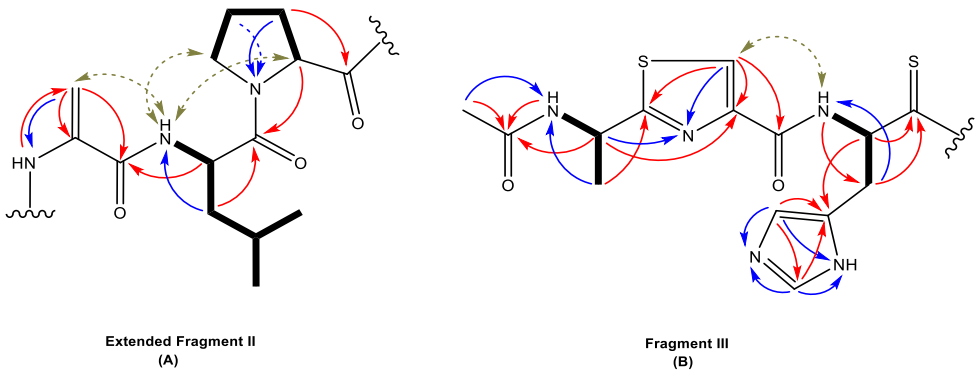

Figure S17. Structural fragments extended **II**, and **III**

The assembly of the highly morphed fragment **IV** was initiated by the guidance of ^{1}H-^{1}H TOCSY, ^{1}H-^{13}C HSQC-TOCSY, and NOESY experiments, which enabled decoding of a common posttranslationally tailored motif as α-aminobutyrate (**Abu**), biosynthetically originating from threonine. Tracing up such spin system (**Abu**) with ^{1}H-^{13}C HMBC, and NOESY correlations uncovered three additional transformed amino acid residues (**AlaS-6**, **AlaS-10**, and **AlaS-11**), comprising typical methyllanthionine (**MeLan = Abu** + **AlaS-10**) (Figures S108-108A), and lanthionine (**Lan = AlaS-6** + **AlaS-11**) bridges,[11] besides an exceptionally δ-oxidized leucine in the form of 4-methylglutamate (**4-Meglu**).[12] As a result of the highly similar (identical) chemical shifts of α- protons of **AlaS-6** and **AlaS-11** across the different datasets (Tables S2-4A), the NOESY analysis did not result in any convincing correlations using neither the β-, or α- protons of the **Lan** residues to validate the crosslink (Figures S108, and S108B-108C).[13] Mainly supervised by the homonuclear correlations arising from NOESY data, **MeLan** and **Lan** blocks were found to be directly bonded to each other on one side whilst being disjointed on the **Abu** flank by **4-Meglu** (Figure S18).

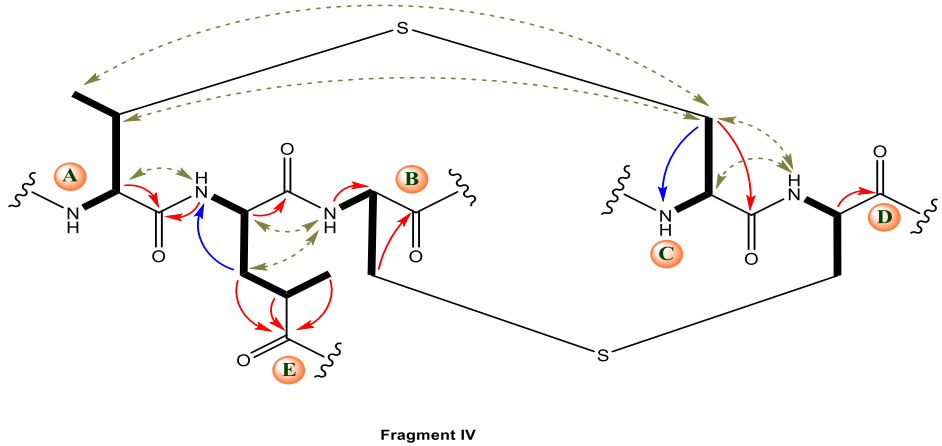

Figure S18. Structural fragment **IV**

Considering the deduced skeletons of fragments (**I–IV**), it was clear that fragment **I** portrayed the C-terminus of the peptide while the amino-terminus was represented as fragment **III** N-capped with an acetyl group.

Besides the heteronuclear connections of αH and βH-**His** to ^{13}C=S, an extra set of aligned couplings (**$\delta_{2H/C,\ major}$** 5.48/65.74, **$\delta_{2H/C,\ minor}$** 5.37/65.74 in d_4-CH_3OH) was identified signifying the αH of the **Abu** motif. The confirmatory observation of ^{1}H-^{15}N HMBC couplings between αH-**His** and NH of the **Abu** offered further unambiguous proof of fitting fragment **III** together with component **IV/A** (Figures S19, and S60). Notably, the uniquely deshielded NH signals of the **Abu** spin system [**$\delta_{H/N}$** 9.77/ 155.59 ppm in d_3-CH_3OH (700/71 MHz)] were also in alignment with its straight association with the thiocarbonyl group (Figure S19). The additional attachment of fragment **I** to **IV/D** was basically gleaned from both ^{1}H-^{13}C HMBC along with ^{1}H-^{1}H NOESY data (Figure S19).

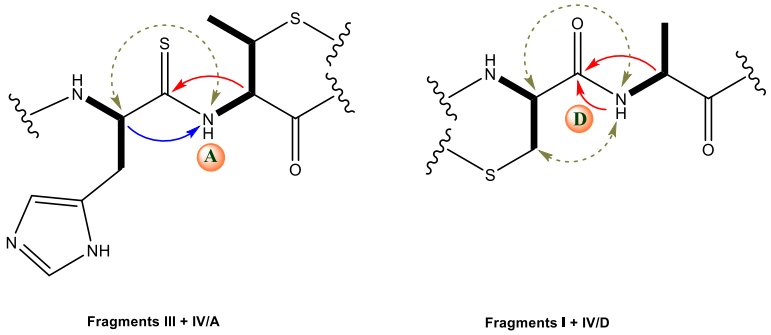

Figure S19. Structural fragments **III**+**IV/A**, and **I**+**IV/D**

Finally, the extended fragment **II** was found to be architecturally inserted within **IV** using solely NOE connections which placed the **Dha** structural brick in association with **AlaS-6** feature (**IV/B**), whereas **Pro** was attached to **AlaS-10** system (**IV/C**) (Figure S20).

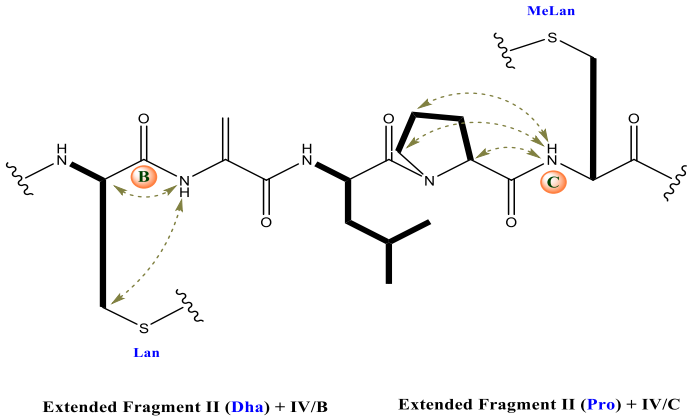

Figure S20. Structural fragments extended **II** (**Dha**) + **IV/B**, and extended **II** (**Pro**) + **IV/D**

Although fragment **IV** possessed five possible attachment sites (**A** – **E**), only four (**A** – **D**) could be structurally ruled out. Unfortunately, meticulous investigation of the different NMR datasets (d_4-CH_3OH, and d_3-CH_3OH) did not infer any valuable couplings that could sort out any structural connection with the last remaining decoration **E**.

However, bearing in mind the anticipated molecular formulae besides its RDB, one final macrocyclization has to be recruited. Driven by the inability to assign δ_H of neither the in-chain NH_2 nor C-terminus CO_2H of **Asn** of fragment **I**, two possible crosslinks have been suggested either as an imide or anhydride macrocyclization, respectively (Figure S21).

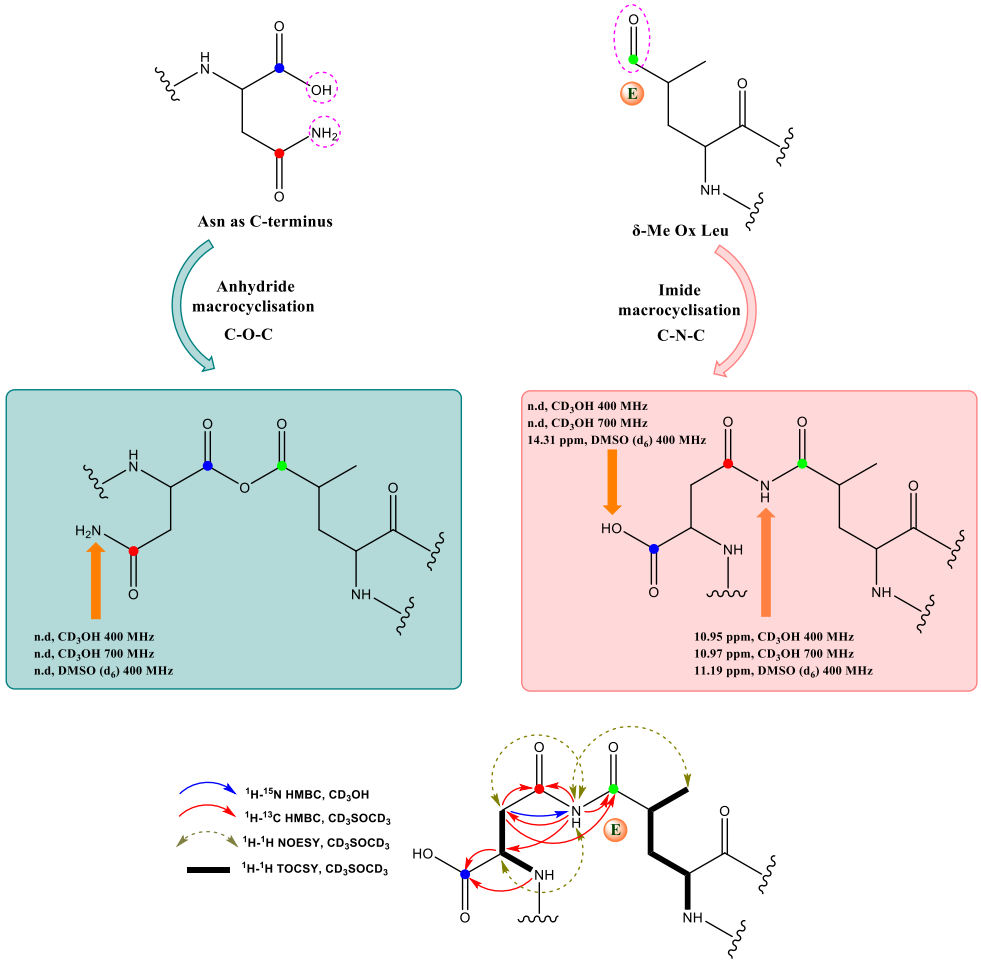

Figure S21. Possible crosslinks between fragment **I-Asn** and fragment **IV/E** (Upper) & Macrocylic imide PTM connected by NMR through NOESY and HMBC correlations (Bottom)

The possibility of having a macrocyclic anhydride makeup was apparently in strong contradiction with **1** in terms of the given chemical stability observed during the extraction, separation, purification and storage as well.

Luckily, the ^{1}H-^{15}N HMBC spectrum of **1** in CD_3OH/700 MHz dataset, in an unintentional partial sweep width (partial SW) experiment, disclosed a so far non-interpreted pair of two unfamiliar cross-peaks ($\delta_{\mathbf{3Ha/Asn}}$ 2.64/ $\delta_{\mathbf{N}}$ 172.80, $\delta_{\mathbf{3Hb/Asn}}$ 2.99/ $\delta_{\mathbf{N}}$ 172.80 ppm) (Figures S60, and S114A) which were consistent with the reported ^{15}N values of imides.[14] Additionally, ^{1}H-^{15}N HSQC of NH glutarimide, an imide-containing standard, ($\delta_{\mathbf{H/N}}$ 10.33/172.25 in d_3-CH_3OH) supported such a range of chemical shifts (Figure S100) and corroborated the imide linkage hypothesis.

Within the course of our preliminary NMR trials recording in various solvents, d_6-DMSO was tested even though the data quality was not good enough to fully elucidate the structure of **1**. Unexpectedly, the ^{1}H-^{15}N HSQC spectrum (Figure S97) showed two characteristic downfield correlations ($\delta_{\mathbf{H/N}}$ 10.55/161.63, and $\delta_{\mathbf{H/N}}$ 11.19/174.72 ppm), which were tracked down by ^{1}H-^{1}H TOCSY, ^{1}H-^{1}H NOESY, and ^{1}H-^{13}C HMBC correlations. The $\delta_{\mathbf{H/N}}$ 10.55/161.63 ppm coupling was assigned to define the thioamide –NH- of **Abu** entity, whereas the sharp singlet $\delta_{\mathbf{H/N}}$ 11.19/174.72 ppm was found to be in an equivocal consistency with the presumed imide crosslink evidenced by a multitude of connectivities (Figures S21, S94, and S99-99A).

Regardless of the unsatisfactory NMR data quality in d_6-DMSO compared to d_3- and d_4-CH_3OH, the dataset could still successfully and efficiently fill the remaining gap regarding the last unprecedented structural ornament and complete the 2D structure of nocathioamide A (**1**) (Figure S22).

Taking into account the suggested molecular formulae of the additional isolated feature, $C_{54}H_{74}N_{16}O_{16}S_4$, it was envisioned that nocathioamide B (**2**) encode an extra oxygen atom within its architecture relative to **1**. Expectedly, **2** exhibited almost identical NMR spectra of **1** except with a lower degree of signals overlap besides a significant drift in the β-carbons chemical shifts of **AlaSO-6** and **AlaSO-11**. The attained ^{1}H-^{13}C HSQC spectra in d_3- and d_4-CH_3OH datasets all share that the **Lan** bridge forming residues (**AlaSO-6**, **AlaSO-11)** inherited an upfield shift with their α-carbons ($\delta_{\mathbf{C\text{-}AlaS6}}$ 55.49 => $\delta_{\mathbf{C\text{-}AlaSO6}}$ 51.50 & $\delta_{\mathbf{C\text{-}AlaS11}}$ 53.60 => $\delta_{\mathbf{C\text{-}AlaSO11}}$ 49.46, d_3-CH_3OH, 176 MHz) whilst the β-carbons resonated strongly downfield ($\delta_{\mathbf{C\text{-}AlaS6}}$ 34.18 => $\delta_{\mathbf{C\text{-}AlaSO6}}$ 55.52 & $\delta_{\mathbf{C\text{-}AlaS11}}$ 35.43/35.52 => $\delta_{\mathbf{C\text{-}AlaSO11}}$ 59.73, d_3-CH_3OH, 176 MHz) (Figures S64, S73, S83, and S118). In addition, the **Lan** crosslink motifs in **2**, unlike **1**, were found to exhibit more resolved NOESY correlations proving the bridge formation between **AlaSO-6**, and **AlaSO-11** (Figures S103, and S121B-121C). Considering such changes in the chemical shifts that typically occurs upon diagnostic oxidation of the thioether functionality,[15] **2** was deduced to be the S-monooxidized congener of **1** (Figure S22).

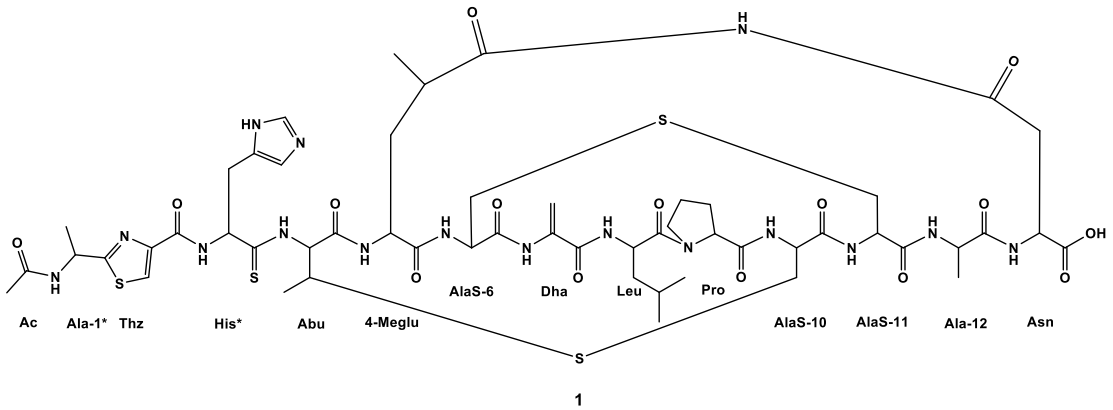

1

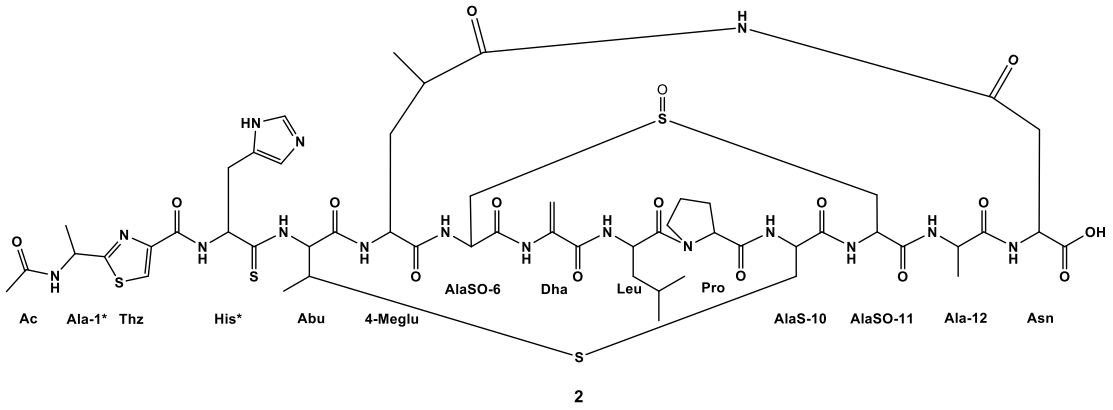

2

Figure S22. Structures of nocathioamide A (**1**), and B (**2**)

Nocathioamide A (**1**): $C_{54}H_{74}N_{16}O_{15}S_4$. White amorphous powder, $[\alpha]_D^{23}$= +2.1 (c 0.75, MeOH); ^{1}H-NMR (400 / 700 MHz, in d_4-CH_3OH, and d_3-CH_3OH): see Tables (S2 – S4); ^{13}C-NMR (100 / 176 MHz, in d_4-CH_3OH, and d_3-CH_3OH): see Tables (S2 – S4); ^{15}N-NMR (40.6 / 71 MHz, in d_4-CH_3OH, and d_3-CH_3OH): see Tables (S2 – S4); FT-IR (ATR) ν (cm^{-1}): 3415, 3254, 2925, 2829, 1651, 1538, 1199, 1023 (see Figure S140); UV (MeOH): λ_{max} (log ε) 272 nm (4.1): see Figure S140. HR-ESIMS *m/z* 658.2276 $[M+2H]^{2+}$ (calcd for $C_{54}H_{76}N_{16}O_{15}S_4$, 658.2274); 1315.4461 $[M+H]^+$ (calcd for $C_{54}H_{75}N_{16}O_{15}S_4$, 1315.4475). HRMSMS: see Figure S2A.

Nocathioamide B (**2**): $C_{54}H_{74}N_{16}O_{16}S_4$. White amorphous powder, $[\alpha]_D^{23}$= -1.6 (c 0.75, MeOH); ^{1}H-NMR (400 / 700 MHz, in d_4-CH_3OH, and d_3-CH_3OH): see Tables (S5 – S7); ^{13}C-NMR (100 / 176 MHz, in d_4-CH_3OH, and d_3-CH_3OH): see Tables (S5 – S7); FT-IR (ATR) ν (cm^{-1}): 3287, 2932, 2832, 1667, 1539, 1428, 1200, 11182, 1137, 1022 (see Figure S140); UV/Vis (MeOH): λ_{max} (log ε) 271 nm (4.0): see Figure S140. HR-ESIMS *m/z* 666.2260 $[M+2H]^{2+}$ (calcd for $C_{54}H_{76}N_{16}O_{16}S_4$, 666.2249); 1331.4433 $[M+H]^+$ (calcd for $C_{54}H_{75}N_{16}O_{16}S_4$, 1331.4424). HRMSMS: see Figure S2A.

Residue	Position	δC / δN	δH, mult (*J* in Hz)	Residue	Position	δC / δN	δH, mult (*J* in Hz)
Ac	1	173.05, C	--------	**Dha**	1	166.77, C	--------
	2	22.64, CH_3	2.02, s		2	138.27, C	--------
Ala-1 *	1	48.92 [b], CH	5.30, p (7.0)		3	107.87, CH_2	5.36, brs
	2	20.98, CH_3	1.60, d (7.0)		-NH-	126.95	10.00, brs
	-NH-	132.2	8.79, d (7.5)	**Leu**	1	173.96, C	--------
Thz	1	163.69, C	--------		2	51.02, CH	4.86, m
	2	149.74, C	--------		3	41.67, CH_2	1.46, m + 1.82, m
	3	126.45, CH	8.15, s		4	26.19, CH	1.70, m
	4	176.73, C	--------		5	22.19, CH_3	0.91, d (6.7)
	=N-	305.66	--------		6	23.75, CH_3	0.97, d (6.6)
His *	1	207.98 [d], C	--------		-NH-	120.49	8.66, d (8.1)
	2	60.64, CH	5.27, m	**Pro**	1	174.72, C	--------
	3	30.69, CH_2	3.44 dd (14.7, 6.9) + 3.56, m		2	62.87, CH	4.68 [b]
	4	130.78, C	--------		3	33.09, CH_2	2.28, m + 2.37, m
	5	119.02, CH	7.46, s		4	22.94, CH_2	1.85, m + 2.07, m
	=N-	184.38	--------		5	47.97, CH_2	3.64, m
	6	135.31, CH	8.80, s		=N-	129.45	--------
	=NH	174.74	--------	**AlaS-10**	1	172.85/172.55 [c], C	--------
	-NH-	123.55	8.97, d (5.8)		2	58.93 [d], CH	4.27, m
Abu	1	170.58, C	--------		3	35.60, CH_2	3.13, m + 3.72, m
	2	65.78, CH	5.47, brs		-NH-	117.43	7.20, brs
	3	44.79, CH	3.93, m	**AlaS-11**	1	171.72, C	--------
	4	20.23, CH_3	1.14, d (7.3)		2	53.39; CH	4.52, m
	-NH-	156.00	9.84, d (5.8)		3	35.61/35.64 [c], CH_2	3.11, m + 3.36, m
4-Meglu	1	172.61, C	--------		-NH-	115.11	8.03 [a], br
	2	53.38, CH	4.64, m	**Ala-12**	1	174.90, C	--------
	3	35.73 [a], CH_2	1.46, m + 2.20, m		2	50.91, CH	4.16, m
	4	36.71, CH	2.45, m		3	18.18, CH_3	1.29, d (7.0)
	5	179.39, C	--------		-NH-	119.65	7.57, brs
	6	18.65, CH_3	0.83 [a], d (6.7)	**Asn**	1	178.95, C	--------
	-NH-	120.33	8.04 [a]		2	51.55, CH	4.54, m
AlaS-6	1	169.60, C	--------		3	37.27, CH_2	2.64, dd (17.7, 5.6) + 2.99, dd (17.7, 9.2)
	2	55.48, CH	4.52, m		4	178.22, C	--------
	3	34.22, CH_2	3.06, m + 3.31, m		-NH-	110.92	8.43, d (7.6)
	-NH-	114.16	7.68, brs		-CONHCO-	n.d	10.96, brs

[*] AA with modified CO within the backbone**,** [a] Overlapped, [b] Masked by water/solvent $^{1}H/^{13}C$-NMR signals, [c] Interchangeable, [d] Weak, [n.d] not determined

Table S2. ^{1}H, ^{13}C, and ^{15}N-NMR data of nocathioamide A (**1**) (d_3-CH_3OH; 400/100/40.6 MHz; major conformer)

Residue	Position	δC / δN	δH, mult (*J* in Hz)	Residue	Position	δC / δN	δH, mult (*J* in Hz)
Ac	1	173.13, C	--------	**Dha**	1	166.70, C	--------
	2	22.67, CH_3	2.04, s		2	138.09, C	--------
Ala-1 *	1	48.95 [b], CH	5.26 [a], m		3	111.69, CH_2	5.43 [a] + 5.50 [a]
	2	20.68, CH_3	1.60, d (7.0)		-NH-	129.92	10.20, s
	-NH-	132.20	8.82, d (7.5)	**Leu**	1	174.12, C	--------
Thz	1	163.87, C	--------		2	57.82, CH	4.31, m
	2	149.85, C	--------		3	38.45, CH_2	1.62, m + 1.88, m
	3	126.42, CH	8.14, s		4	26.37, CH	1.79, m
	4	176.94, C	--------		5	22.16, CH_3	0.93, d (6.5)
	=N-	n.d	n.d		6	23.18, CH_3	1.00, d (6.5)
His *	1	207.03 [d], C	--------		-NH-	135.57	9.01 [a], brs
	2	60.99, CH	5.10, m	**Pro**	1	n.d	--------
	3	30.39, CH_2	n.d + 3.65, m		2	64.87, CH	4.35, m
	4	131.01, C	--------		3	30.39, CH_2	2.07, m + 2.36, m
	5	118.88, C	7.36, s		4	27.08, CH_2	1.98, m + 2.13, m
	=N-	188.01	--------		5	48.88 [b], CH_2	3.73, m + 3.86, m
	6	n.d	8.76 [a], s		=N-	n.d	--------
	=NH	174.08	--------	**AlaS-10**	1	n.d	--------
	-NH-	122.30	9.05, d (5.8)		2	56.16, CH	4.96 [b]
Abu	1	171.24, C	--------		3	38.88, CH_2	3.15 [a], m + 3.59 [a], m
	2	65.70, CH	5.36 [a], m		-NH-	106.11	6.66, d (9.0)
	3	45.27, CH	3.90, m	**AlaS-11**	1	n.d	n.d
	4	n.d	1.13 [a]		2	n.d	n.d
	-NH-	155.1	9.51, brs		3	n.d	n.d
4-Meglu	1	172.03, C	--------		-NH-	n.d	n.d
	2	54.06, CH	4.47 [b]	**Ala-12**	1	175.08, C	--------
	3	35.73, CH_2	1.42 [a], m + 2.19 [a], m		2	51.27, CH	4.31, m
	4	36.71, CH	2.40 [a], m		3	17.71, CH_3	1.42, d (6.7)
	5	179.39 [a], C	--------		-NH-	120.17	7.88, d (6.7)
	6	18.52, CH_3	0.72, d (7.0)	**Asn**	1	178.91, C	--------
	-NH-	119.50	7.92, d (8.0)		2	51.41, CH	4.60, m
AlaS-6	1	169.75, C	--------		3	37.34, CH_2	2.60, m + 2.94, m
	2	55.79, CH	4.64, m		4	n.d	--------
	3	34.38, CH_2	2.94, m + 3.20, m		-NH-	111.15	8.30, d (7.7)
	-NH-	113.86	7.32 [a], m		-CONHCO-	n.d	n.d

[*] AA with modified CO within the backbone**,** [a] Overlapped, [b] Masked by water/solvent $^{1}H/^{13}C$-NMR signals, [c] Interchangeable, [d] Weak, [n.d] not determined

Table S2A. ^{1}H, ^{13}C, and ^{15}N-NMR data of nocathioamide A (**1**) (d_3-CH_3OH; 400/100/40.6 MHz; minor conformer)

Residue	Position	δC / δN	δH, mult (*J* in Hz)	Residue	Position	δC / δN	δH, mult (*J* in Hz)
Ac	1	173.07, C	--------	**Dha**	1	166.70, C	--------
	2	22.64, CH_3	2.02, s		2	138.33, C	--------
Ala-1 *	1	48.89 [b], CH	5.30, p (7.0)		3	111.63, CH_2	5.35, brs
	2	20.94, CH_3	1.60, d (7.0)		-NH-	127.35	10.05, brs
	-NH-	132.3	8.81, d (7.4)	**Leu**	1	174.00, C	--------
Thz	1	163.68, C	--------		2	50.94, CH	4.86 [b]
	2	149.73, C	--------		3	41.66, CH_2	1.45, m + 1.82, m
	3	126.43, CH	8.16, s		4	26.19, CH	1.70, m
	4	176.64, C	--------		5	22.17, CH_3	0.91, d (6.5)
	=N-	305.80	--------		6	23.75, CH_3	0.97, d (6.5)
His *	1	208.21 [d], C	--------		-NH-	120.58	8.68 [a]
	2	60.94, CH	5.23, m	**Pro**	1	174.85, C	--------
	3	30.89; CH_2	3.43, m + 3.54, m		2	62.89, CH	4.67, m
	4	131.22, C	--------		3	33.15, CH_2	2.27, m + 2.36, m
	5	118.95, CH	7.40, s		4	22.93, CH_2	1.84, m + 2.05, m
	=N-	189.63	--------		5	47.98, CH_2	3.63, m
	6	135.57, CH	8.67, s		=N-	129.27	--------
	=NH	175.21	--------	**AlaS-10**	1	172.84/172.59 [c], C	--------
	-NH-	123.78	8.94, d (5.1)		2	59.21, CH	4.26, brs
Abu	1	170.70, C	--------		3	35.43/35.52 [c], CH_2	3.13, m + 3.69, m
	2	65.62, CH	5.48, brs		-NH-	117.55	7.23, very brs
	3	44.77, CH	3.96, m	**AlaS-11**	1	171.77, C	--------
	4	20.24, CH_3	1.12, d (7.1)		2	53.60, CH	4.51 [a], m
	-NH-	155.59	9.77, brs		3	35.52/35.43 [c], CH_2	3.11, m + 3.35, m
4-Meglu	1	172.63 [a], C	--------		-NH-	114.99	8.02, brs
	2	53.41, CH	4.63, m	**Ala-12**	1	174.94, C	--------
	3	35.70, CH_2	1.48, m + 2.18, m		2	50.94, CH	4.15, m
	4	36.75, CH	2.44, m		3	18.17, CH_3	1.30, d (5.7)
	5	179.54, C	--------		-NH-	119.70	7.56, brs
	6	18.65, CH_3	0.83, brs	**Asn**	1	179.00, C	--------
	-NH-	120.30	8.09, brs		2	51.56, CH	4.54, m
AlaS-6	1	169.62, C	--------		3	37.26, CH_2	2.64, dd (18.0, 5.6) + 2.99, dd (18.0, 9.3)
	2	55.49, CH	4.51 [a], m		4	178.27, C	--------
	3	34.18, CH_2	3.05, m + 3.29, m		-NH-	110.93	8.44, d (7.3)
	-NH-	114.08	7.66, very brs		-CONHCO-	172.80 [d]	10.94, very brs

[*] AA with modified CO within the backbone**,** [a] Overlapped, [b] Masked by water/solvent $^{1}H/^{13}C$-NMR signals, [c] Interchangeable, [d] Weak, [n.d] not determined

Table S3. ^{1}H, ^{13}C, and ^{15}N-NMR data of nocathioamide A (**1**) (d_3-CH_3OH; 700/176/71 MHz; major conformer)

Residue	Position	δC / δN	δH, mult (*J* in Hz)	Residue	Position	δC / δN	δH, mult (*J* in Hz)
Ac	1	173.14, C	--------	**Dha**	1	166.80, C	--------
	2	22.65, CH_3	2.03, s		2	138.09, C	--------
Ala-1 *	1	48.97 [b], CH	5.26 [a], m		3	111.61, CH_2	5.42 + 5.49, brs
	2	20.96, CH_3	1.59, d		-NH-	129.08	10.22, brs
	-NH-	132.3	8.84, d (7.4)	**Leu**	1	174.15, C	--------
Thz	1	163.87, C	--------		2	57.86, CH	4.31, m
	2	149.85, C	--------		3	38.43, CH_2	1.62, m + 1.87, m
	3	126.40, CH	8.14, s		4	26.36, CH	1.78, m
	4	176.87, C	--------		5	22.15, CH_3	0.93, d (6.5)
	=N-	305.8	--------		6	23.18, CH_3	1.00, d (6.5)
His *	1	207.30 [d], C	--------		-NH-	135.70	9.04 [a]
	2	61.30, CH	5.07 [b]	**Pro**	1	n.d	--------
	3	30.72, CH_2	3.41, m + 3.61, m		2	64.90, CH	4.34, t (8.1)
	4	131.56, C	--------		3	30.40, CH_2	2.06, m + 2.35, m
	5	118.68, CH	7.29, s		4	27.09, CH_2	1.97, m + 2.13, m
	=N-	191.86	--------		5	48.95 [b], CH_2	3.73, m + 3.86, m
	6	135.52, CH	8.62, s		=N-	130.18	--------
	=NH	174.32	--------	**AlaS-10**	1	n.d	--------
	-NH-	122.62	9.03, d (5.0)		2	56.13, CH	4.96, m
Abu	1	171.33, C	--------		3	38.81, CH_2	3.15, m + 3.58, m
	2	65.62 [a], CH	5.35 [a]		-NH-	106.32	6.68, brs
	3	45.19, CH	3.89, m	**AlaS-11**	1	n.d	n.d
	4	20.65, CH_3	1.09, d (7.1)		2	n.d	n.d
	-NH-	154.69	9.45, brs		3	n.d	n.d
4-Meglu	1	172.58/172.84 [c], C	--------		-NH-	n.d	n.d
	2	53.41 & 54.05, CH	4.62 [a] & 4.47 [b] , m	**Ala-12**	1	175.12, C	--------
	3	35.70 [a], CH_2	1.45 + 2.17, m & 1.54 + 2.19, m		2	51.27, CH	4.31, m
	4	36.75 [a], CH	2.43 [a] & 2.47 [a]		3	17.69, CH_3	1.42, d (7.2)
	5	n.d	--------		-NH-	120.38	7.91, d (6.4)
	6	18.65, CH_3	0.74, d (7.2) & 0.82 [a]	**Asn**	1	178.95, C	--------
	-NH-	119.70	7.97 [a] & 7.99 [a]		2	51.42, CH	4.60, m
AlaS-6	1	169.78, C	--------		3	37.33, CH_2	2.61 [a] + 2.77 [a], dd
	2	55.82, CH	4.64, m		4	178.26, C	--------
	3	34.35, CH_2	2.91 + 3.18, m		-NH-	111.15	8.32, d (7.8)
	-NH-	113.90	7.32, brs		-CONHCO-	n.d	n.d

[*] AA with modified CO within the backbone**,** [a] Overlapped, [b] Masked by water/solvent $^{1}H/^{13}C$-NMR signals, [c] Interchangeable, [d] Weak, [n.d] not determined

Table S3A. ^{1}H, ^{13}C, and ^{15}N-NMR data of nocathioamide A (**1**) (d_3-CH_3OH; 700/176/71 MHz; minor conformer)

Residue	Position	δC / δN	δH, mult (*J* in Hz)	Residue	Position	δC / δN	δH, mult (*J* in Hz)
Ac	1	173.15, C	--------	**Dha**	1	166.76, C	--------
	2	22.70, CH_3	2.02, s		2	138.21, C	--------
Ala-1 *	1	48.97 [b], CH	5.31, m (7.0)		3	108.13, CH_2	5.37, brs
	2	21.04, CH_3	1.61, d (7.0)		-NH-	--------	--------
	-NH-	--------	--------	**Leu**	1	174.19, C	--------
Thz	1	163.84, C	--------		2	51.11, CH	4.87, m
	2	149.79, C	--------		3	41.71, CH_2	1.47, m + 1.84, m
	3	126.66, CH	8.16, s		4	26.34, CH	1.72, m
	4	177.08, C	--------		5	22.30, CH_3	0.92, d (6.2)
	=N-	--------	--------		6	23.86, CH_3	0.98, d (6.5)
His *	1	207.99 [d], C	--------		-NH-	--------	--------
	2	60.71, CH	5.25, t (7.5)	**Pro**	1	174.83, C	--------
	3	30.52, CH_2	3.47, dd (14.7, 7.5) + 3.59, dd (14.7, 7.5)		2	63.01, CH	4.69, m
	4	130.69, C	--------		3	33.23, CH_2	2.28, m + 2.37, m
	5	119.05, CH	7.48, s		4	23.06, CH_2	1.87, m + 2.08, m
	=N-	--------	--------		5	48.13, CH_2	3.66, m
	6	135.23, CH	8.86, s		=N-	--------	--------
	=NH	--------	--------	**AlaS-10**	1	172.93/172.64 [c], C	--------
	-NH-	--------	--------		2	65.74, CH	5.48, brs
Abu	1	170.68, C	--------		3	44.76, CH_2	3.98, m
	2	65.74, CH	5.48, brs		-NH-	--------	--------
	3	44.76, CH	3.98, m	**AlaS-11**	1	171.82, C	--------
	4	20.24, CH_3	1.15, d (6.8)		2	53.37, CH	4.52 [a]
	-NH-	--------	--------		3	35.49/35.67 [c], CH_2	3.12 [a] + 3.36 [a]
4-Meglu	1	172.64 [a], C	--------		-NH-	--------	--------
	2	53.37, CH	4.65, m	**Ala-12**	1	174.99, C	--------
	3	35.79, CH_2	1.47, m + 2.19, m		2	50.92, CH	4.17 [a]
	4	36.79, CH	2.46, m		3	18.25, CH_3	1.31, d (6.9)
	5	179.48, C	--------		-NH-	--------	--------
	6	18.73, CH_3	0.85 [a]	**Asn**	1	178.99, C	--------
	-NH-	--------	--------		2	51.58, CH	4.56 [a]
AlaS-16	1	169.70, C	--------		3	37.34, CH_2	2.65, dd (17.7, 5.5) + 3.00, dd (17.7, 9.3)
	2	55.53, CH	4.53 [a]		4	178.28, C	--------
	3	34.32, CH_2	3.06 [a] + 3.32 [a]		-NH-	--------	--------
	-NH-	--------	--------		-CONHCO-	--------	--------

[*] AA with modified CO within the backbone**,** [a] Overlapped, [b] Masked by water/solvent $^1H/^{13}C$-NMR signals, [c] Interchangeable, [d] Weak, [n.d] not determined

Table S4. ^1H, and ^{13}C-NMR data of nocathioamide A (**1**) (d_4-CH_3OH; 400/100 MHz; major conformer)

Residue	Position	δC / δN	δH, mult (*J* in Hz)	Residue	Position	δC / δN	δH, mult (*J* in Hz)
Ac	1	173.23, C	--------	**Dha**	1	166.76, C	--------
	2	22.73, CH_3	2.04, s		2	138.04, C	--------
Ala-1 *	1	49.00 [b], CH	5.25 [a], m		3	111.63, CH_2	5.42 [a] + 5.49 [a]
	2	21.02 [a], CH_3	1.61, d (7.0)		-NH-	--------	--------
	-NH-	--------	--------	**Leu**	1	174.28, C	--------
Thz	1	163.99, C	--------		2	57.83, CH	4.32, m
	2	149.93, C	--------		3	38.50, CH_2	1.62, m + 1.90, m
	3	126.60, CH	8.14, s		4	26.50, CH	1.79, m
	4	177.08, C	--------		5	22.26, CH_3	0.93 [a]
	=N-	--------	--------		6	23.30, CH_3	1.01, d (6.5)
His *	1	206.90 [d], C	--------		-NH-	--------	--------
	2	60.91, CH	5.09, t (7.5)	**Pro**	1	n.d	--------
	3	30.32, CH_2	n.d + 3.68 [a]		2	65.00, CH	4.36 [a]
	4	130.92, C	--------		3	30.53 [a], CH_2	2.08 [a] + 2.36 [a]
	5	118.88, CH	7.37, s		4	27.21, CH_2	1.99 [a] + 2.14 [a]
	=N-	--------	--------		5	49.00, CH_2	3.72 [a] + 3.88 [a]
	6	135.17; CH	8.82, s		=N-	--------	--------
	=NH	--------	--------	**AlaS-10**	1	n.d	--------
	-NH-	--------	--------		2	56.20, CH	4.97 [b]
Abu	1	171.40, C	--------		3	38.97, CH_2	3.16 [a] + 3.61 [a]
	2	65.74 [a], CH	5.37, brs		-NH-	--------	--------
	3	45.40, CH	3.92, m	**AlaS-11**	1	n.d	n.d
	4	n.d	1.14 [a]		2	n.d	n.d
	-NH-	--------	--------		3	n.d	n.d
4-Meglu	1	n.d	--------		-NH-	--------	--------
	2	n.d	4.62 [a]	**Ala-12**	1	175.18, C	--------
	3	35.79 [a], CH_2	1.44 [a] + 2.18 [a]		2	51.29, CH	4.32 a
	4	36.79 [a], CH	2.43, m		3	17.79, CH_3	1.43, d (7.0)
	5	n.d	--------		-NH-	--------	--------
	6	18.62, CH_3	0.74, d (7.2)	**Asn**	1	178.93, C	--------
	-NH-	--------	--------		2	51.42, CH	4.62 [a]
AlaS-6	1	n.d	--------		3	37.41, CH_2	2.62 [a], m+ 2.96 [a], m
	2	55.82, CH	4.60, m		4	n.d	--------
	3	n.d	n.d		-NH-	--------	--------
	-NH-	--------	--------		-CONHCO-	--------	--------

[*] AA with modified CO within the backbone**,** [a] Overlapped, [b] Masked by water/solvent $^{1}H/^{13}C$-NMR signals, [c] Interchangeable, [d] Weak, [n.d] not determined

Table S4A. ^{1}H, and ^{13}C-NMR data of nocathioamide A (**1**) (d_4-CH_3OH; 400/100 MHz; minor conformer)

Residue	Position	δC / δN	δH, mult (*J* in Hz)	Residue	Position	δC / δN	δH, mult (*J* in Hz)
Ac	1	173.15, C	--------	**Dha**	1	166.44, C	--------
	2	22.59, CH_3	2.01, s		2	138.79, C	--------
Ala-1 *	1	48.97 [b], CH	5.30, m		3	109.33, CH_2	5.25 + 5.32, brs
	2	20.95, CH_3	1.60, d (7.0)		-NH-	--------	10.20, s
	-NH-	**--------**	8.81, d (7.7)	**Leu**	1	173.77, C	--------
Thz	1	163.87, C	--------		2	50.63, CH	4.84 [a]
	2	149.77, C	--------		3	42.12, CH_2	1.44, m + 1.80, m
	3	126.38, CH	8.17, s		4	26.12, CH	1.66, m
	4	176.81, C	--------		5	21.97, CH_3	0.91, d (6.5)
	=N-	--------	--------		6	23.70, CH_3	0.96, d (6.6)
His *	1	208.53 [d], C	--------		-NH-	--------	8.59, d (7.7)
	2	61.00, CH	5.16 [b]	**Pro**	1	175.10, C	--------
	3	30.49, CH_2	3.46, m + 3.55, m		2	62.90, CH	4.57 [a]
	4	130.87, C	--------		3	33.16, CH_2	2.33, m
	5	119.04, CH	7.44, s		4	23.04, CH_2	1.83, m + 2.05, m
	=N-	--------	--------		5	48.16, CH_2	3.62, m
	6	135.44, CH	8.79, s		=N-	--------	--------
	=NH	--------	--------	**AlaS-10**	1	172.14, C	--------
	-NH-	--------	9.00, d (5.5)		2	58.82, CH	4.23, m
Abu	1	170.55, C	--------		3	34.68, CH_2	3.09, m + 3.48, m
	2	65.73, CH	5.56, brs		-NH-	--------	7.07, brs
	3	44.66, CH	3.97, m	**AlaSO-11**	1	171.06, C	--------
	4	20.08, CH_3	1.13, d (6.97)		2	49.47, CH	5.13 [b]
	-NH-	--------	9.87, brs		3	59.74, CH_2	3.44, m + 3.68, m
4-Meglu	1	172.70, C	--------		-NH-	--------	7.90 [a]
	2	53.36, CH	4.67 [b]	**Ala-12**	1	175.22, C	--------
	3	35.52, CH_2	1.51, m + 2.21, m		2	51.27, CH	4.14, m
	4	36.75, CH	2.39, m		3	18.14, CH_3	1.37, d (7.1)
	5	179.60, C	--------		-NH-	--------	7.48, d (5.8)
	6	18.50, CH_3	0.80, d (7.0)	**Asn**	1	179.04, C	--------
	-NH-	--------	7.94 [a]		2	51.58, CH	4.52, m
AlaSO-6	1	167.62, C	--------		3	37.20, CH_2	2.64, dd (17.8, 5.5) + 2.97, dd (17.8, 9.4)
	2	51.52, CH	4.70 [a]		4	178.24, C	--------
	3	55.52, CH_2	3.35, m + 3.83, m		-NH-	--------	8.58, d (7.9)
	-NH-	--------	8.09 [a], brs		-CONHCO-	--------	11.00, brs

[*] AA with modified CO within the backbone**,** [a] Overlapped, [b] Masked by water/solvent $^1H/^{13}C$-NMR signals, [c] Interchangeable, [d] Weak, [nd] not determined

Table S5. ^1H, and ^{13}C-NMR data of nocathioamide B (**2**) (d_3-CH_3OH; 400/100 MHz; major conformer)

Residue	Position	δC / δN	δH, mult (*J* in Hz)	Residue	Position	δC / δN	δH, mult (*J* in Hz)
Ac	1	nd	--------	**Dha**	1	nd	--------
	2	22.62, CH_3	2.03, s		2	nd	--------
Ala-1 *	1	49.03 [b], CH	5.26 [a]		3	nd	nd
	2	20.92, CH_3	1.60 [a]		-NH-	--------	nd
	-NH-	--------	8.84 [a]	**Leu**	1	nd	--------
Thz	1	nd	--------		2	nd	4.48 [b]
	2	149.84, C	--------		3	nd	nd
	3	126.00, CH	8.13, s		4	26.33, CH	1.75 [a]
	4	176.85, C	--------		5	nd	0.93 d (6.6)
	=N-	--------	--------		6	nd	0.99, d (6.6)
His *	1	nd	--------		-NH-	--------	nd
	2	nd	nd	**Pro**	1	nd	--------
	3	30.16, CH_2	3.46, [a] + 3.55, [a]		2	64.74, CH	4.32, m
	4	131.12, C	--------		3	30.15, CH_2	1.99, m + 2.35, m
	5	118.84, CH	7.34, s		4	26.90, CH_2	2.00, m + 2.13, m
	=N-	--------	--------		5	49.10, CH_2	3.69, m + 3.86, m
	6	135.32, CH	8.75, s		=N-	--------	--------
	=NH	--------	--------	**AlaS-10**	1	nd	--------
	-NH-	--------	nd		2	nd	nd
Abu	1	nd	--------		3	nd	nd
	2	nd	nd		-NH-	--------	nd
	3	nd	nd	**AlaSO-11**	1	nd	--------
	4	nd	nd		2	nd	nd
	-NH-	--------	9.62, brs		3	nd	nd
4-Meglu	1	nd	--------		-NH-	--------	nd
	2	nd	nd	**Ala-12**	1	175.33, C	--------
	3	nd	nd		2	51.36, CH	4.33, m
	4	nd	nd		3	17.65, CH_3	1.45, d (7.0)
	5	nd	--------		-NH-	--------	8.14 [a]
	6	nd	nd	**Asn**	1	179.11, C	--------
	-NH-	--------	nd		2	51.41, CH	4.57, m
AlaSO-6	1	nd	--------		3	37.20 [a], CH_2	2.64 [a], m + 2.97 [a], m
	2	nd	nd		4	nd	--------
	3	nd	nd		-NH-	--------	8.43, d (6.8)
	-NH-	-------	nd		-CONHCO-	--------	nd

[*] AA with modified CO within the backbone**,** [a] Overlapped, [b] Masked by water/solvent $^{1}H/^{13}C$-NMR signals, [c] Interchangeable, [d] Weak, [nd] not determined

Table S5A. ^{1}H, and ^{13}C-NMR data of nocathioamide B (**2**) (d_3-CH_3OH; 400/100 MHz; minor conformer)

Residue	Position	δC / δN	δH, mult (*J* in Hz)	Residue	Position	δC / δN	δH, mult (*J* in Hz)
Ac	1	173.15, C	--------	**Dha**	1	166.41, C	--------
	2	22.60, CH_3	2.01, s		2	138.82, C	--------
Ala-1 *	1	48.94 [b], CH	5.31, m		3	109.30, CH_2	5.24 + 5.32, brs
	2	20.88, CH_3	1.60, d (6.9)		-NH-	--------	10.25, s
	-NH-	**--------**	8.83, d (7.4)	**Leu**	1	173.71, C	--------
Thz	1	163.81, C	--------		2	50.57, CH	4.85 [b]
	2	149.76, C	--------		3	42.15; CH_2	1.43, m + 1.80, m
	3	126.31, CH	8.16, s		4	26.10, CH	1.65, m
	4	176.67, C	--------		5	21.97, CH_3	0.91, d (6.5)
	=N-	--------	--------		6	23.70, CH_3	0.96, d (6.5)
His *	1	208.75 [d], C	--------		-NH-	--------	8.62 [a]
	2	61.29, CH	5.15 [b]	**Pro**	1	175.12, C	--------
	3	30.97, CH_2	3.44, m + 3.54, m		2	62.89, CH	4.57, m
	4	131.60, C	--------		3	33.23, CH_2	2.32, m
	5	118.87, CH	7.37, s		4	23.04, CH_2	1.82, m + 2.05, m
	=N-	--------	--------		5	48.17, CH_2	3.60, m
	6	135.81, CH	8.62, s		=N-	--------	--------
	=NH	--------	--------	**AlaS-10**	1	172.16, C	--------
	-NH-	--------	8.94, d (5.1)		2	59.03, CH	4.23, m
Abu	1	170.67, C	--------		3	34.59, CH_2	3.08, m + 3.47, m
	2	65.62, CH	5.57, brs		-NH-	--------	7.15, brs
	3	44.68, CH	3.97, m	**AlaSO-11**	1	171.07, C	--------
	4	20.04, CH_3	1.11, d (6.4)		2	49.46, CH	5.14/5.15 [a], m
	-NH-	--------	9.80, very brs		3	59.73, CH_2	3.44, m + 3.70, m
4-Meglu	1	172.73, C	--------		-NH-	--------	7.90, d (9.0)
	2	53.44, CH	4.68, m	**Ala-12**	1	175.20, C	--------
	3	35.56, CH_2	1.52, m + 2.21, m		2	51.30, CH	4.13, p (6.7)
	4	36.84, CH	2.41, m		3	18.13, CH_3	1.38, d (7.1)
	5	179.72, C	--------		-NH-	--------	7.46, d (4.7)
	6	18.54, CH_3	0.80, d (6.9)	**Asn**	1	179.06, C	--------
	-NH-	--------	8.01, d (7.6)		2	51.57, CH	4.53, m
AlaSO-6	1	167.61, C	--------		3	37.19, CH_2	2.64, dd (17.8, 5.5) + 2.97, dd (17.8, 9.5)
	2	51.52/51.50 [c]	4.71 [b]		4	178.25, C	--------
	3	55.52	3.36, m + 3.82, m		-NH-	--------	8.60 [a]
	-NH-	--------	8.10, brs		-CONHCO-	--------	11.00, very brs

[*] AA with modified CO within the backbone**,** [a] Overlapped, [b] Masked by water/solvent $^1H/^{13}C$-NMR signals, [c] Interchangeable, [d] Weak, [nd] not determined

Table S6. ^1H, and ^{13}C-NMR data of nocathioamide B (**2**) (d_3-CH_3OH; 700/176 MHz; major conformer)

Residue	Position	δC / δN	δH, mult (*J* in Hz)	Residue	Position	δC / δN	δH, mult (*J* in Hz)
Ac	1	173.20, C	--------	**Dha**	1	nd	--------
	2	22.62, CH_3	2.03, s		2	137.71, C	--------
Ala-1 *	1	49.05 [b], CH	5.27 [a]		3	nd	nd
	2	20.92, CH_3	1.59 [a]		-NH-	--------	nd
	-NH-	--------	8.85, d (7.2)	**Leu**	1	nd	--------
Thz	1	nd	--------		2	nd	4.44 [b]
	2	149.86, C	--------		3	nd	nd
	3	126.16, CH	8.14, s		4	26.33, CH	1.75 [a]
	4	176.77, C	--------		5	nd	0.94, d (6.4)
	=N-	--------	--------		6	nd	0.99, d (6.4)
His *	1	nd	--------		-NH-	--------	nd
	2	61.21, CH	5.15 [b]	**Pro**	1	nd	--------
	3	30.75, CH_2	3.44, [a] + 3.54, [a]		2	64.81, CH	4.32, m
	4	131.75, C	--------		3	30.13, CH_2	1.96, m + 2.35, m
	5	118.64, CH	7.28, s		4	26.96, CH_2	1.99, m+ 2.14, m
	=N-	--------	--------		5	49.14, CH_2	3.68, m + 3.86, m
	6	135.56, CH	8.60, s		=N-	--------	--------
	=NH	--------	--------	**AlaS-10**	1	nd	--------
	-NH-	--------	--------		2	nd	nd
Abu	1	nd	--------		3	nd	nd
	2	nd	nd		-NH-	--------	nd
	3	nd	nd	**AlaSO-11**	1	nd	--------
	4	nd	nd		2	nd	nd
	-NH-	--------	9.55, very brs		3	nd	nd
4-Meglu	1	nd	--------		-NH-	--------	nd
	2	nd	nd	**Ala-12**	1	175.40, C	--------
	3	nd	nd		2	51.35, CH	4.32, m
	4	nd	nd		3	17.64, CH_3	1.45, d (7.1)
	5	nd	--------		-NH-	--------	8.18 [a]
	6	18.63, CH_3	nd	**Asn**	1	179.13, C	--------
	-NH-	--------	nd		2	51.50/51.52 [c], CH	4.57, m
AlaSO-6	1	nd	--------		3	37.24, CH_2	2.64 [a] + 2.97 [a]
	2	nd	nd		4	nd	--------
	3	nd	nd		-NH-	--------	8.45, brs
	-NH-	-------	nd		-CONHCO-	--------	n.d

[*] AA with modified CO within the backbone**,** [a] Overlapped, [b] Masked by water/solvent $^{1}H/^{13}C$-NMR signals, [c] Interchangeable, [d] Weak, [nd] not determined

Table S6A. ^{1}H, and ^{13}C-NMR data of nocathioamide B (**2**) (d_3-CH_3OH; 700/176 MHz; minor conformer)

Residue	Position	δC / δN	δH, mult (*J* in Hz)	Residue	Position	δC / δN	δH, mult (*J* in Hz)
Ac	1	173.21, C	--------	**Dha**	1	166.48, C	--------
	2	22.67, CH_3	2.02, s		2	138.74, C	--------
Ala-1 *	1	49.09 [b], CH	5.31, m		3	109.46, CH_2	5.26 + 5.33, brs
	2	21.05, CH_3	1.61, d (7.1)		-NH-	--------	--------
	-NH-	--------	--------	**Leu**	1	173.88, C	--------
Thz	1	163.95, C	--------		2	50.69, CH	4.87 [b]
	2	149.87, C	--------		3	42.20, CH_2	1.45, m + 1.81, m
	3	126.55, CH	8.18, s		4	26.26, CH	1.67, m
	4	176.97, C	--------		5	22.10, CH_3	0.93, d (6.7)
	=N-	--------	--------		6	23.82, CH_3	0.97, d (6.7)
His *	1	208.43 [d], C	--------		-NH-	--------	--------
	2	60.90, CH	5.18, t (7.6)	**Pro**	1	175.14, C	--------
	3	30.45, CH_2	3.48, m + 3.58, m		2	63.01, CH	4.59, m
	4	130.75, C	--------		3	33.26, CH_2	2.34, m
	5	119.06, CH	7.47, s		4	23.17, CH_2	1.84, m + 2.06, m
	=N-	--------	--------		5	48.30, CH_2	3.64, m
	6	135.30, CH	8.86, s		=N-	--------	--------
	=NH	--------	--------	**AlaS-10**	1	172.15, C	--------
	-NH-	--------	--------		2	58.79, CH	3.10 dd (13.4, 4.2) + 3.50 [a]
Abu	1	170.59, C	--------		3	34.78, CH_2	4.24, dd (13.4, 4.0)
	2	65.85, CH	5.55, brs		-NH-	--------	--------
	3	44.77, CH	3.97, m	**AlaSO-11**	1	171.11, C	--------
	4	20.21, CH_3	1.13, d (7.0)		2	49.52, CH	5.14, m
	-NH-	--------	--------		3	59.84, CH_2	3.45, m + 3.68, m
4-Meglu	1	172.74, C	--------		-NH-	--------	--------
	2	53.34, CH	4.68, m	**Ala-12**	1	175.24, C	--------
	3	35.58, CH_2	1.52, m + 2.22, m		2	51.27, CH	4.16, m
	4	36.81, CH	2.40, m		3	18.21, CH_3	1.38, d (7.2)
	5	179.51, C	--------		-NH-	--------	--------
	6	18.60, CH_3	0.81, d (7.0)	**Asn**	1	179.02, C	--------
	-NH-	--------	--------		2	51.58, CH	4.52, dd (9.1, 5.7)
AlaSO-6	1	167.64, C	--------		3	37.28, CH_2	2.65, dd (17.8, 5.7) + 2.98, dd (17.8, 9.1)
	2	51.54, CH	4.71, m		4	178.23, C	--------
	3	55.63, CH_2	3.37, m + 3.83, m		-NH-	--------	--------
	-NH-	--------	--------		-CONHCO-	--------	--------

[*] AA with modified CO within the backbone**,** [a] Overlapped, [b] Masked by water/solvent $^{1}H/^{13}C$-NMR signals, [c] Interchangeable, [d] Weak, [nd] not determined

Table S7. ^{1}H, and ^{13}C-NMR data of nocathioamide B (**2**) (d_4-CH_3OH; 400/100 MHz; major conformer)

Residue	Position	δC / δN	δH, mult (*J* in Hz)	Residue	Position	δC / δN	δH, mult (*J* in Hz)
Ac	1	nd	--------	**Dha**	1	nd	--------
	2	21.01, CH_3	2.04, s		2	nd	--------
Ala-1 *	1	49.09 [b], CH	5.26 [a]		3	nd	nd
	2	21.05, CH_3	1.61 [a]		-NH-	-------	--------
	-NH-	--------	--------	**Leu**	1	nd	--------
Thz	1	nd	--------		2	nd	4.50
	2	149.95, C	--------		3	nd	nd
	3	126.38, CH	8.14, s		4	26.47, CH	1.77
	4	177.00, C	--------		5	nd	0.95 [a]
	=N-	--------	--------		6	nd	1.00, d (6.6)
His *	1	nd	--------		-NH-	-------	--------
	2	nd	5.15, m	**Pro**	1	n.d	--------
	3	30.30, CH_2	3.48 [a] + 3.58 [a]		2	64.87, CH	4.33, m
	4	131.03, C	--------		3	30.29, CH_2	2.00, m + 2.36, m
	5	118.88, CH	7.37, s		4	27.07, CH_2	2.00, m + 3.14, m
	=N-	--------	--------		5	49.28, CH_2	3.68, m + 3.88, m
	6	135.20, CH	8.81, s		=N-	-------	--------
	=NH	--------	--------	**AlaS-10**	1	nd	--------
	-NH-	--------	--------		2	nd	nd
Melan	1	nd	--------		3	nd	nd
	2	nd	nd		-NH-	-------	--------
	3	nd	nd	**AlaSO-11**	1	nd	--------
	4	nd	nd		2	nd	nd
	-NH-	--------	--------		3	nd	nd
4-Meglu	1	nd	--------		-NH-	-------	--------
	2	nd	nd	**Ala-12**	1	175.34, C	--------
	3	nd	nd		2	51.36, CH	4.33, m
	4	nd	nd		3	17.73, CH_3	1.46, d (7.0)
	5	nd	--------		-NH-	-------	--------
	6	nd	nd	**Asn**	1	179.10, C	--------
	-NH-	--------	--------		2	nd	4.57, m
AlaSO-6	1	nd	--------		3	37.32, CH_2	2.65 [a] + 2.98 [a]
	2	nd	nd		4	nd	--------
	3	nd	nd		-NH-	-------	--------
	-NH-	-------	--------		-CONHCO-	-------	--------

[*] AA with modified CO within the backbone**,** [a] Overlapped, [b] Masked by water/solvent $^{1}H/^{13}C$-NMR signals, [c] Interchangeable, [d] Weak, [nd] not determined

Table S7A. ^{1}H, and ^{13}C-NMR data of nocathioamide B (**2**) (d_4-CH_3OH; 400/100 MHz; minor conformer)

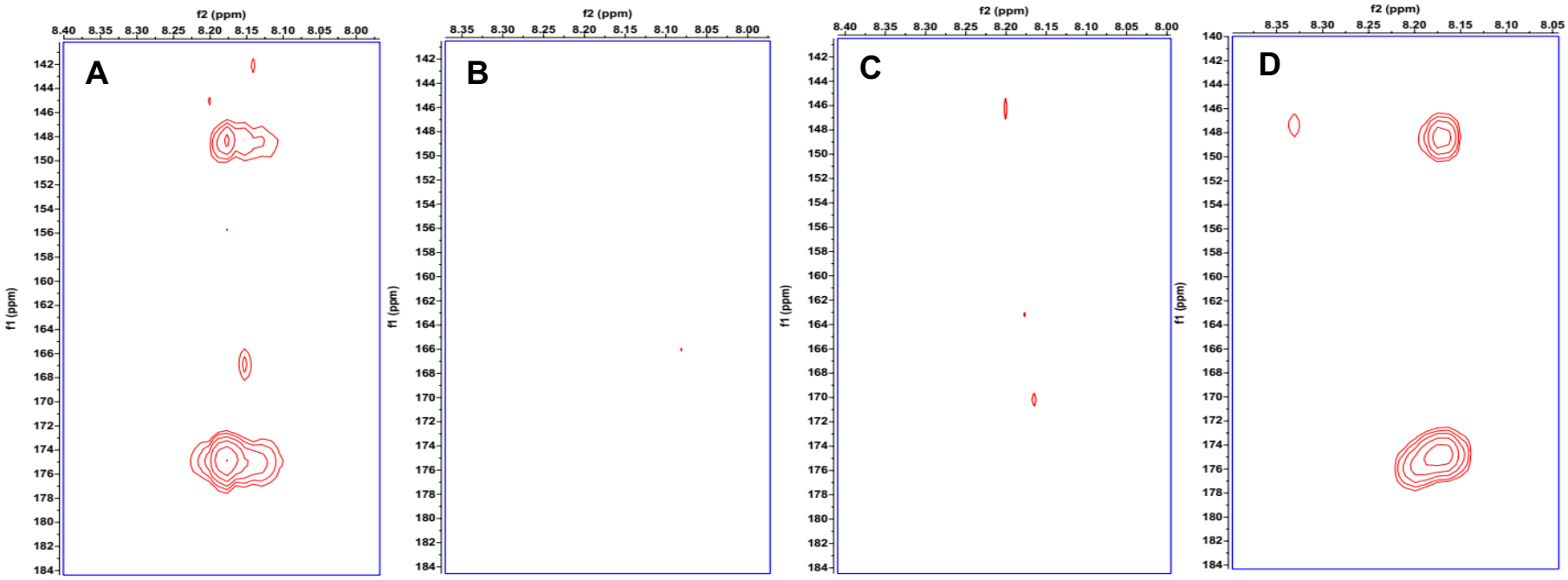

Figure S23. ^{1}H-^{13}C HMBC spectra of fractions 70% (panel A), 80% (panel B), 90% (panel C), and B LH20_70% (panel D) MeOH (d_4-CH_3OH, 400/100 MHz), respectively exhibiting cross correlations typical for oxazole and/or thiazole entities ($\delta_{H/C}$, 8.18/148.32 and $\delta_{H/C}$, 8.18/174.91 ppm). Only fraction 70% and the LH20_70% fractions show the correlations of interest, while these resonances are absent in the 80% and 90% fractions.

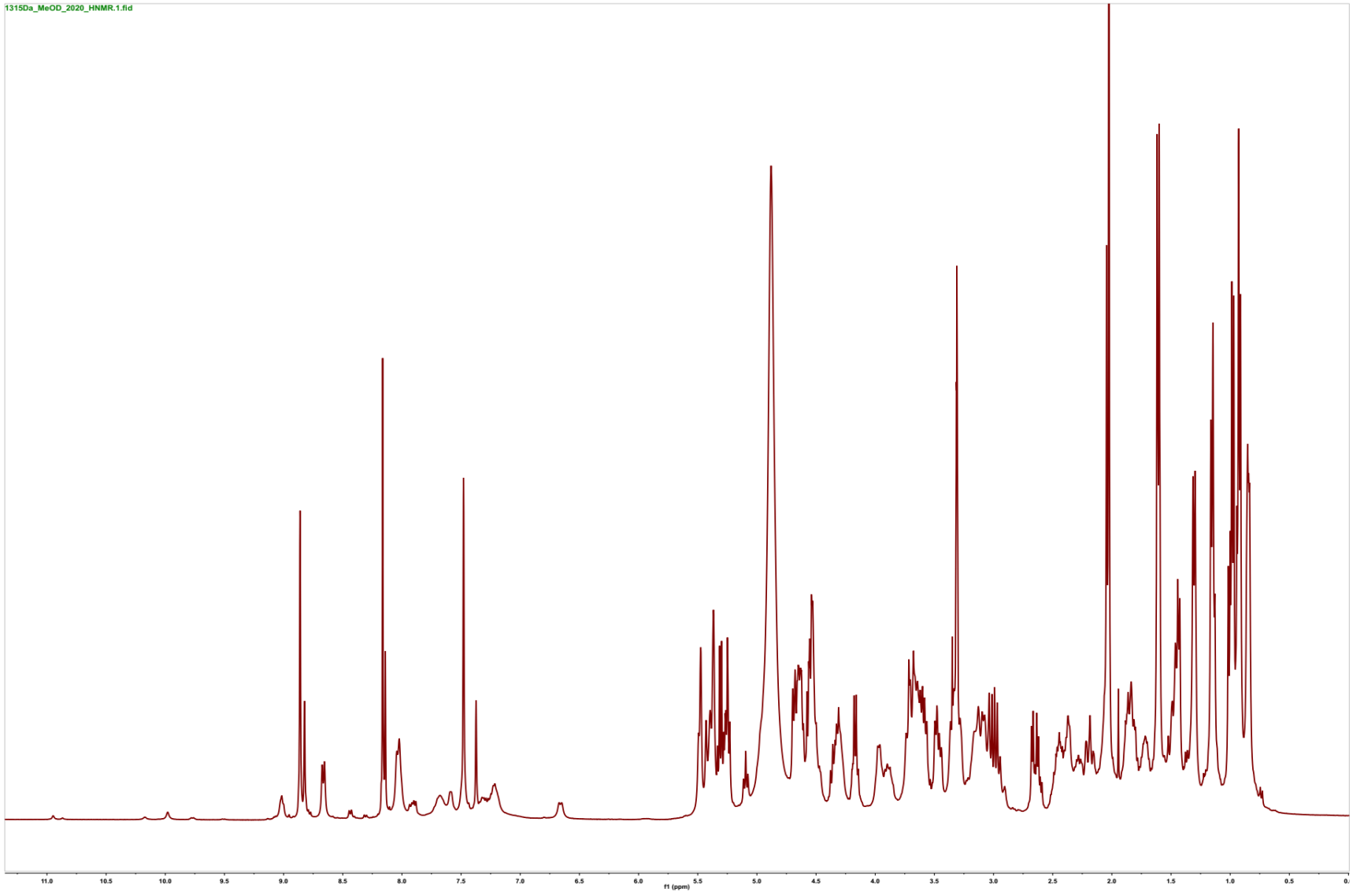

Figure S24. ^{1}H-NMR spectrum of nocathioamide A (**1**) (d_4-CH_3OH, 400 MHz)

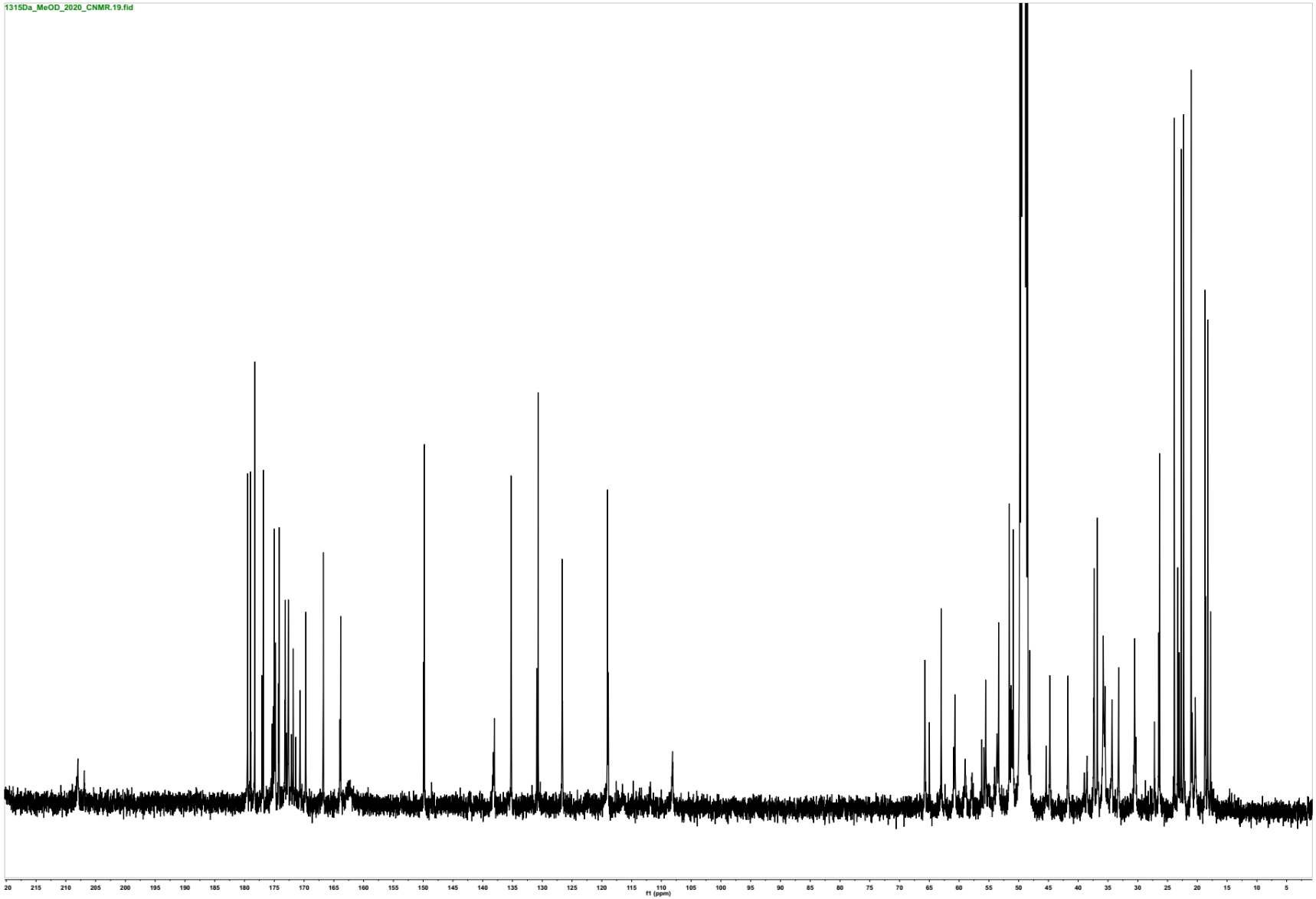

Figure S25. ^{13}C-NMR spectrum of nocathioamide A (**1**) (d_4-CH_3OH, 100 MHz)

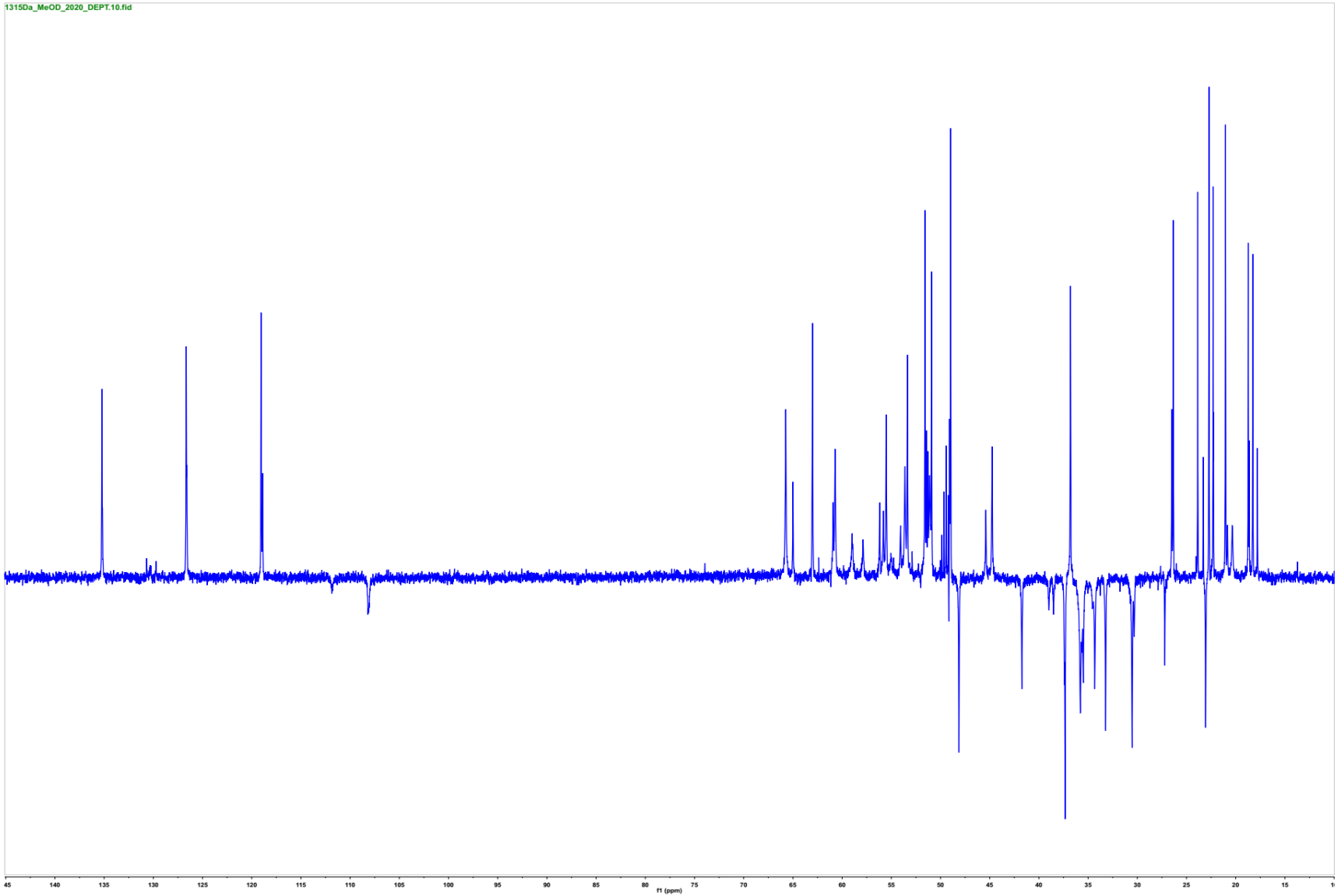

Figure S26. DEPT-135 spectrum of nocathioamide A (**1**) (d_4-CH_3OH, 100 MHz)

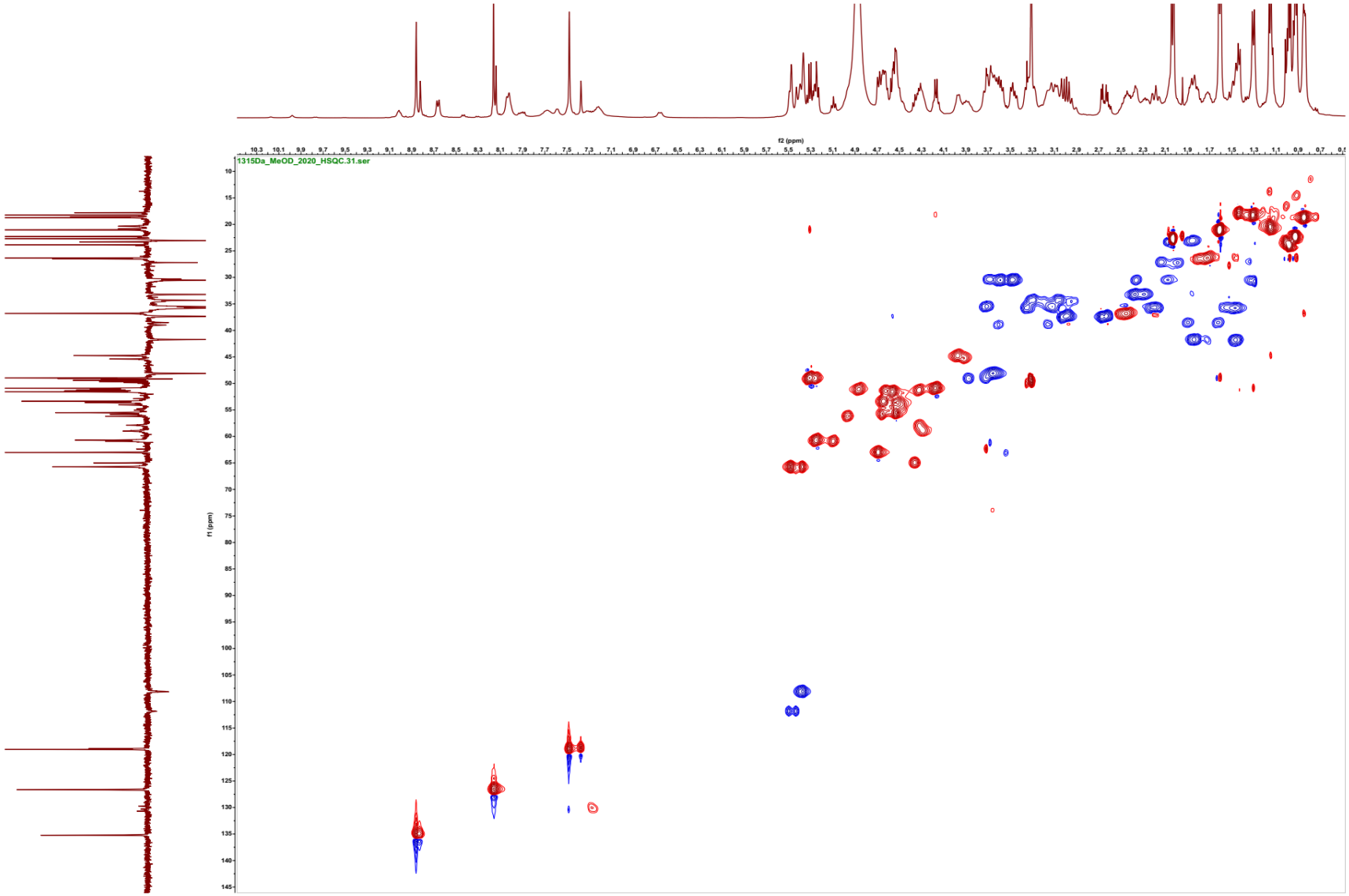

Figure S27. ^{1}H-^{13}C HSQC spectrum of nocathioamide A (**1**) (d_4-CH_3OH, 400/100 MHz)

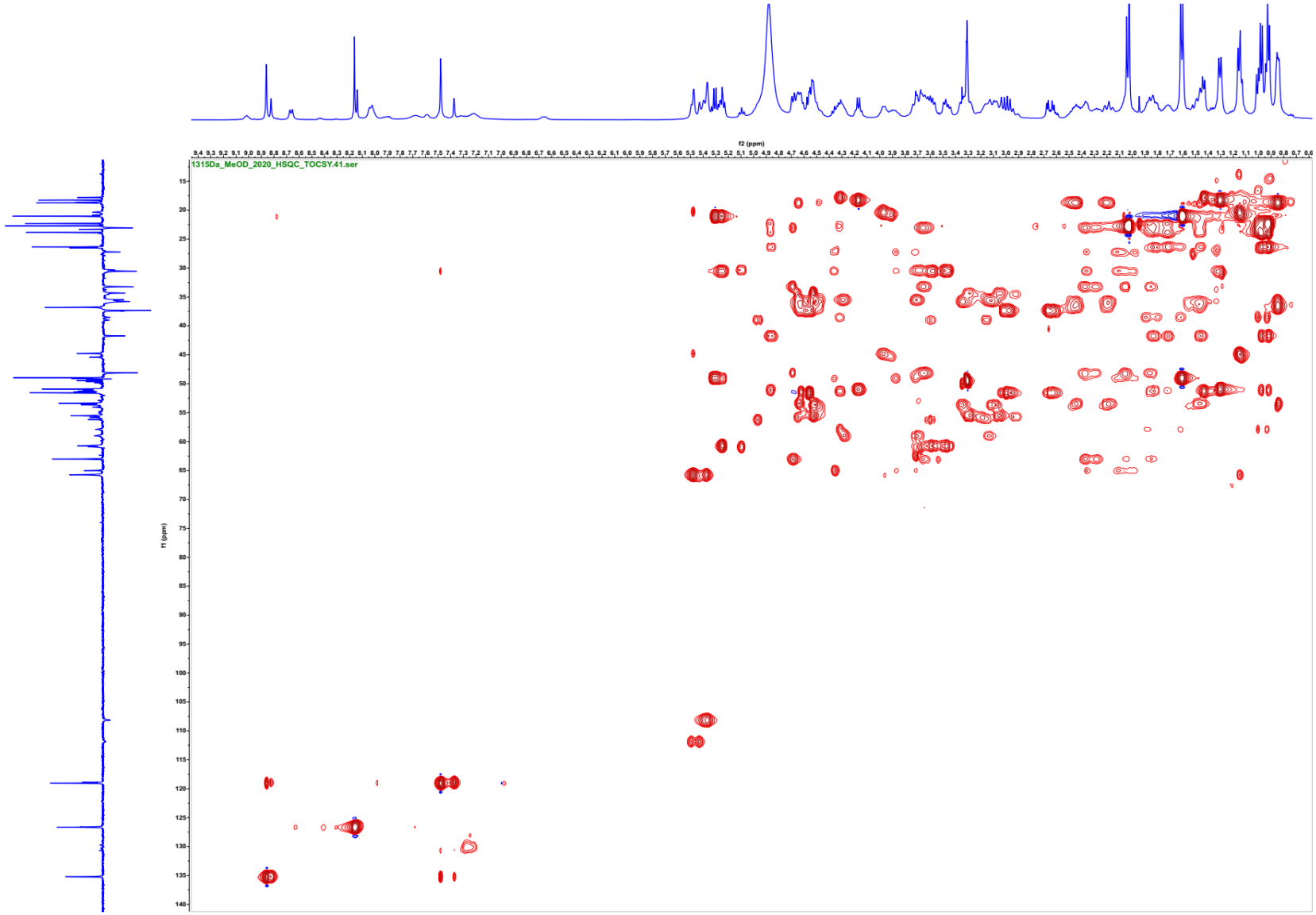

Figure S28. ^{1}H-^{13}C HSQC-TOCSY spectrum of nocathioamide A (**1**) (d_4-CH_3OH, 400/100 MHz)

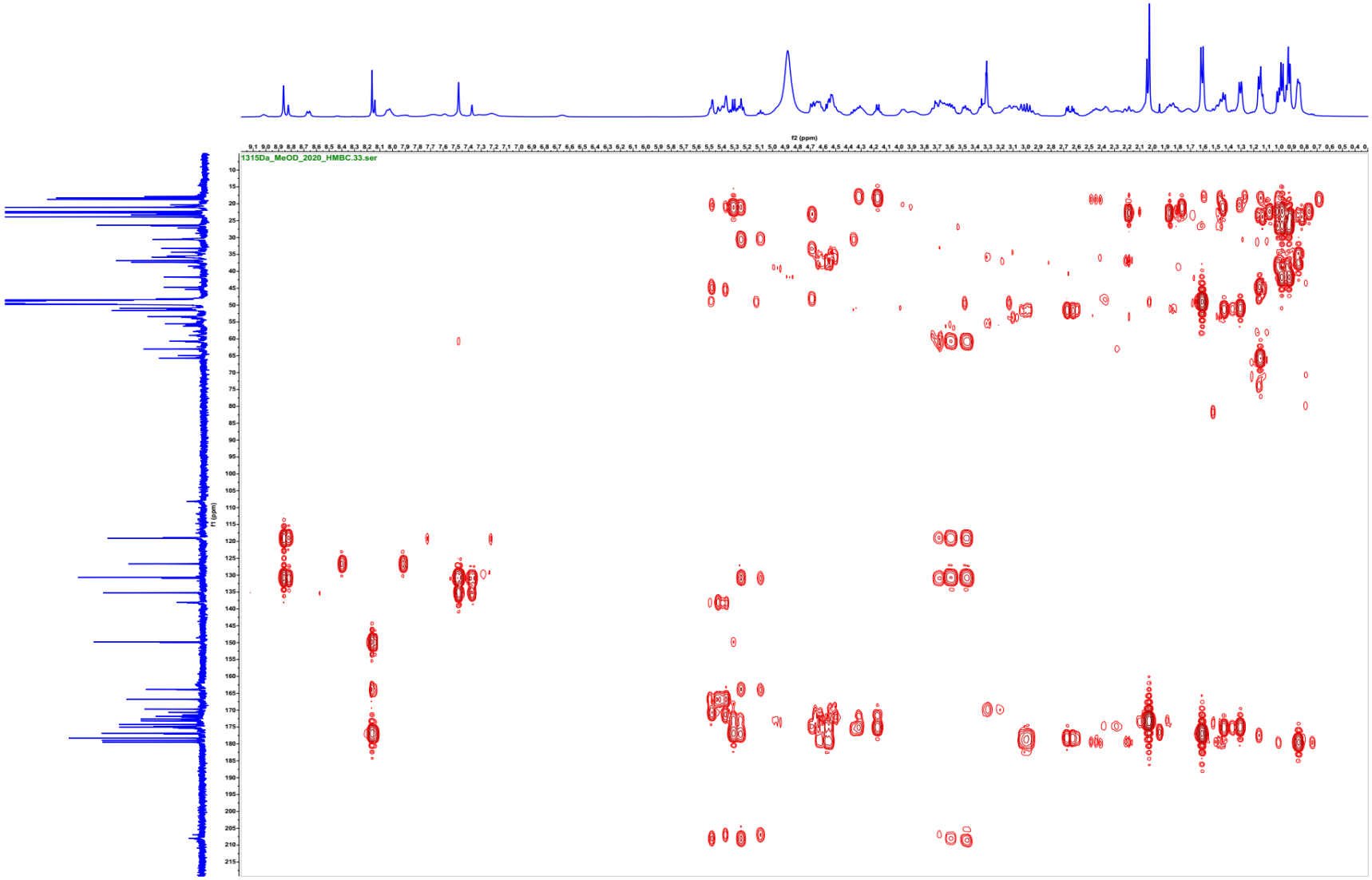

Figure S29. ^{1}H-^{13}C HMBC spectrum of nocathioamide A (**1**) (d_4-CH_3OH, 400/100 MHz)

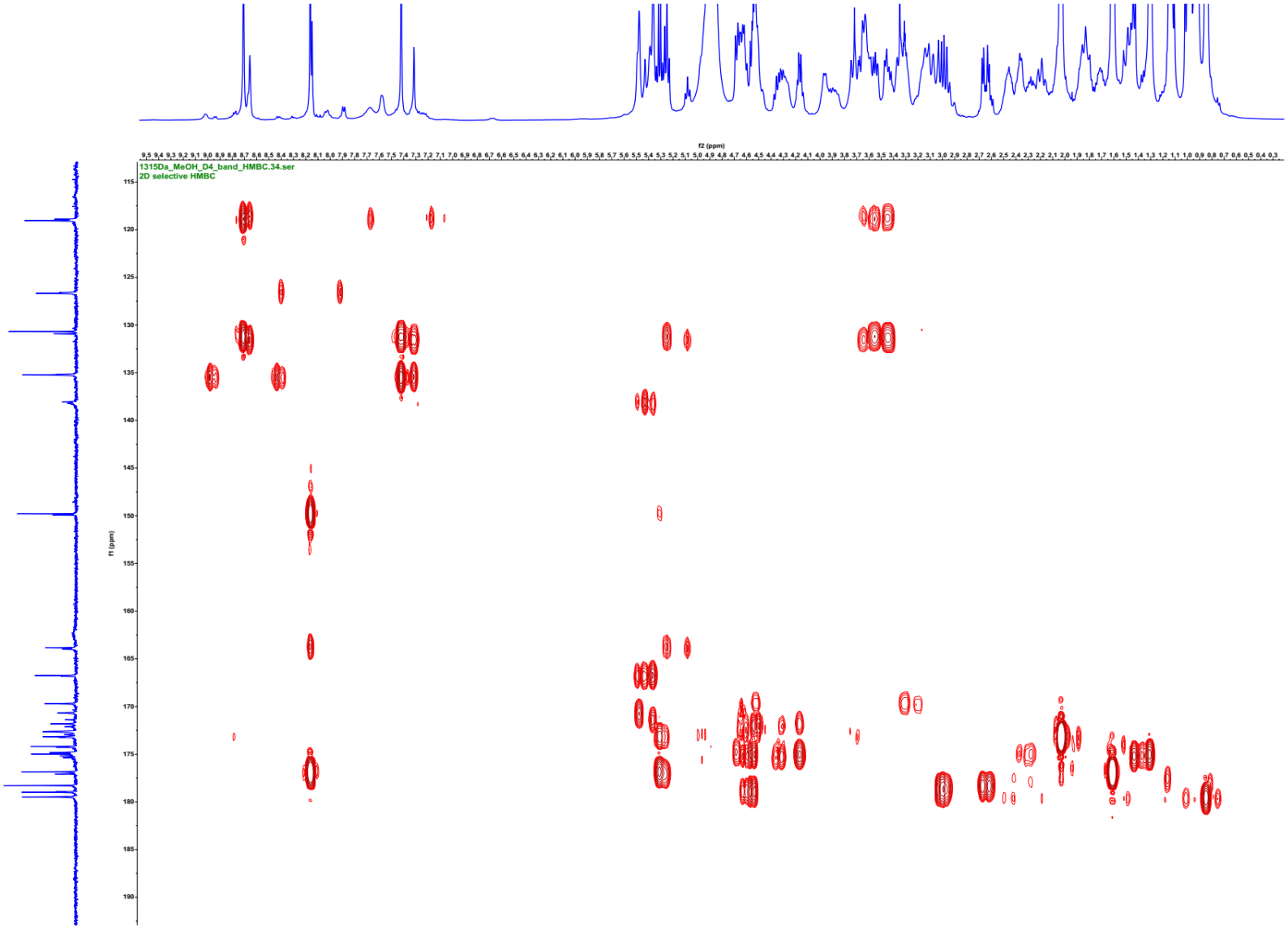

Figure S30. Band-Selective ^{1}H-^{13}C-HMBC spectrum of nocathioamide A (**1**) (d_4-CH_3OH, 400/100 MHz)

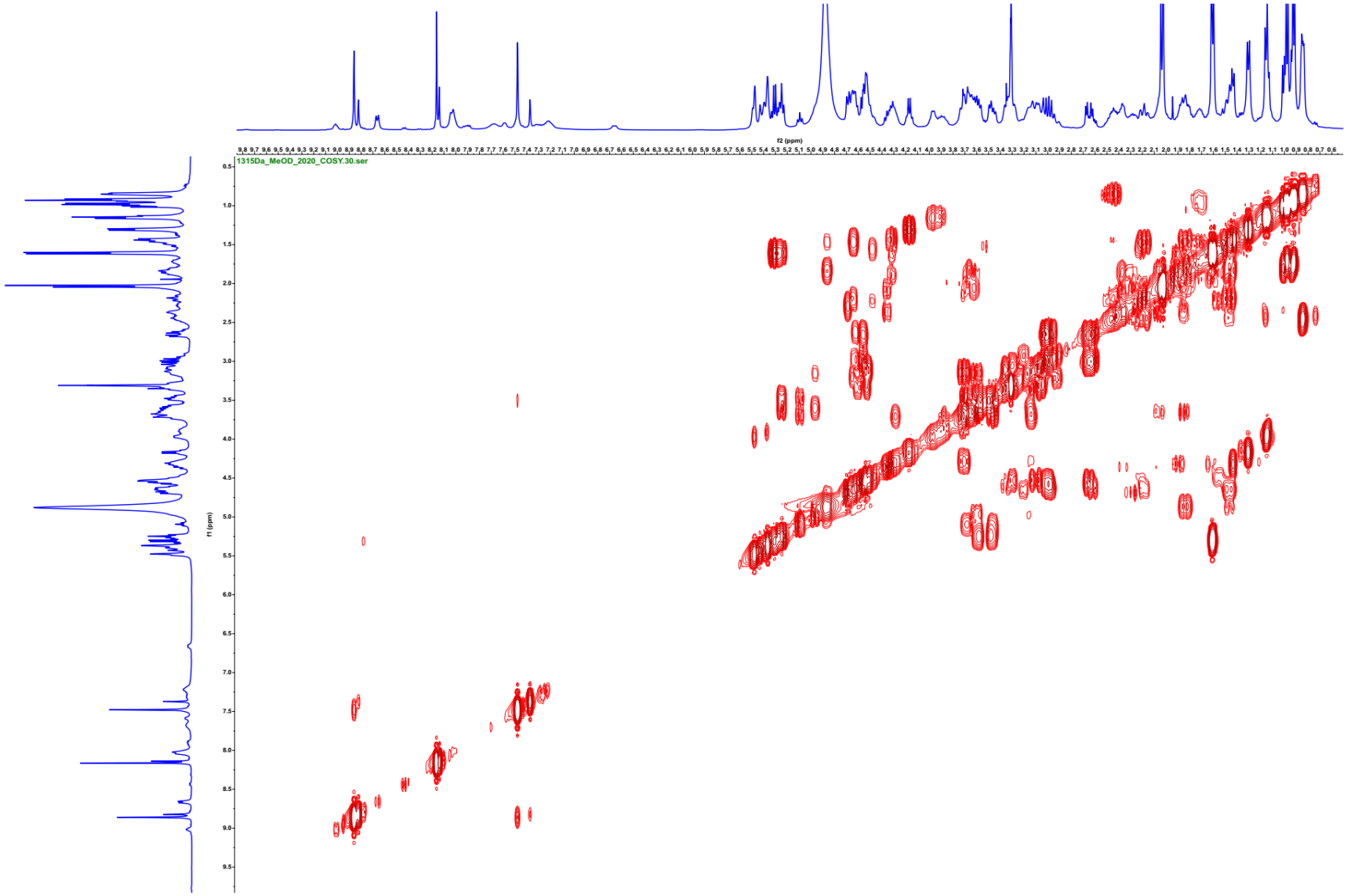

Figure S31. ^{1}H-^{1}H COSY spectrum of nocathioamide A (**1**) (d_4-CH_3OH, 400/400 MHz)

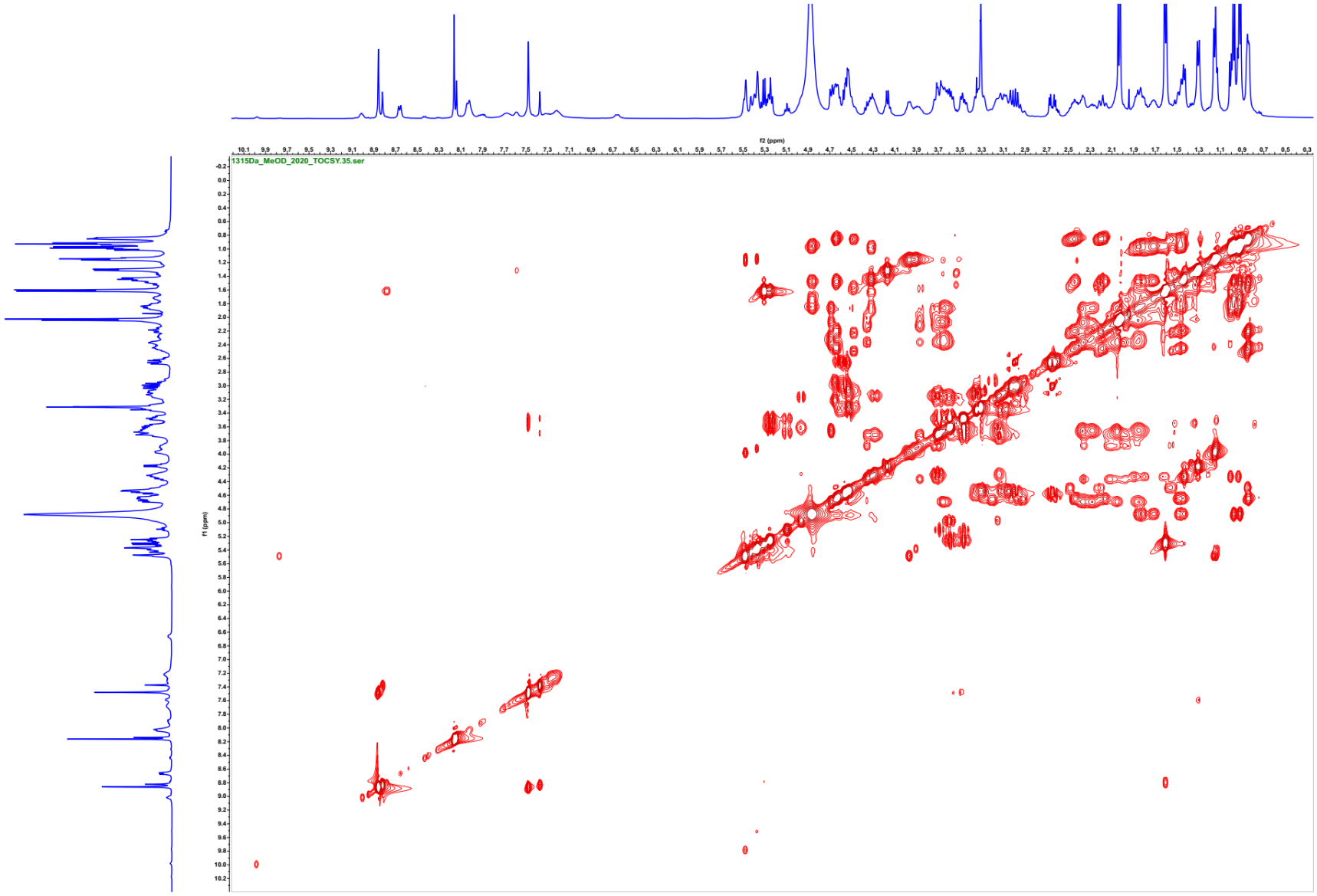

Figure S32. ^{1}H-^{1}H TOCSY spectrum of nocathioamide A (**1**) (d_4-CH_3OH, 400/400 MHz)

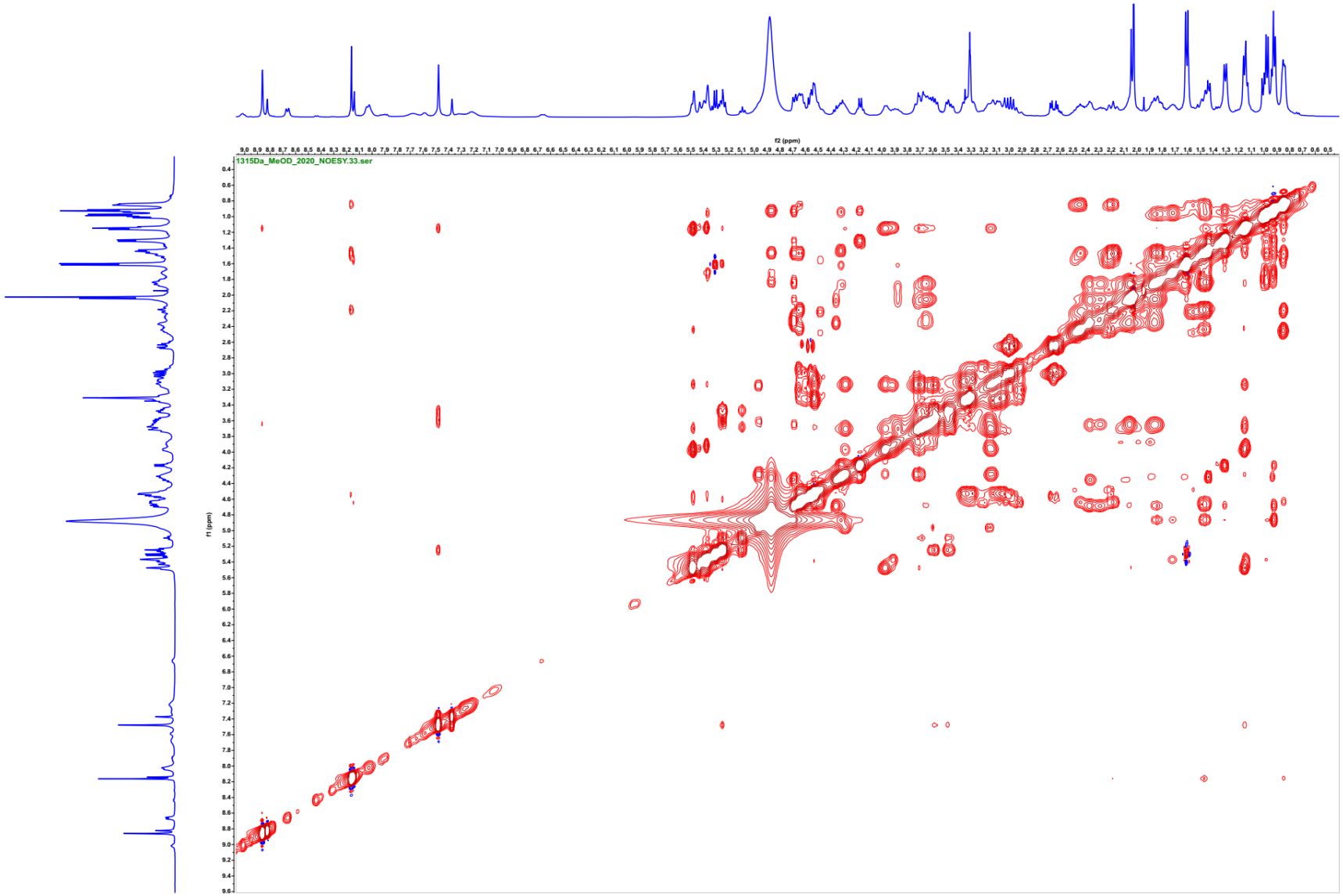

Figure S33. ^{1}H-^{1}H NOESY spectrum of nocathioamide A (**1**) (d_4-CH_3OH, 400/400 MHz, d8 = 300 msec)

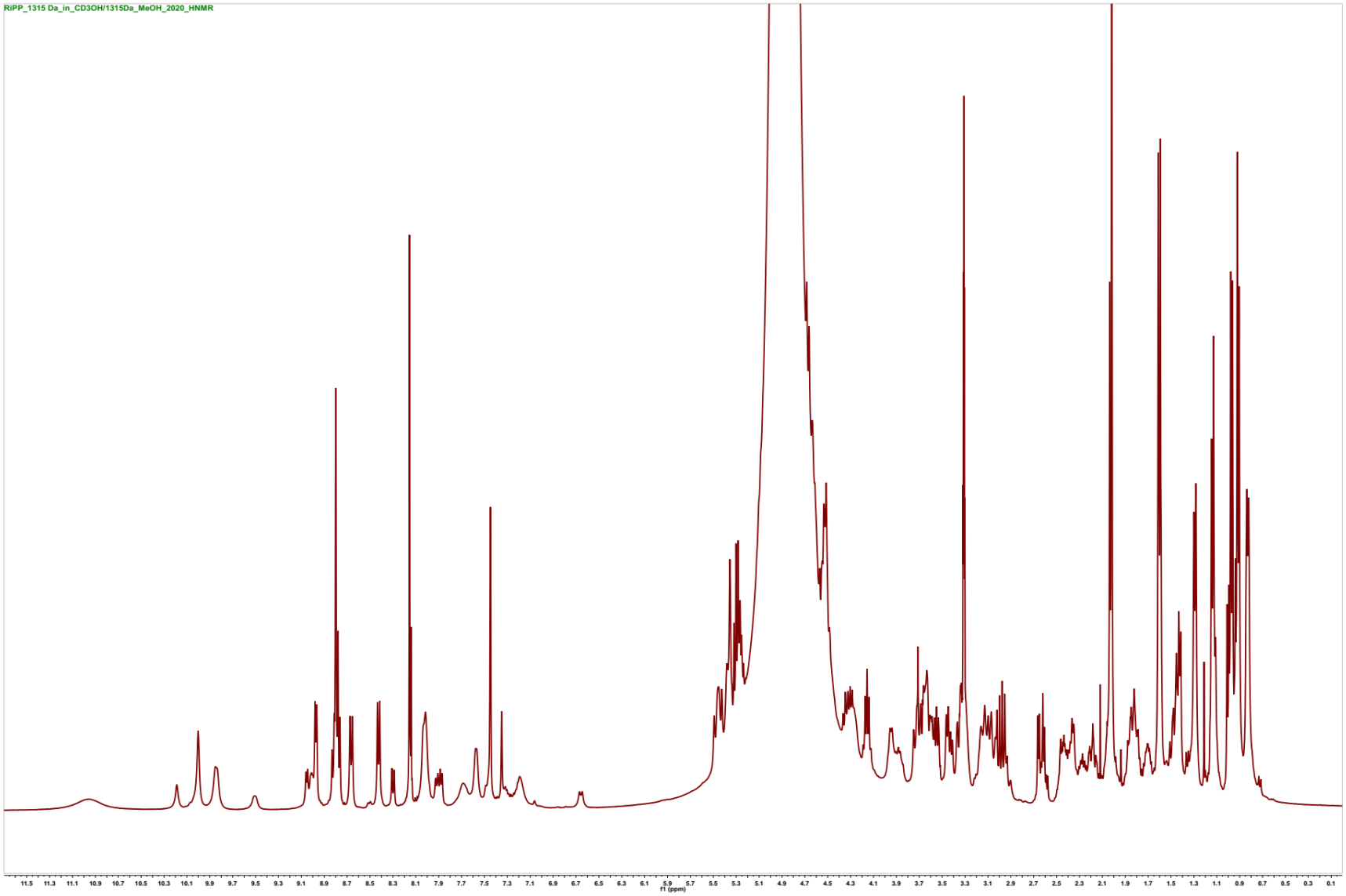

Figure S34. ^{1}H-NMR spectrum of nocathioamide A (**1**) (d_3-CH_3OH, 400 MHz)

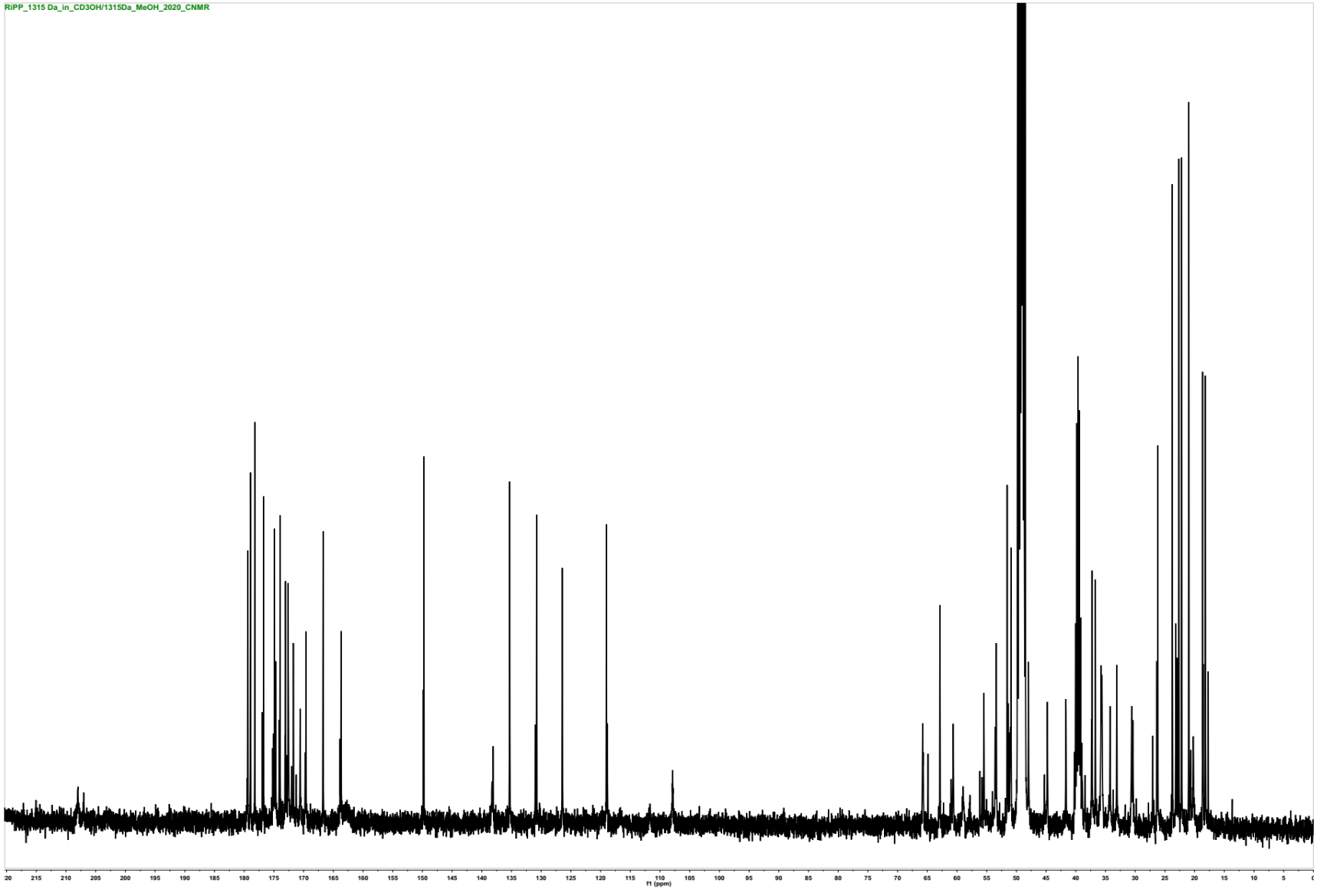

Figure S35. ^{13}C-NMR spectrum of nocathioamide A (**1**) (d_3-CH_3OH, 100 MHz)

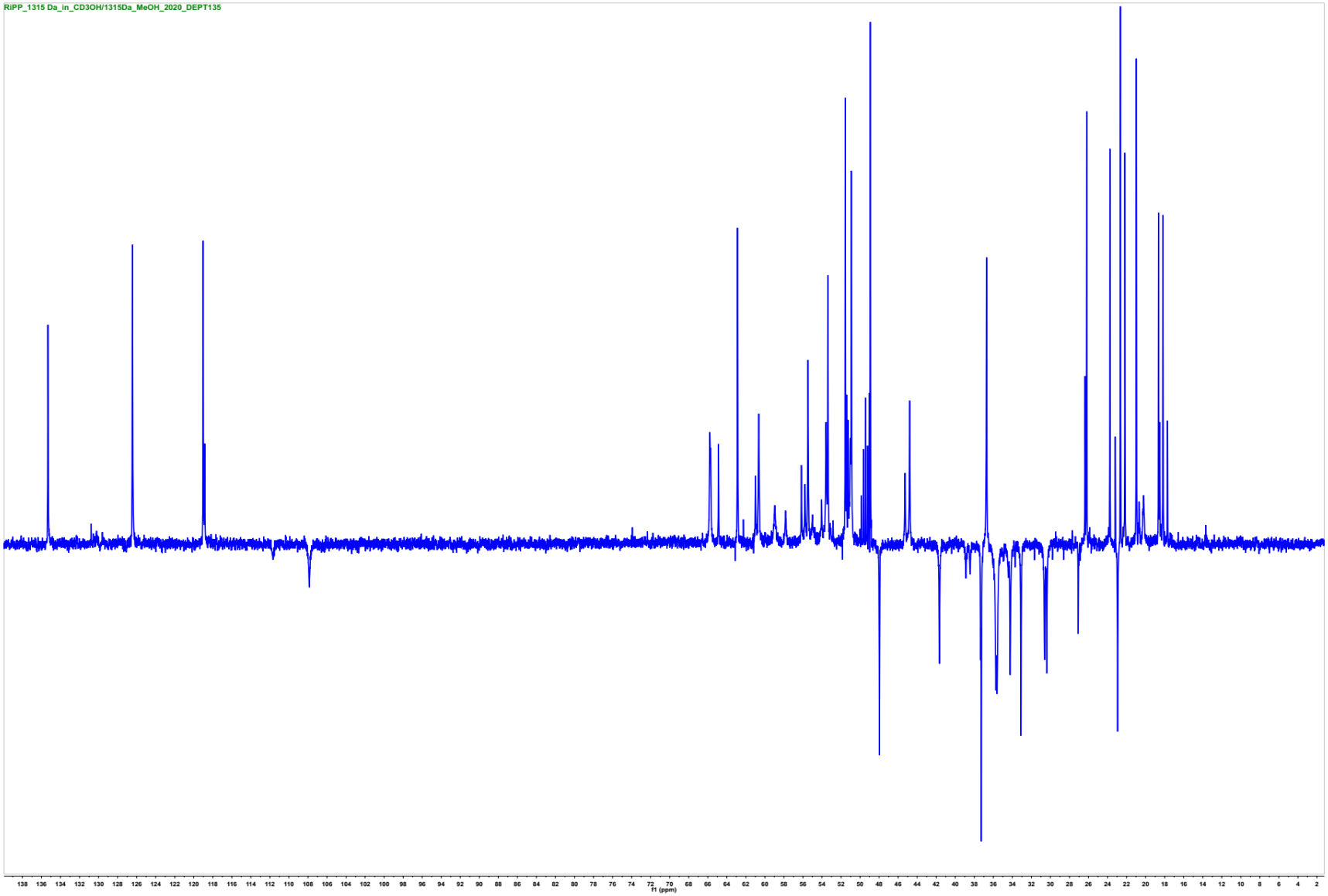

Figure S36. DEPT-135 spectrum of nocathioamide A (**1**) (d_3-CH_3OH, 100 MHz)

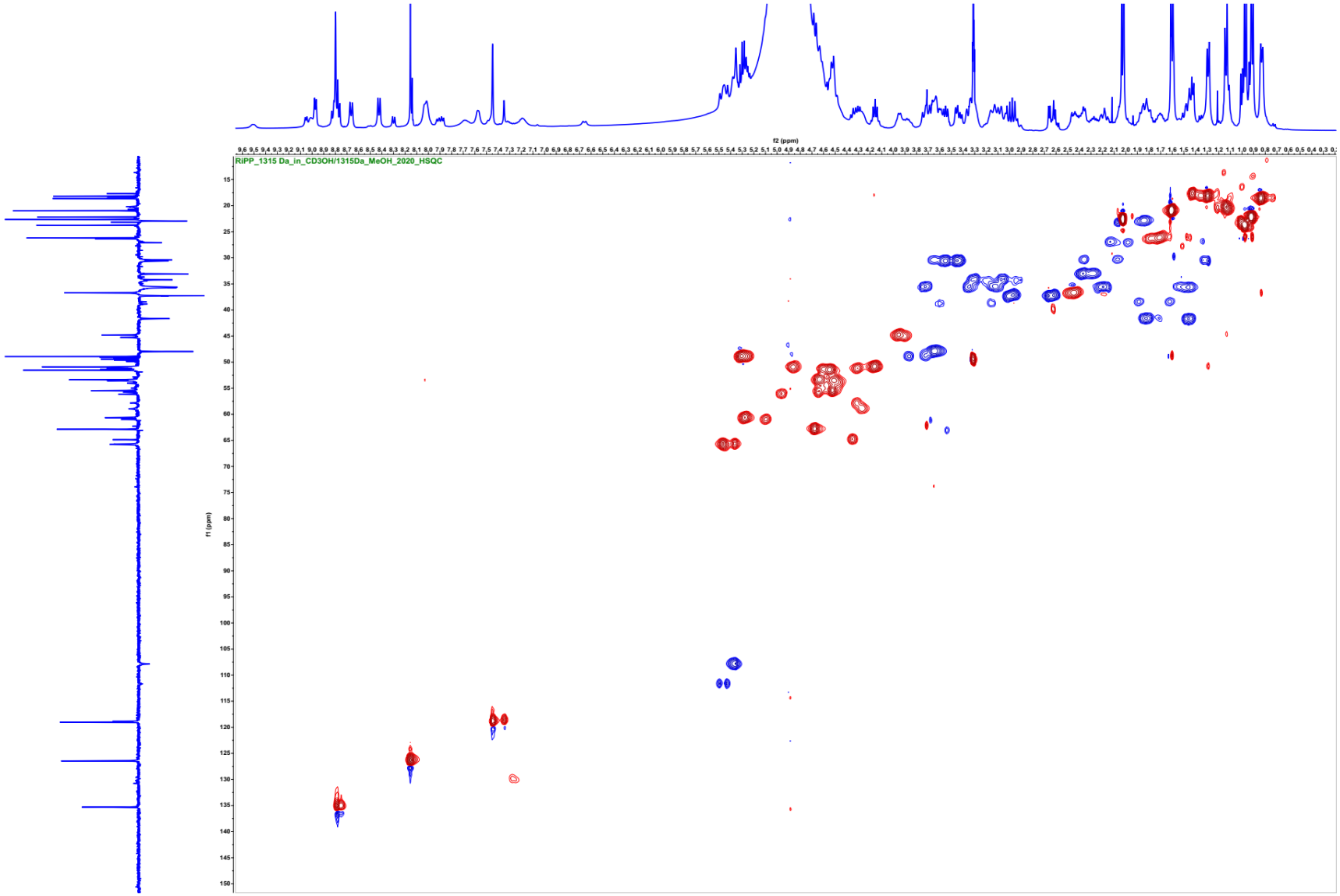

Figure S37. ^{1}H-^{13}C HSQC spectrum of nocathioamide A (**1**) (d_3-CH_3OH, 400/100 MHz)

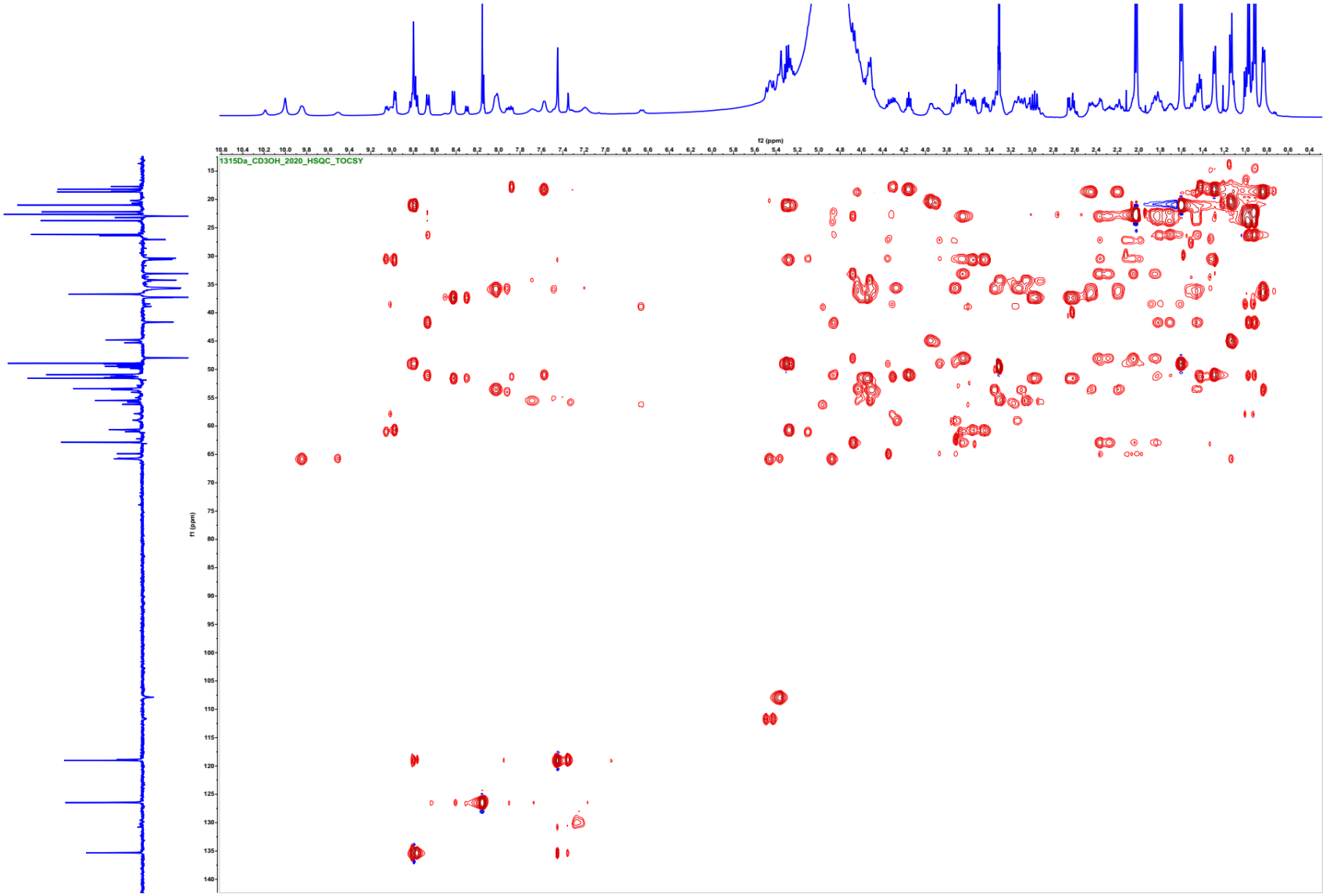

Figure S38. ^{1}H-^{13}C HSQC-TOCSY spectrum of nocathioamide A (**1**) (d_3-CH_3OH, 400/100 MHz)

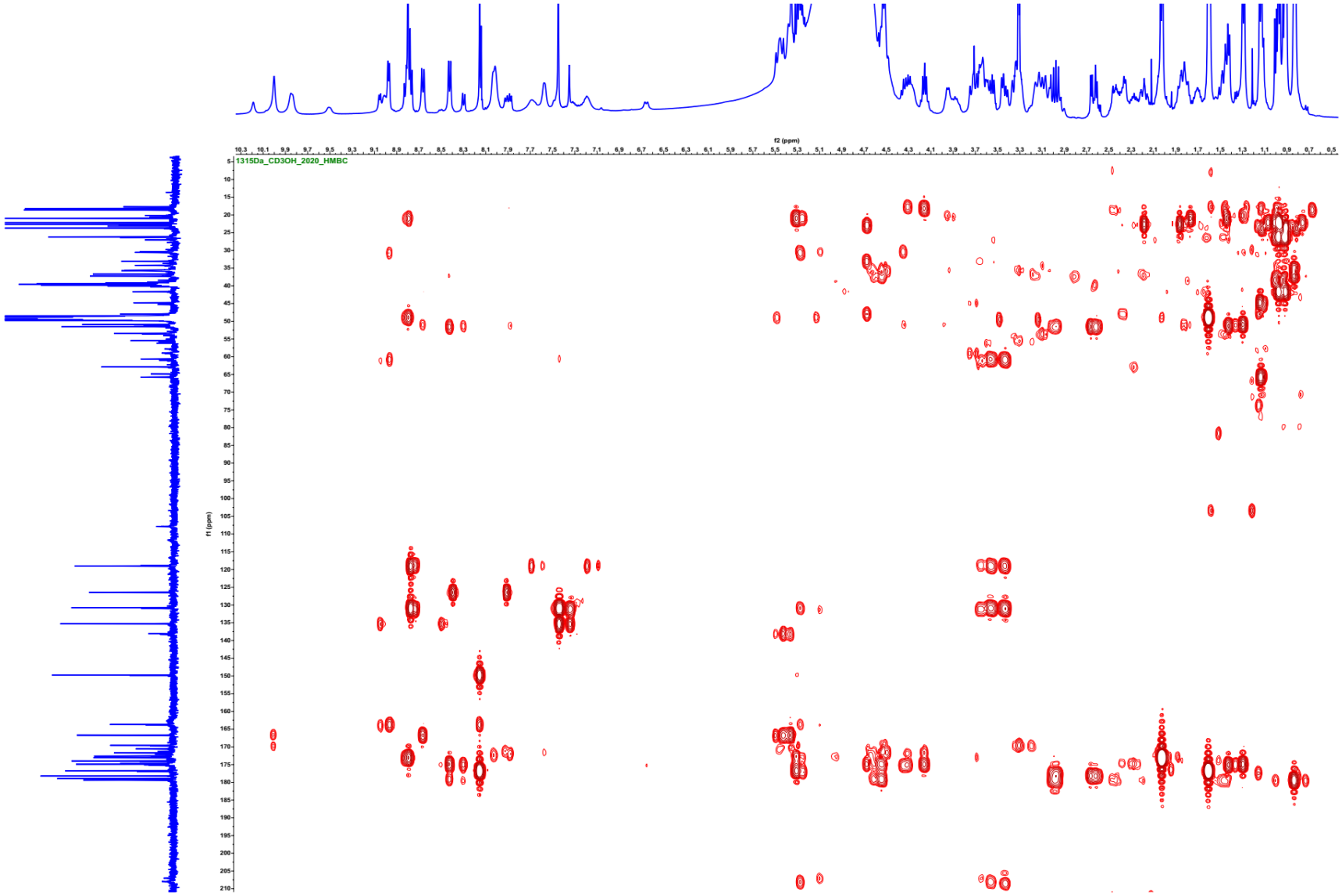

Figure S39. ^{1}H-^{13}C HMBC spectrum of nocathioamide A (**1**) (d_3-CH_3OH, 400/100 MHz)

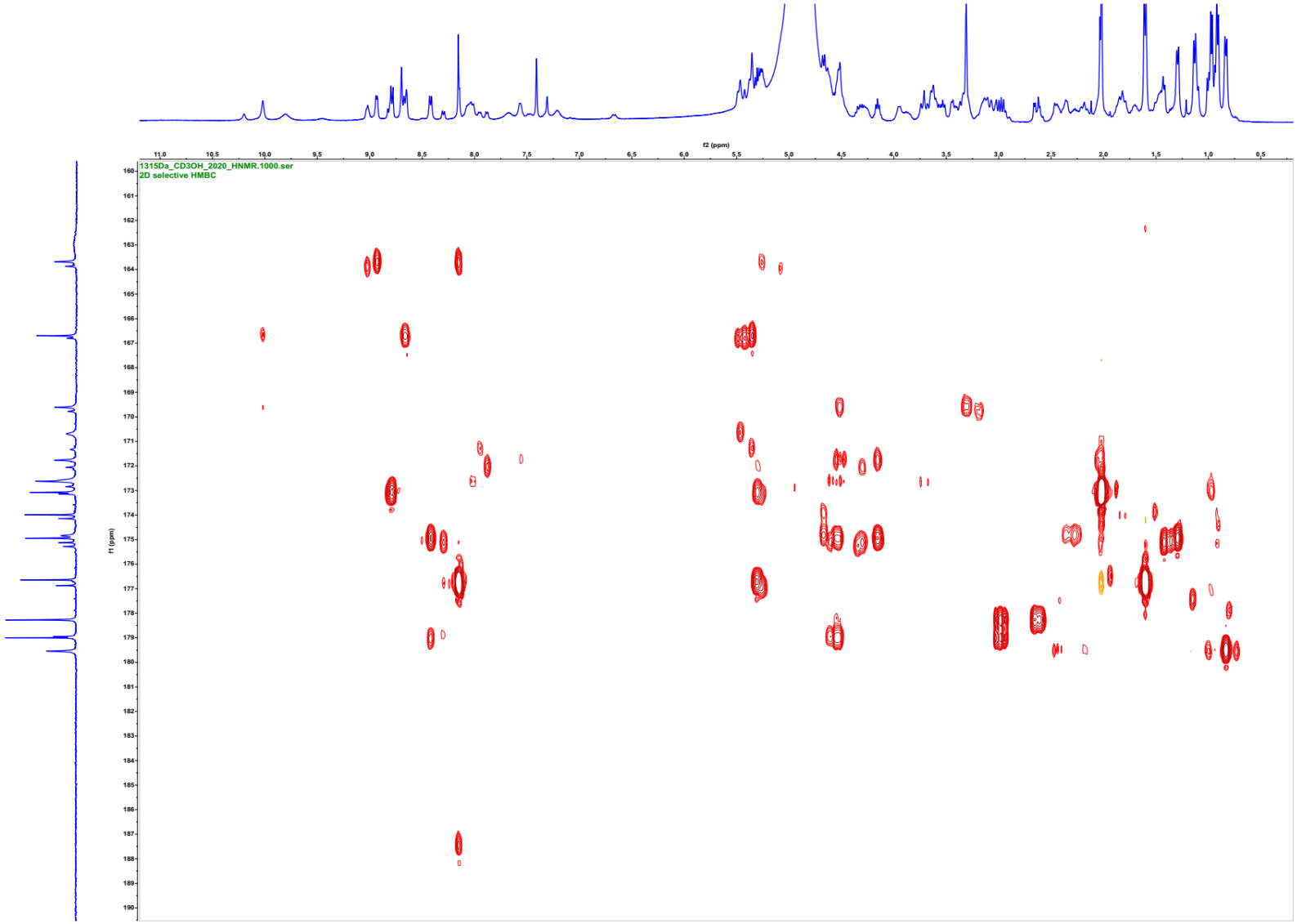

Figure S40. ^{1}H-^{13}C Band-Selective HMBC spectrum of nocathioamide A (**1**) (d_3-CH_3OH, 400/100 MHz)

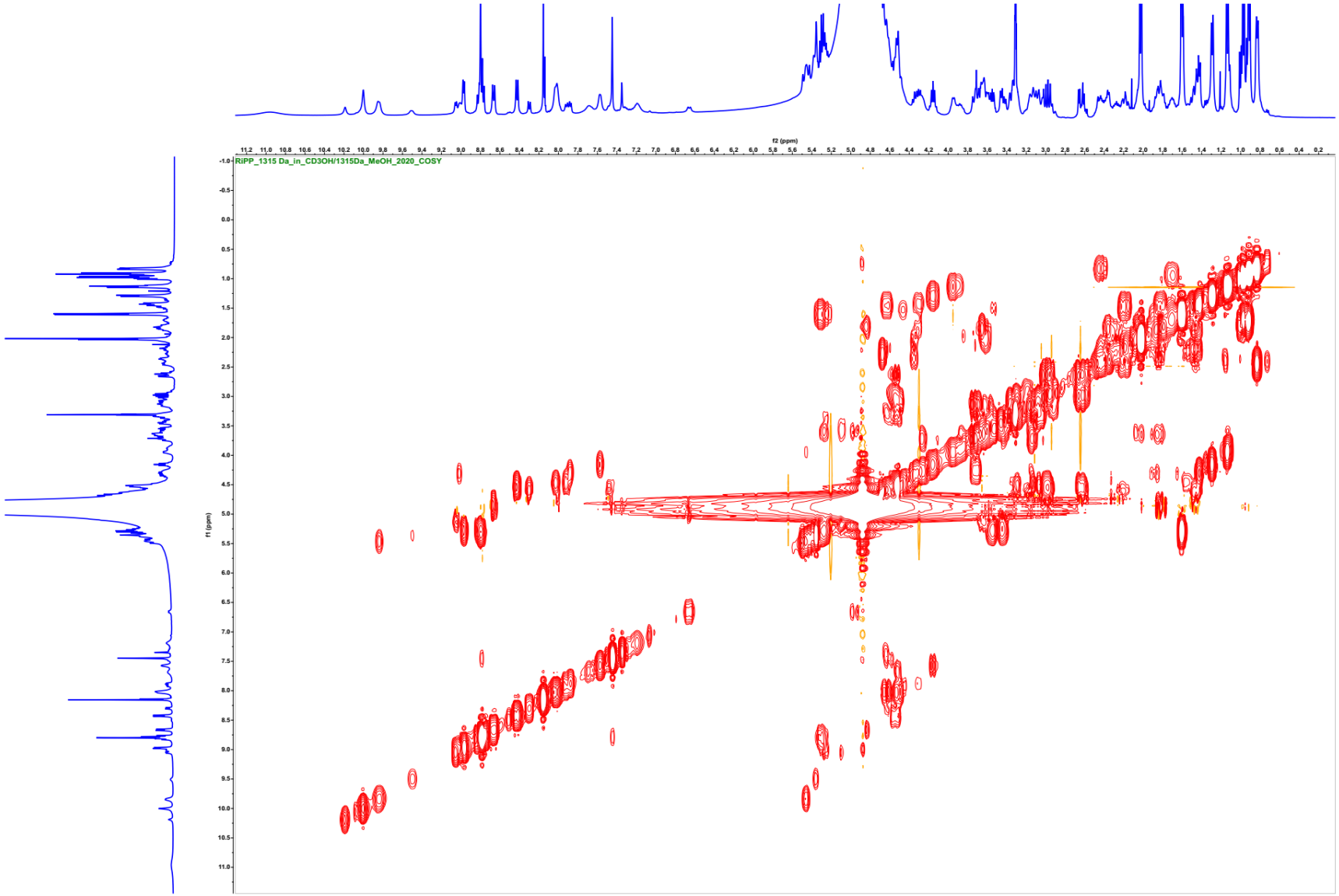

Figure S41. ^{1}H-^{1}H COSY spectrum of nocathioamide A (**1**) (d_3-CH_3OH, 400/400 MHz)

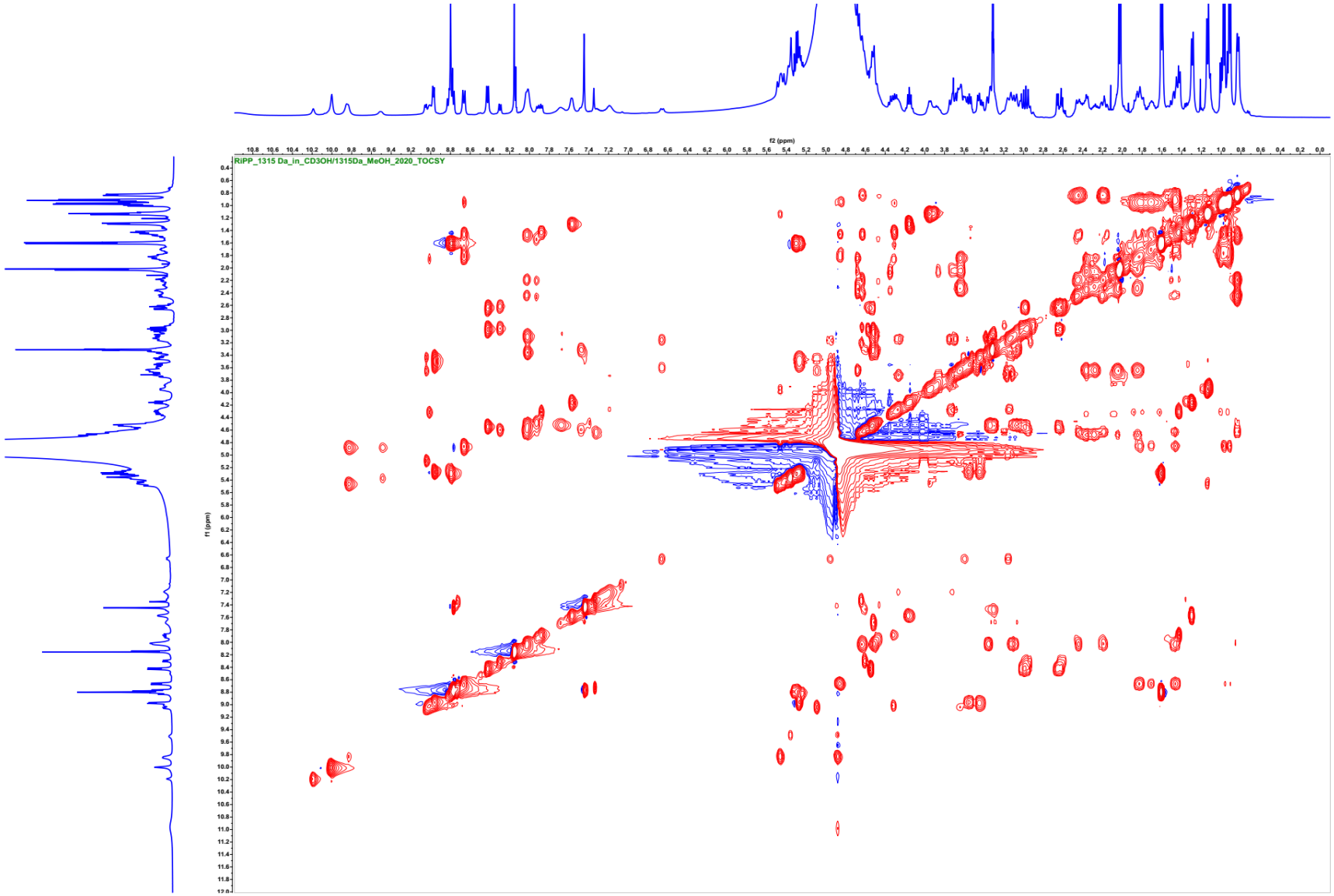

Figure S42. ^{1}H-^{1}H TOCSY spectrum of nocathioamide A (**1**) (d_3-CH_3OH, 400/400 MHz)

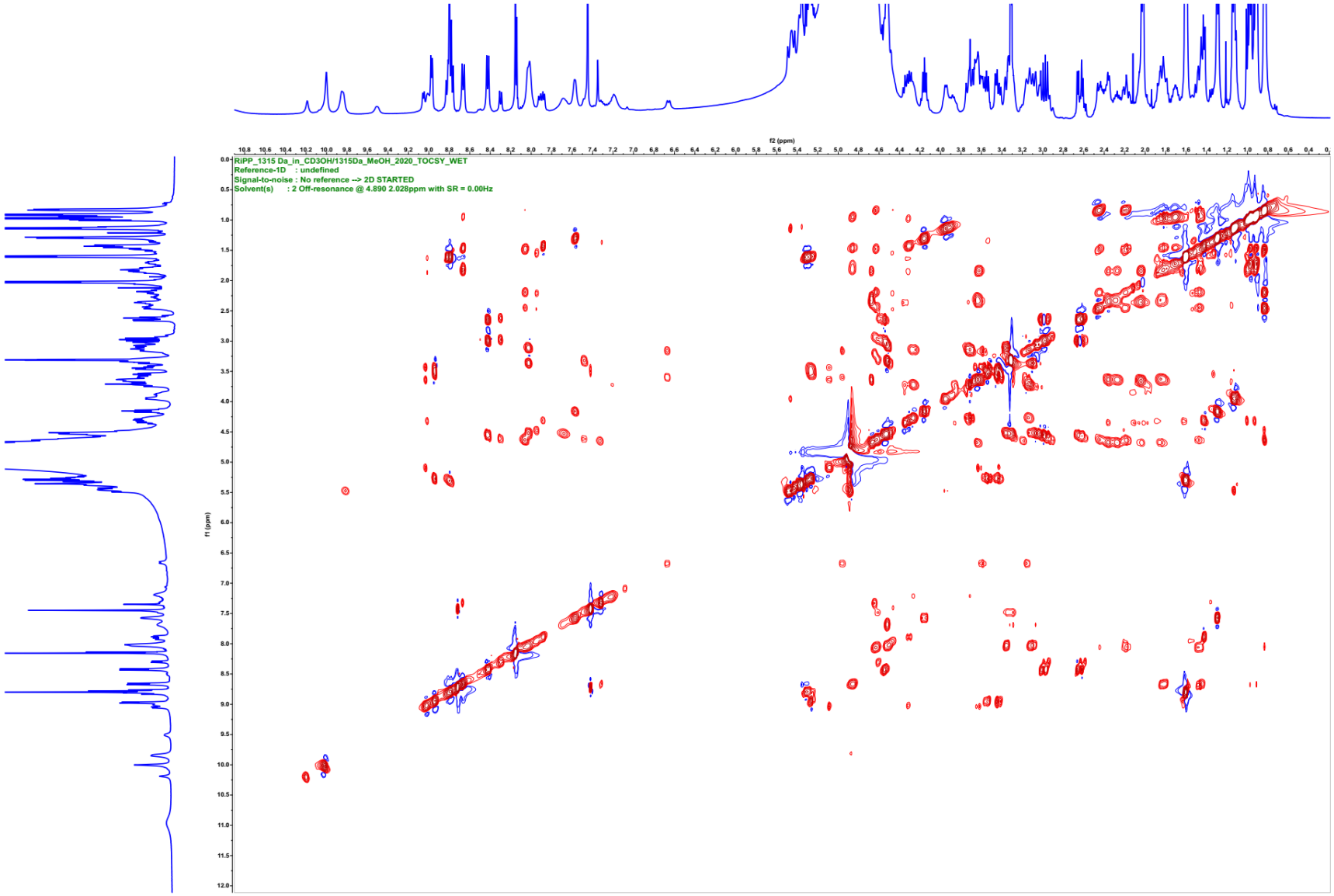

Figure S43. ^{1}H-^{1}H TOCSY WET spectrum of nocathioamide A (**1**) (d_3-CH_3OH, 400/400 MHz)

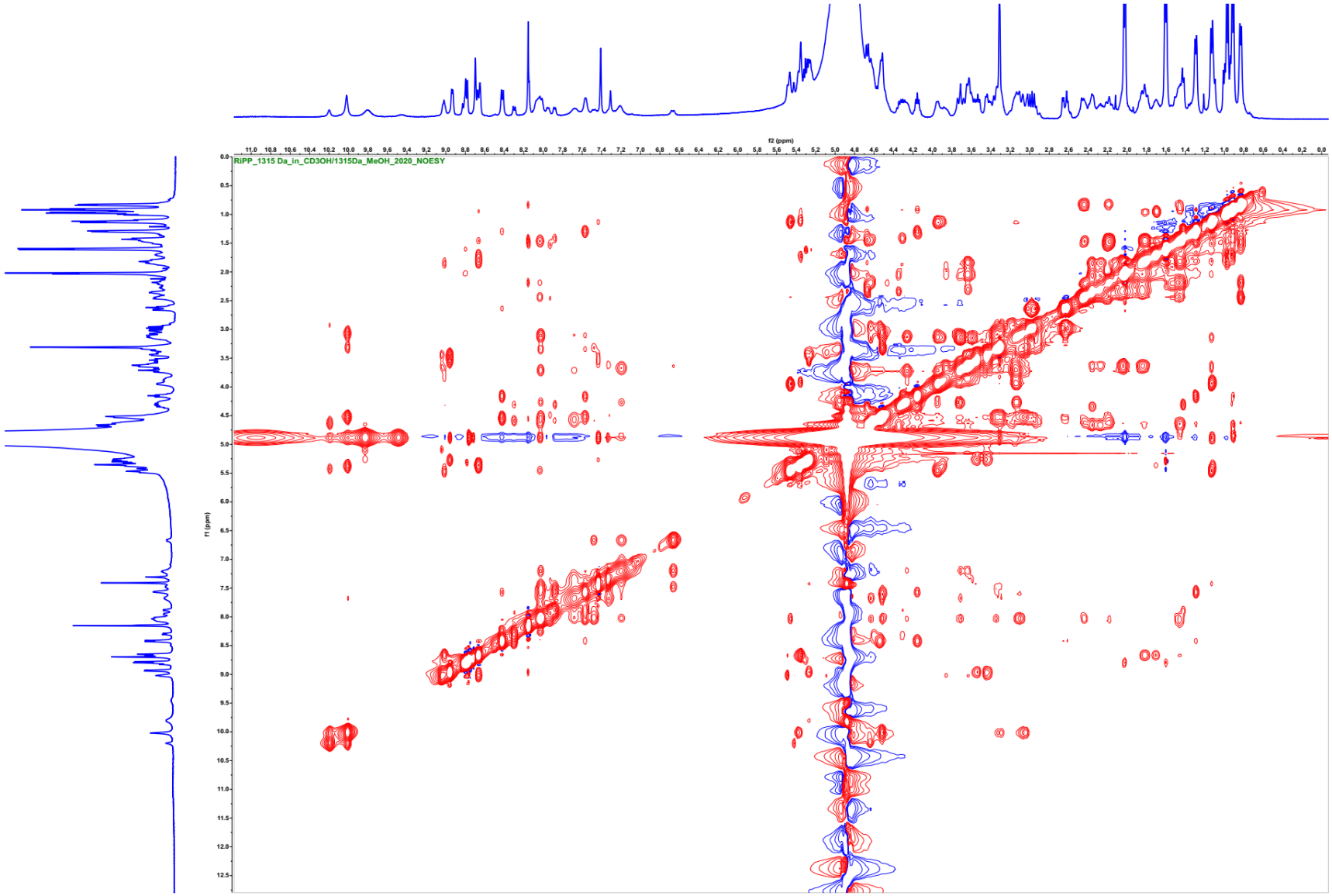

Figure S44. ^{1}H-^{1}H NOESY spectrum of nocathioamide A (**1**) (d_3-CH_3OH, 400/400 MHz, d8 = 300 msec)

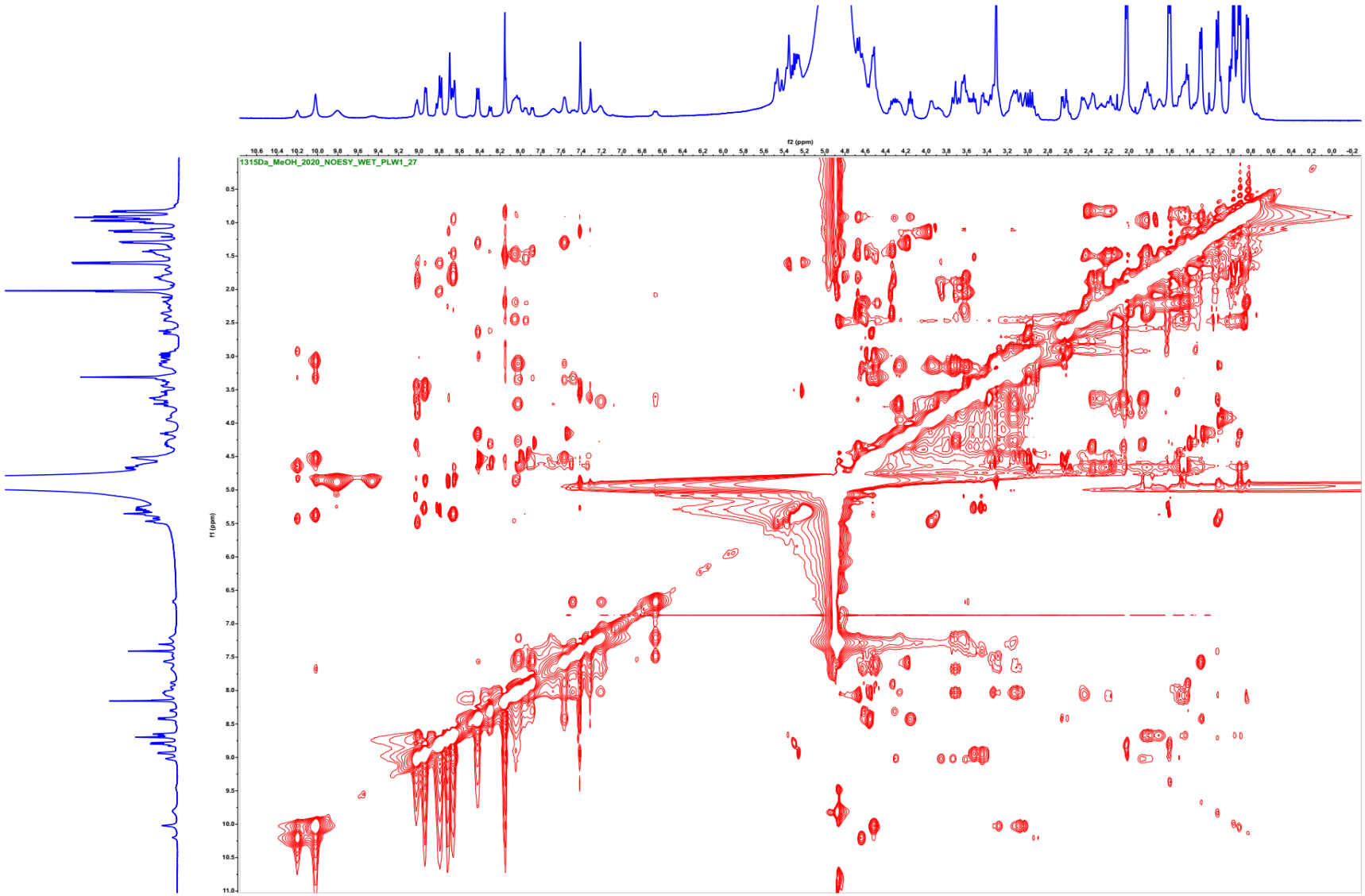

Figure S45. ^{1}H-^{1}H NOESY WET spectrum of nocathioamide A (**1**) (d_3-CH_3OH, 400/400 MHz, d8 = 300 msec, PLW1 = 27)

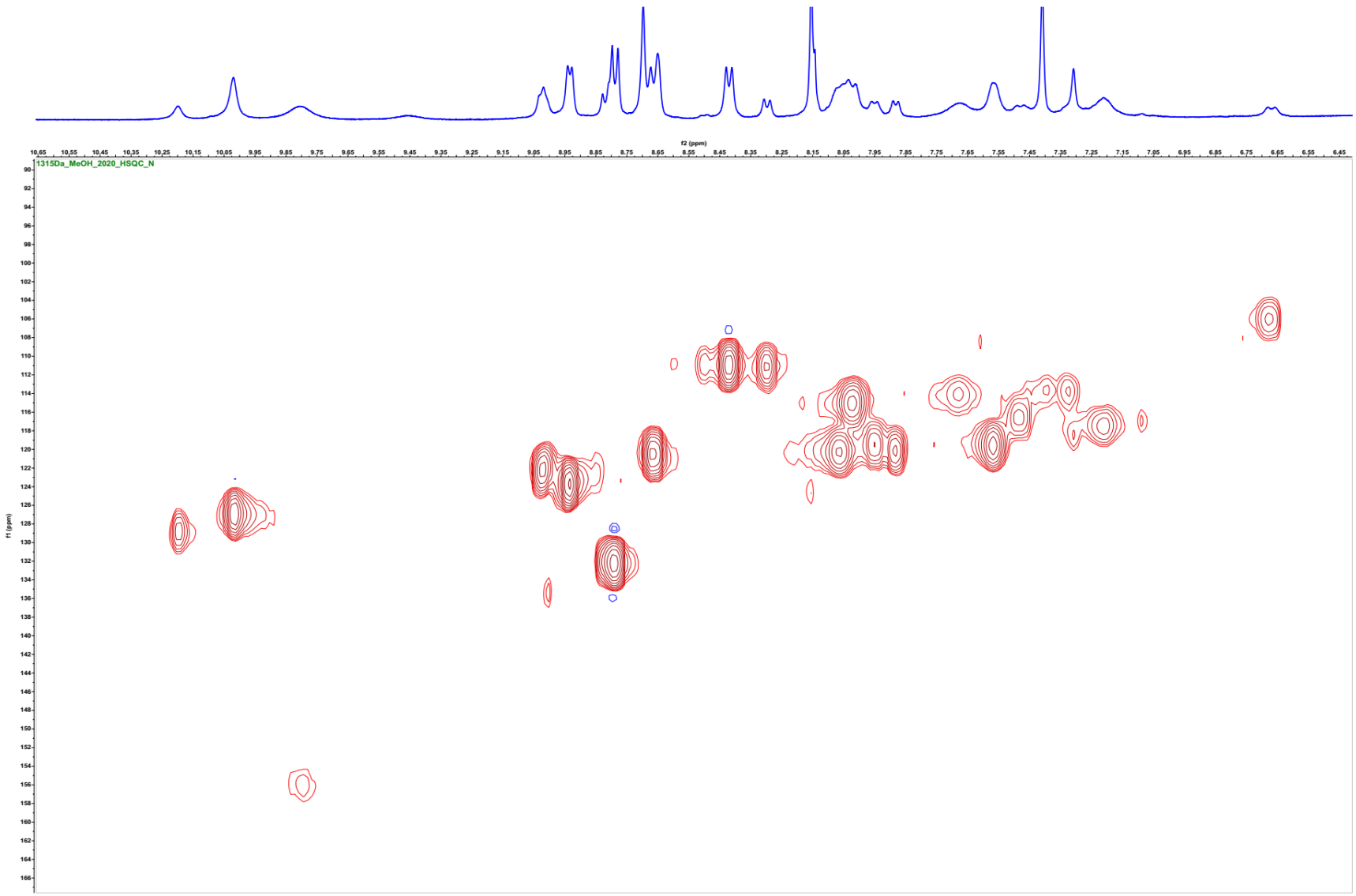

Figure S46. ^{1}H-^{15}N HSQC spectrum of nocathioamide A (**1**) (d_3-CH_3OH, 400/40.6 MHz)

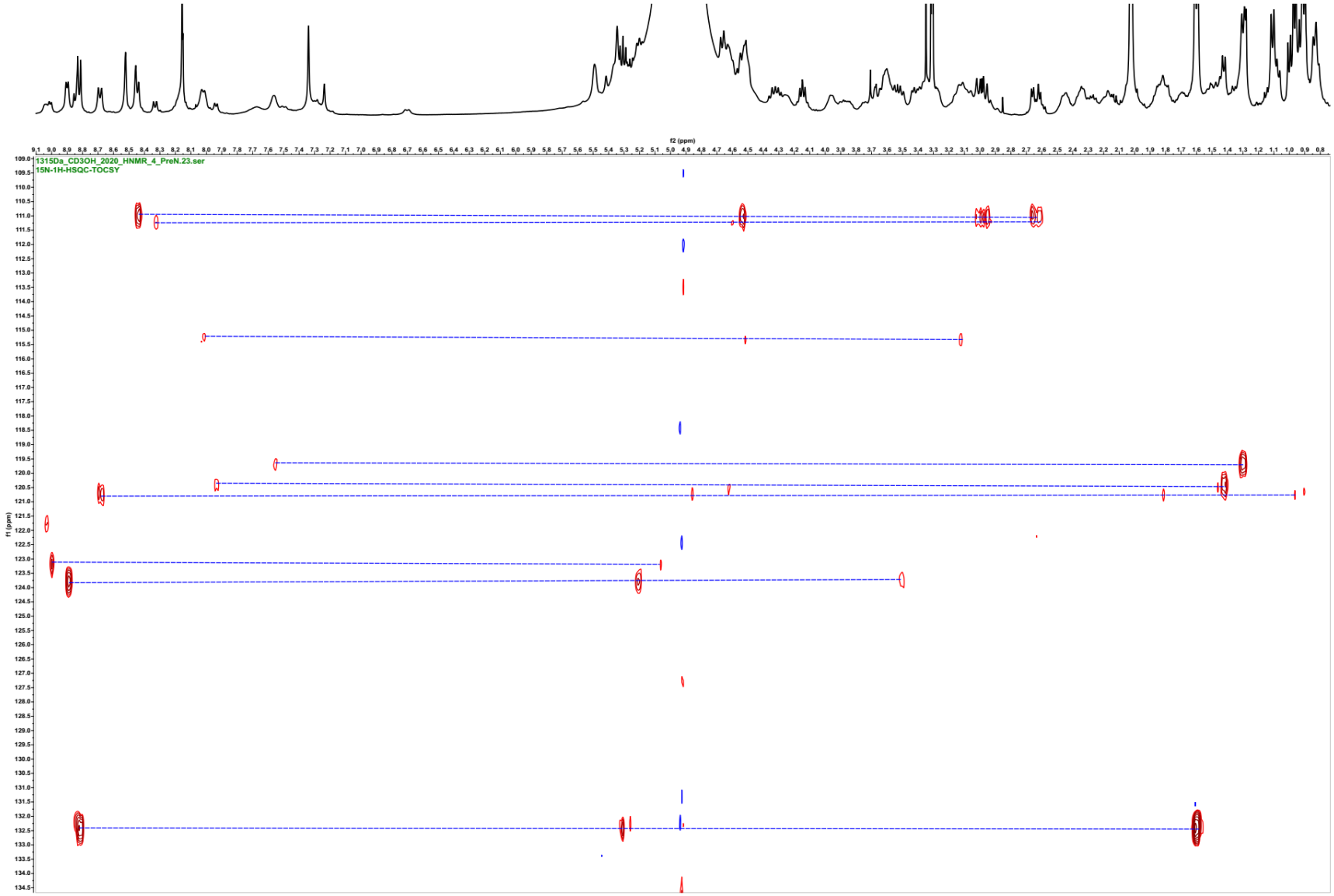

Figure S47. Enlarged ^{1}H-^{15}N HSQC-TOCSY spectrum of nocathioamide A (**1**) (d_3-CH_3OH, 400/40.6 MHz)

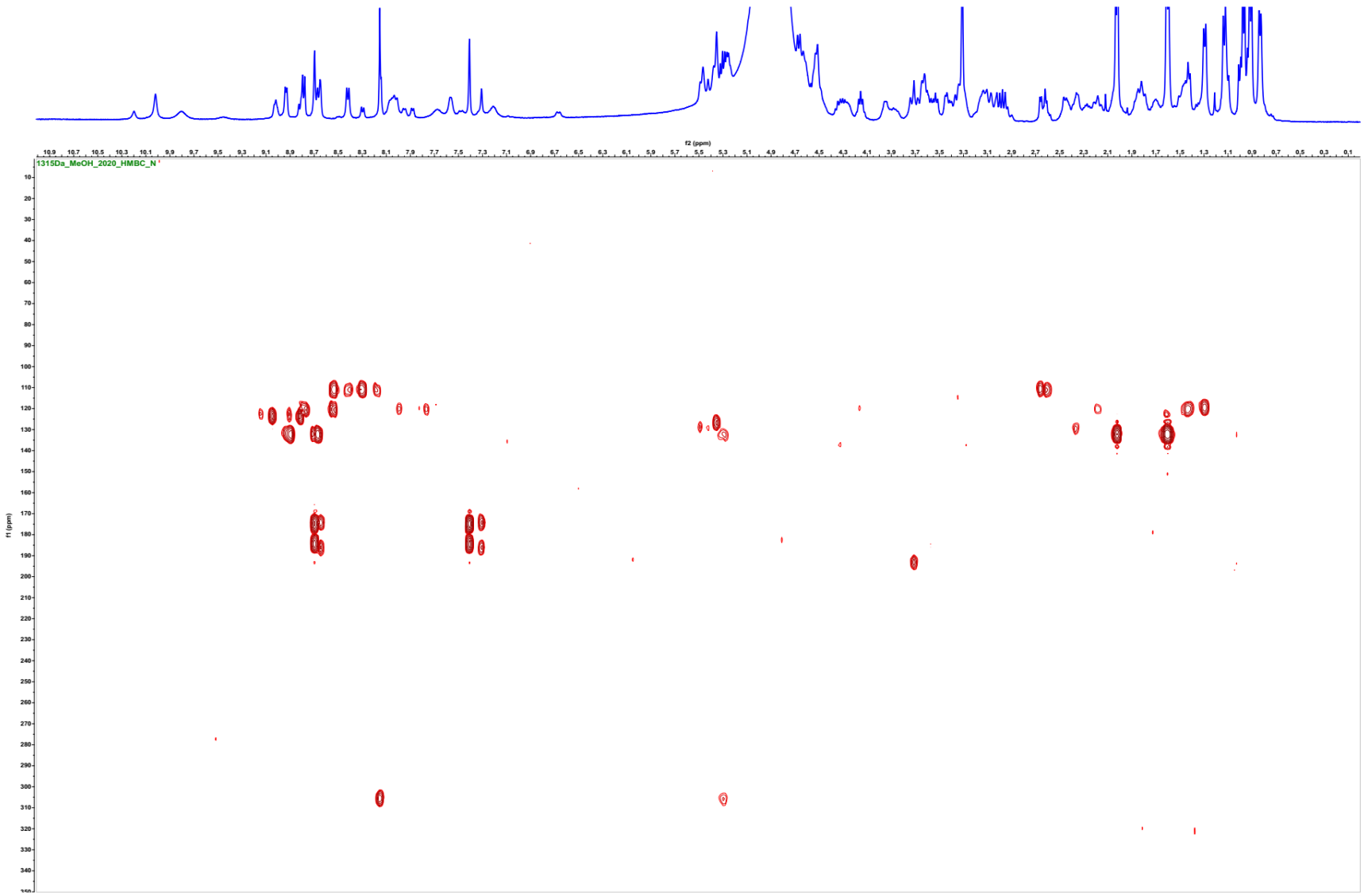

Figure S48. ^{1}H-^{15}N HMBC spectrum of nocathioamide A (**1**) (d_3-CH_3OH, 400/40.6 MHz)

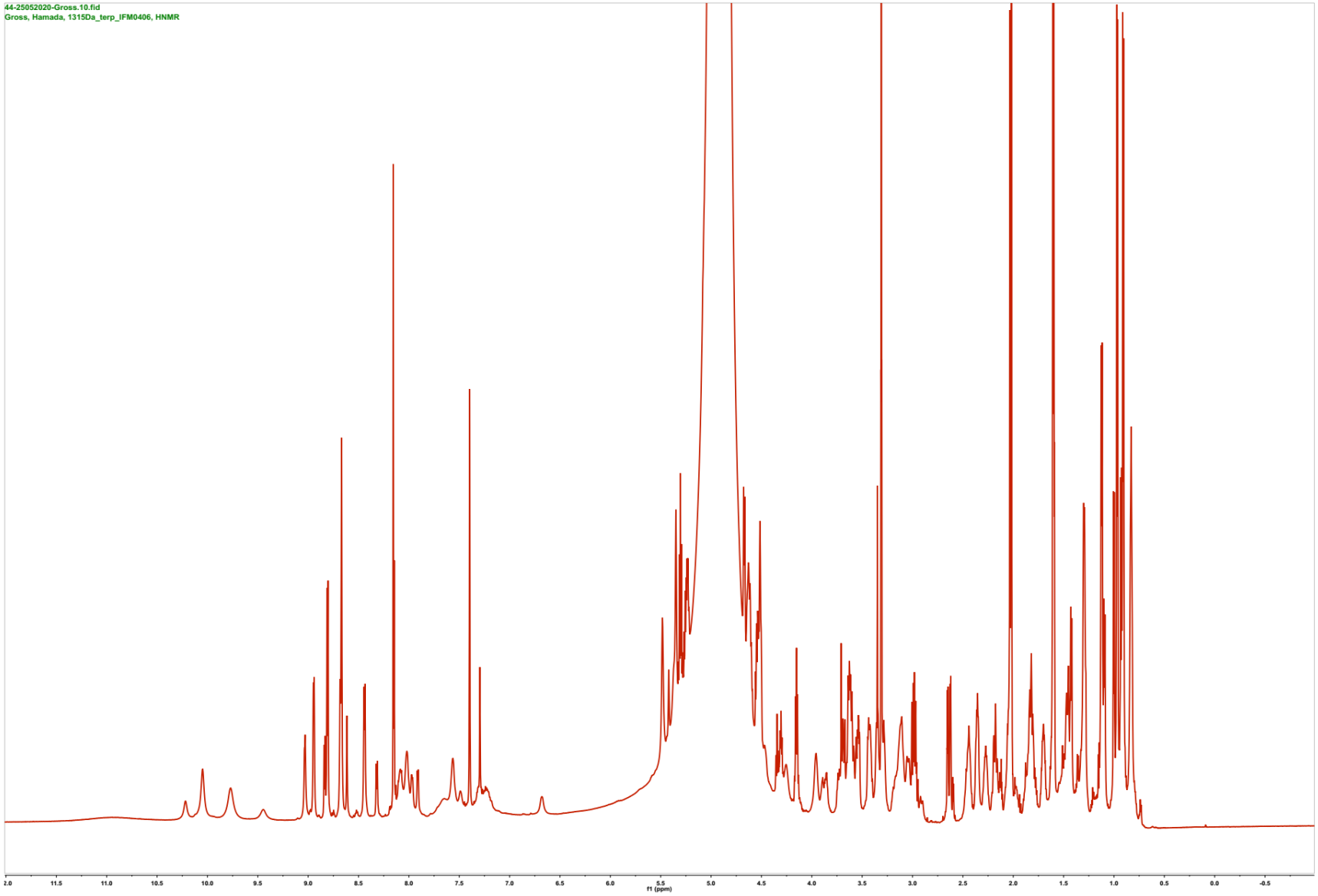

Figure S49. ^{1}H-NMR spectrum of nocathioamide A (**1**) (d_3-CH_3OH, 700 MHz)

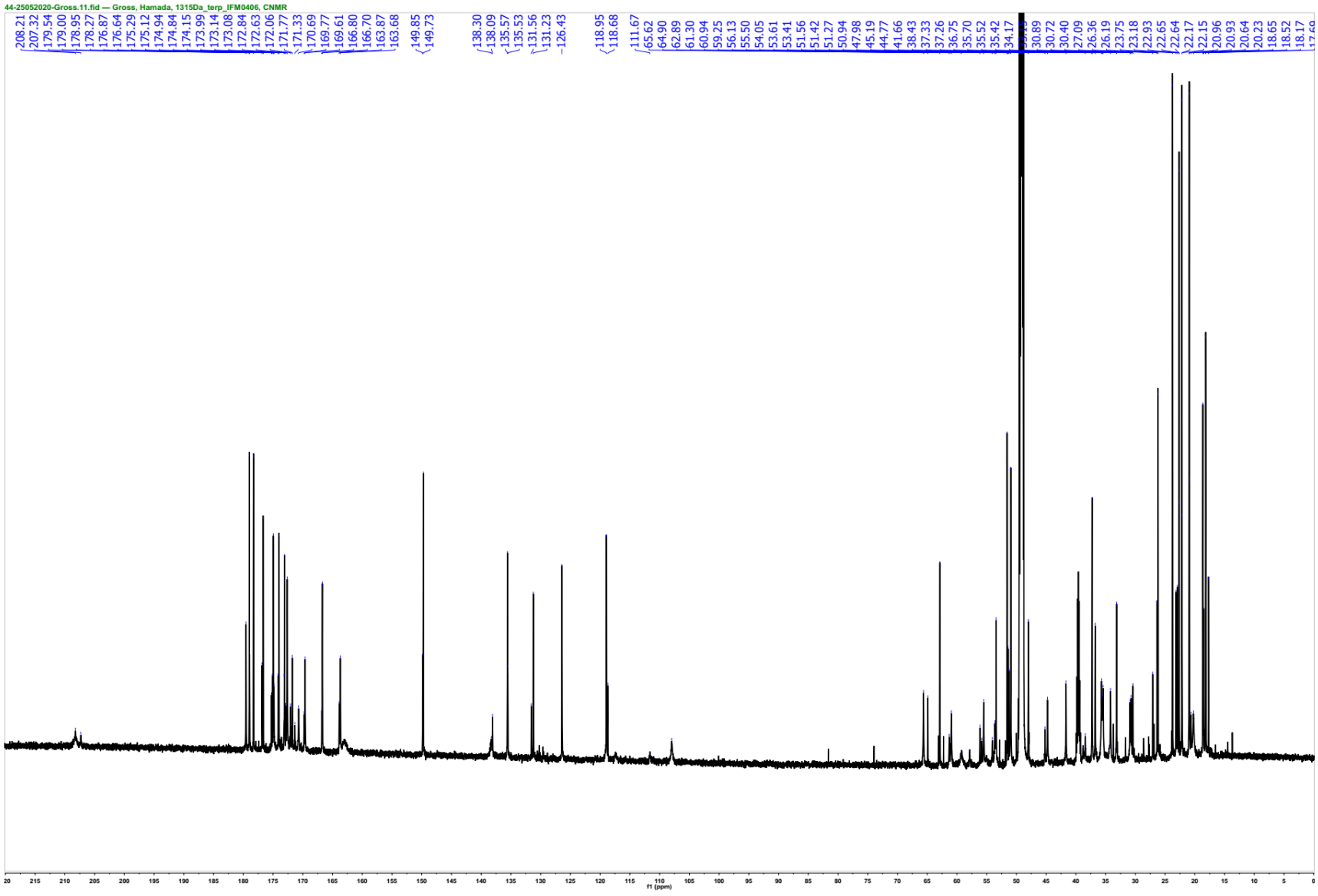

Figure S50. ^{13}C-NMR spectrum of nocathioamide A (**1**) (d_3-CH_3OH, 176 MHz)

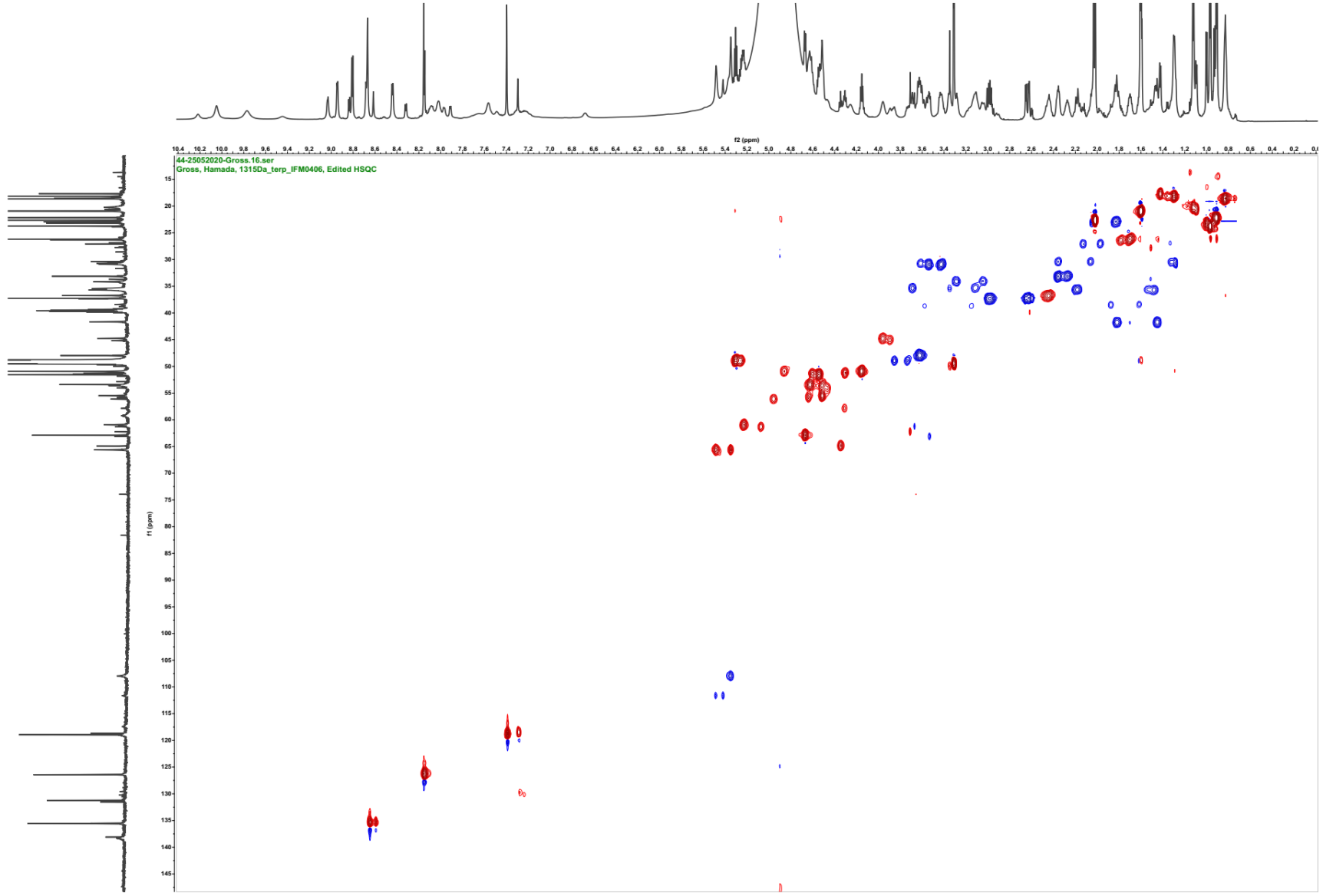

Figure S51. ^{1}H-^{13}C HSQC spectrum of nocathioamide A (**1**) (d_3-CH_3OH, 700/176 MHz)

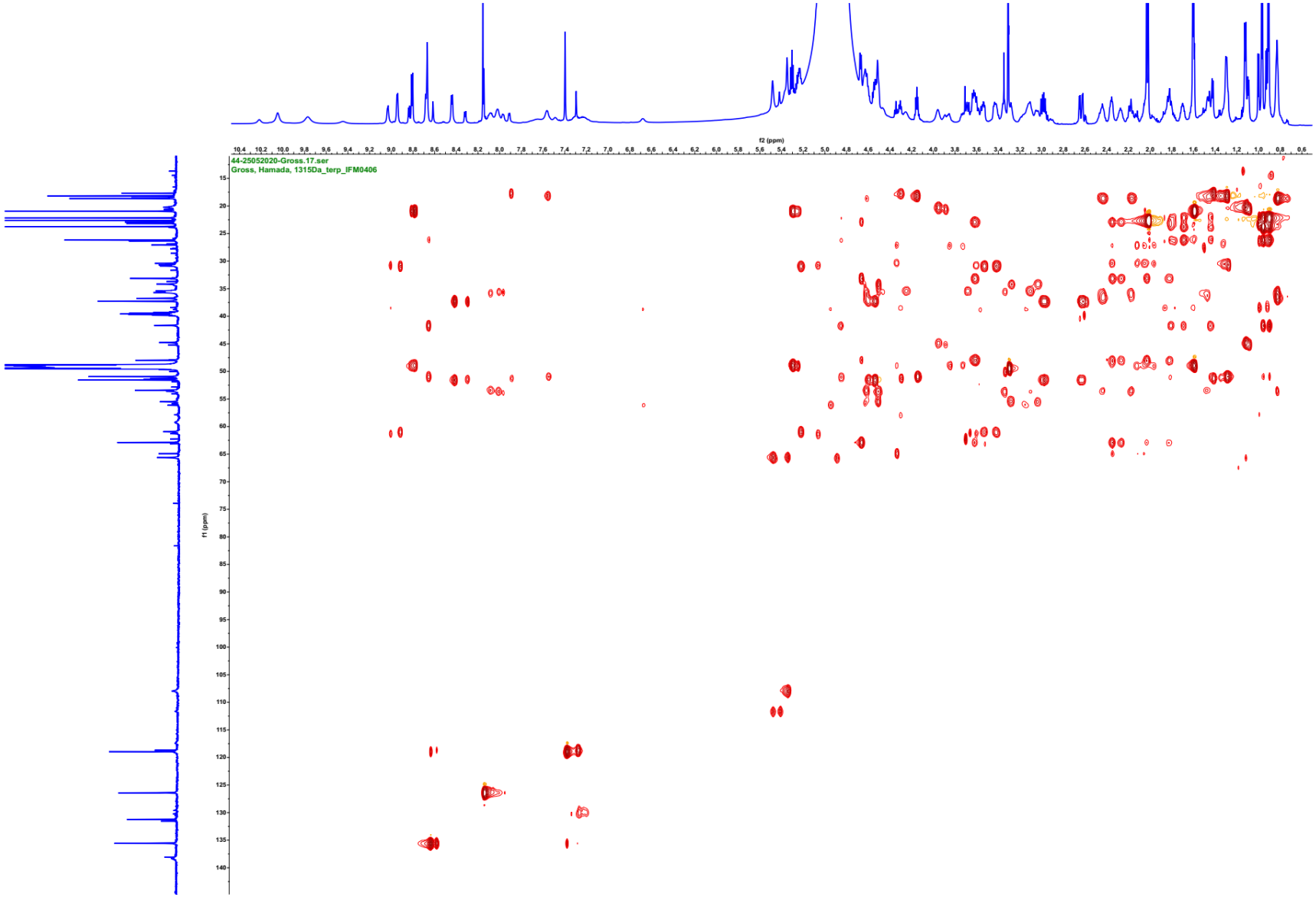

Figure S52. ^{1}H-^{13}C HSQC-TOCSY spectrum of nocathioamide A (**1**) (d_3-CH_3OH, 700/176 MHz)

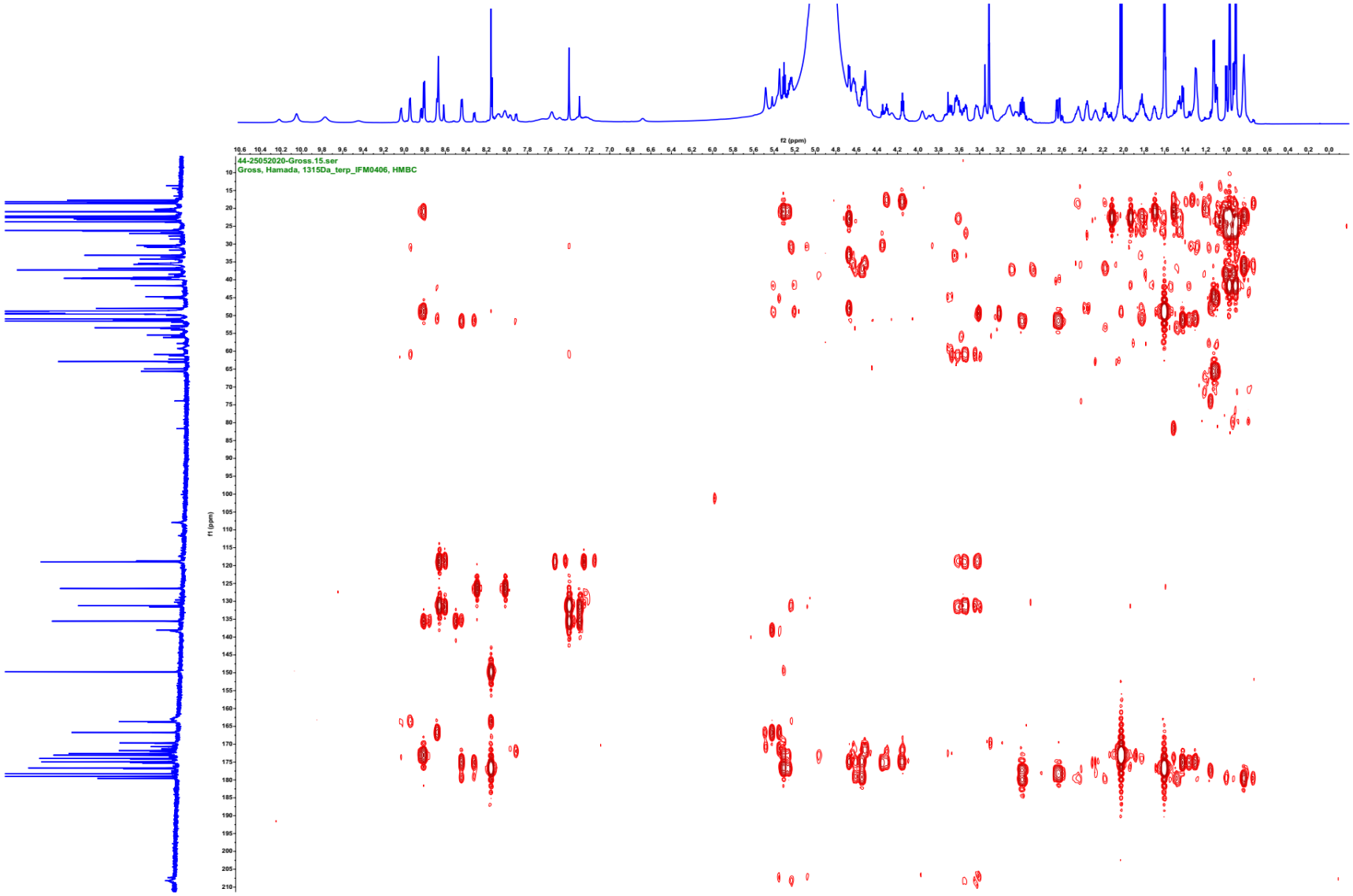

Figure S53. ^{1}H-^{13}C HMBC spectrum of nocathioamide A (**1**) (d_3-CH_3OH, 700/176 MHz)

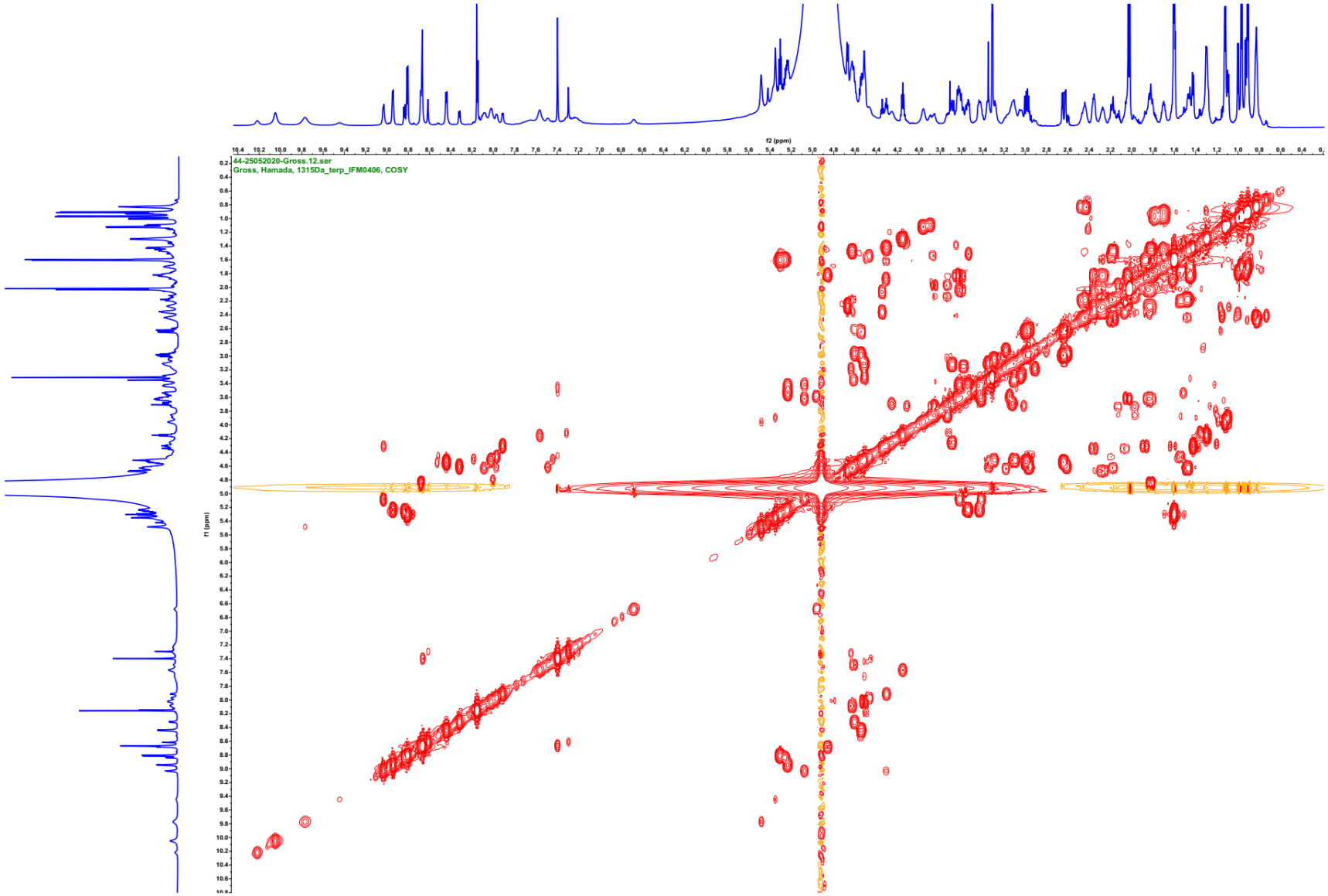

Figure S54. ^{1}H-^{1}H COSY spectrum of nocathioamide A (**1**) (d_3-CH_3OH, 700/700 MHz)

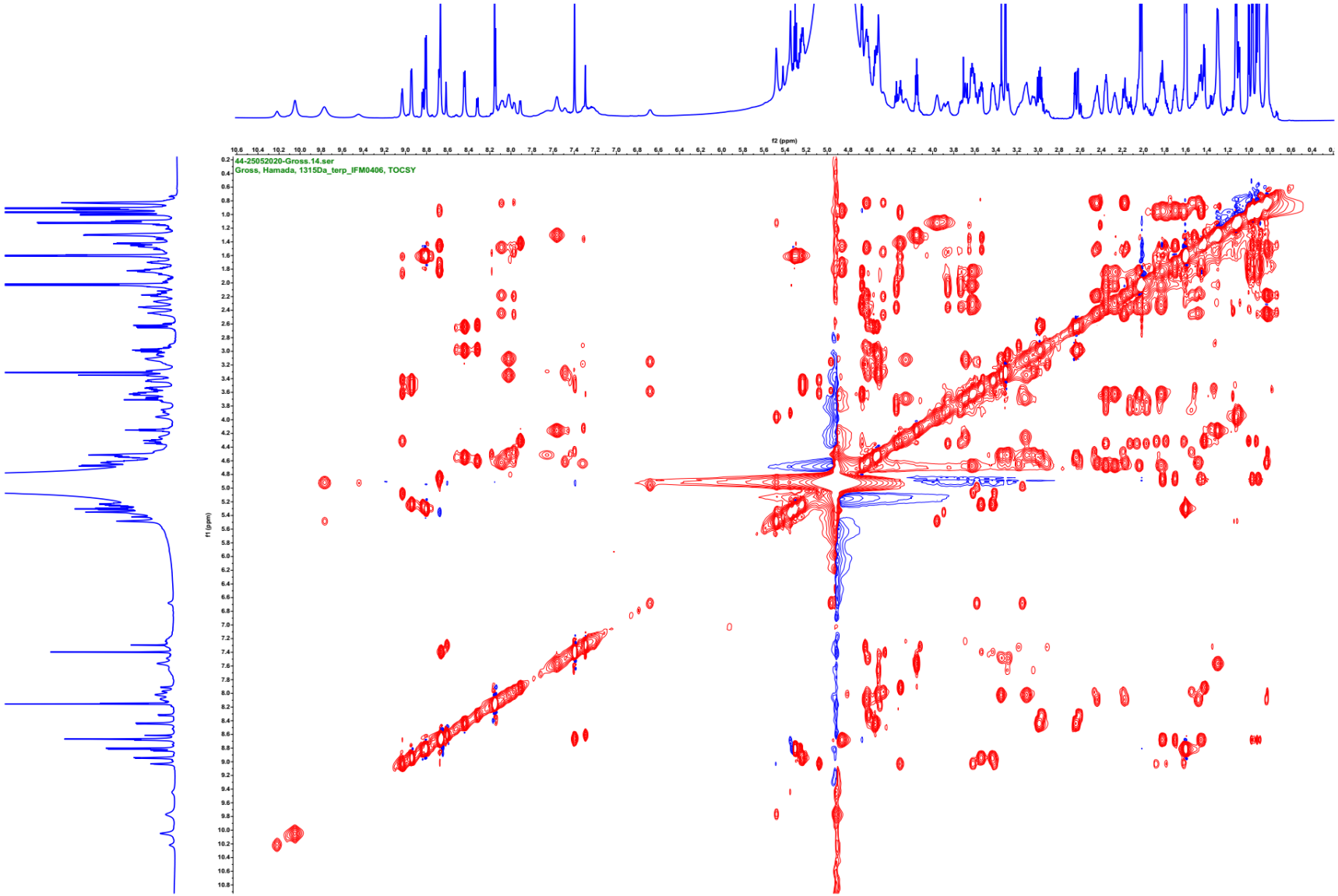

Figure S55. ^{1}H-^{1}H TOCSY spectrum of nocathioamide A (**1**) (d_3-CH_3OH, 700/700 MHz)

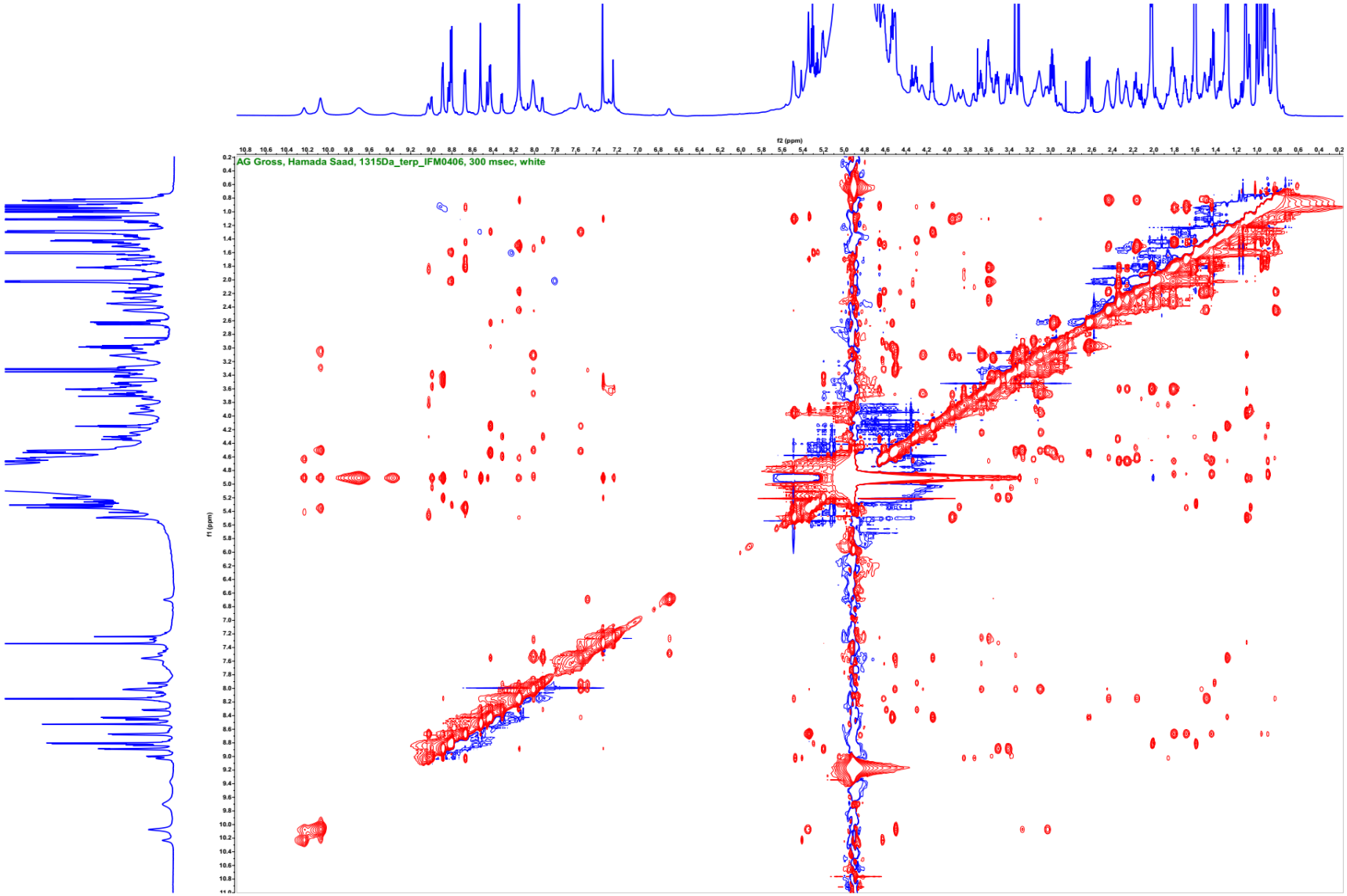

Figure S56. ^{1}H-^{1}H NOESY spectrum of nocathioamide A (**1**) (d_3-CH_3OH, 700/700 MHz; d8 = 300 msec)

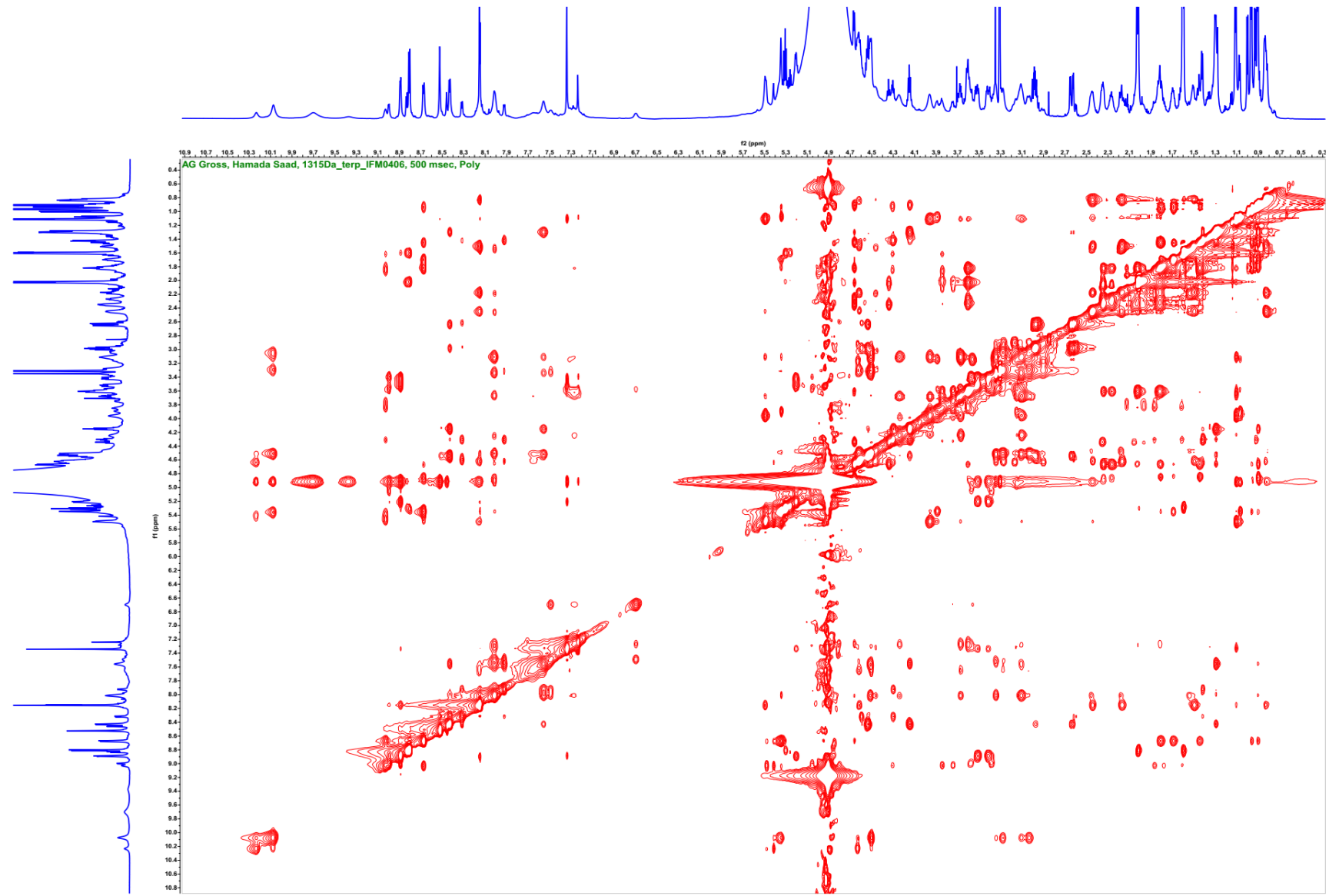

Figure S57. ^{1}H-^{1}H NOESY spectrum of nocathioamide A (**1**) (d_3-CH_3OH, 700/700 MHz; d8 = 500 msec)

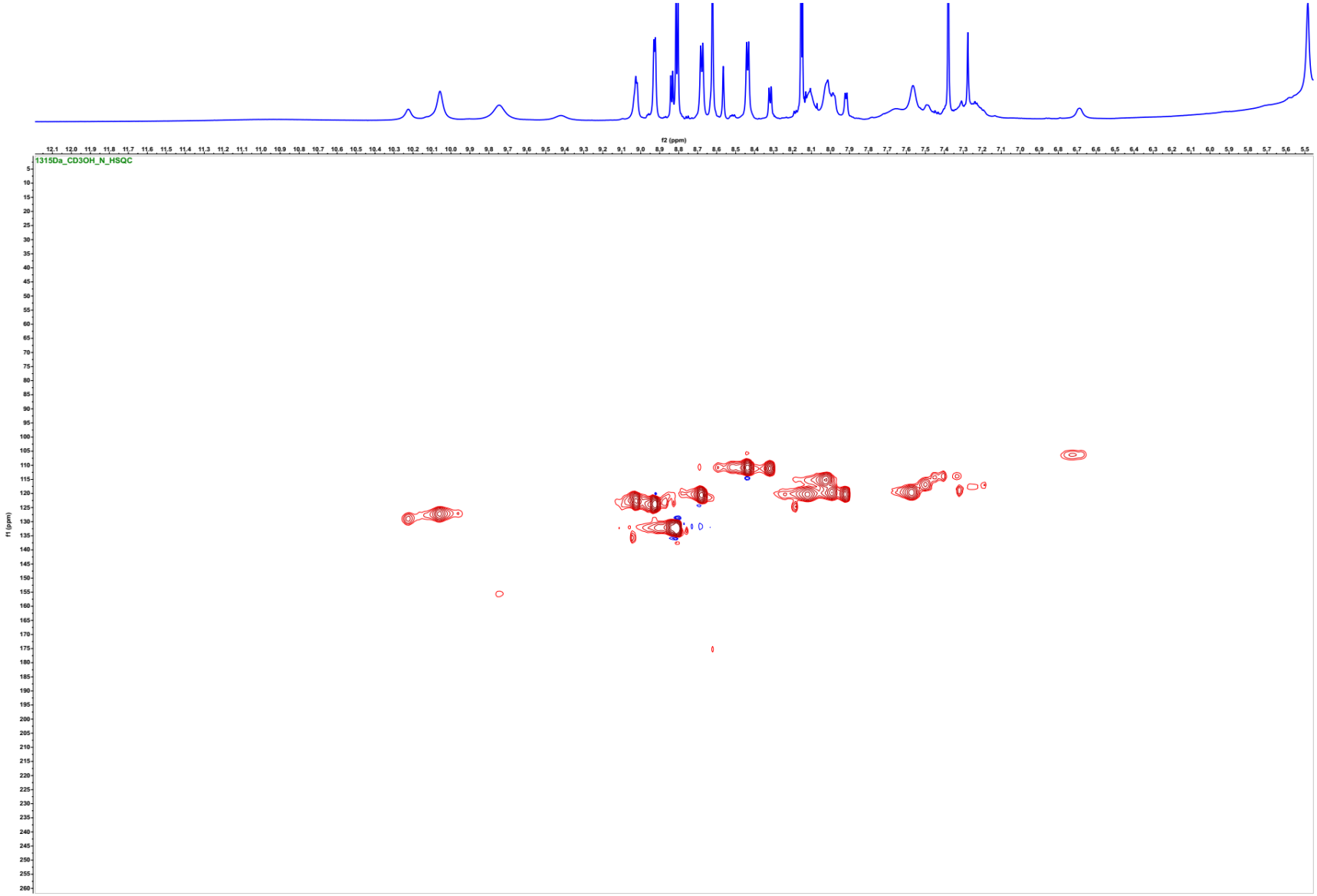

Figure S58. ^{1}H-^{15}N HSQC spectrum of nocathioamide A (**1**) (d_3-CH_3OH, 700/71 MHz)

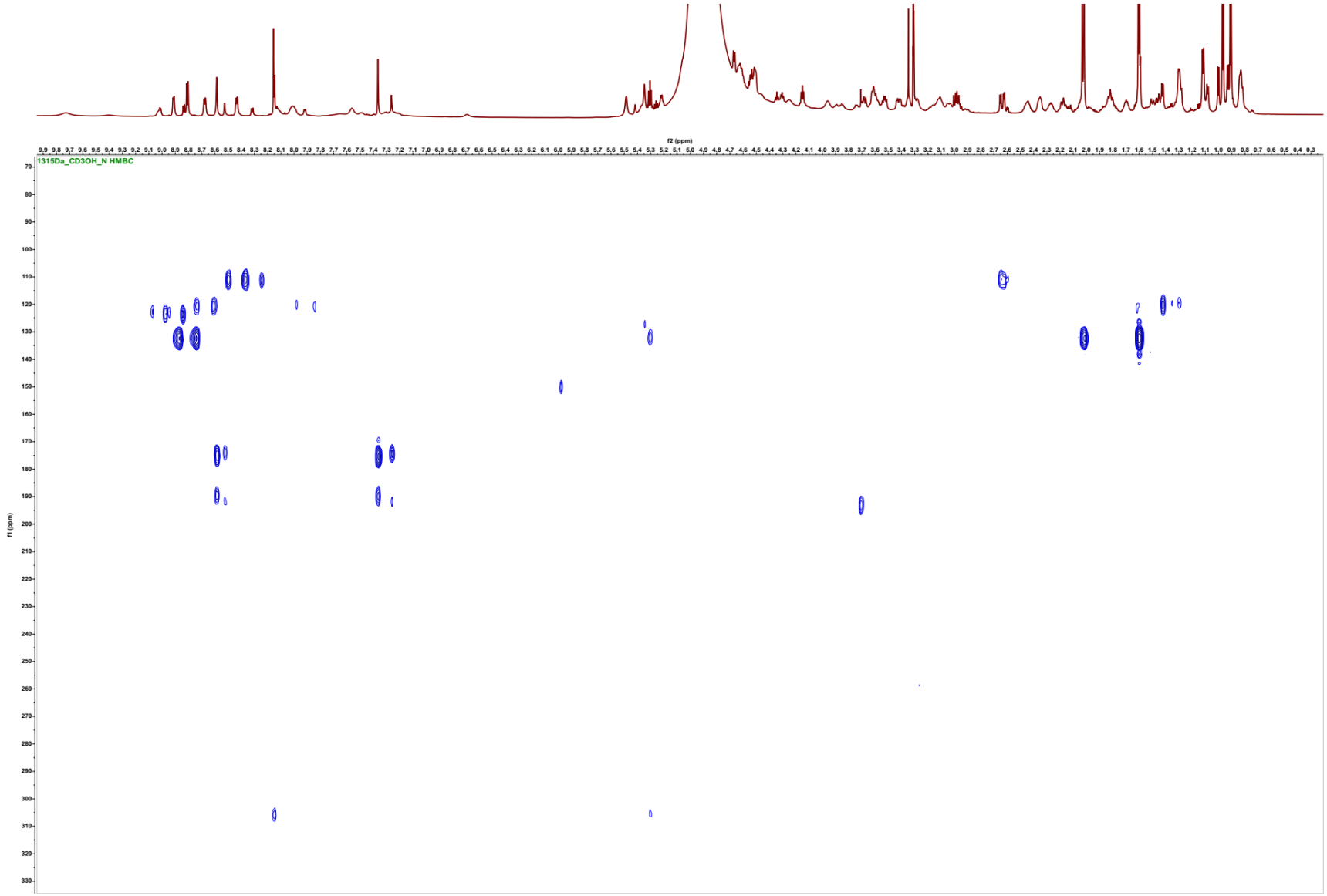

Figure S59. ^{1}H-^{15}N HMBC spectrum of nocathioamide A (**1**) (d_3-CH_3OH, 700/71 MHz)

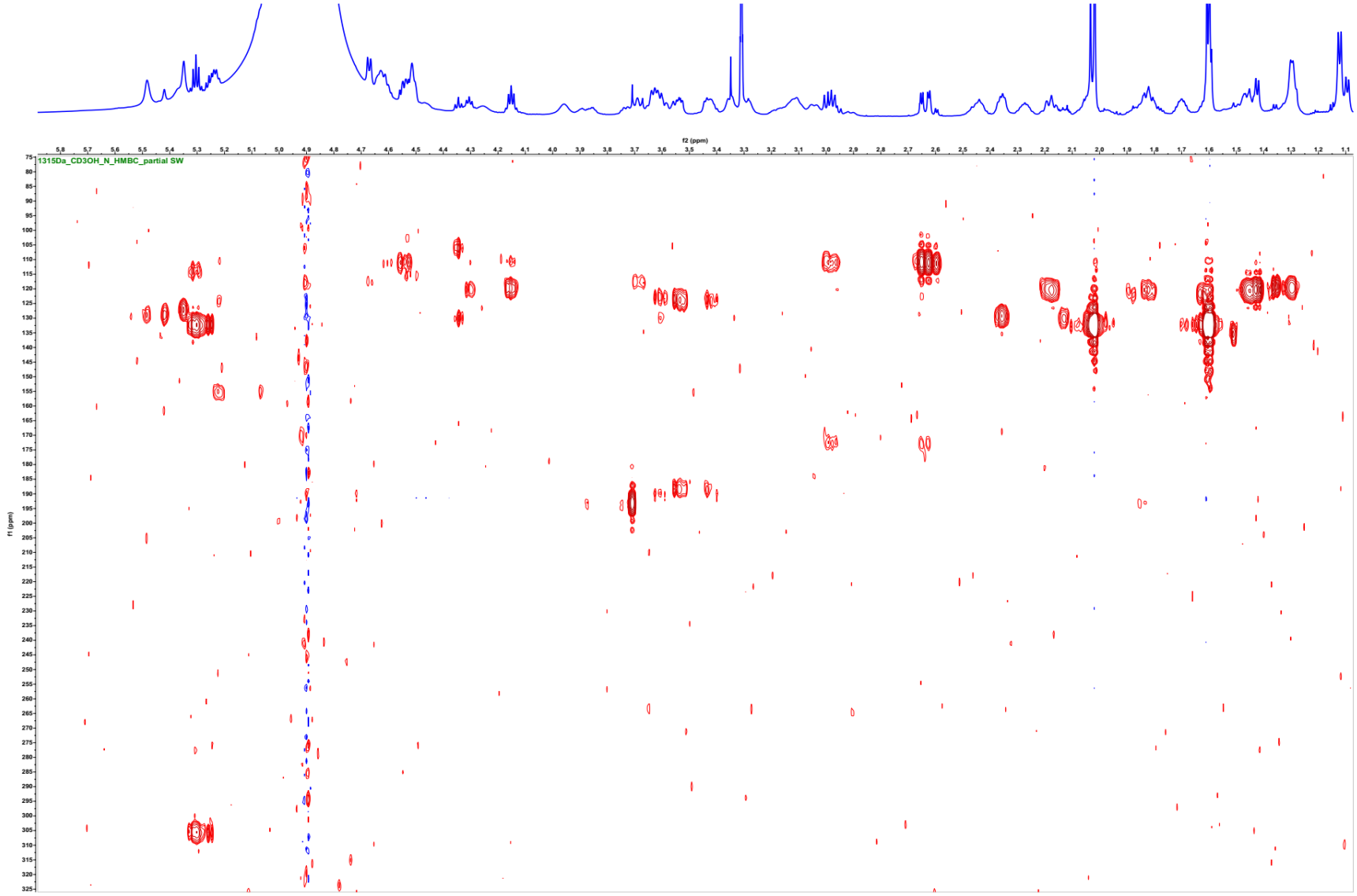

Figure S60. ^{1}H-^{15}N HMBC partial SW spectrum of nocathioamide A (**1**) (d_3-CH_3OH, 700/71 MHz)

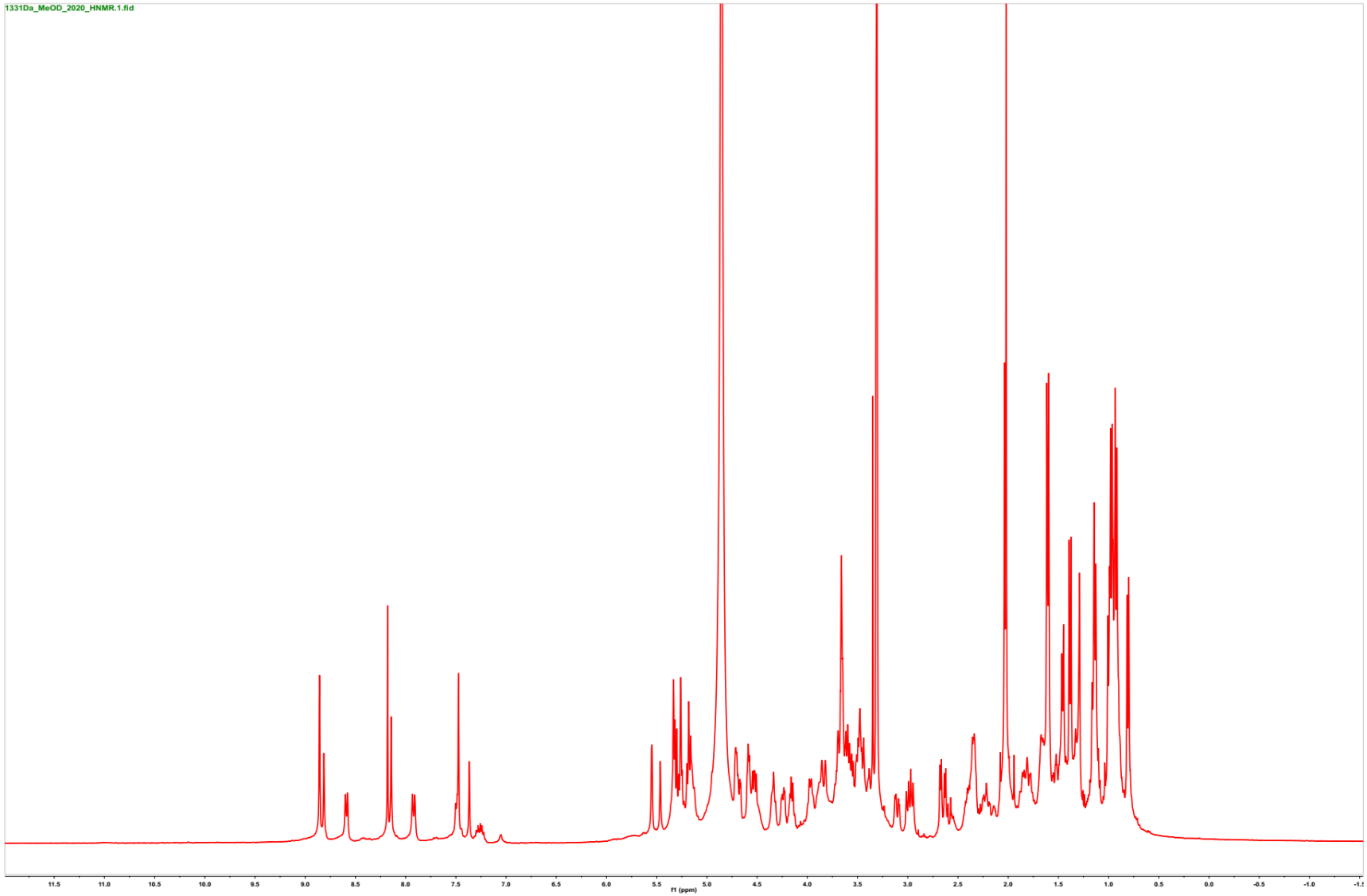

Figure S61. ^{1}H-NMR spectrum of nocathioamide B (**2**) (d_4-CH_3OH, 400 MHz)

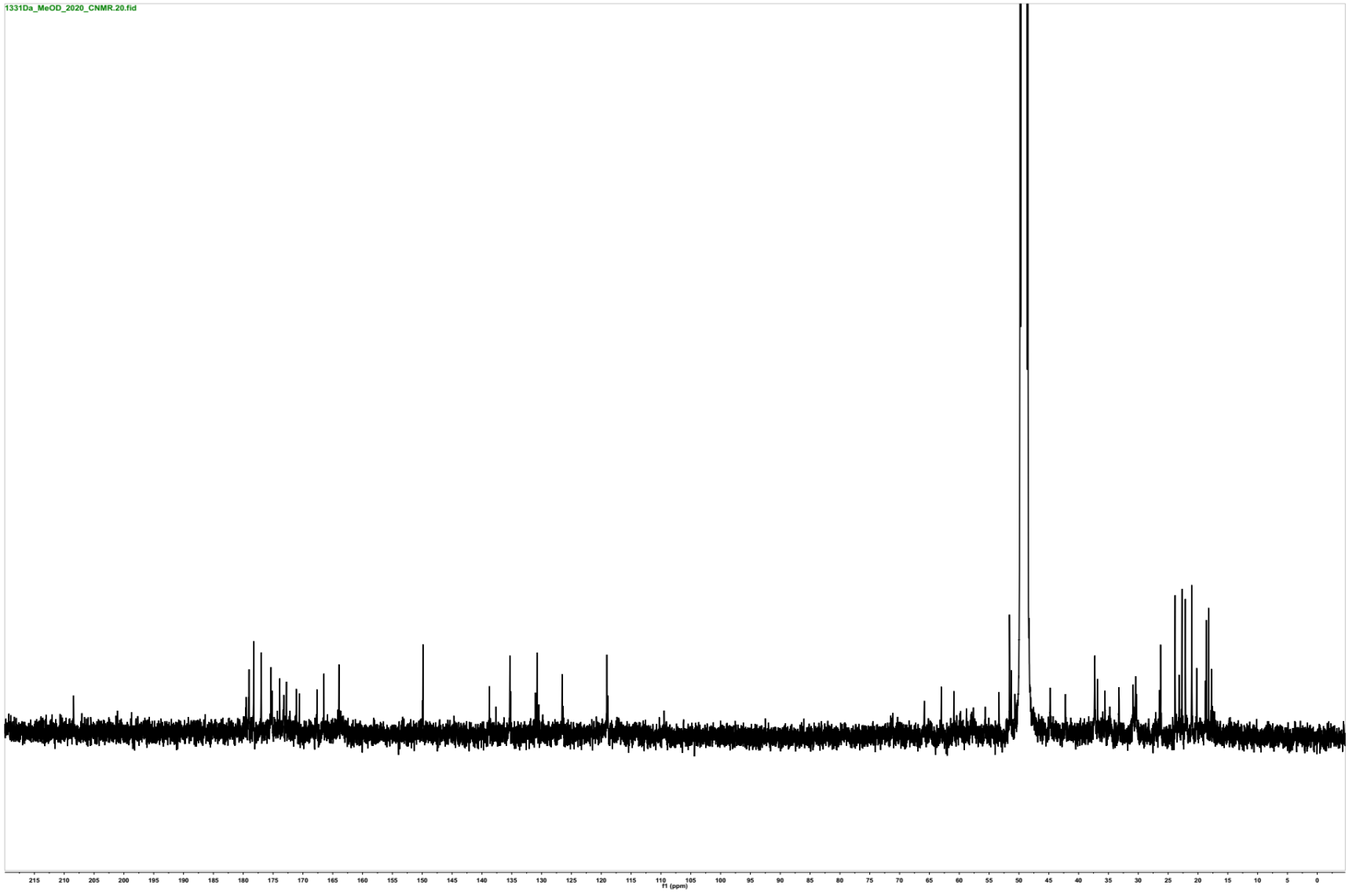

Figure S62. ^{13}C-NMR spectrum of nocathioamide B (**2**) (d_4-CH_3OH, 100 MHz)

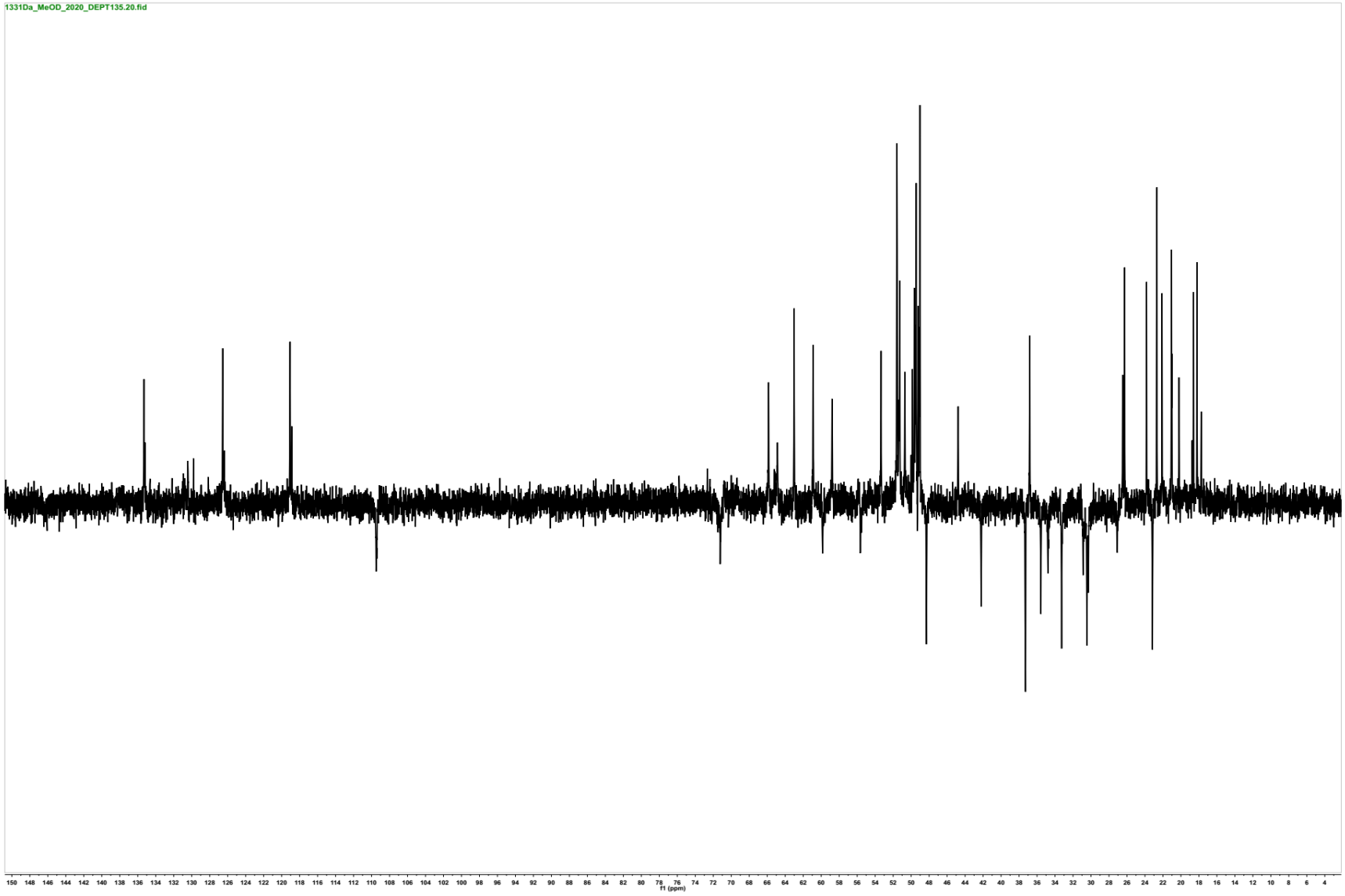

Figure S63. DEPT-135 spectrum of nocathioamide B (**2**) (d_4-CH_3OH, 100 MHz)

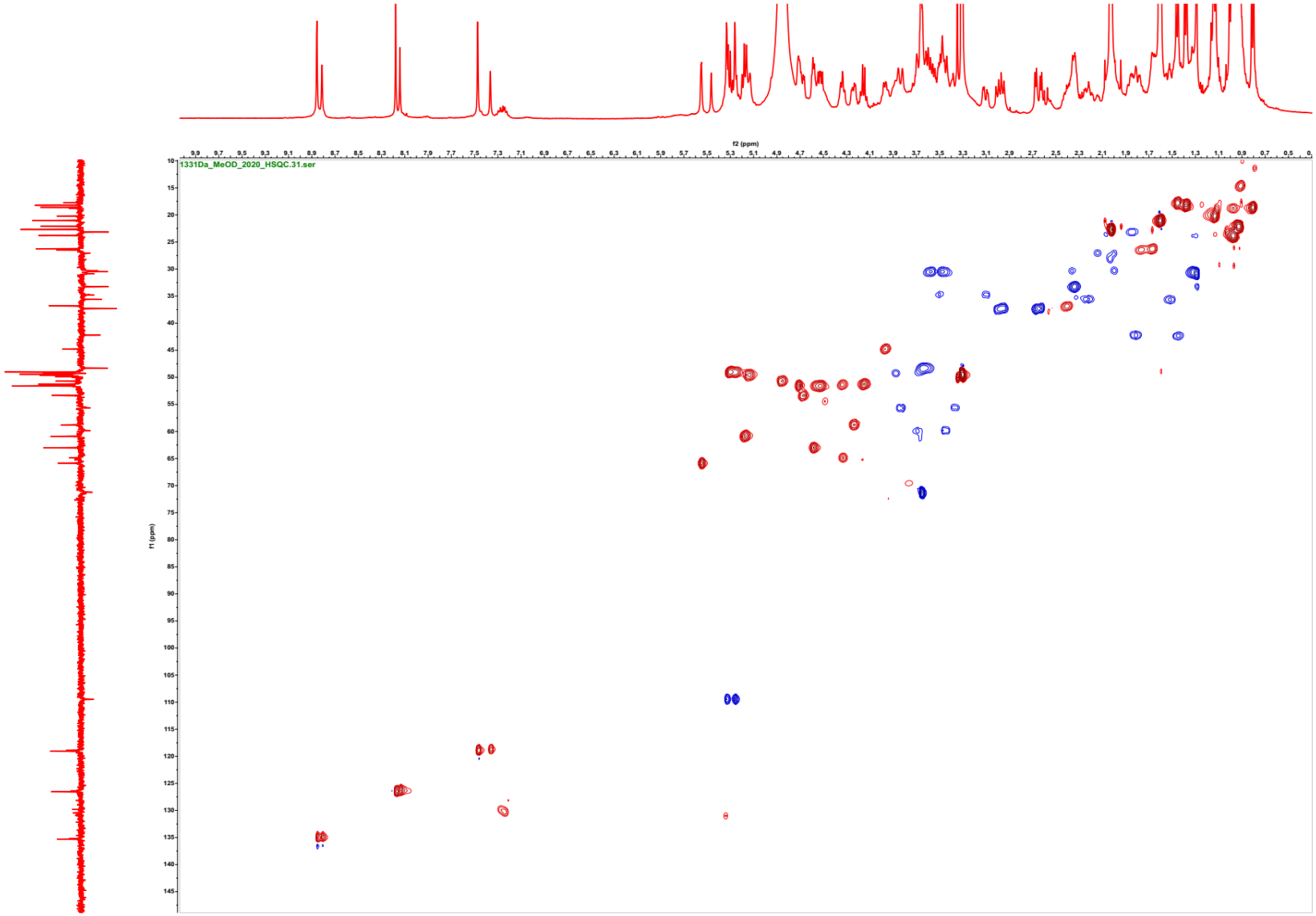

Figure S64. ^{1}H-^{13}C HSQC spectrum of nocathioamide B (**2**) (d_4-CH_3OH, 400/100 MHz)

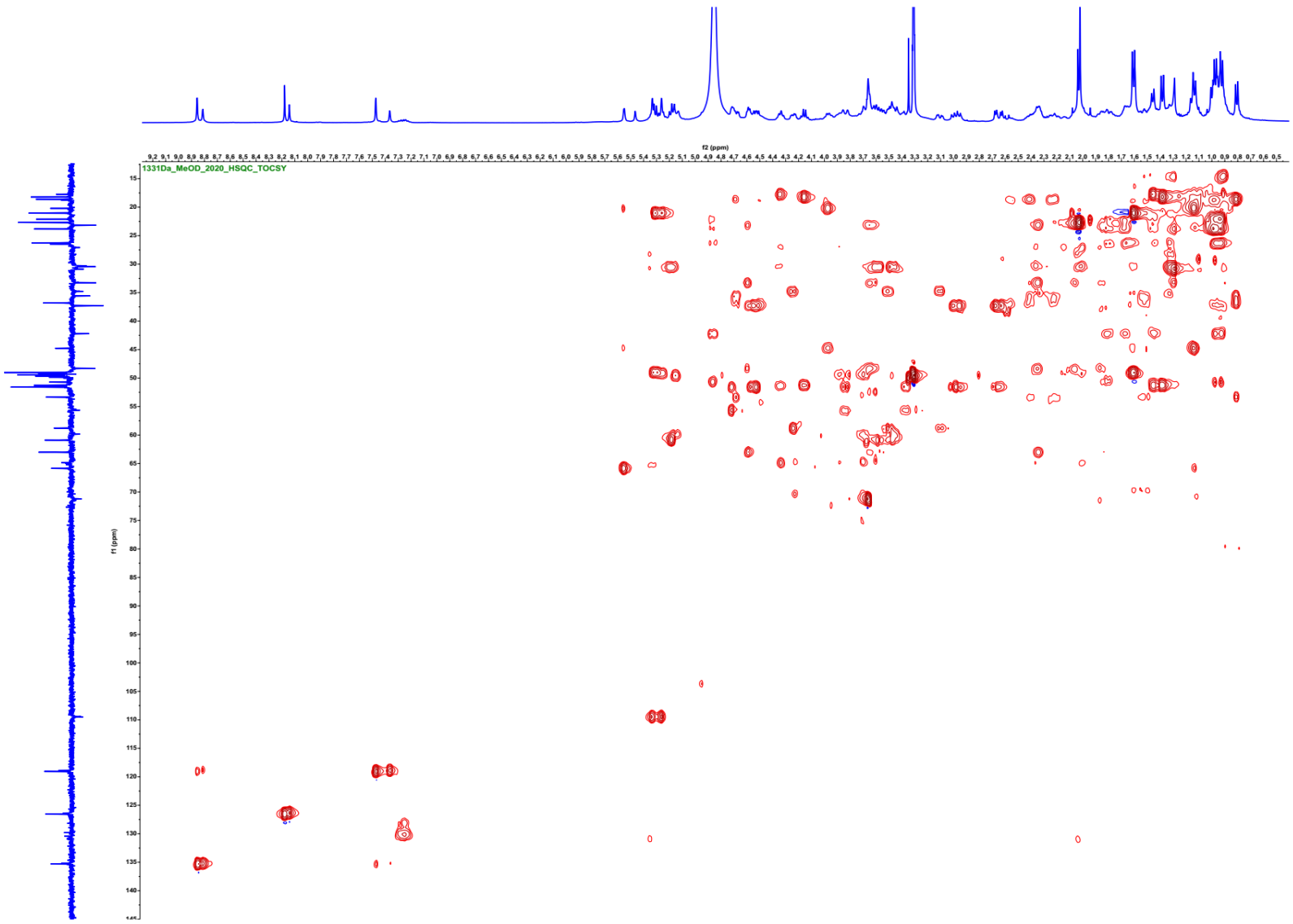

Figure S65. ^{1}H-^{13}C HSQC-TOCSY spectrum of nocathioamide B (**2**) (d_4-CH_3OH, 400/100 MHz)

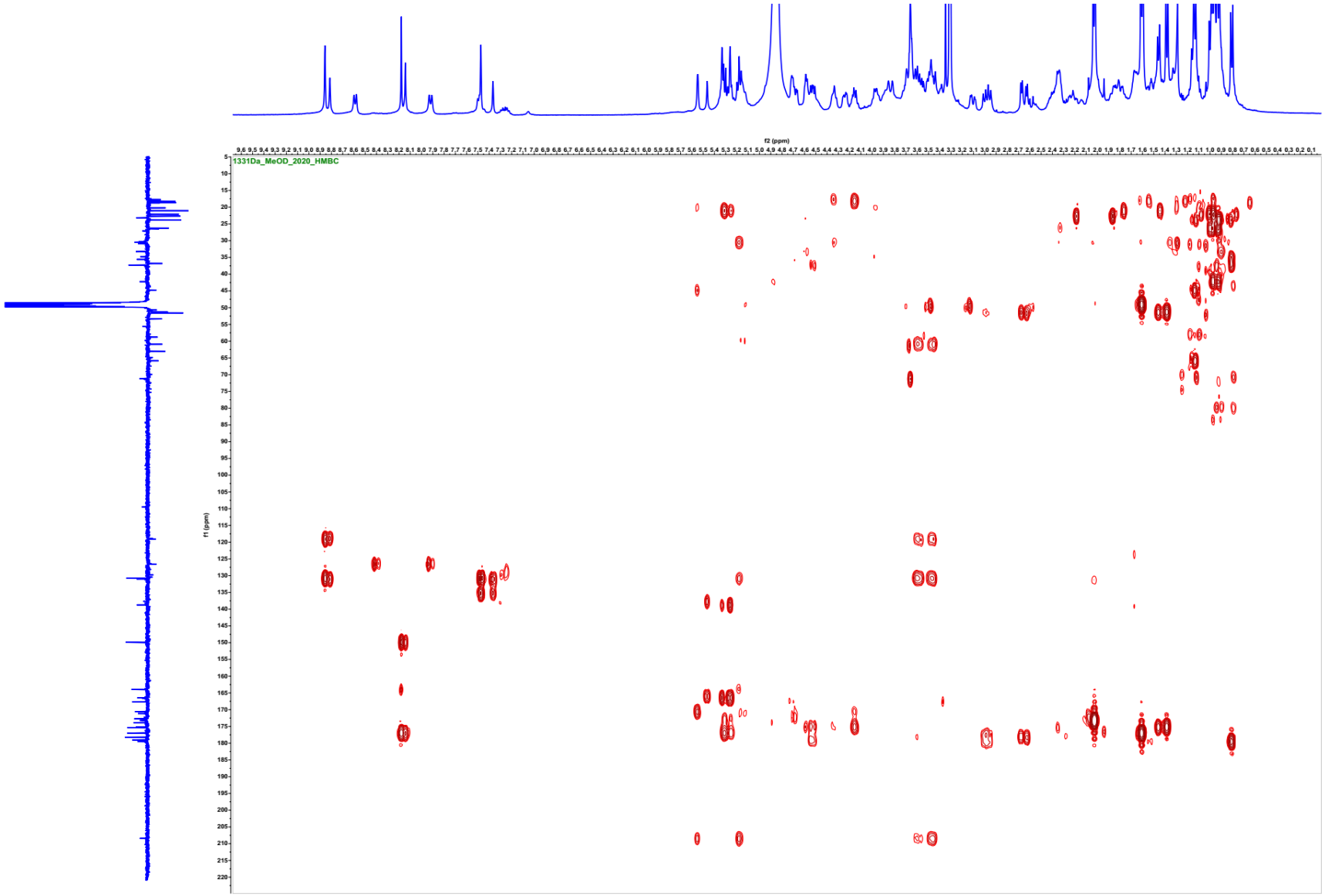

Figure S66. ^{1}H-^{13}C HMBC spectrum of nocathioamide B (**2**) (d_4-CH_3OH, 400/100 MHz)

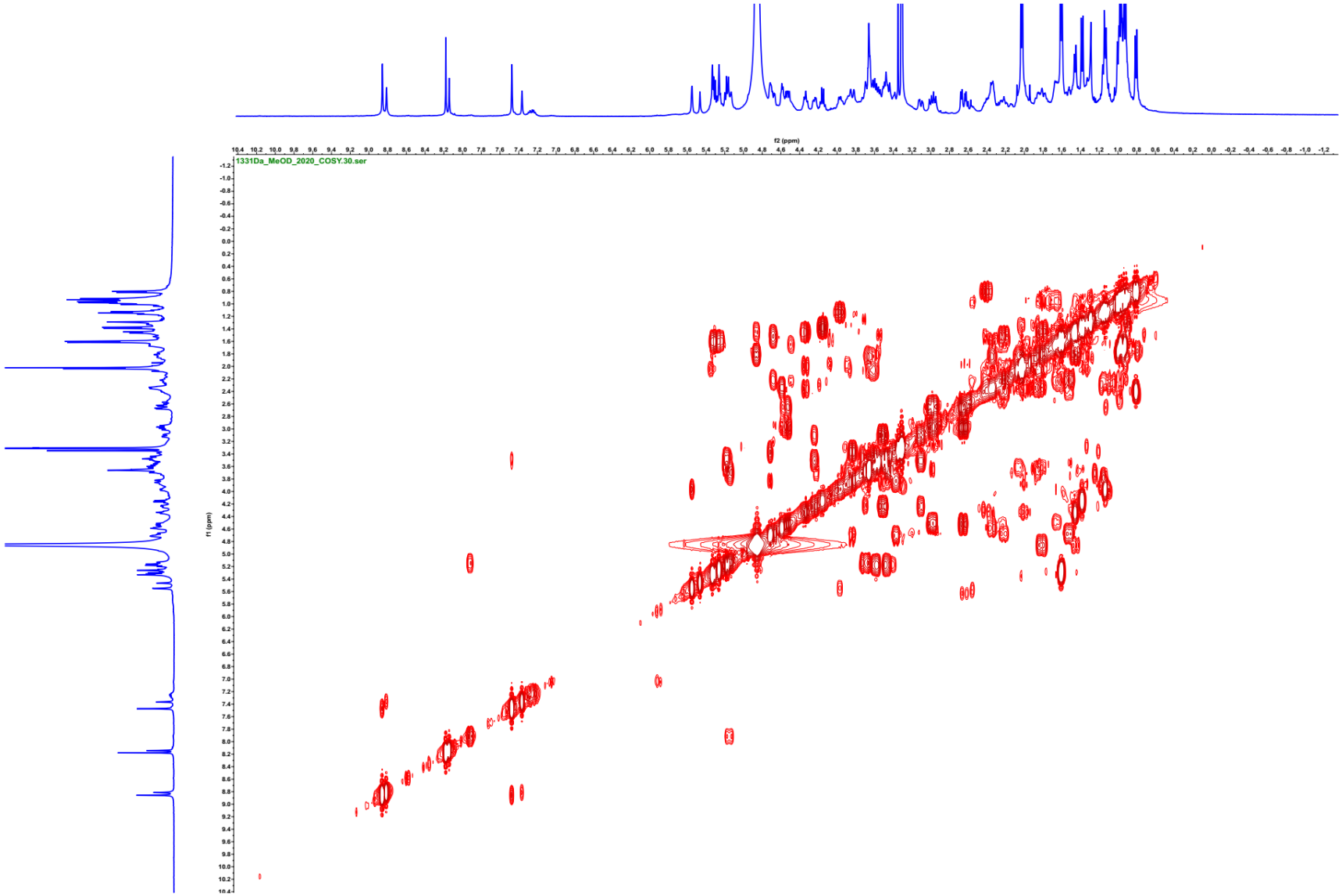

Figure S67. ^{1}H-^{1}H COSY spectrum of nocathioamide B (**2**) (d_4-CH_3OH, 400/400 MHz)

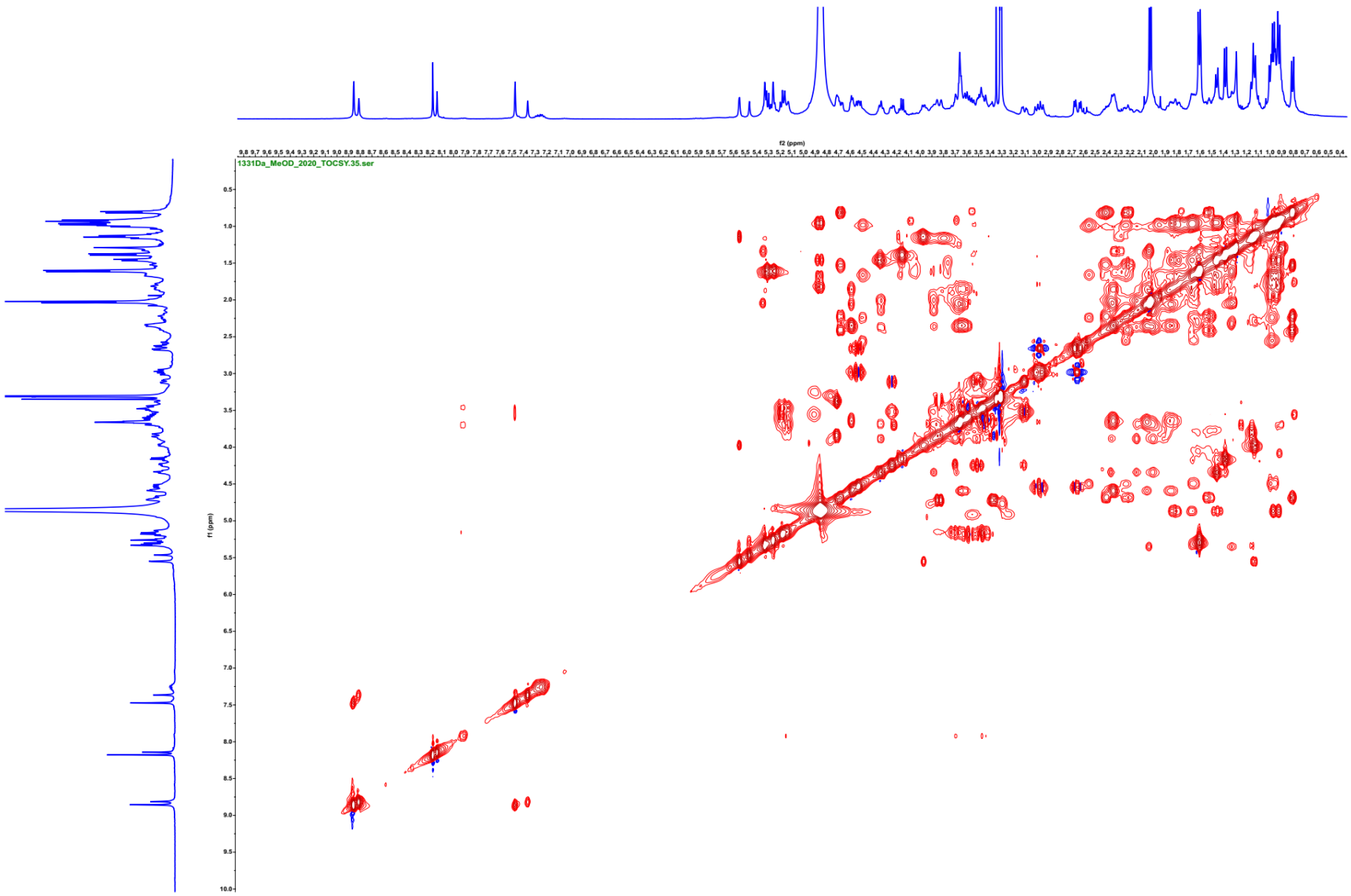

Figure S68. ^{1}H-^{1}H TOCSY spectrum of nocathioamide B (**2**) (d_4-CH_3OH, 400/400 MHz)

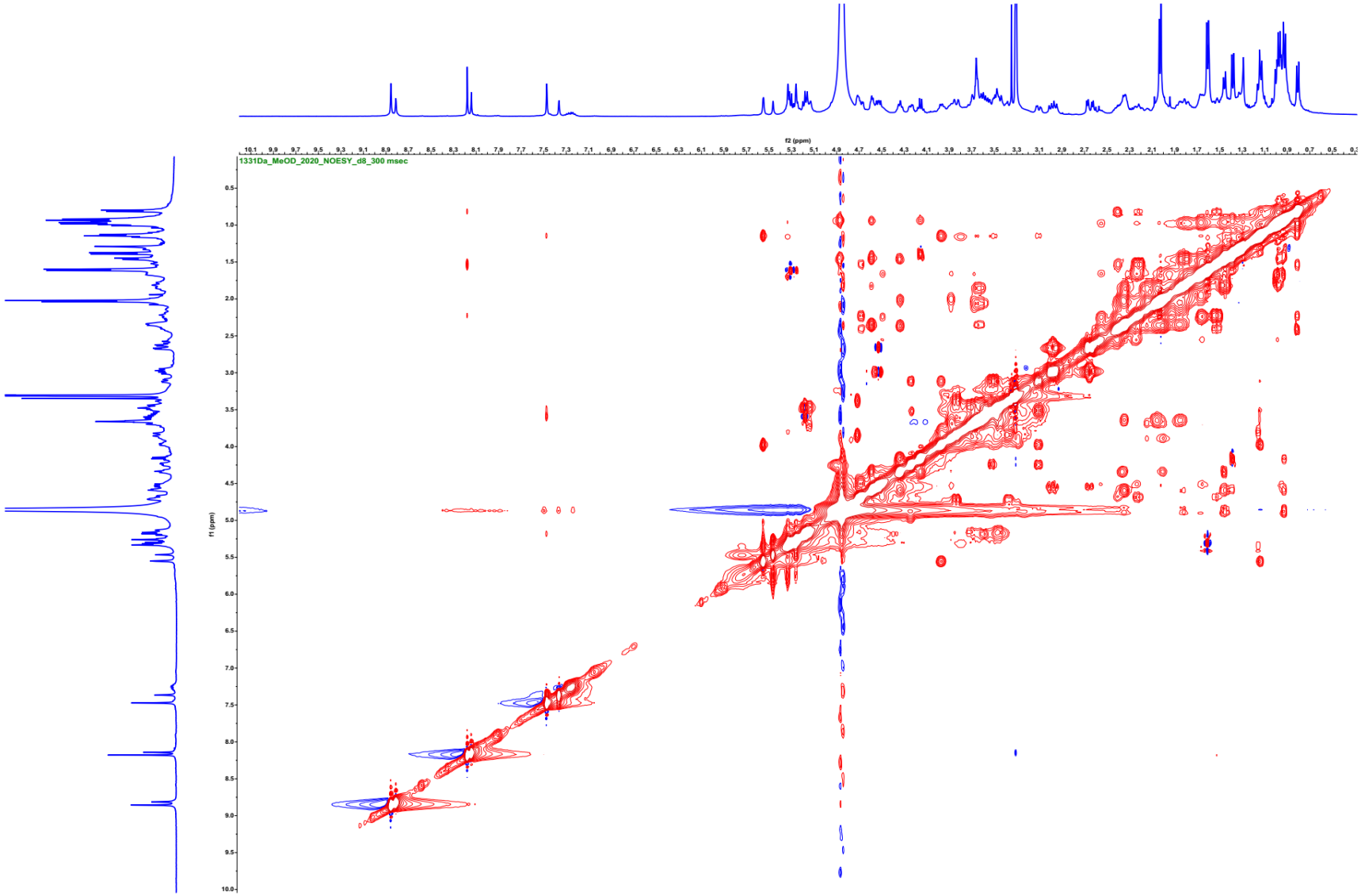

Figure S69. ^{1}H-^{1}H NOESY spectrum of nocathioamide B (**2**) (d_4-CH_3OH, 400/400 MHz, d8 = 300 msec)

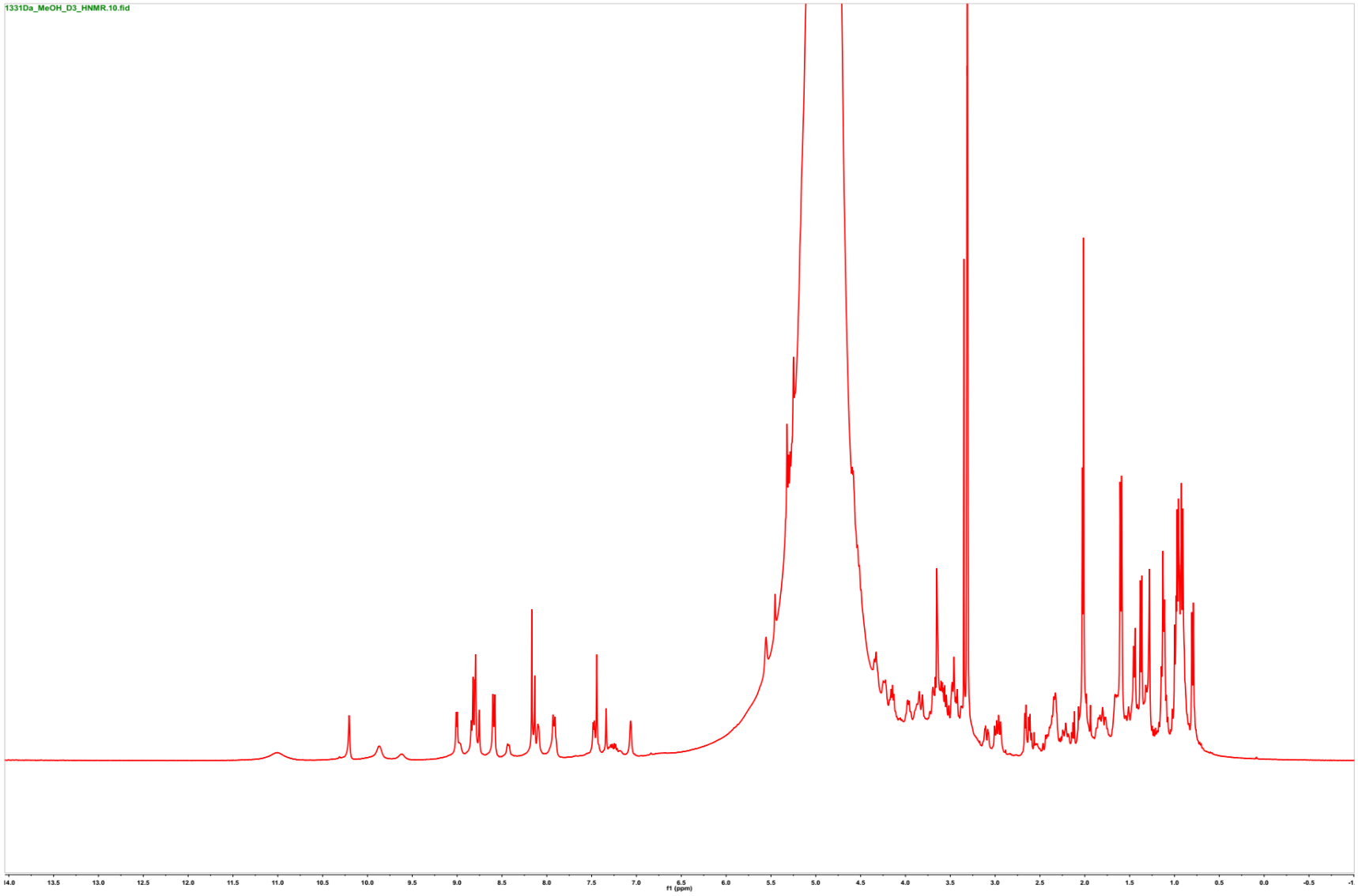

Figure S70. ^{1}H-NMR spectrum of nocathioamide B (**2**) (d_3-CH_3OH, 400 MHz)

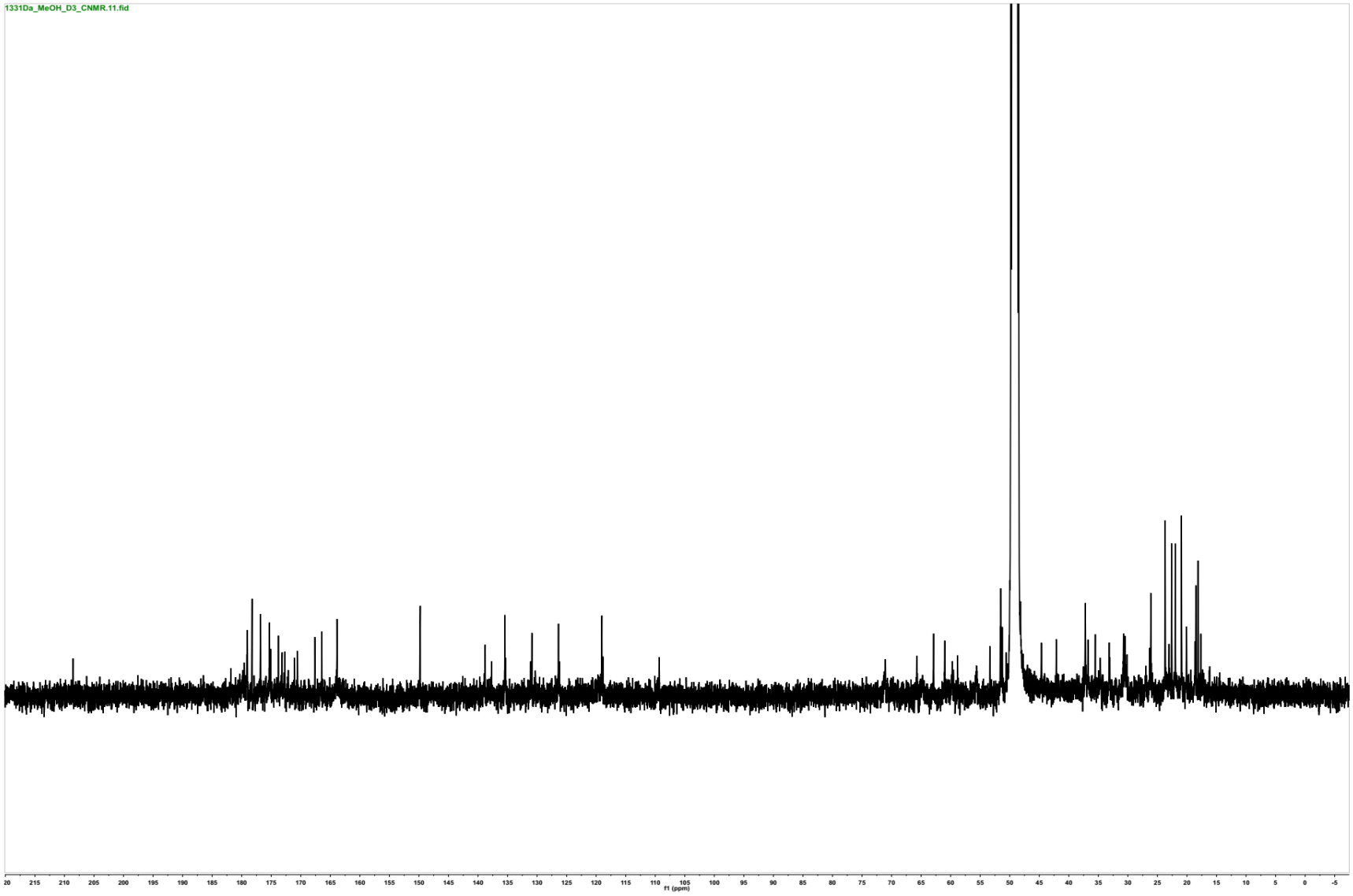

Figure S71. ^{13}C-NMR spectrum of nocathioamide B (**2**) (d_3-CH_3OH, 100 MHz)

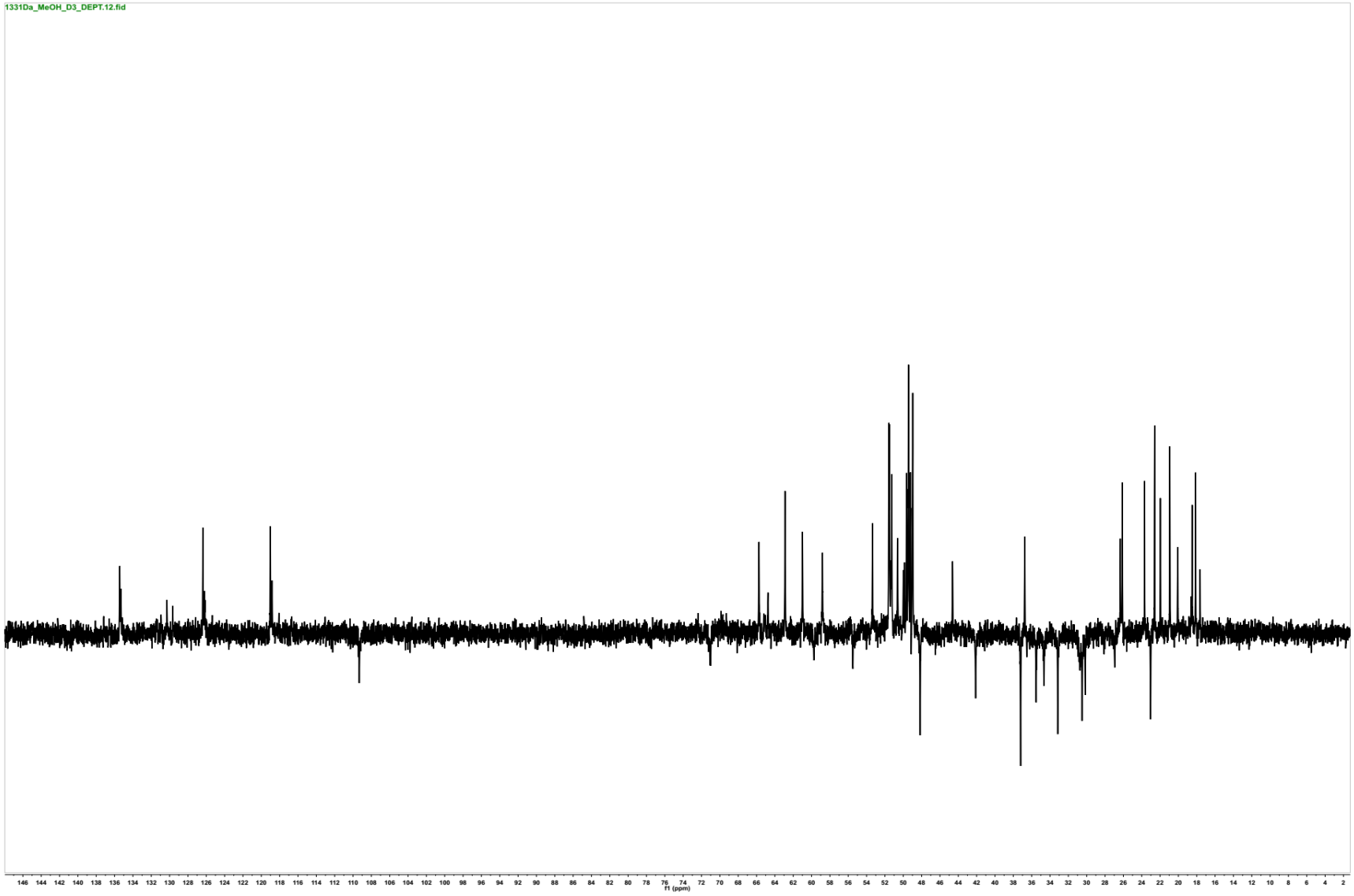

Figure S72. DEPT-135 spectrum of nocathioamide B (**2**) (d_3-CH_3OH, 100 MHz)

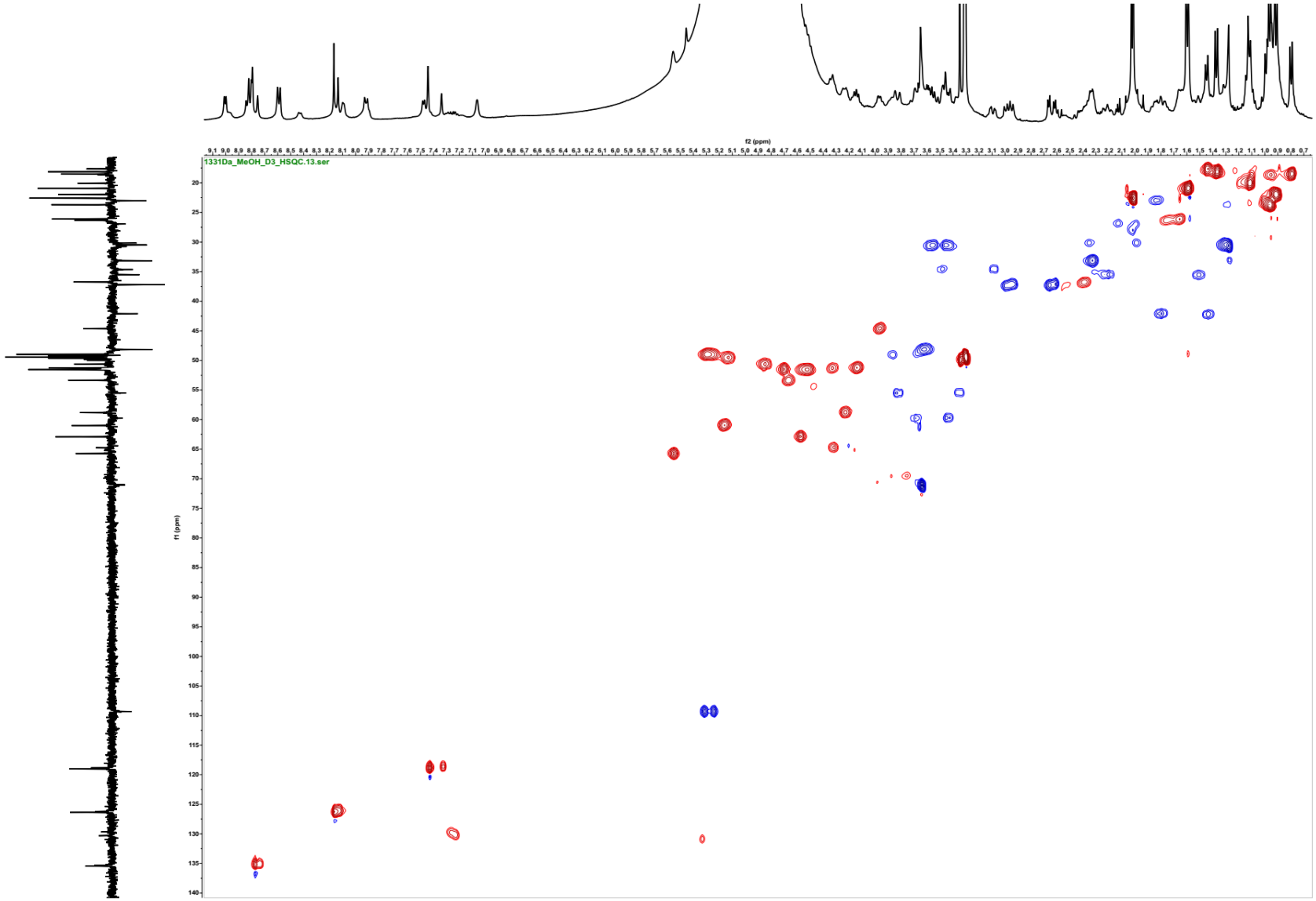

Figure S73. ^{1}H-^{13}C HSQC spectrum of nocathioamide B (**2**) (d_3-CH_3OH, 400/100 MHz)

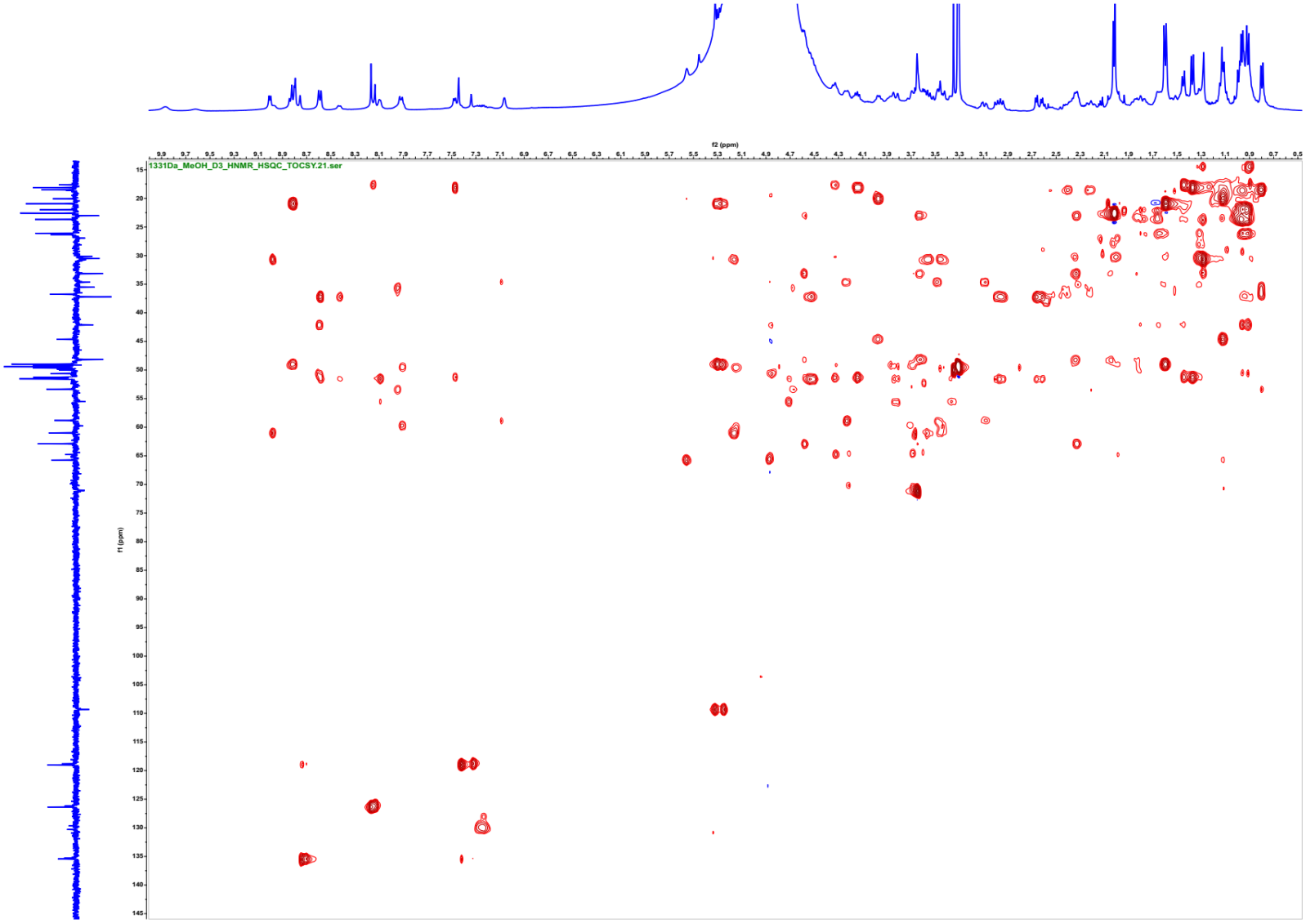

Figure S74. ^{1}H-^{13}C HSQC-TOCSY spectrum of nocathioamide B (**2**) (d_3-CH_3OH, 400/100 MHz)

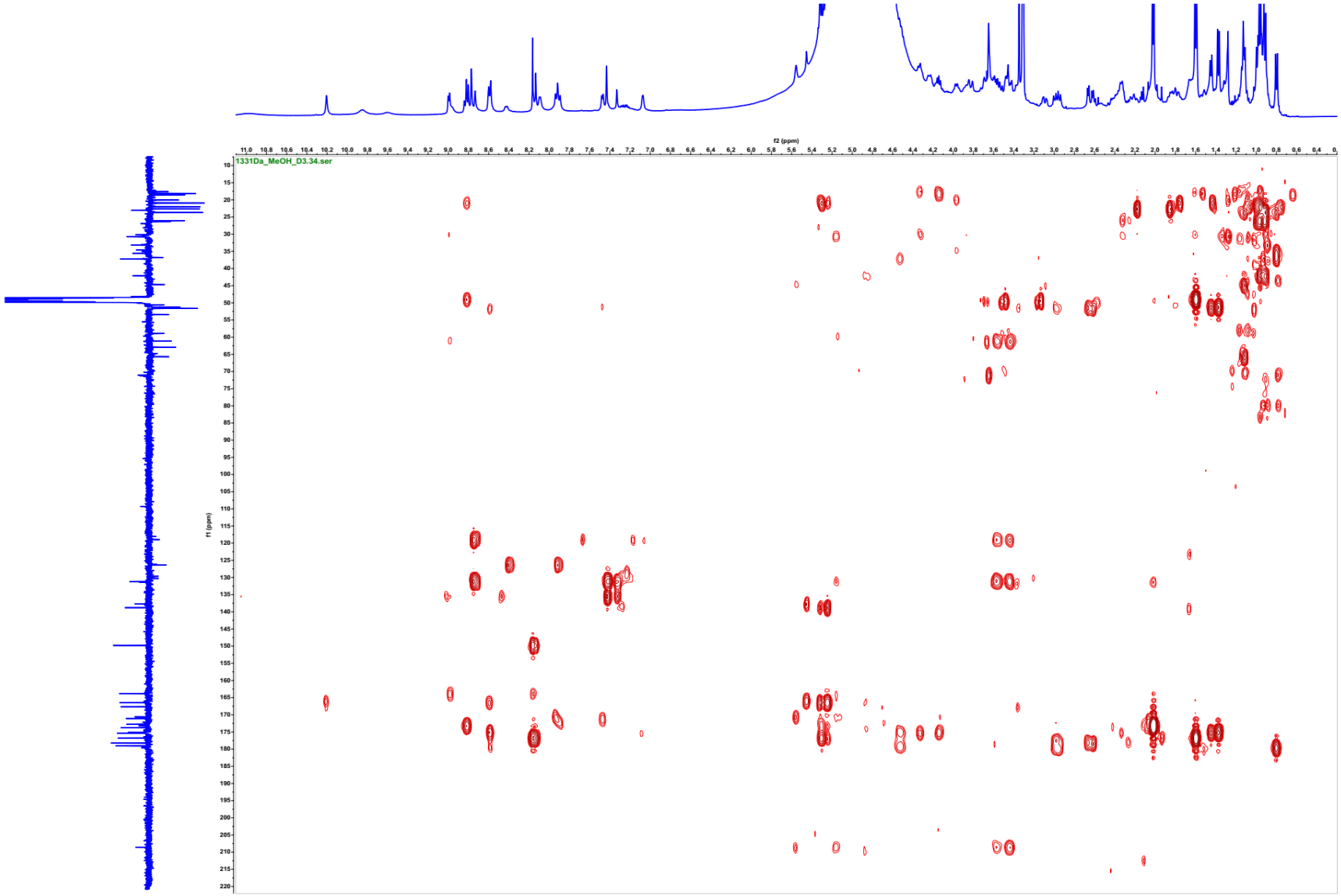

Figure S75. ^{1}H-^{13}C HMBC spectrum of nocathioamide B (**2**) (d_3-CH_3OH, 400/100 MHz)

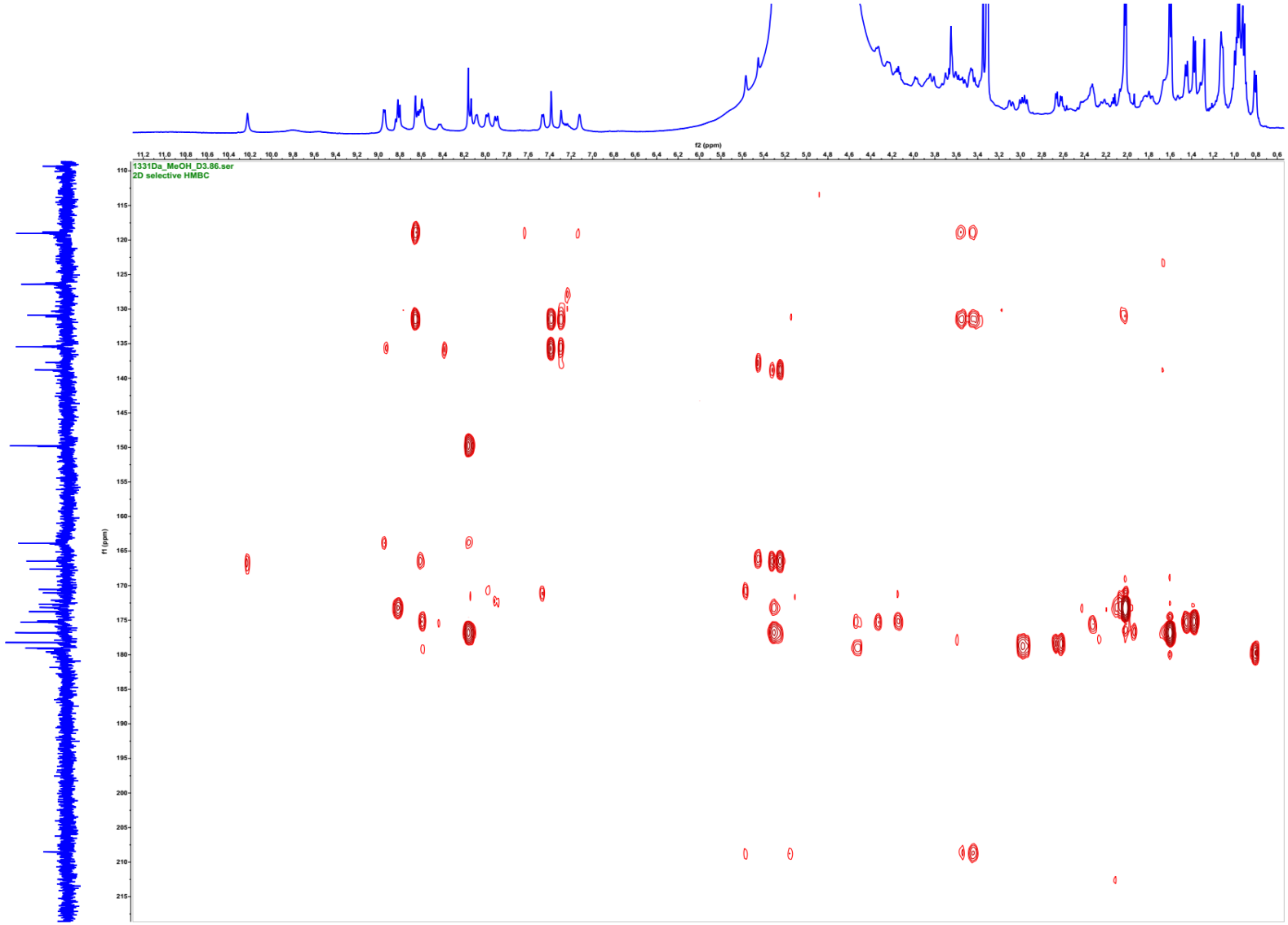

Figure S76. Band-Selective HMBC spectrum of nocathioamide B (**2**) (d_3-CH_3OH, 400/100 MHz)

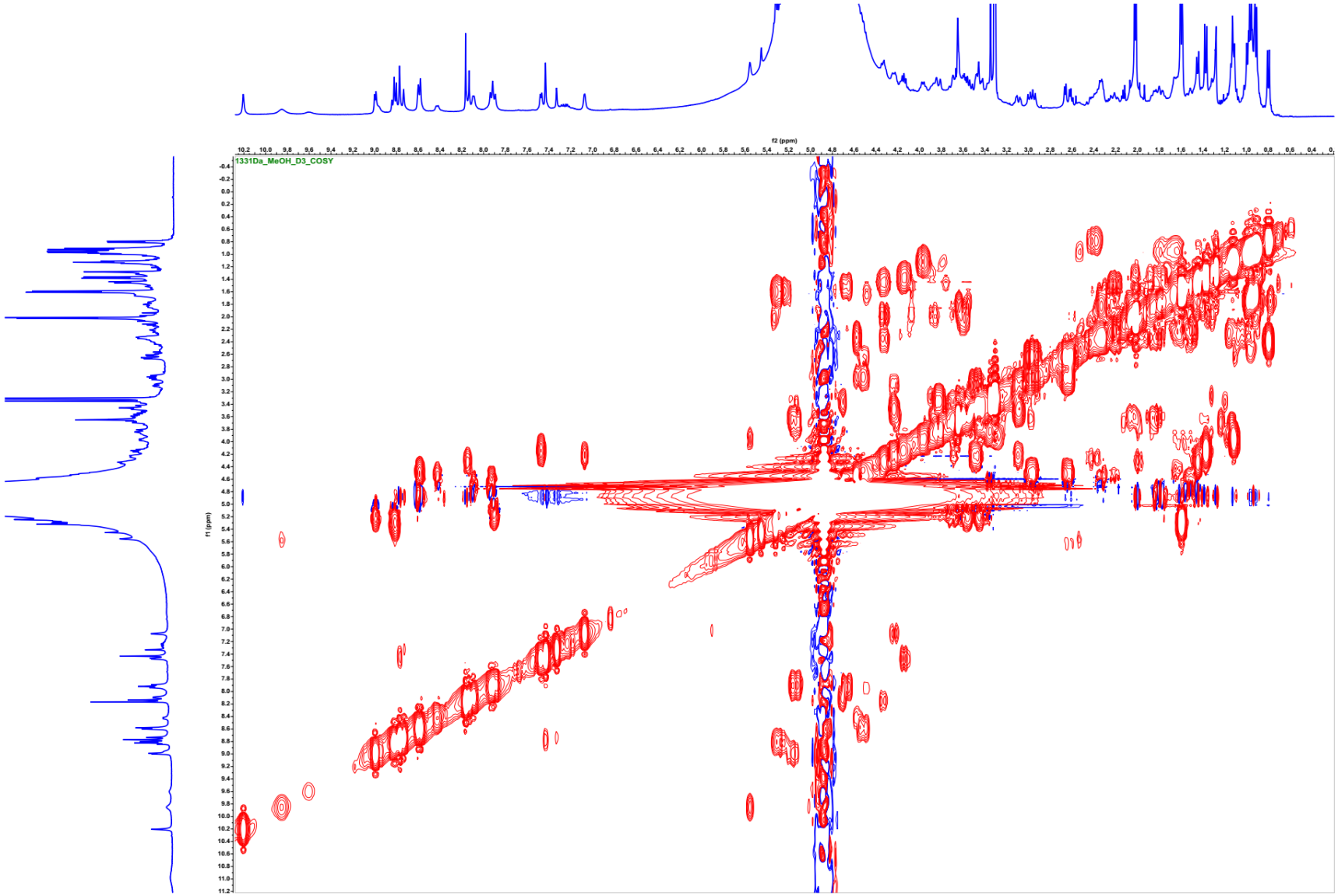

Figure S77. ^{1}H-^{1}H COSY spectrum of nocathioamide B (**2**) (d_3-CH_3OH, 400/400 MHz)

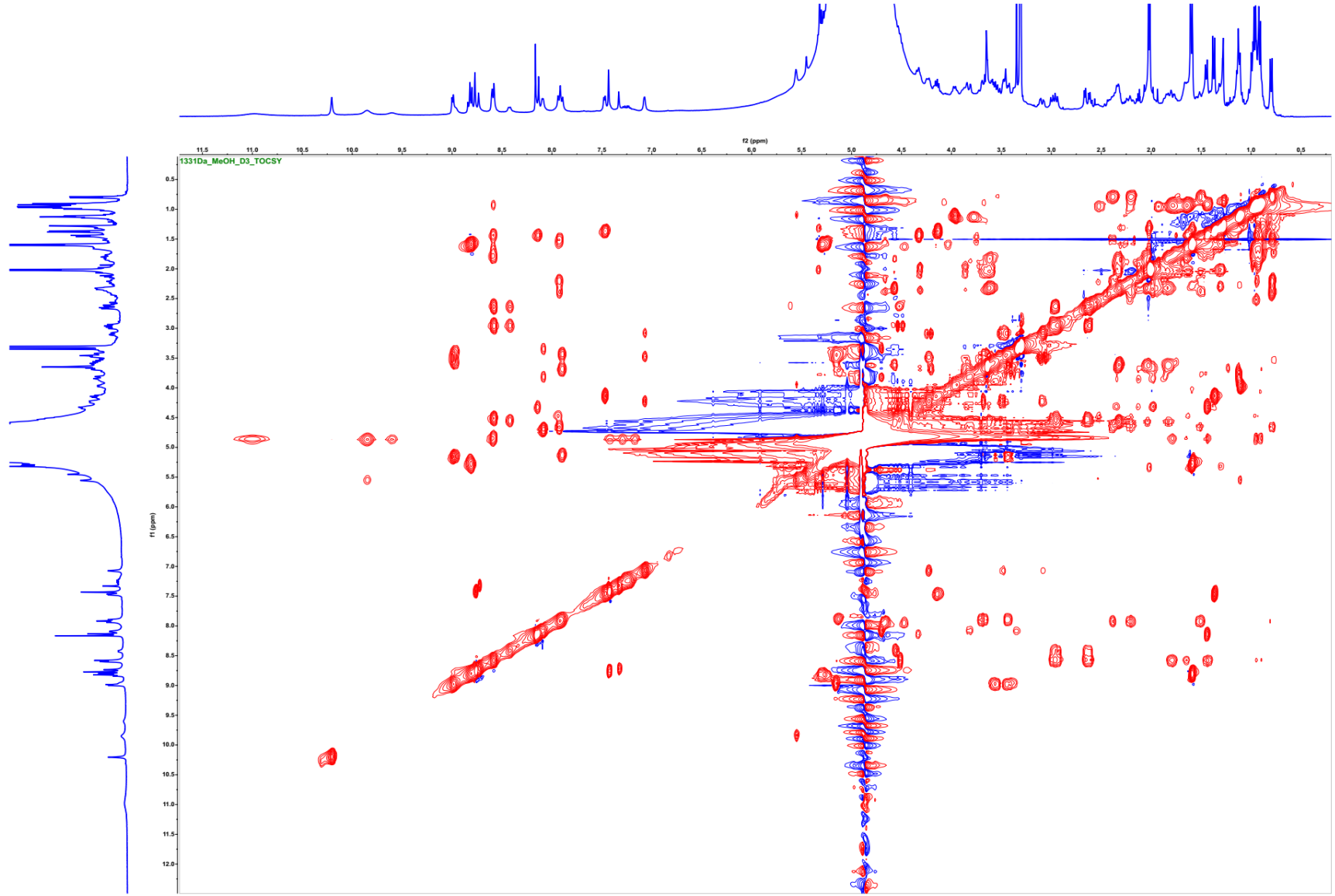

Figure S78. ^{1}H-^{1}H TOCSY spectrum of nocathioamide B (**2**) (d_3-CH_3OH, 400/400 MHz)

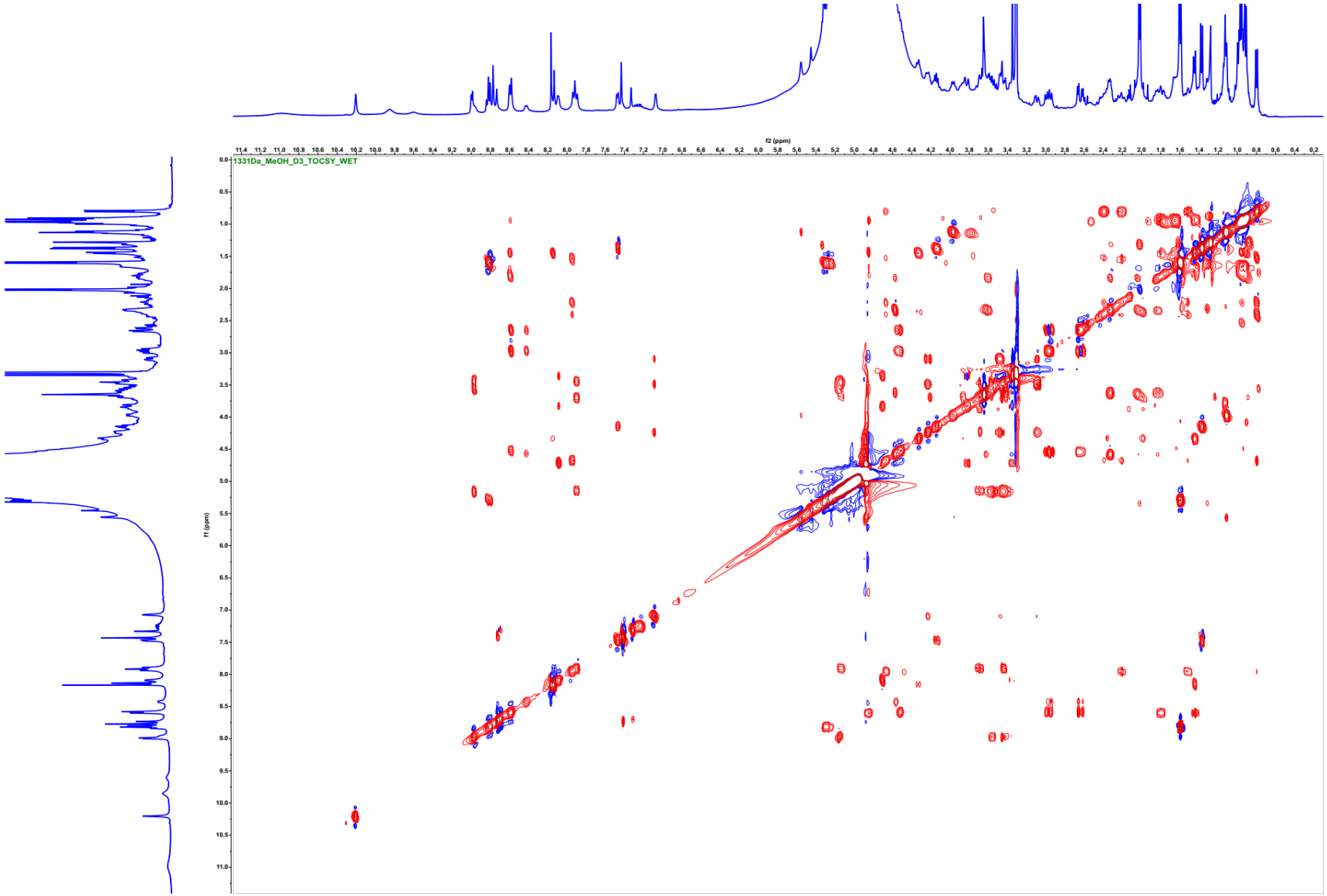

Figure S79. ^{1}H-^{1}H TOCSY WET spectrum of nocathioamide B (**2**) (d_3-CH_3OH, 400/400 MHz)

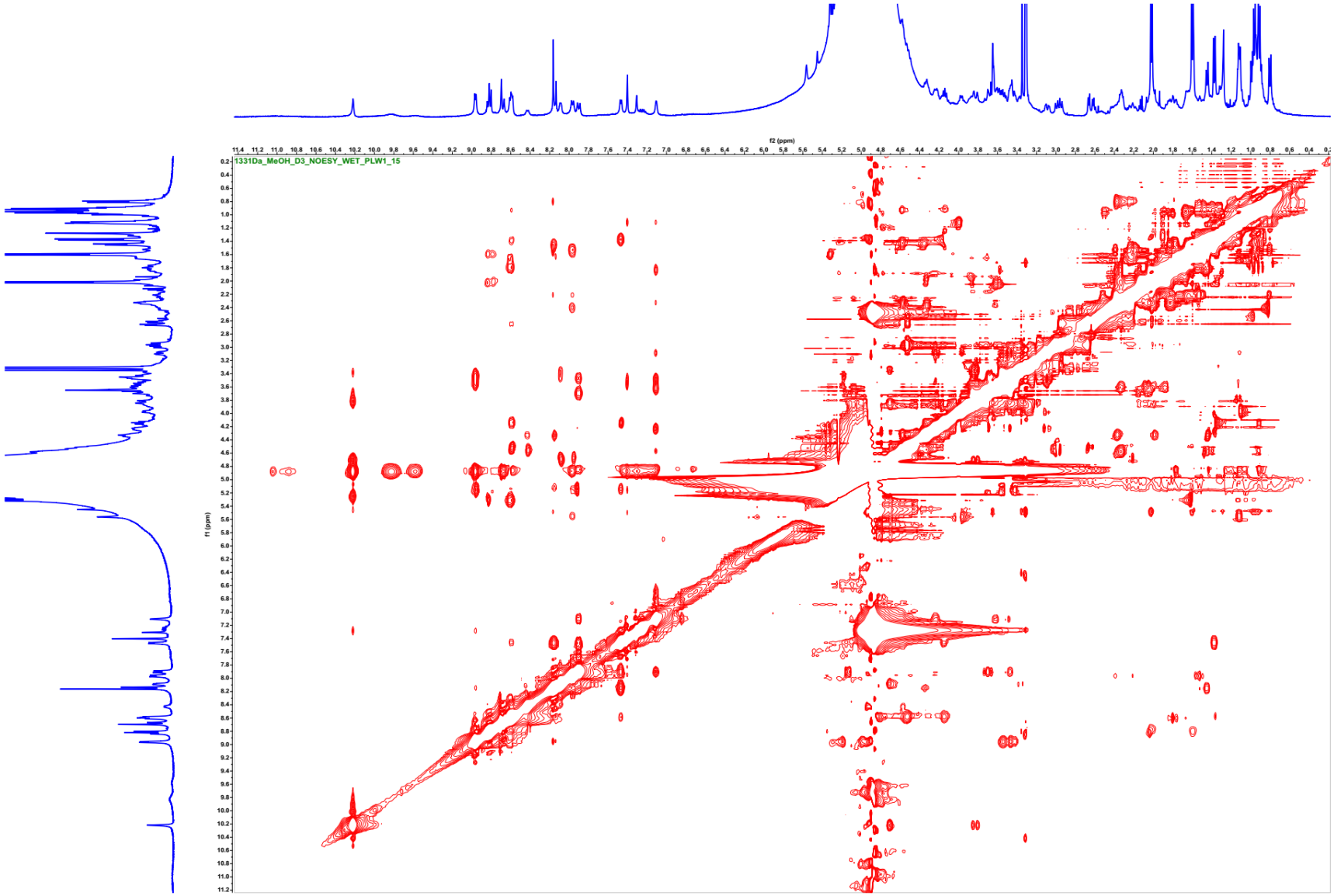

Figure S80. ^{1}H-^{1}H NOESY WET spectrum of nocathioamide B (**2**) (d_3-CH_3OH, 400/400 MHz, d8 = 300 msec, PLW1=15)

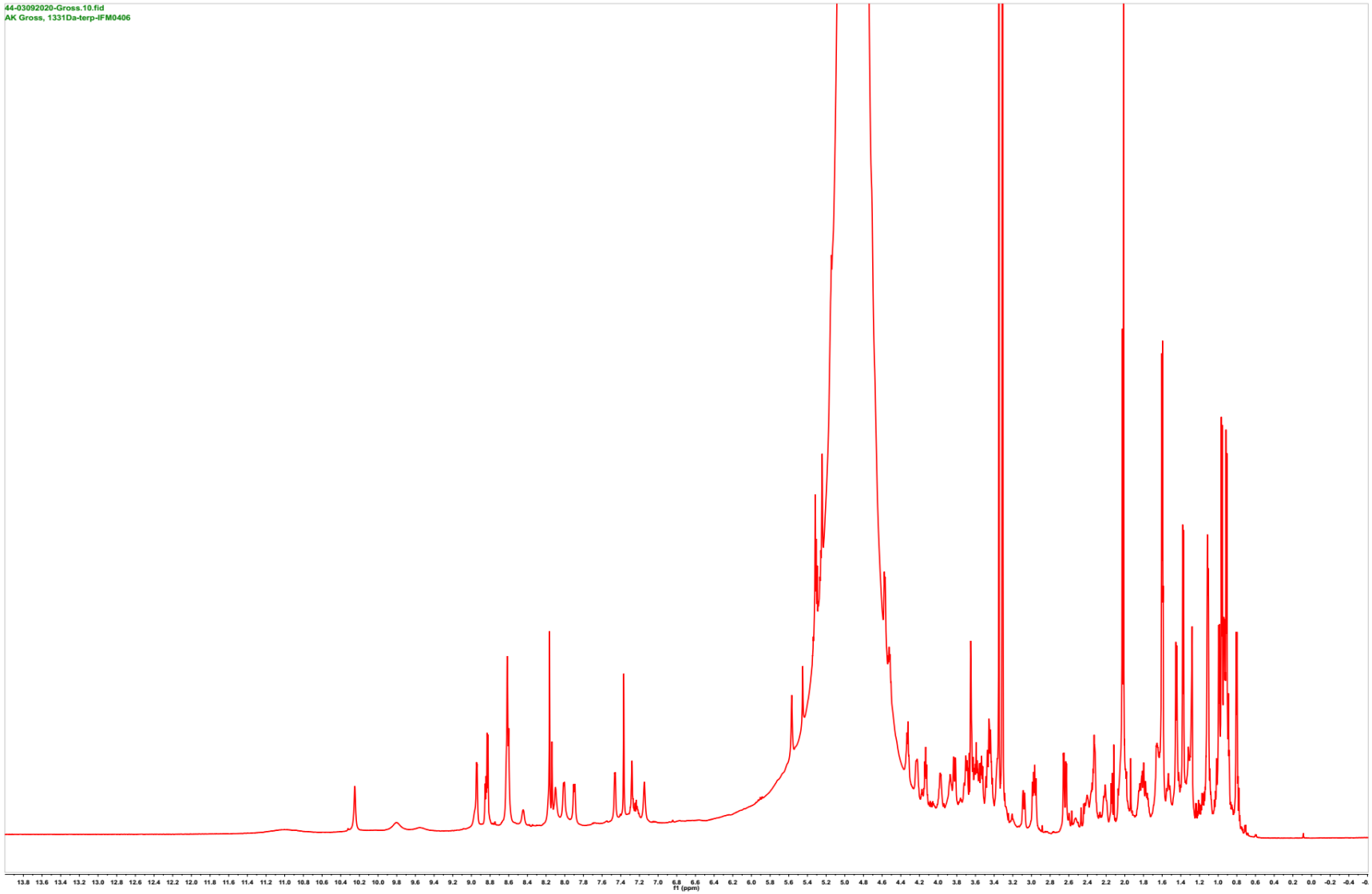

Figure S81. ^{1}H-NMR spectrum of nocathioamide B (**2**) (d_3-CH_3OH, 700 MHz)

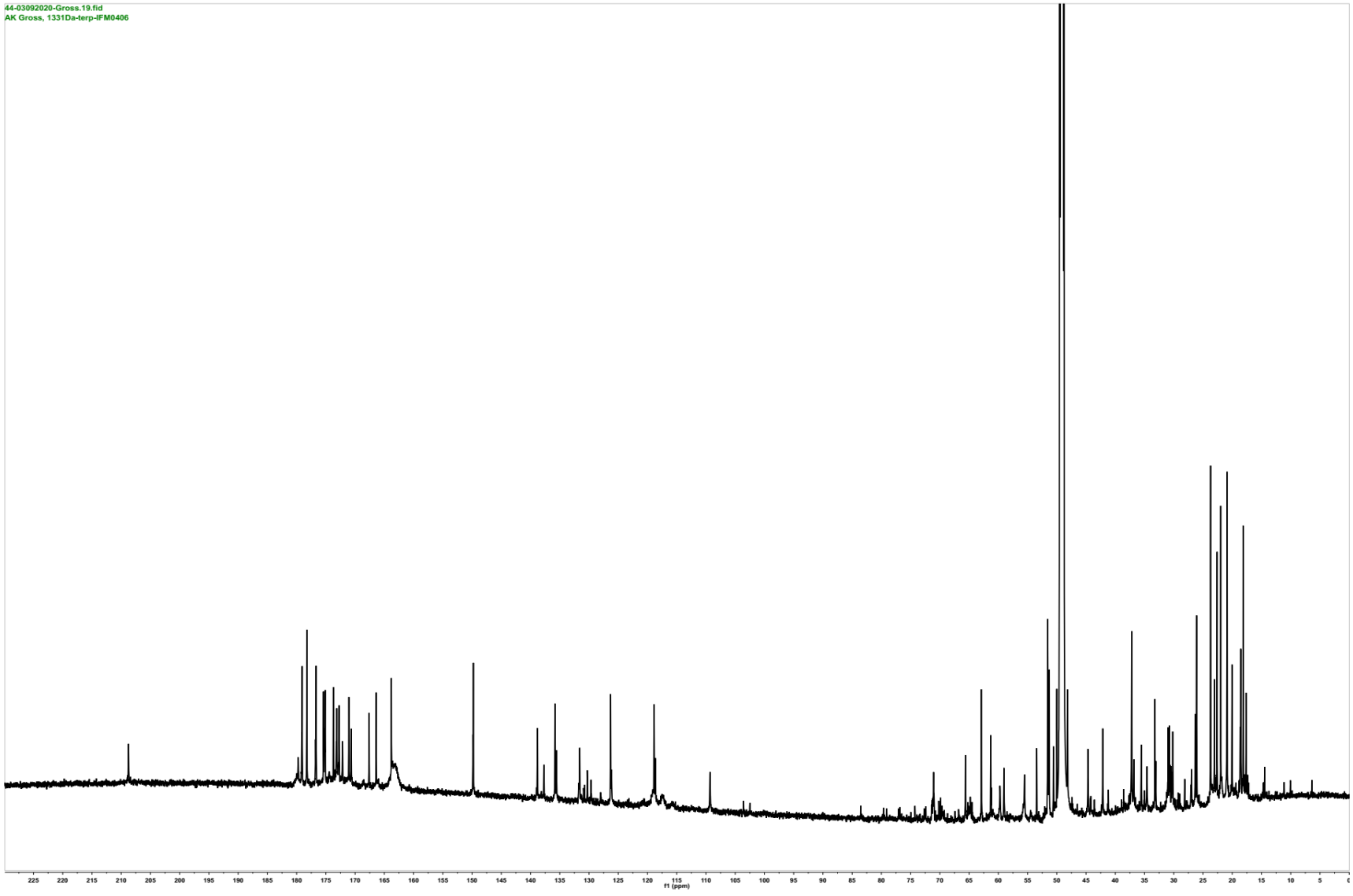

Figure S82. ^{13}C-NMR spectrum of nocathioamide B (**2**) (d_3-CH_3OH, 176 MHz)

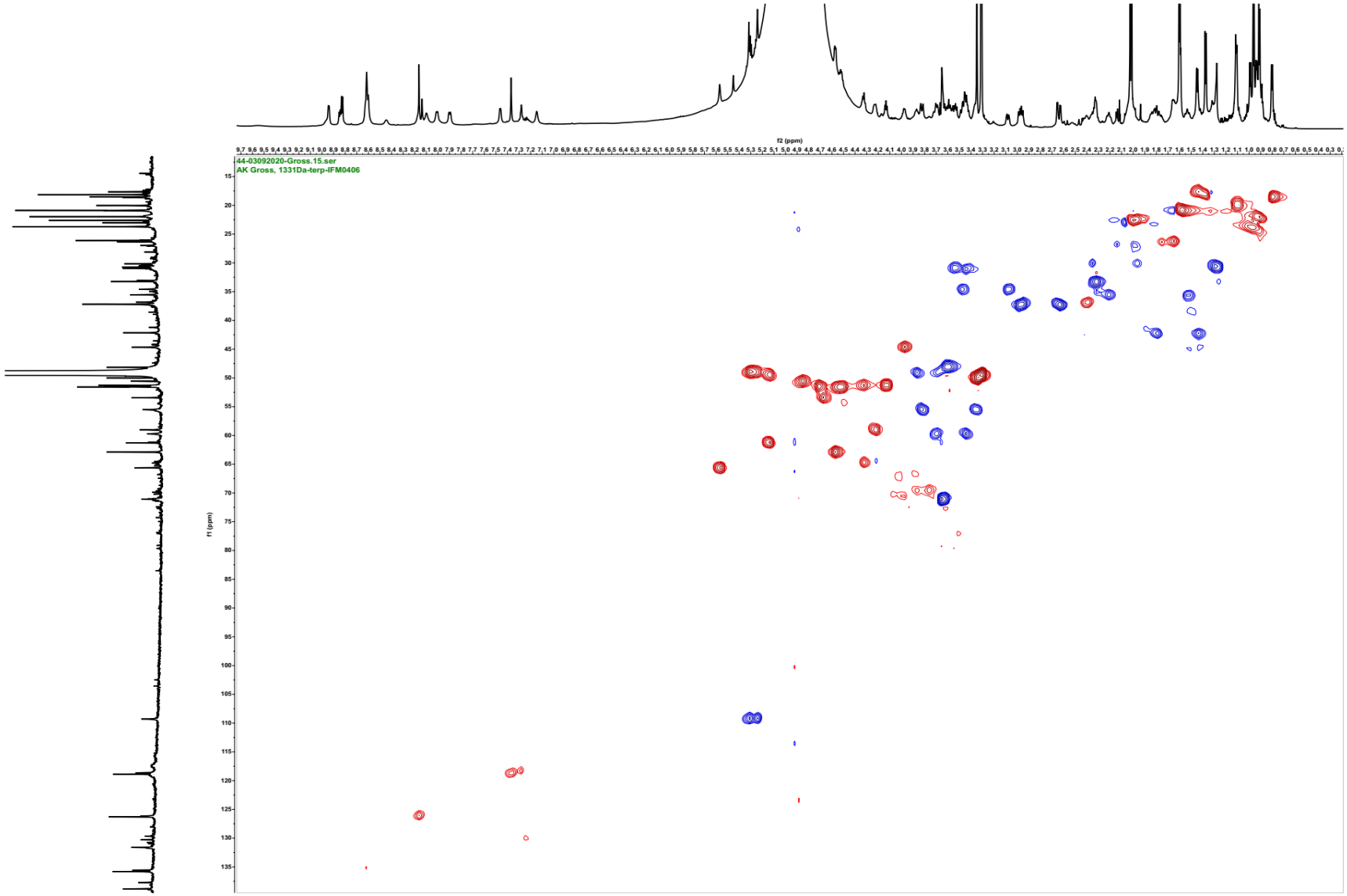

Figure S83. ^{1}H-^{13}C HSQC spectrum of nocathioamide B (**2**) (d_3-CH_3OH, 700/176 MHz)

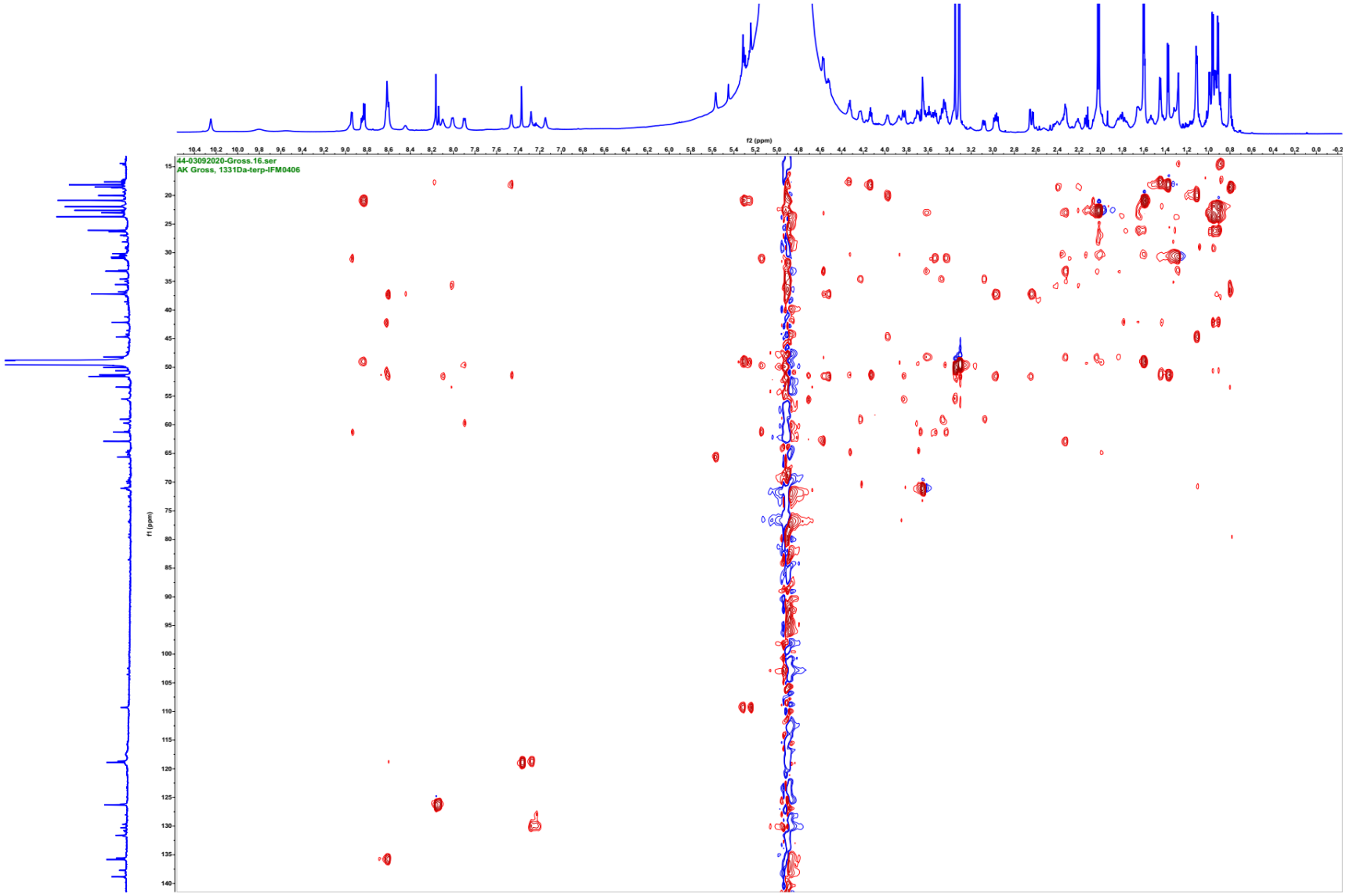

Figure S84. ^{1}H-^{13}C HSQC-TOCSY spectrum of nocathioamide B (**2**) (d_3-CH_3OH, 700/176 MHz)

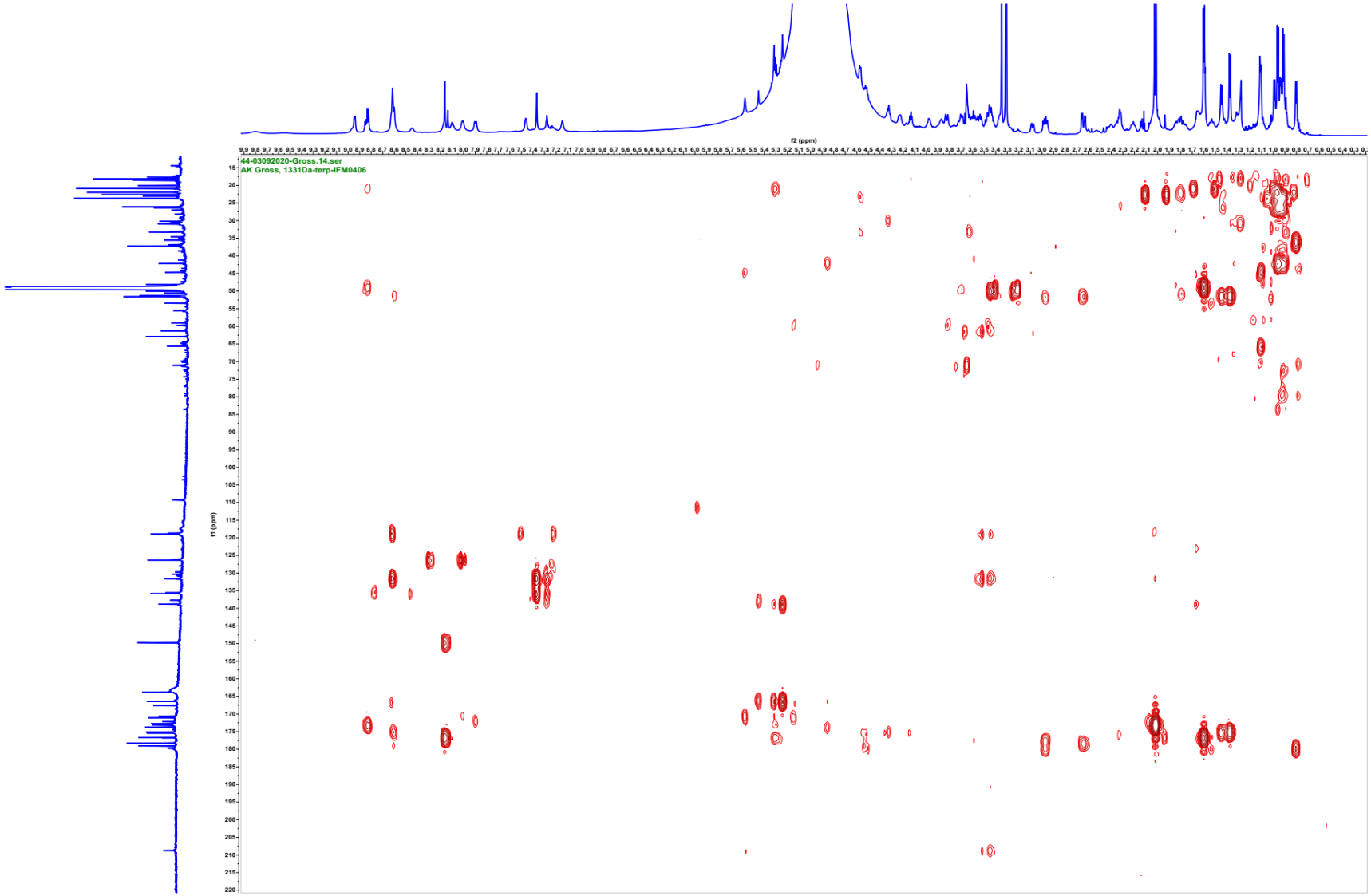

Figure S85. ^{1}H-^{13}C HMBC spectrum of nocathioamide B (**2**) (d_3-CH_3OH, 700/176 MHz)

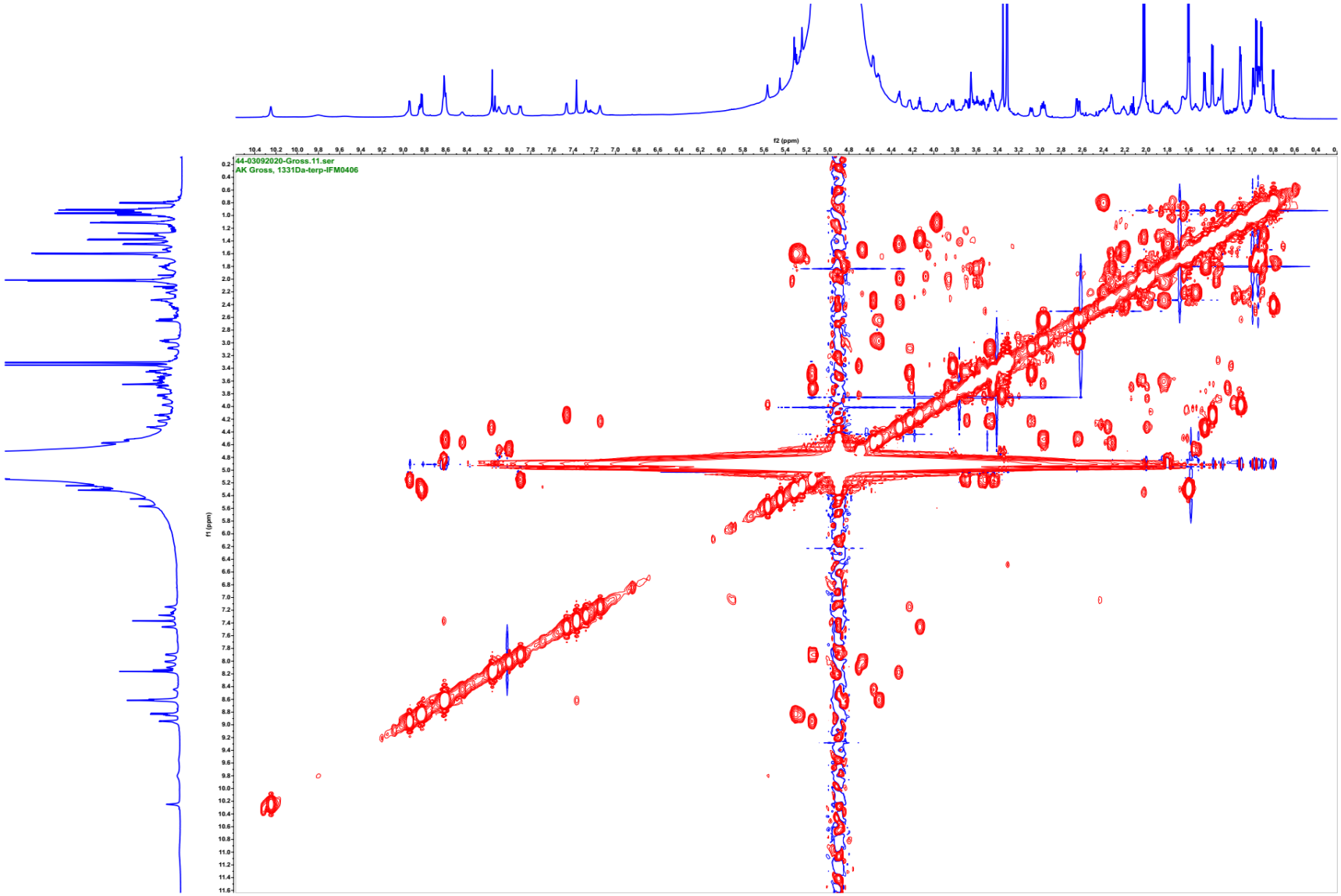

Figure S86. ^{1}H-^{1}H COSY spectrum of nocathioamide B (**2**) (d_3-CH_3OH, 700/700 MHz)

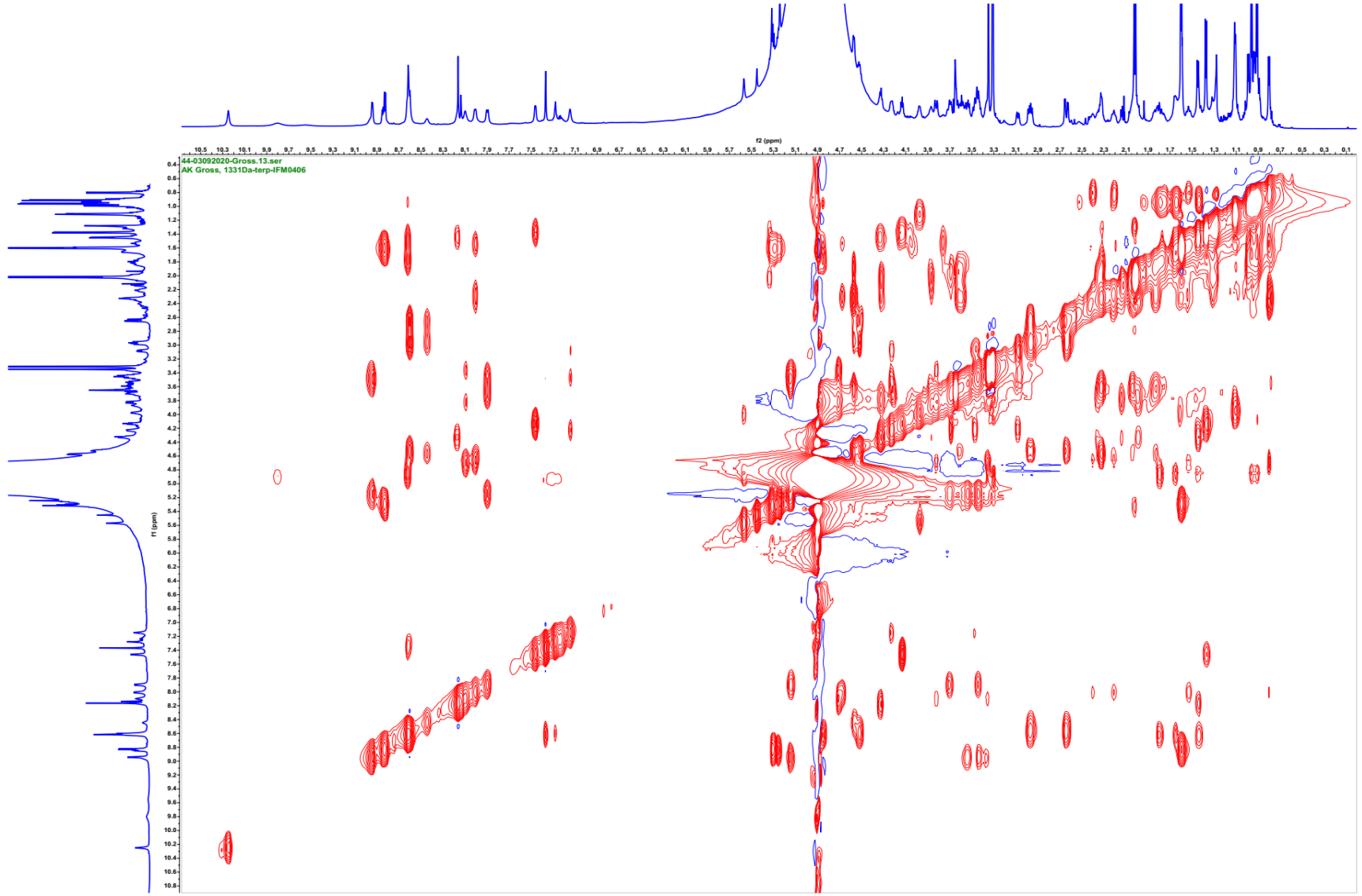

Figure S87. ^{1}H-^{1}H TOCSY spectrum of nocathioamide B (**2**) (d_3-CH_3OH, 700/700 MHz)

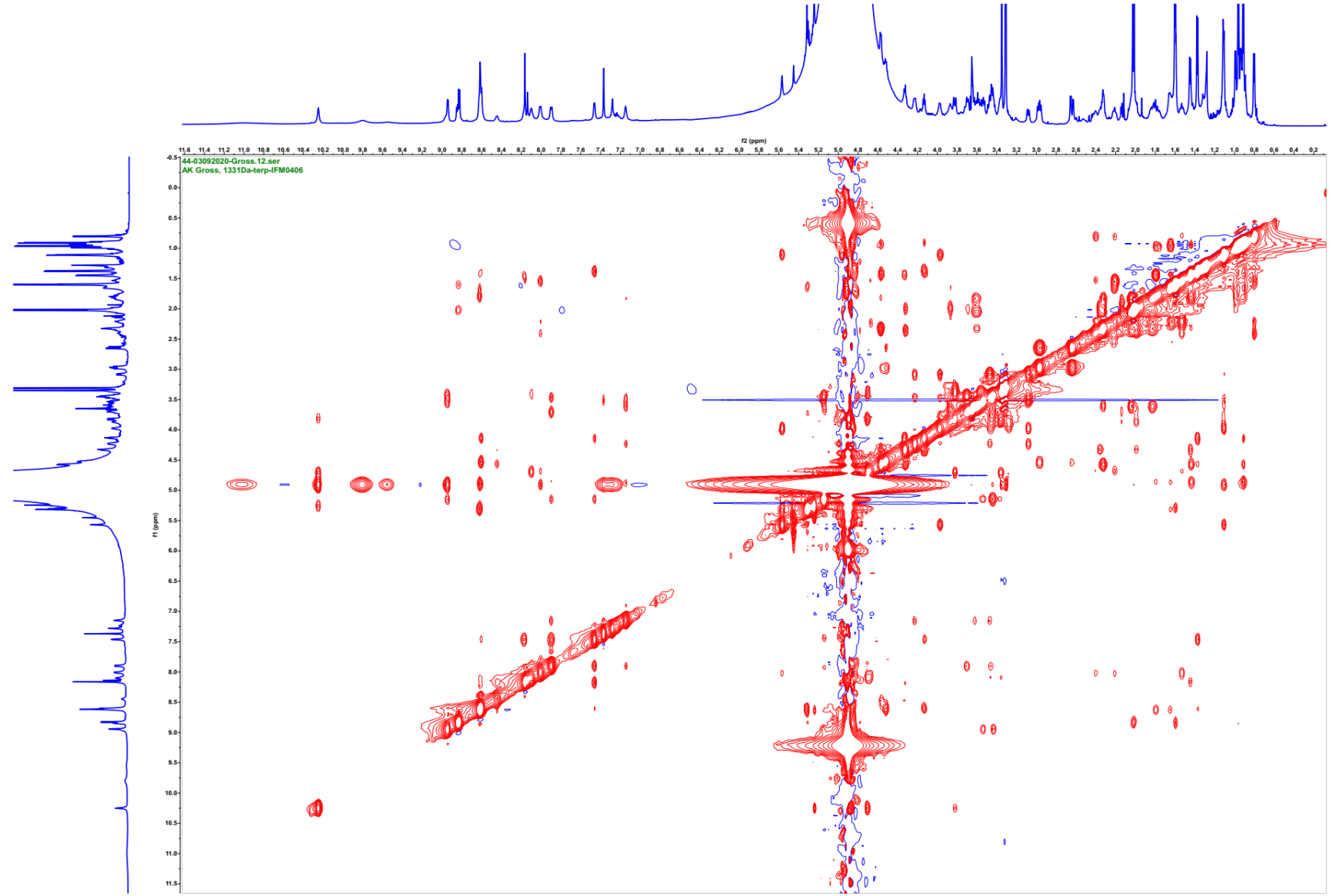

Figure S88. ^{1}H-^{1}H NOESY spectrum of nocathioamide B (**2**) (d_3-CH_3OH, 700/700 MHz, d8 = 300 msec)

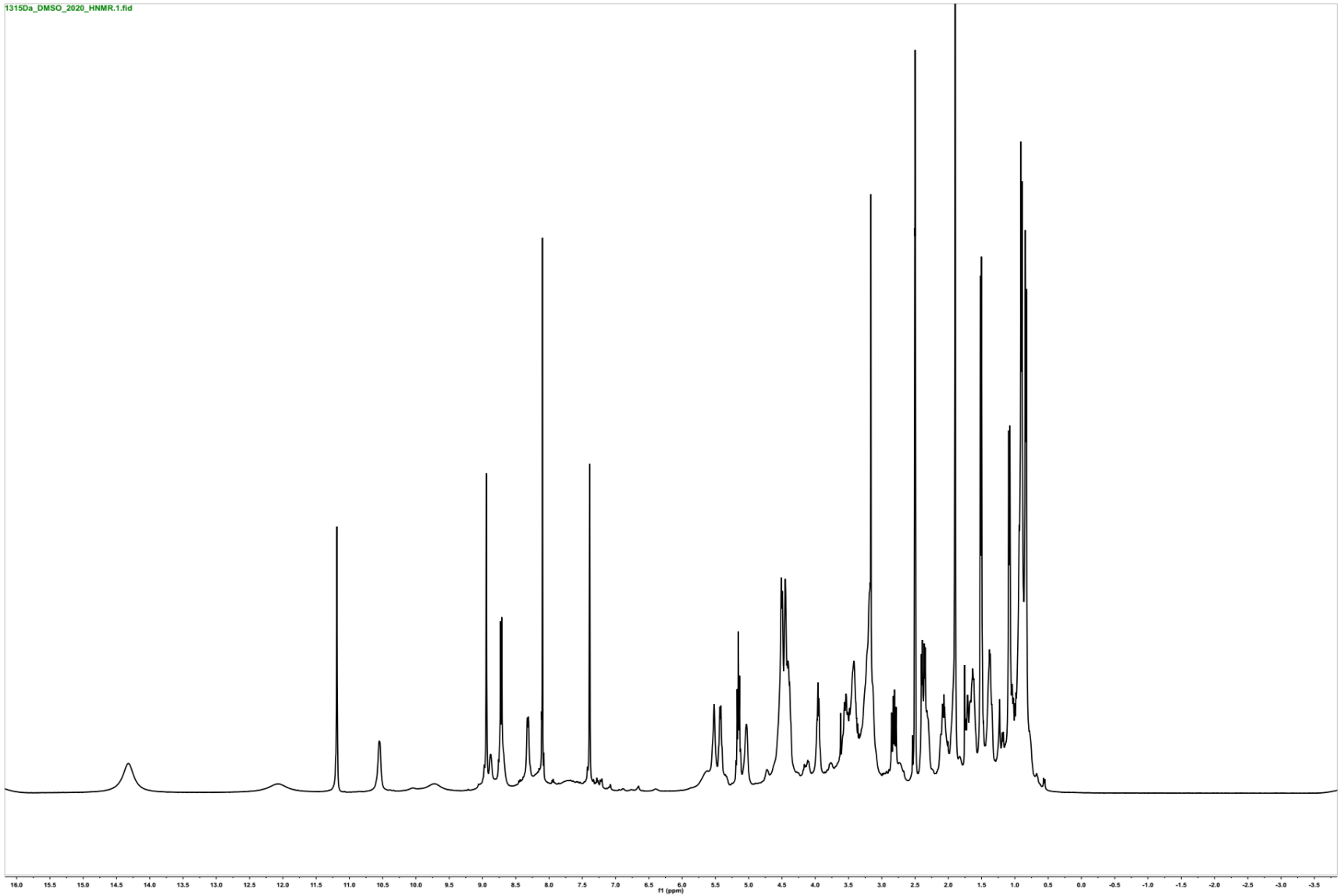

Figure S89. ^{1}H-NMR spectrum of nocathioamide A (**1**) (d_6-DMSO, 400 MHz)

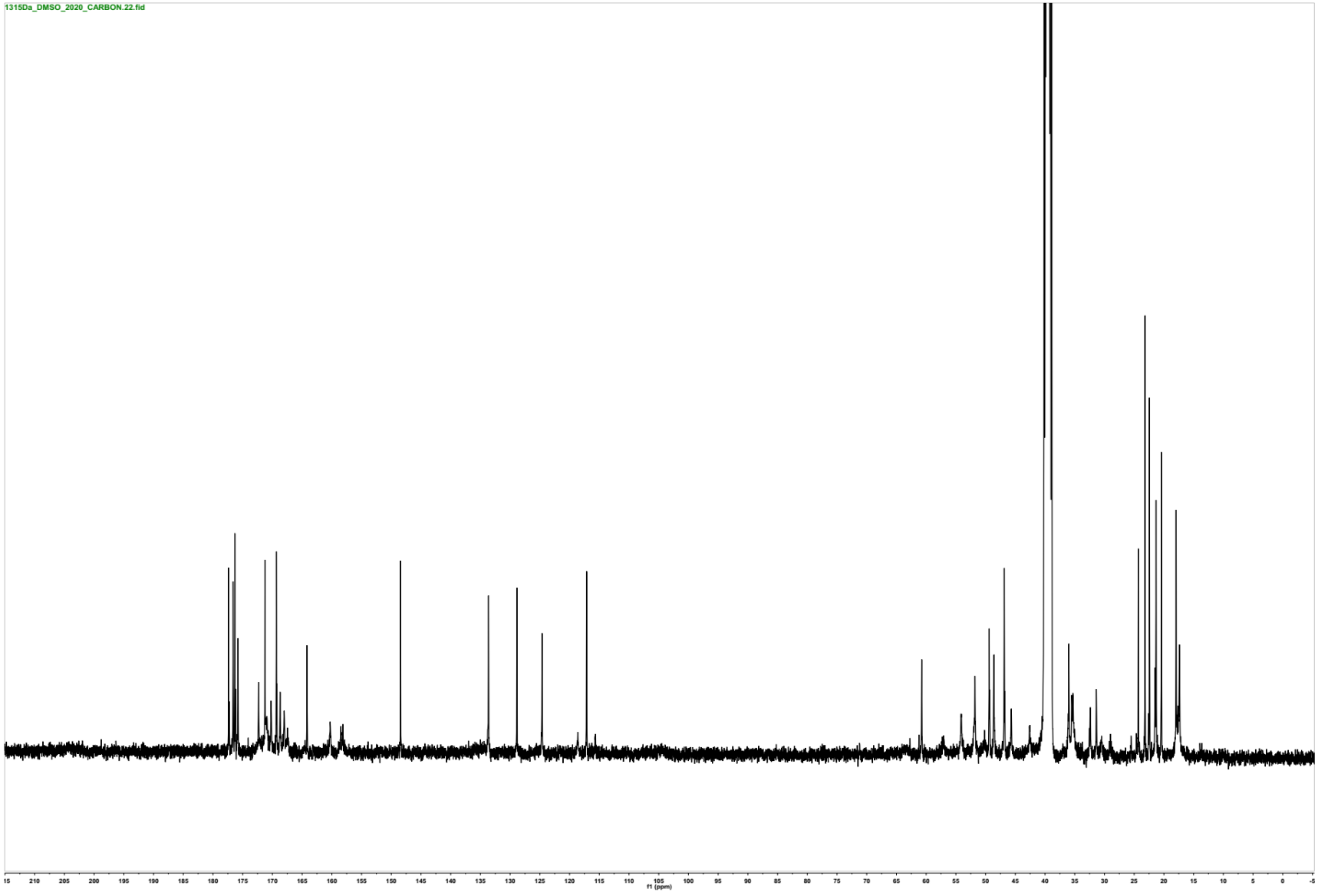

Figure S90. ^{13}C-NMR spectrum of nocathioamide A (**1**) (d_6-DMSO, 100 MHz)

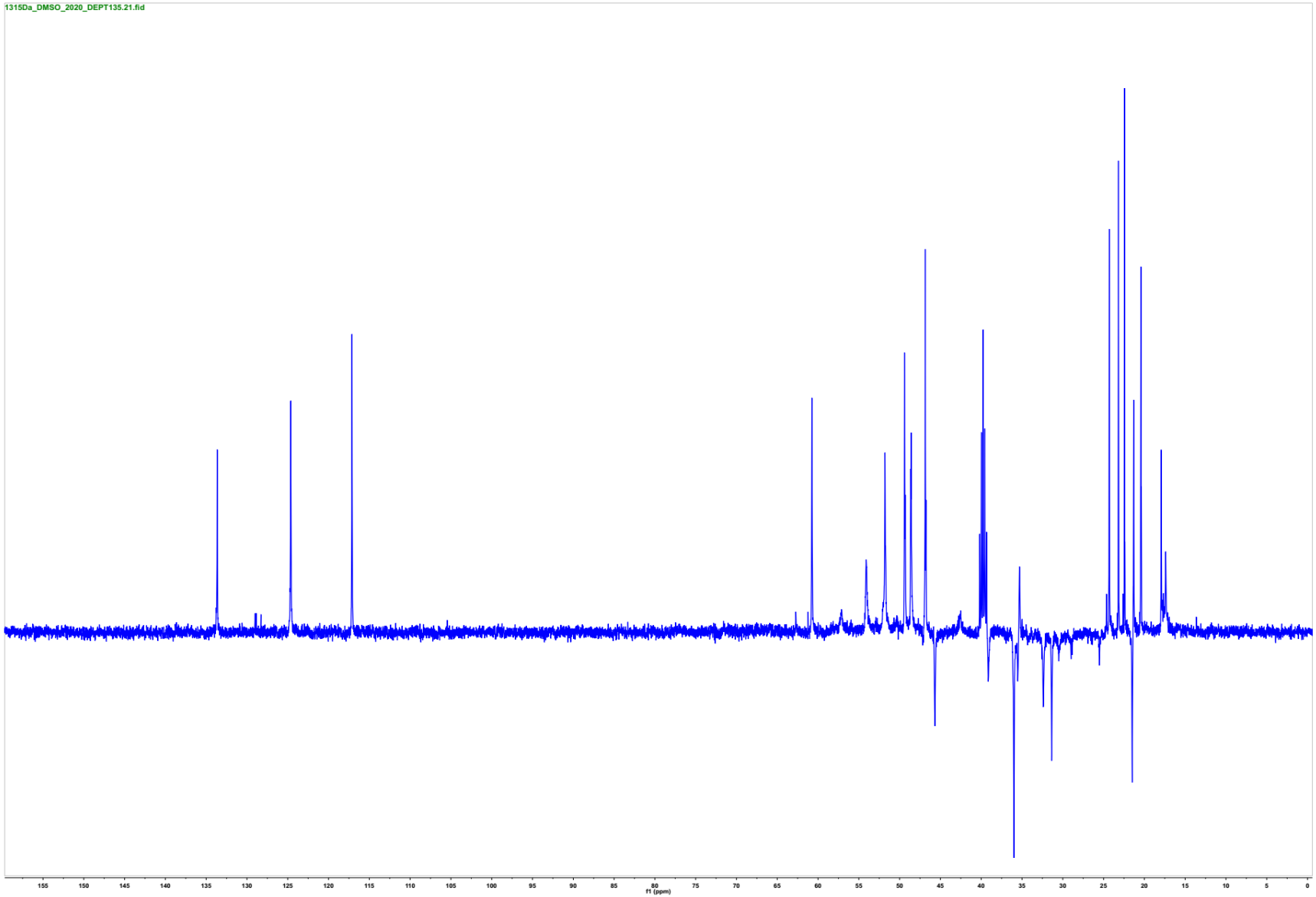

Figure S91. DEPT-135 spectrum of nocathioamide A (**1**) (d_6-DMSO, 100 MHz)

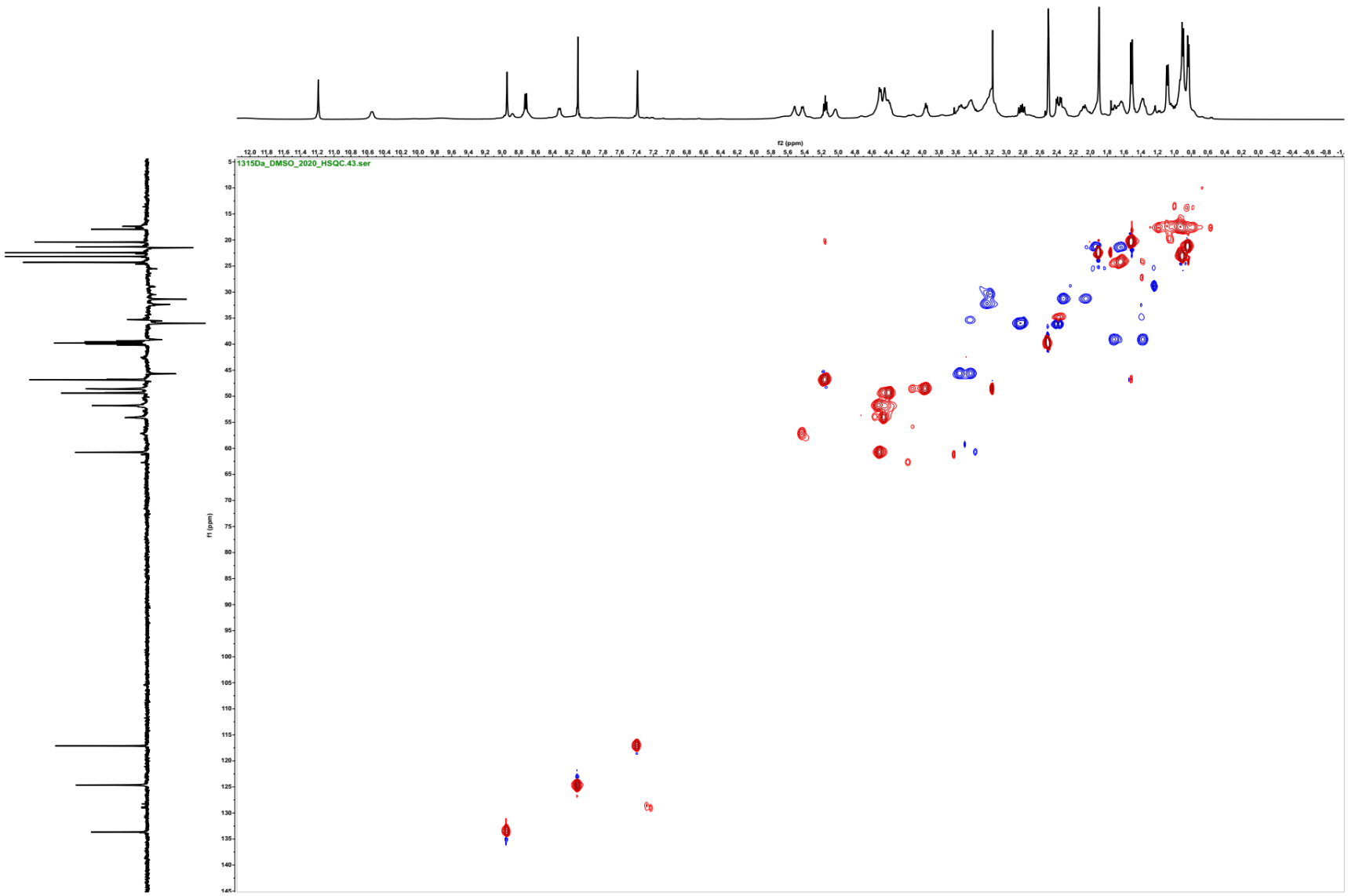

Figure S92. ^{1}H-^{13}C HSQC spectrum of nocathioamide A (**1**) (d_6-DMSO, 400/100 MHz)

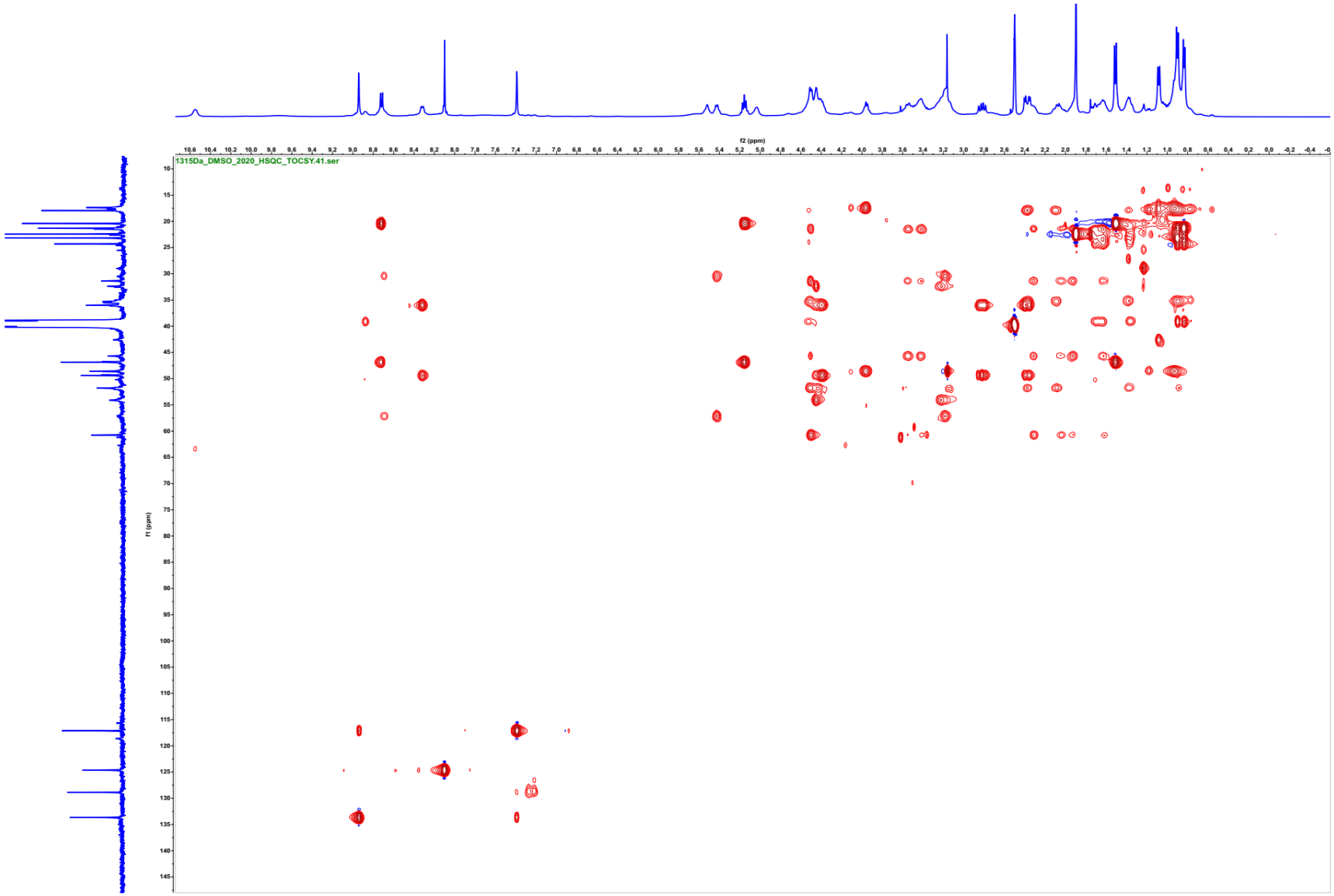

Figure S93. ^{1}H-^{13}C HSQC-TOCSY spectrum of nocathioamide A (**1**) (d_6-DMSO, 400/100 MHz)

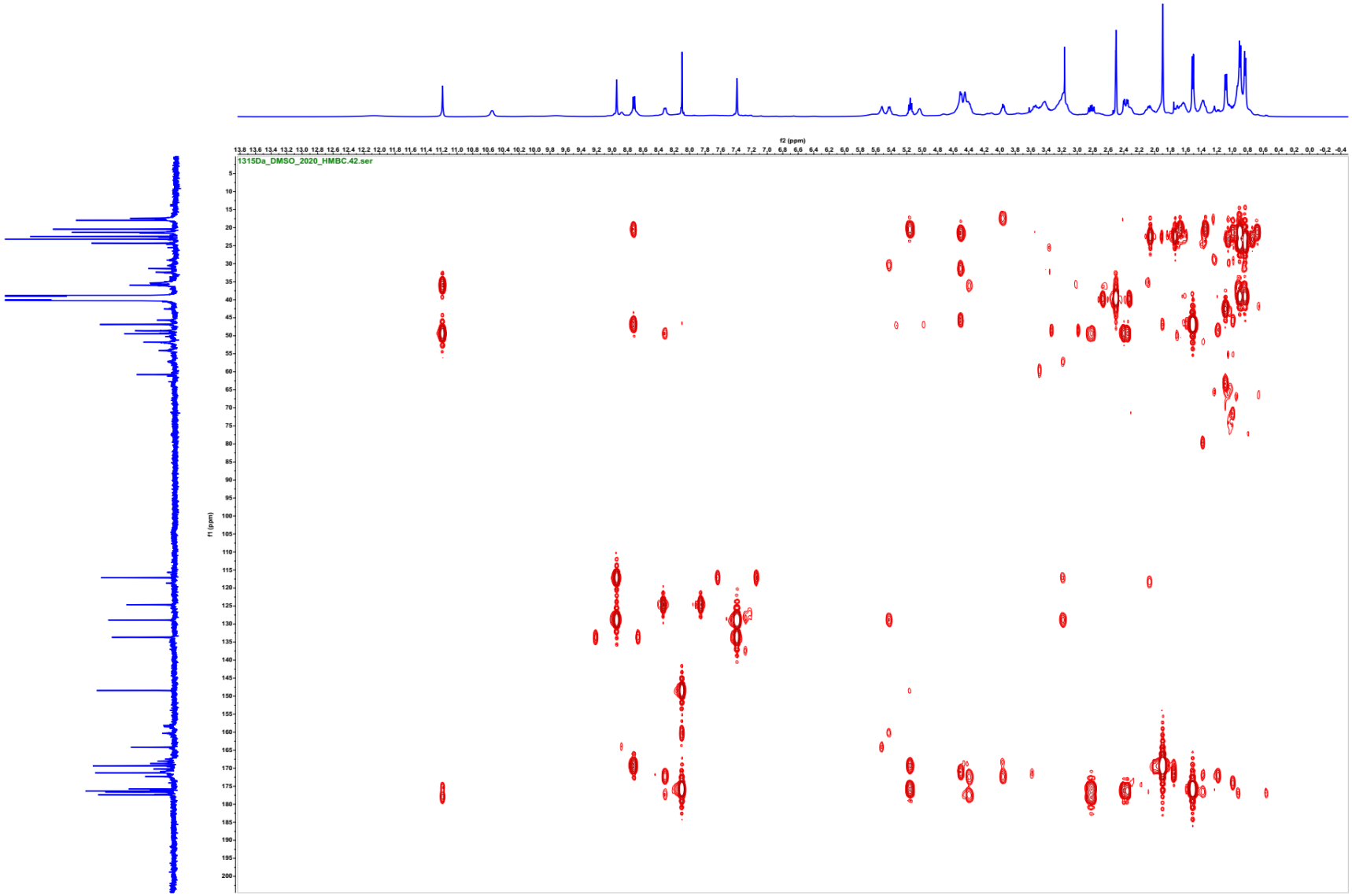

Figure S94. ^{1}H-^{13}C HMBC spectrum of nocathioamide A (**1**) (d_6-DMSO, 400/100 MHz)

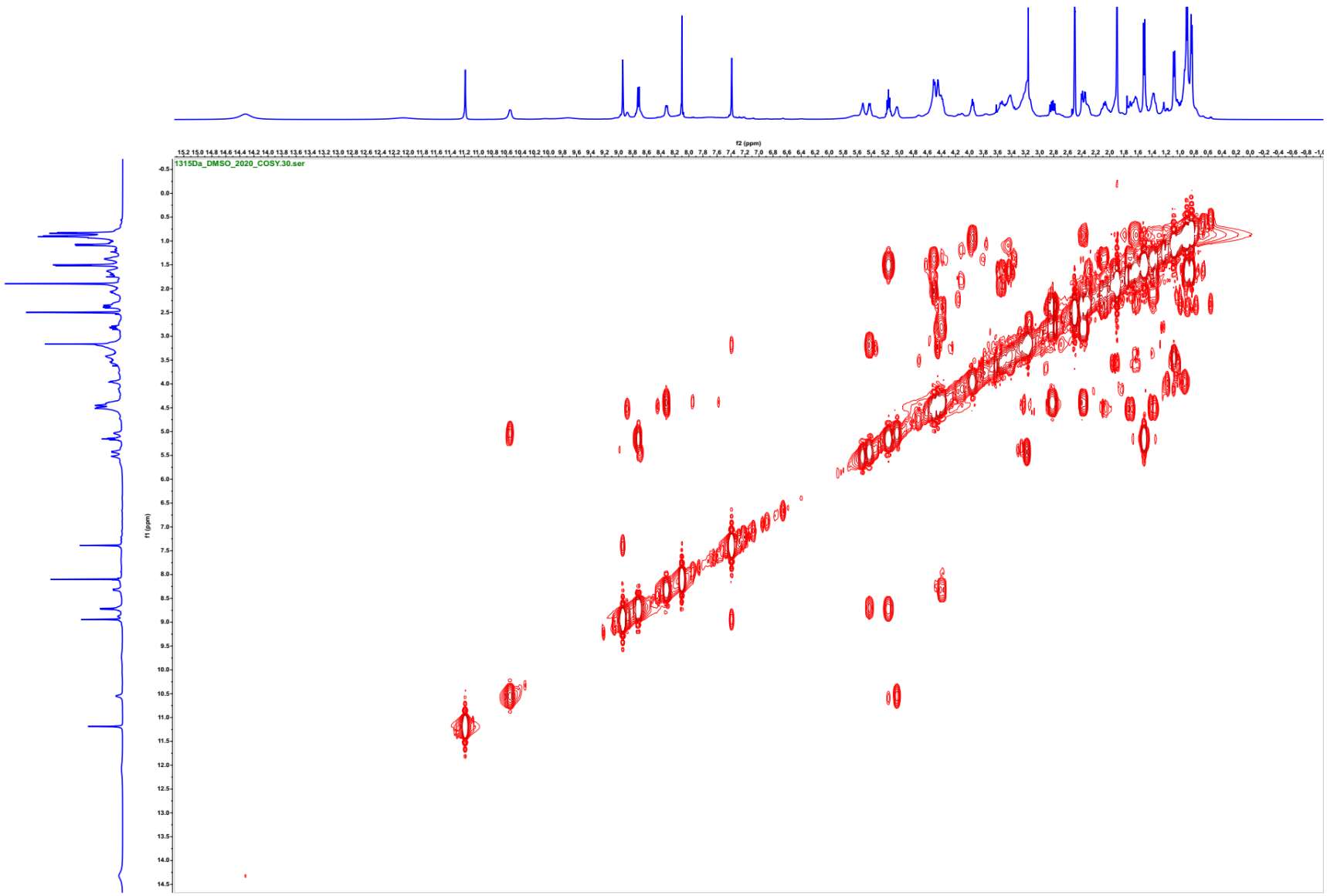

Figure S95. ^{1}H-^{1}H COSY spectrum of nocathioamide A (**1**) (d_6-DMSO, 400/400 MHz)

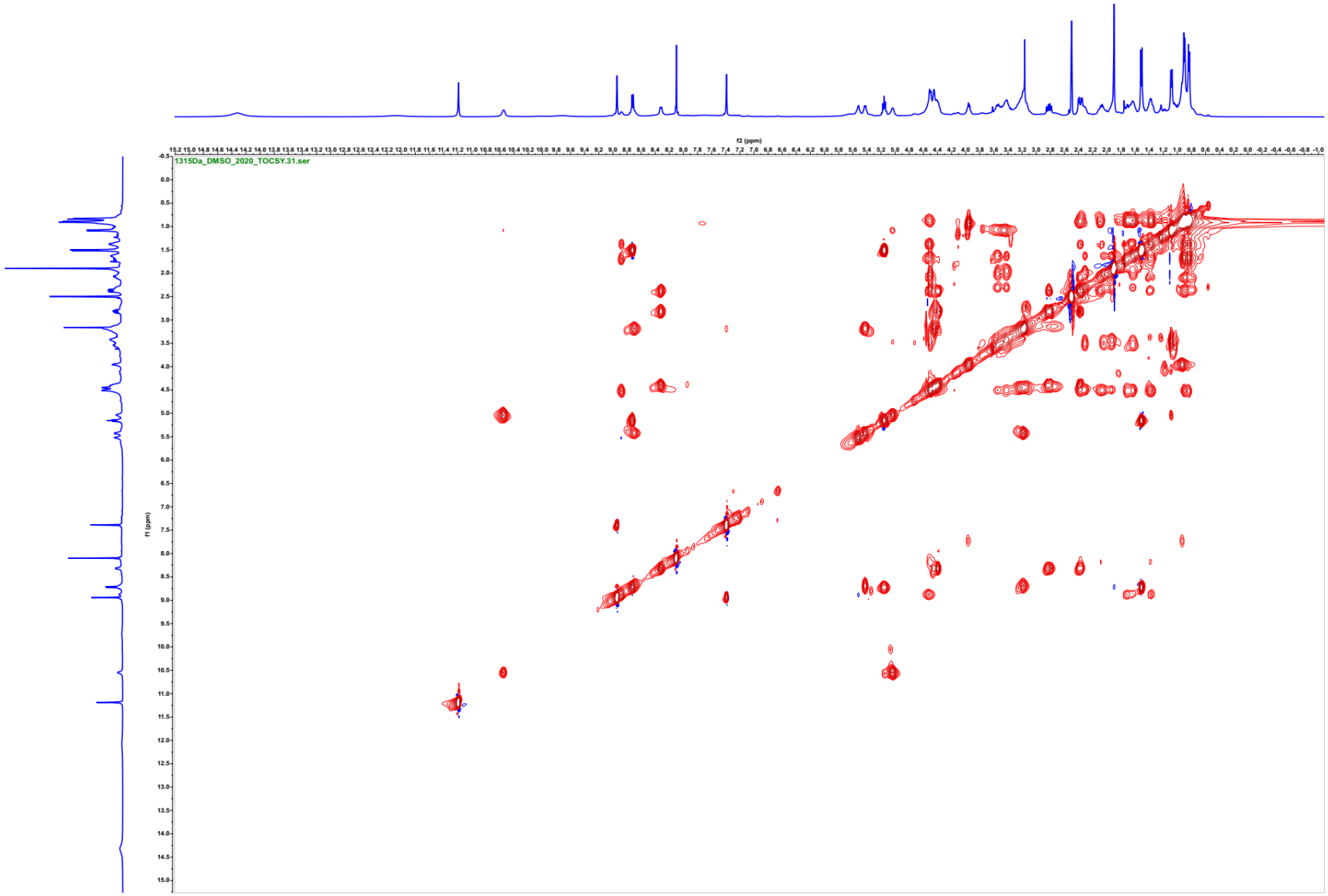

Figure S96. ^{1}H-^{1}H TOCSY spectrum of nocathioamide A (**1**) (d_6-DMSO, 400/400 MHz)

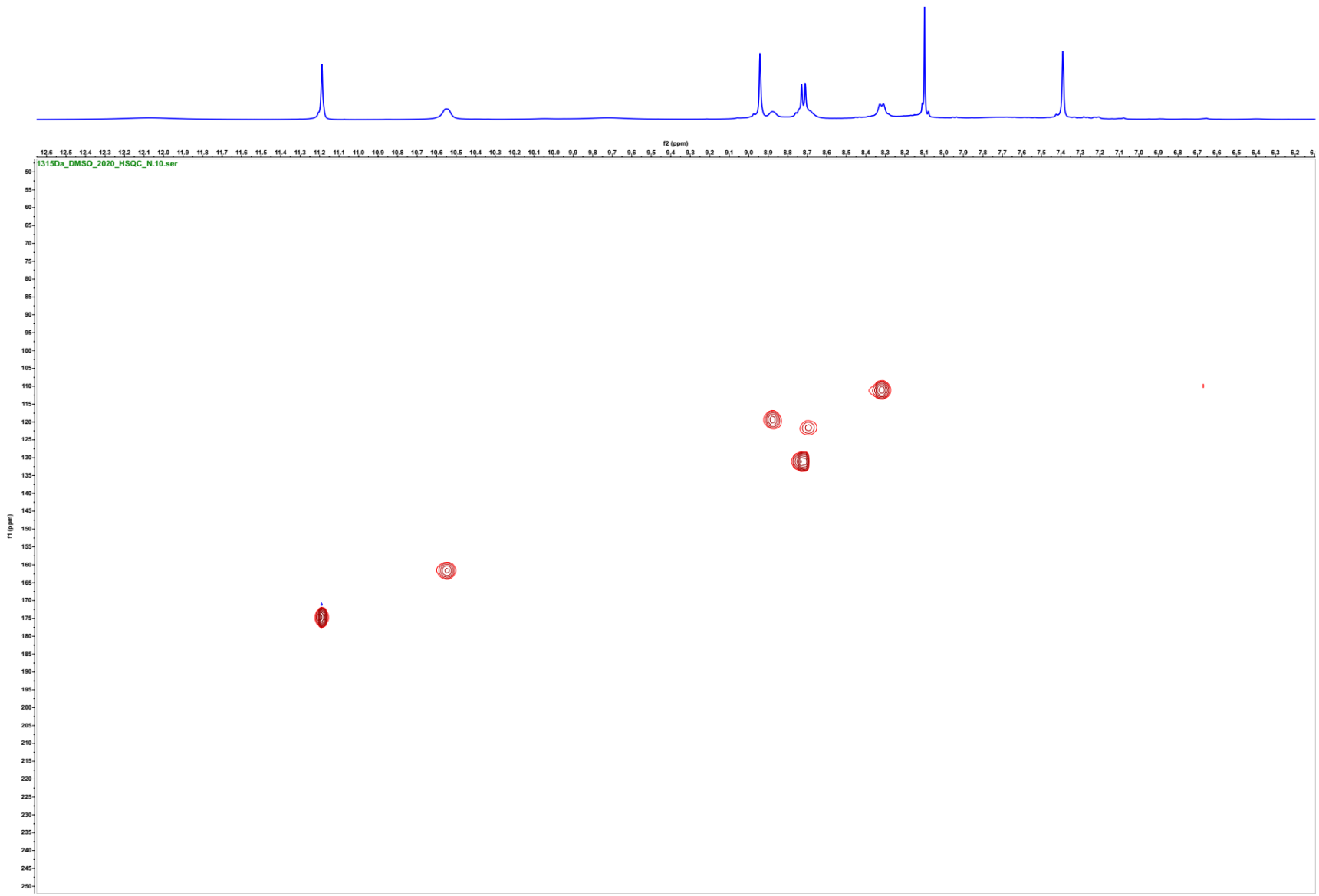

Figure S97. ^{1}H-^{15}N HSQC spectrum of nocathioamide A (**1**) (d_6-DMSO, 400/40.6 MHz)

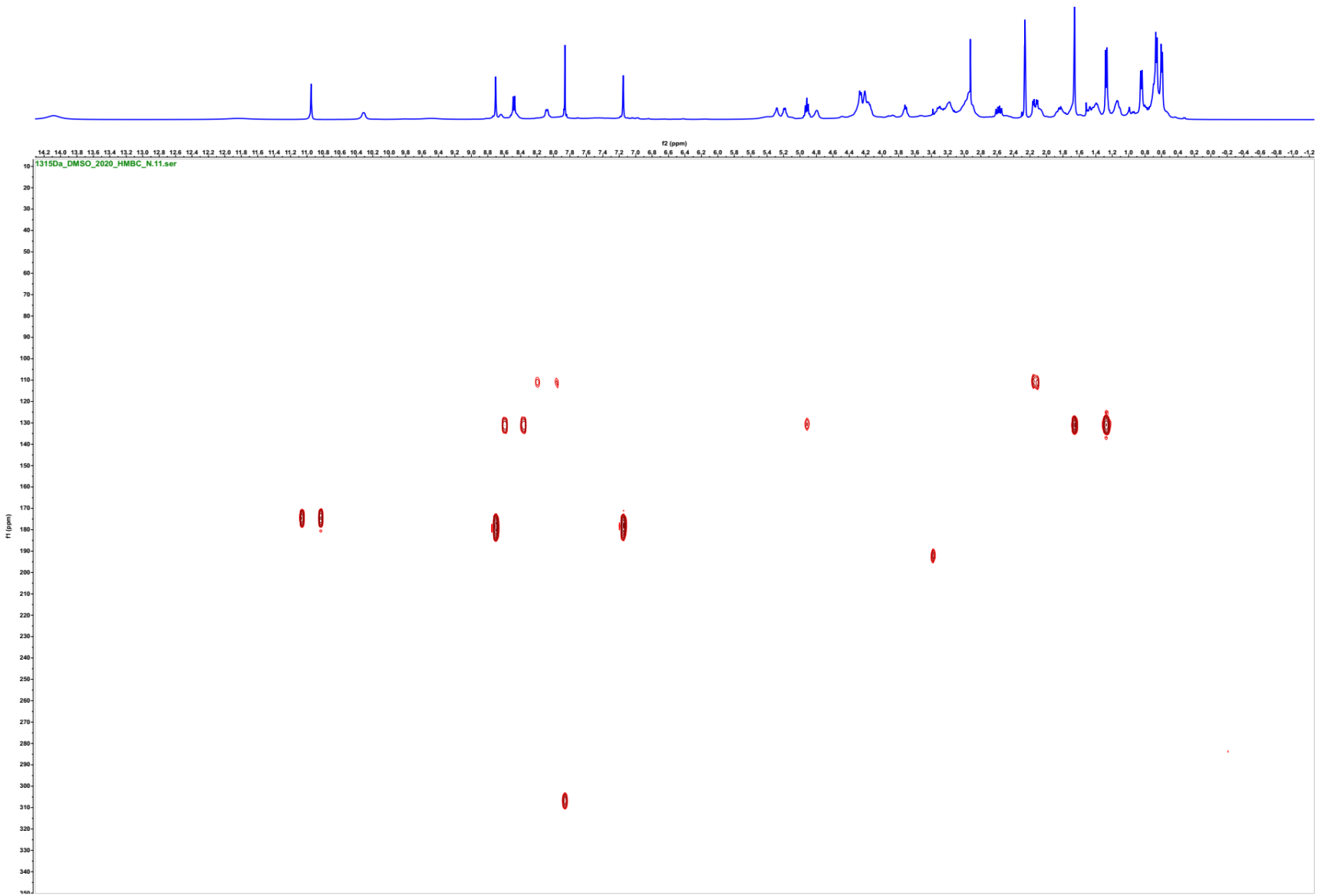

Figure S98. ^{1}H-^{15}N HMBC spectrum of nocathioamide A (**1**) (d_6-DMSO, 400/40.6 MHz)

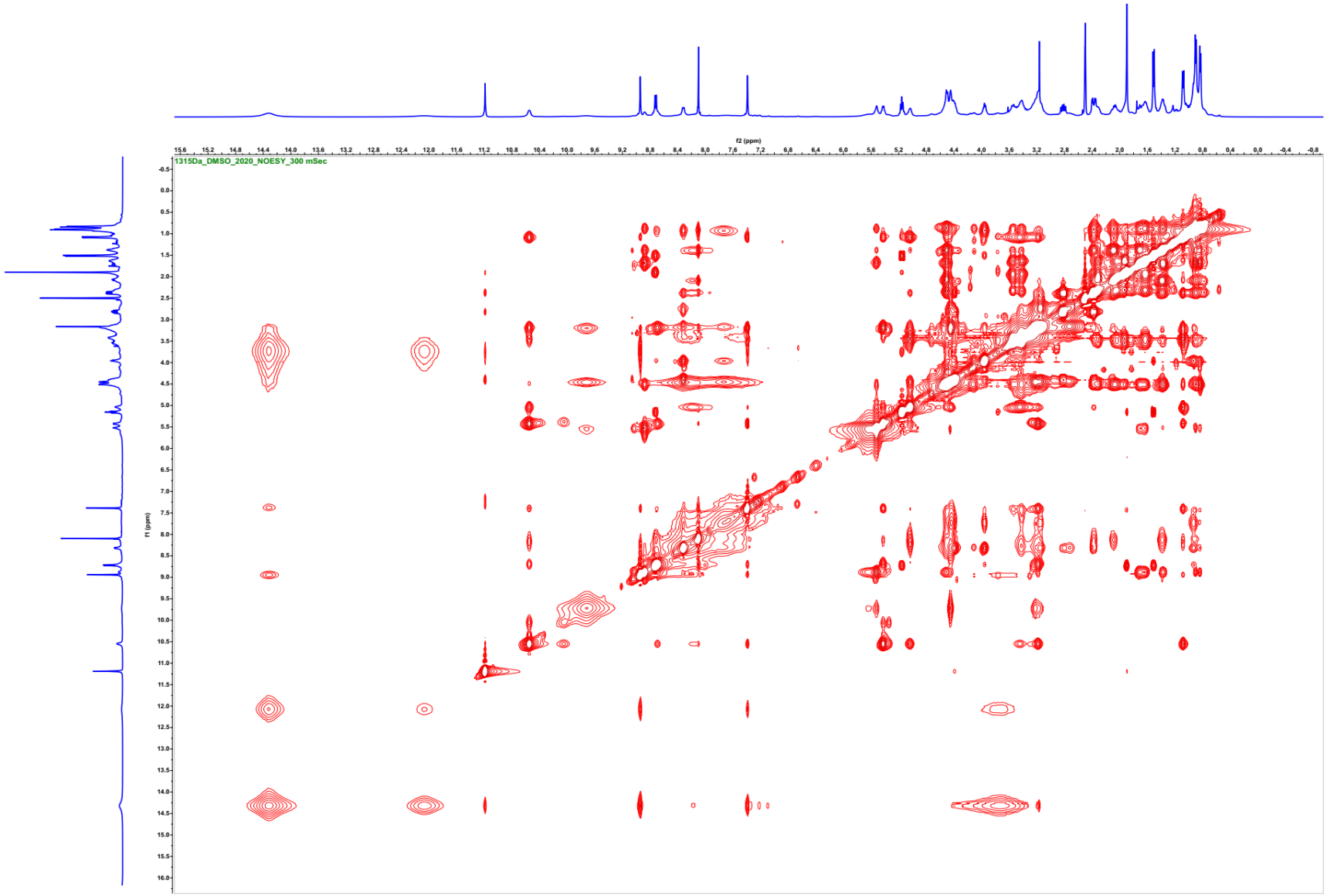

Figure S99. ^{1}H-^{1}H NOESY spectrum of nocathioamide A (**1**) (d_6-DMSO, 400/400 MHz, d8 = 300 msec)

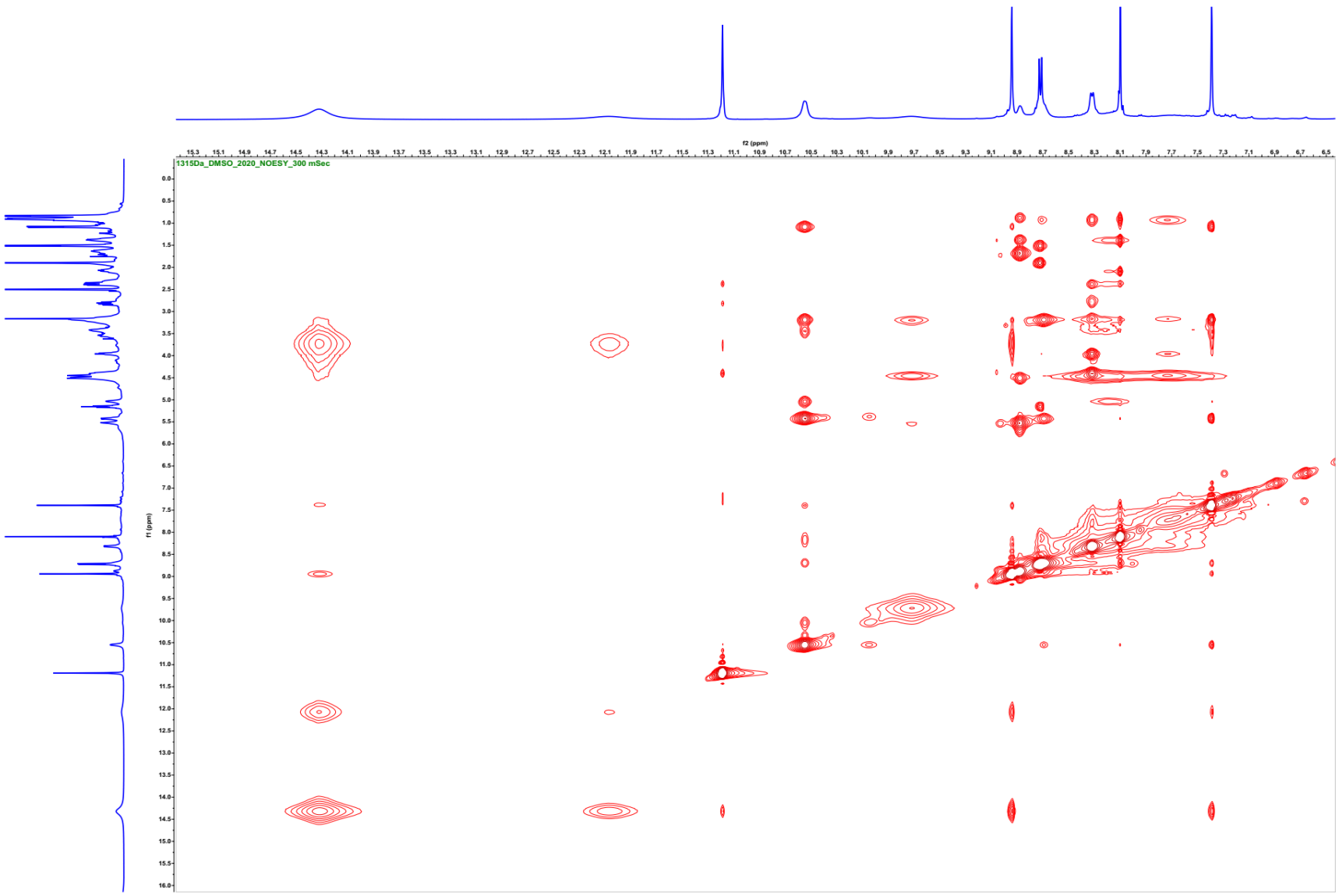

Figure S99A. Enlarged ^{1}H-^{1}H NOESY spectrum of nocathioamide A (**1**) (d_6-DMSO, 400/400 MHz, d8 = 300 msec)

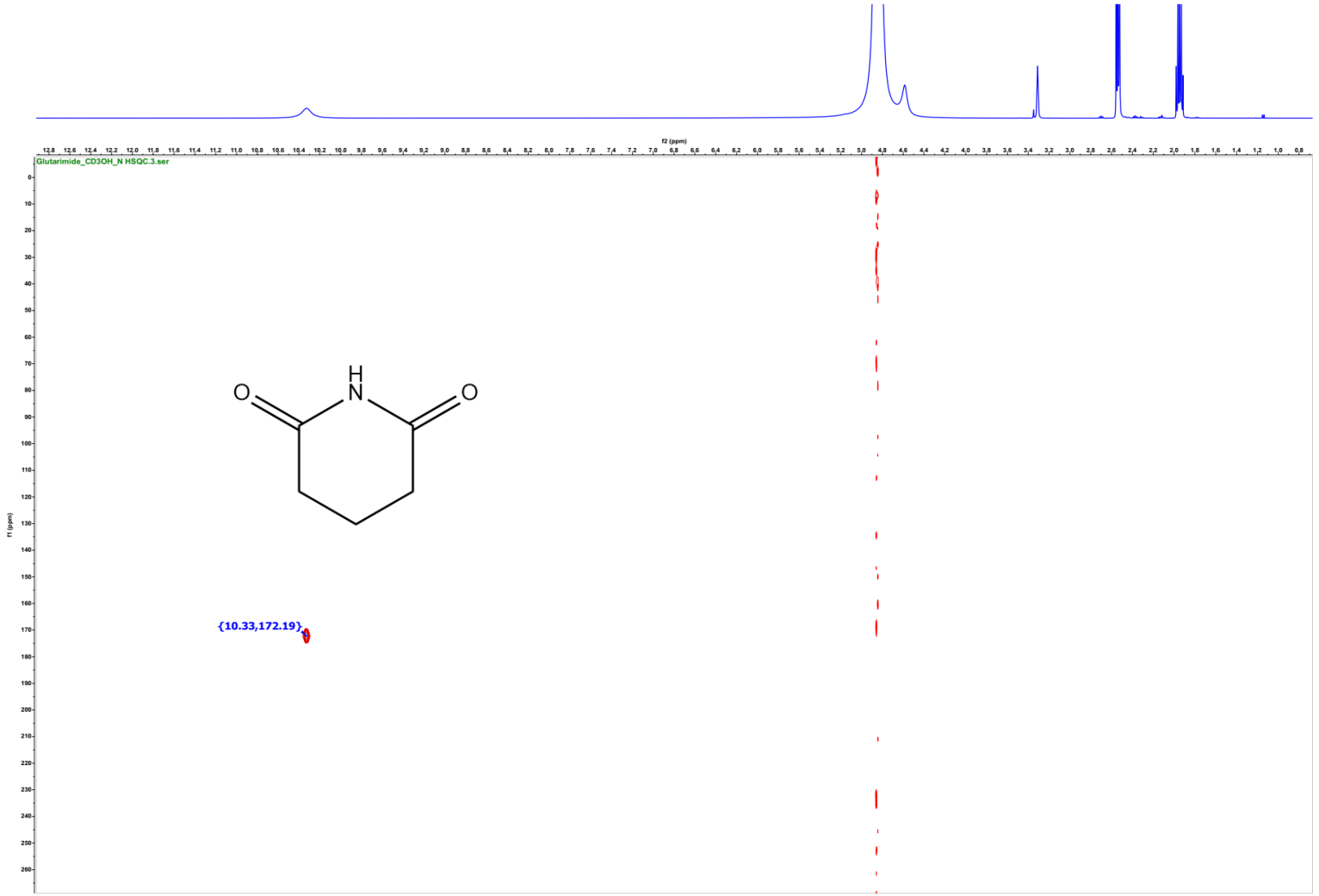

Figure S100. ^{1}H-^{15}N HSQC spectrum of glutarimide (d_3-CH_3OH, 400/40.6 MHz)

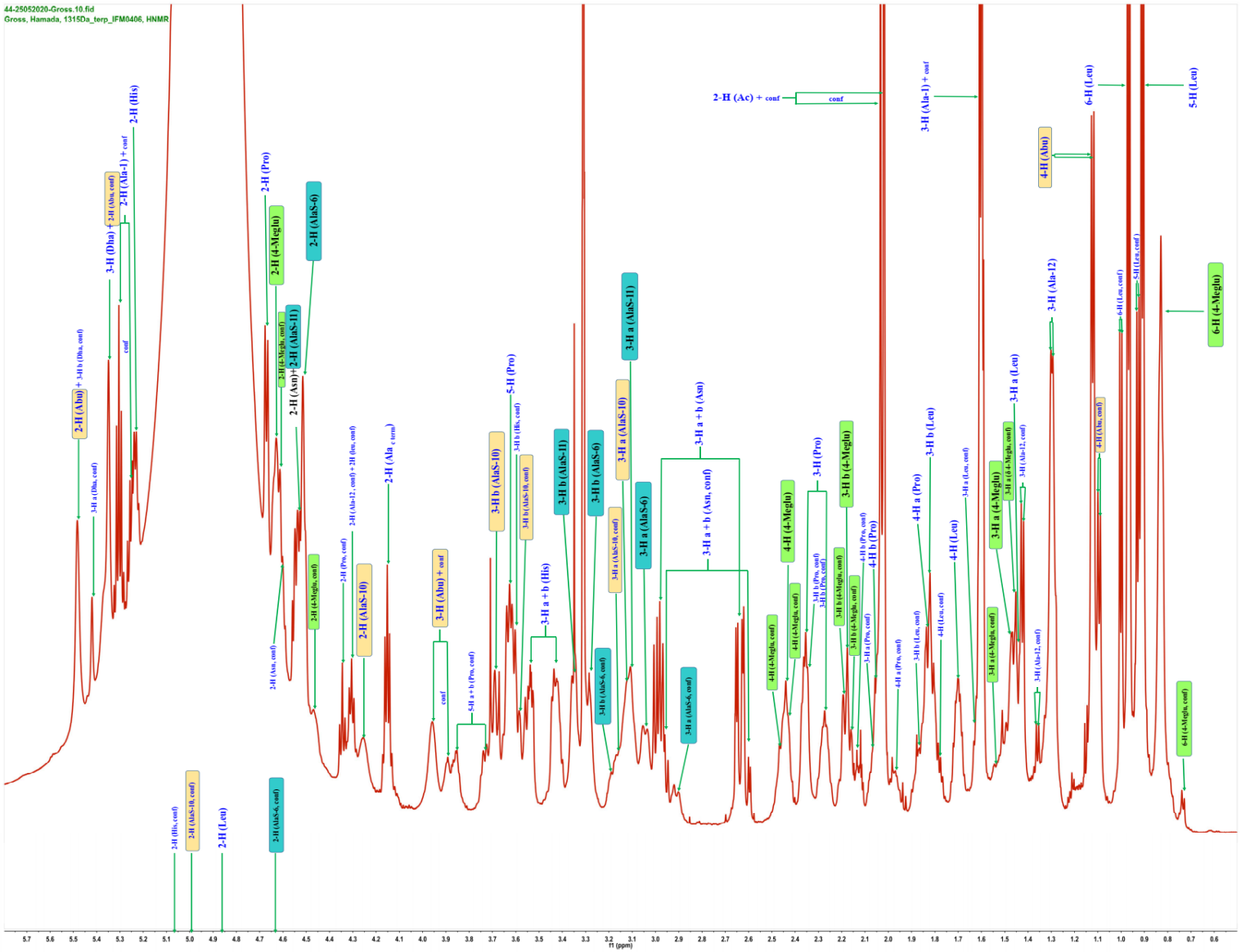

Figure S101. Annotated ^{1}H-NMR spectrum of nocathioamide A (**1**) (d_3-CH_3OH, 700 MHz)

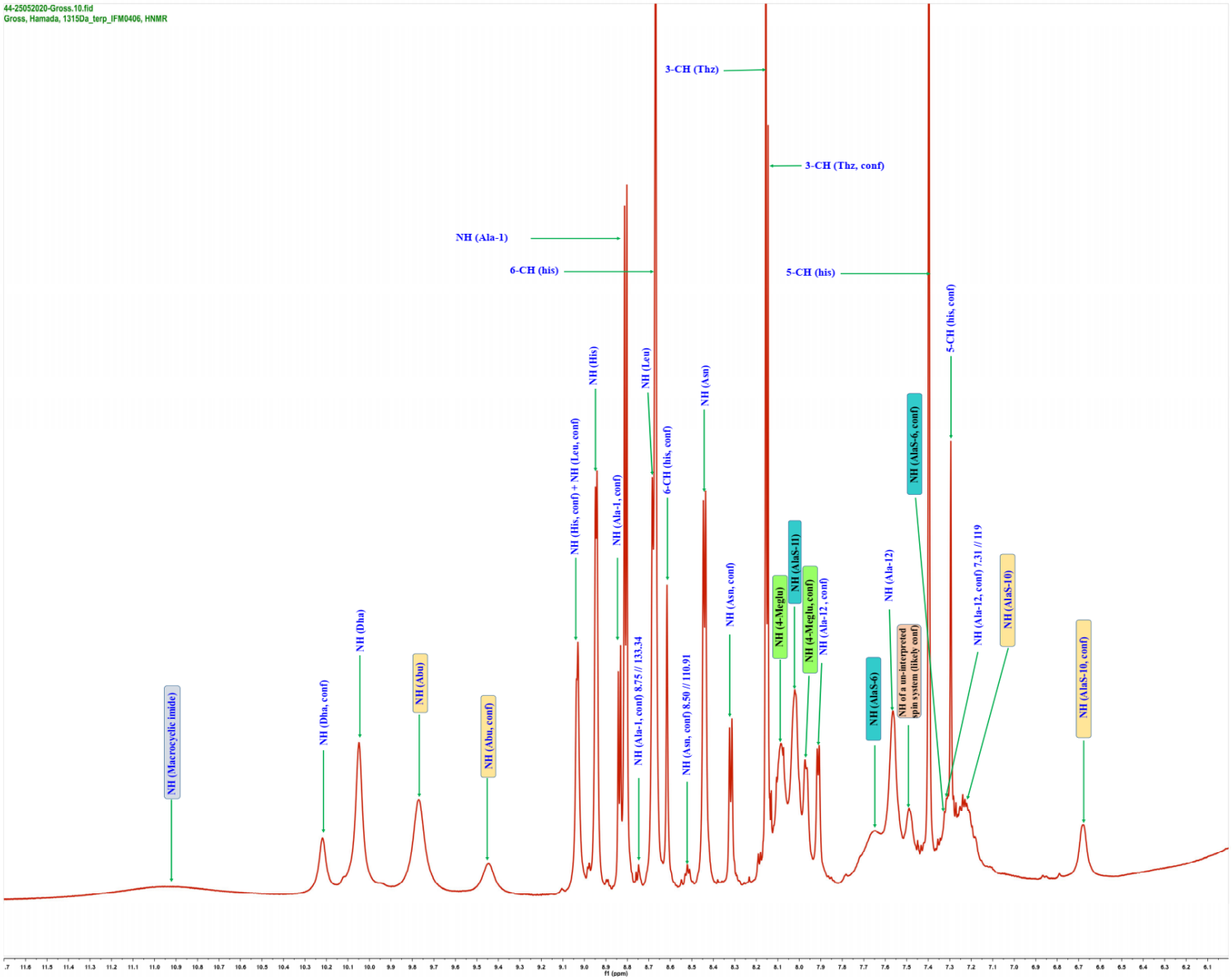

Figure S101A. Annotated ^{1}H-NMR spectrum of nocathioamide A (**1**) (d_3-CH_3OH, 700 MHz)

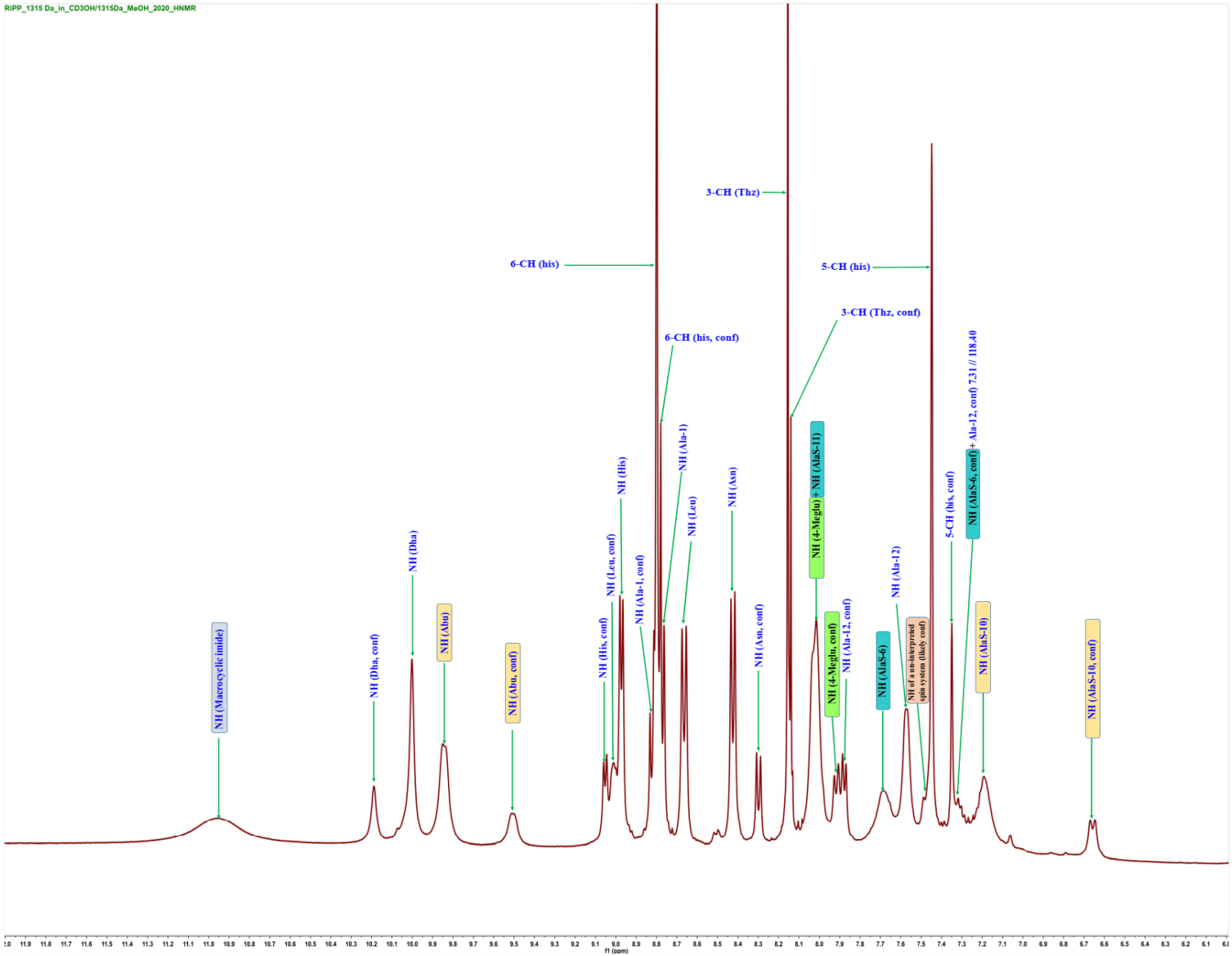

Figure S101B. Annotated ^{1}H-NMR spectrum of nocathioamide A (**1**) (d_3-CH_3OH, 400 MHz)

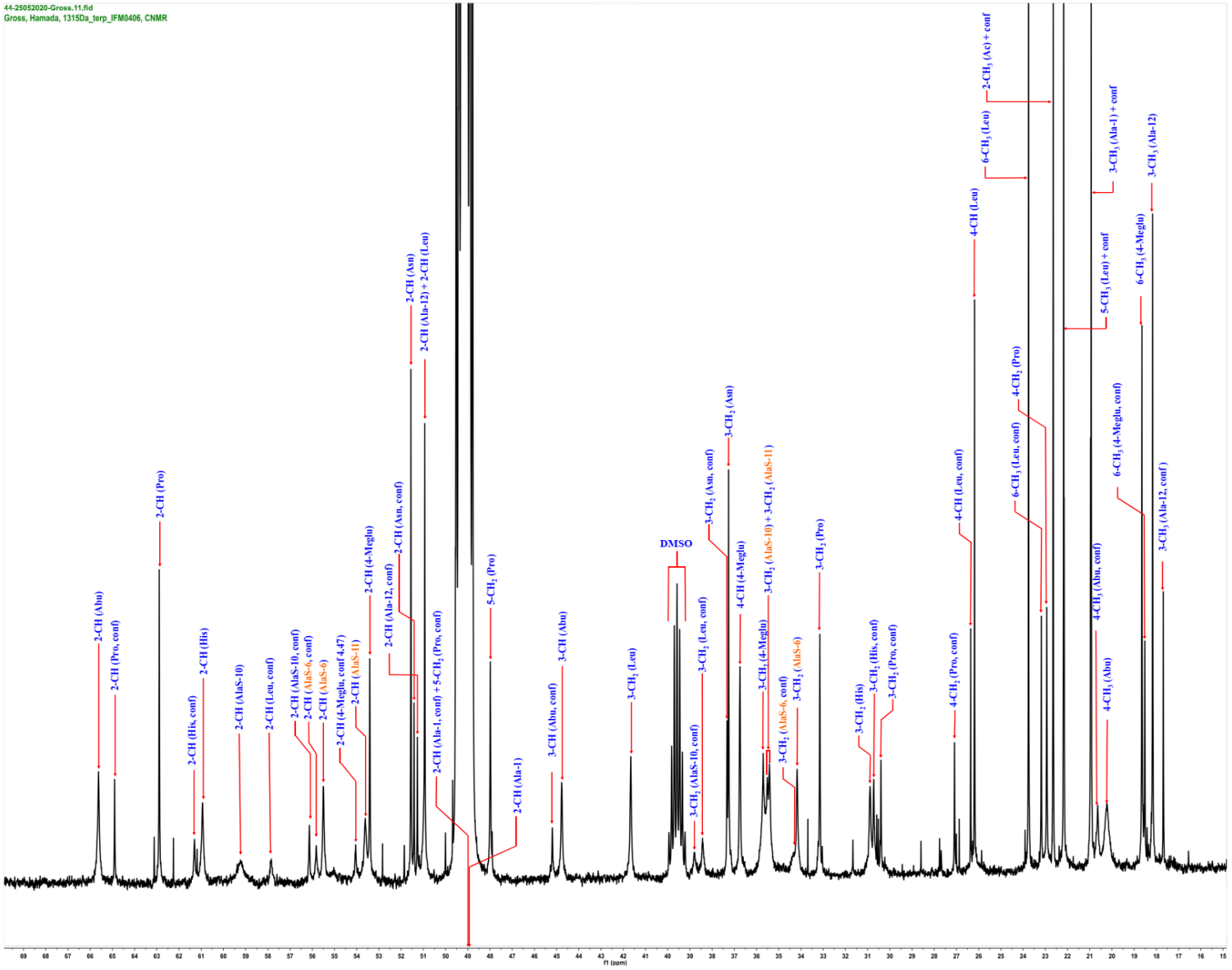

Figure S102. Annotated ^{13}C-NMR spectrum of nocathioamide A (**1**) (d_3-CH_3OH, 176 MHz)

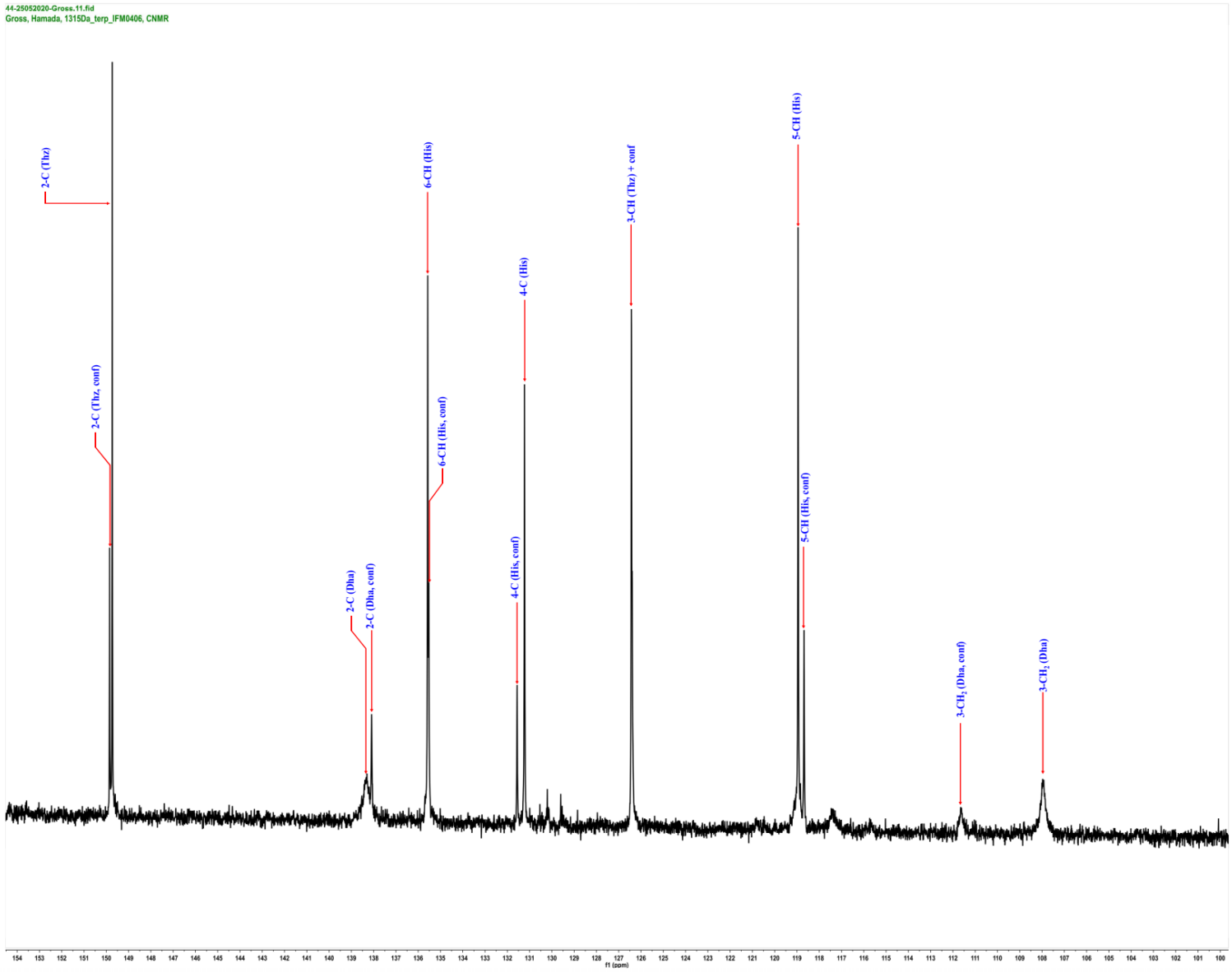

Figure S102A. Annotated ^{13}C-NMR spectrum of nocathioamide A (**1**) (d_3-CH_3OH, 176 MHz)

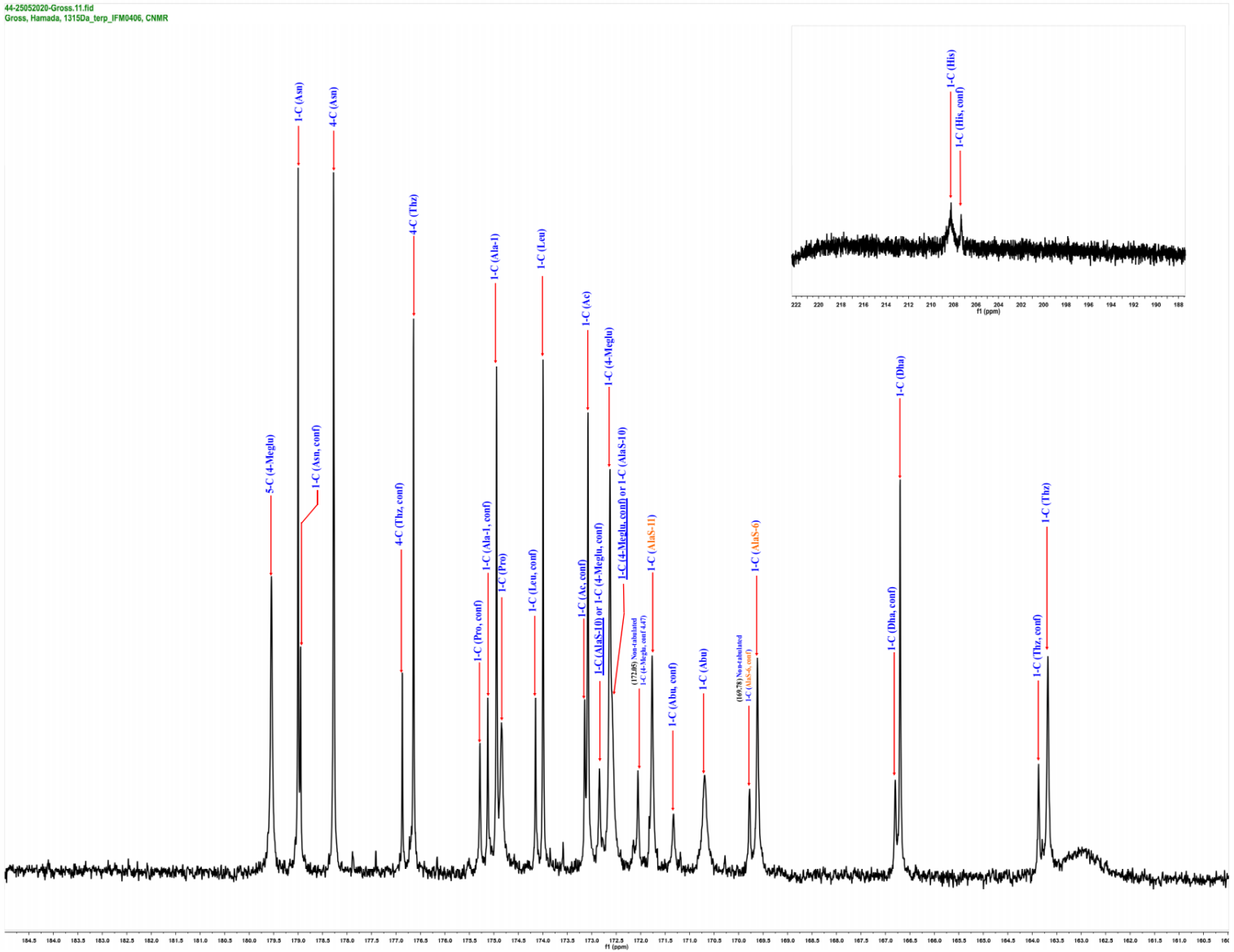

Figure S102B. Annotated ^{13}C-NMR spectrum of nocathioamide A (**1**) (d_3-CH_3OH, 176 MHz)

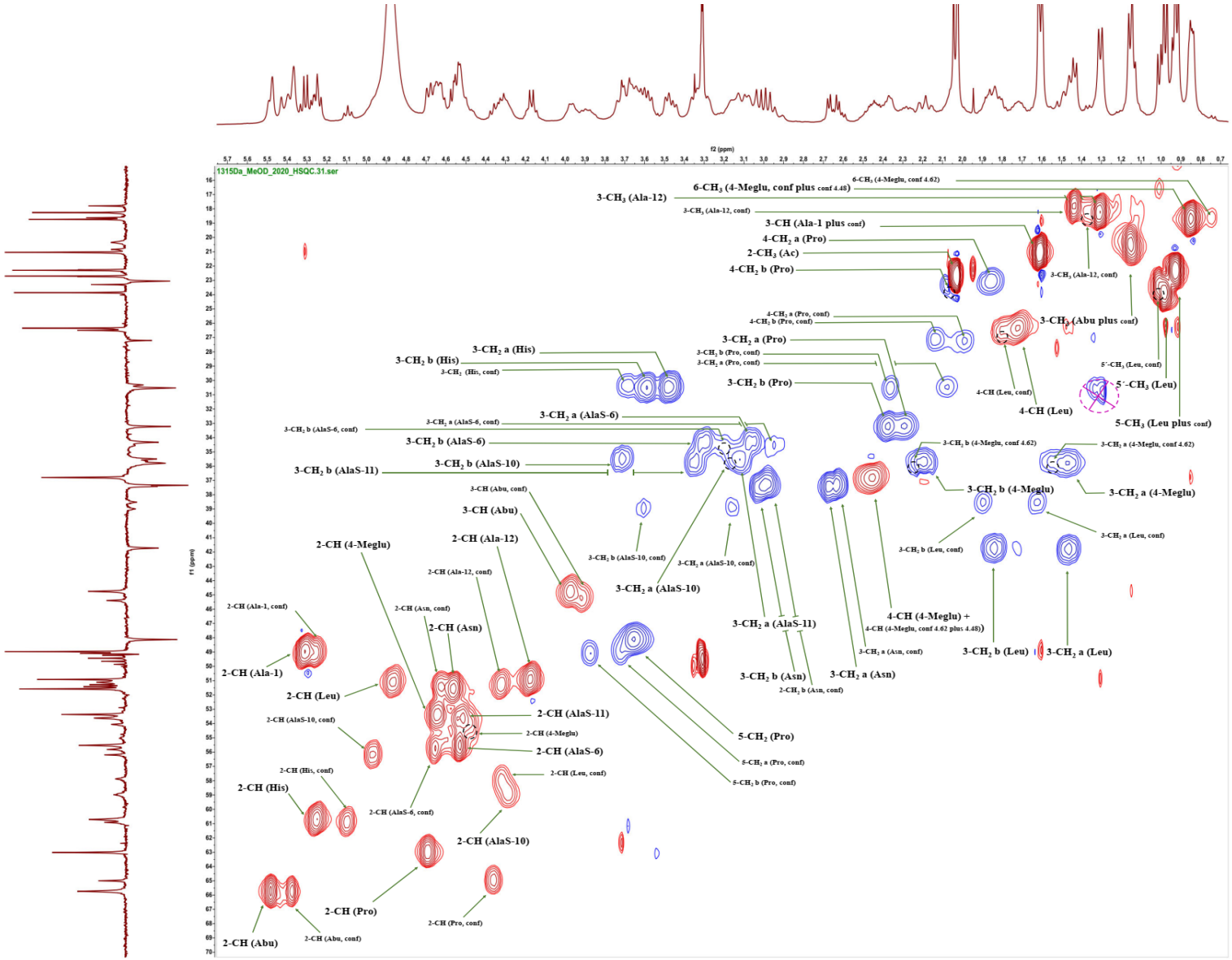

Figure S103. Annotated ^{1}H-^{13}C HSQC spectrum of nocathioamide A (**1**) (d_4-CH_3OH, 400/100 MHz)

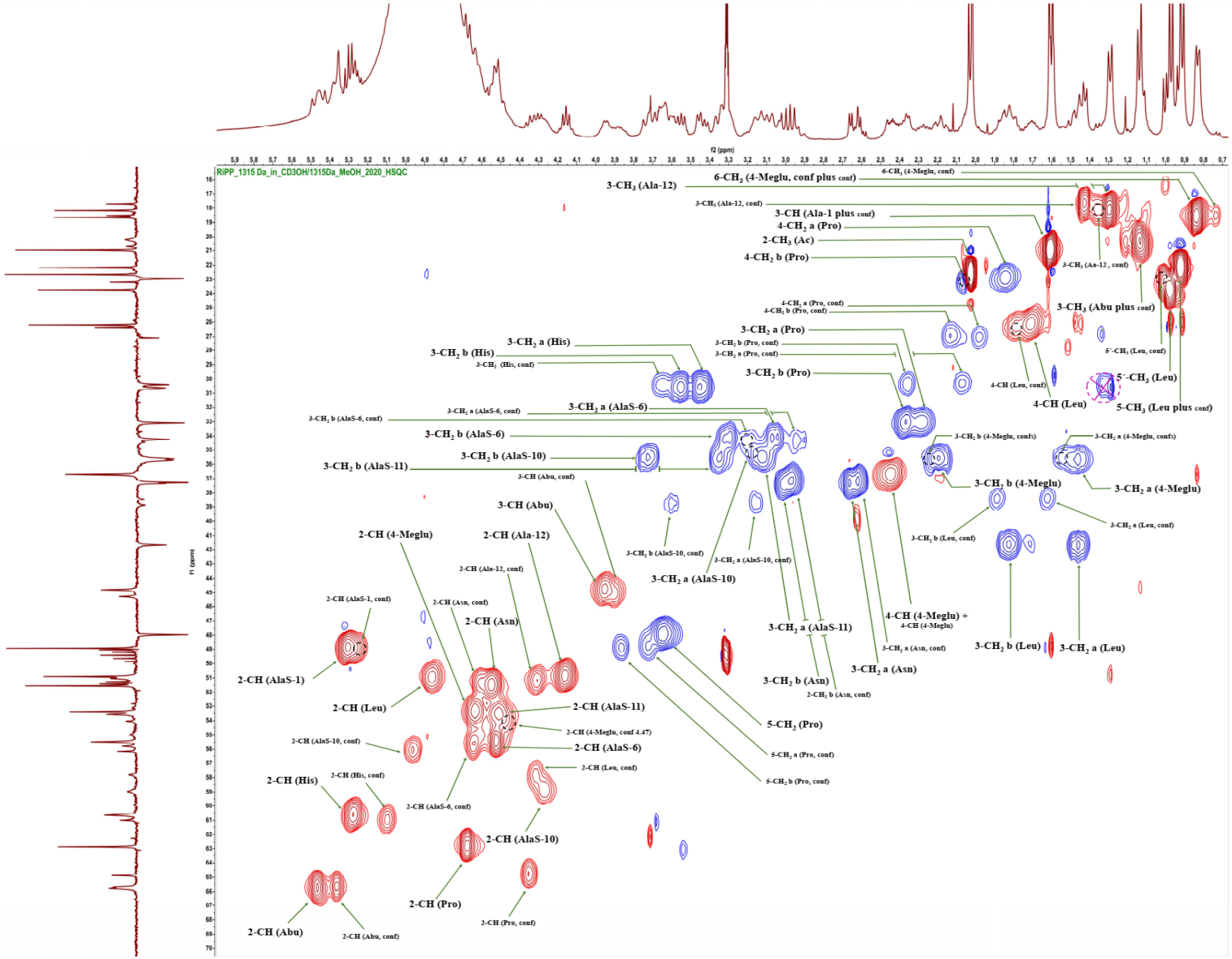

Figure S104. Annotated ^{1}H-^{13}C HSQC spectrum of nocathioamide A (**1**) (d_3-CH_3OH, 400/100 MHz)

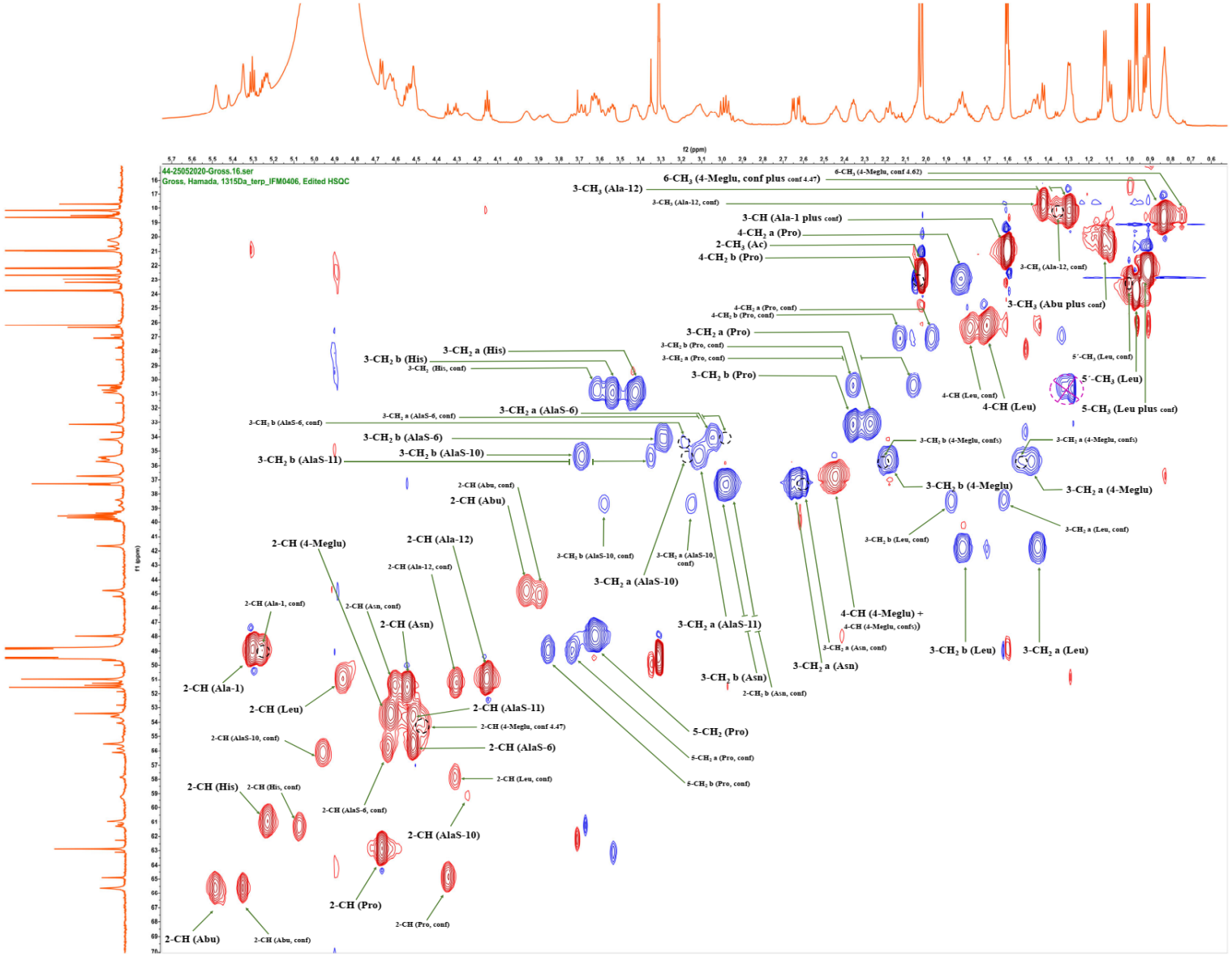

Figure S105. Annotated ^{1}H-^{13}C HSQC spectrum of nocathioamide A (**1**) (d_3-CH_3OH, 700/176 MHz)

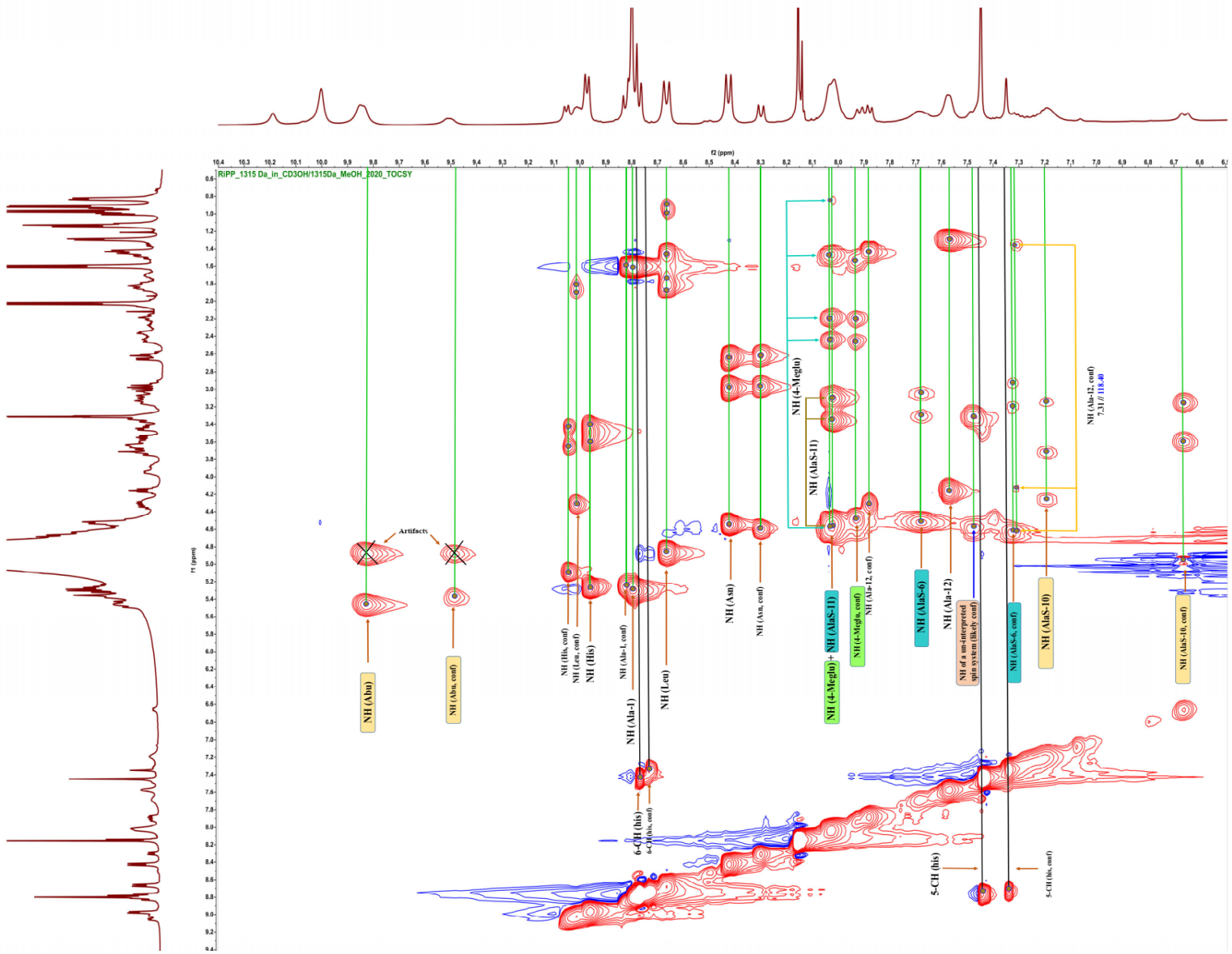

Figure S106. Annotated ^{1}H-^{1}H TOCSY spectrum of nocathioamide A (**1**) (d_3-CH_3OH, 400/400 MHz)

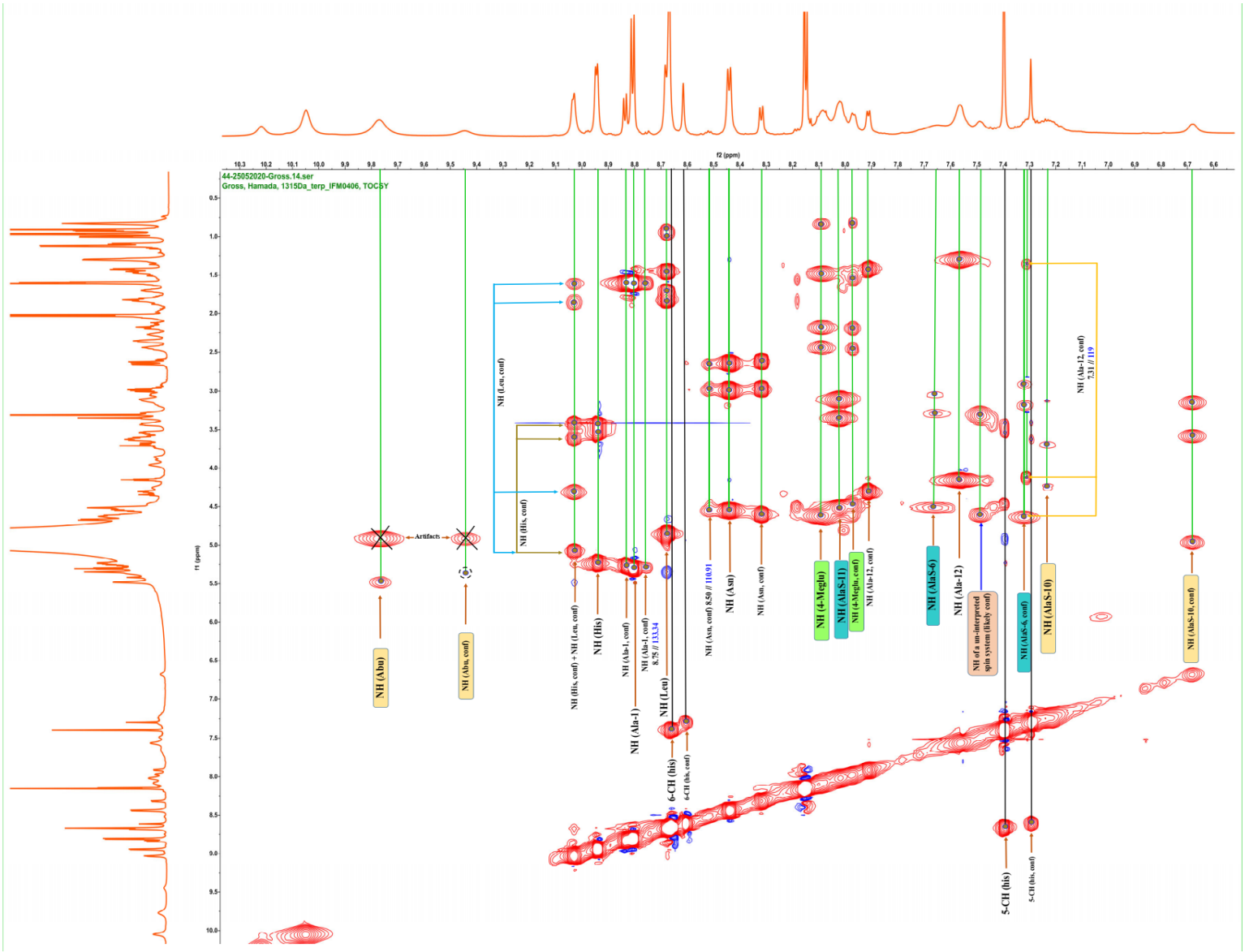

Figure S107. Annotated ^{1}H-^{1}H TOCSY spectrum of nocathioamide A (**1**) (d_3-CH_3OH, 700/700 MHz)

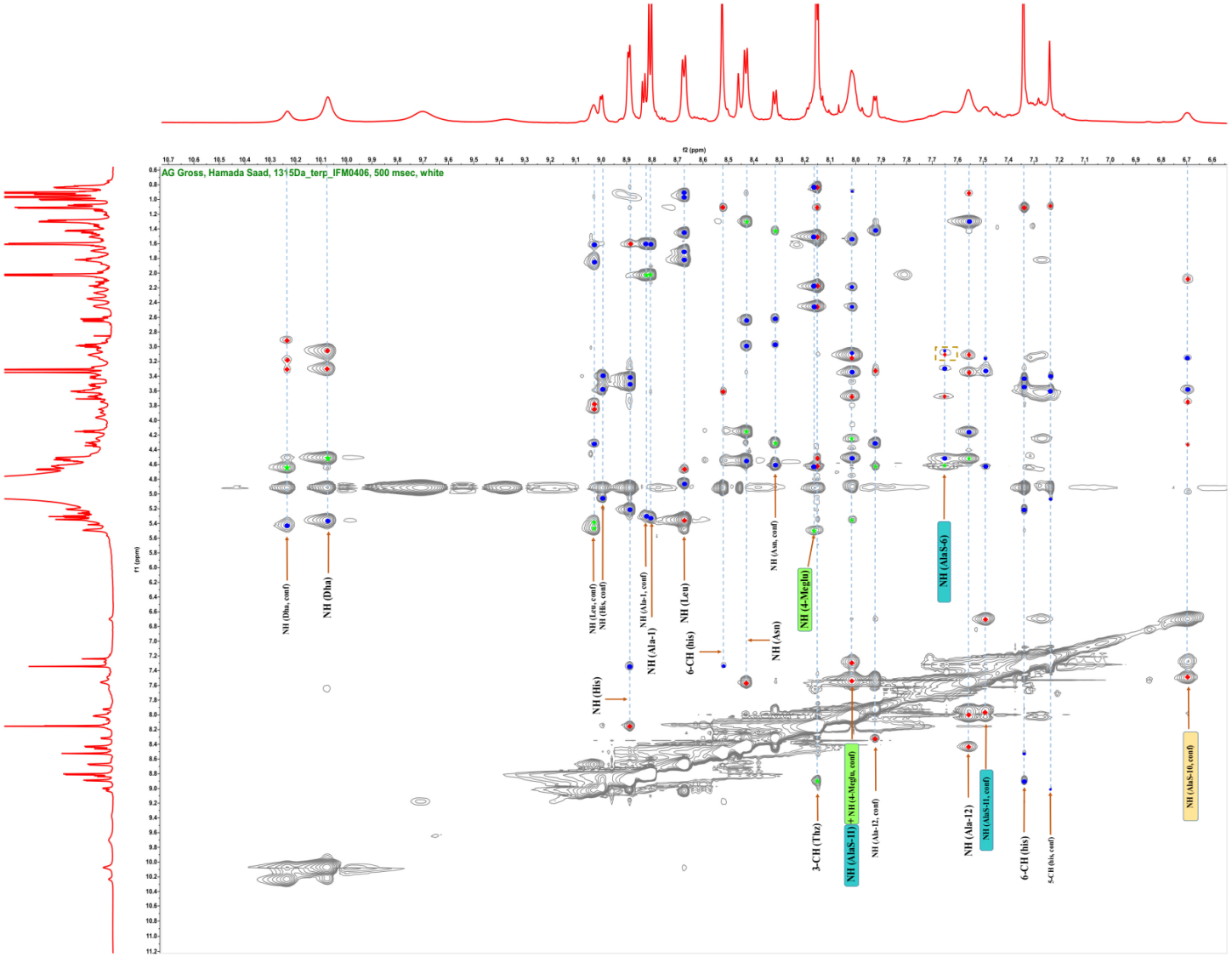

Figure S108. Annotated ^{1}H-^{1}H NOESY spectrum of nocathioamide A (**1**) (d_3-CH_3OH, 700/700 MHz). Cross correlations color code: a blue circle indicates resonances, observed within each amino acid residue; a green asterisk indicates through-space interactions with the adjacent amino acids of the peptidic backbone; a red diamond indicates through-space interactions with distant/unexpected residues.

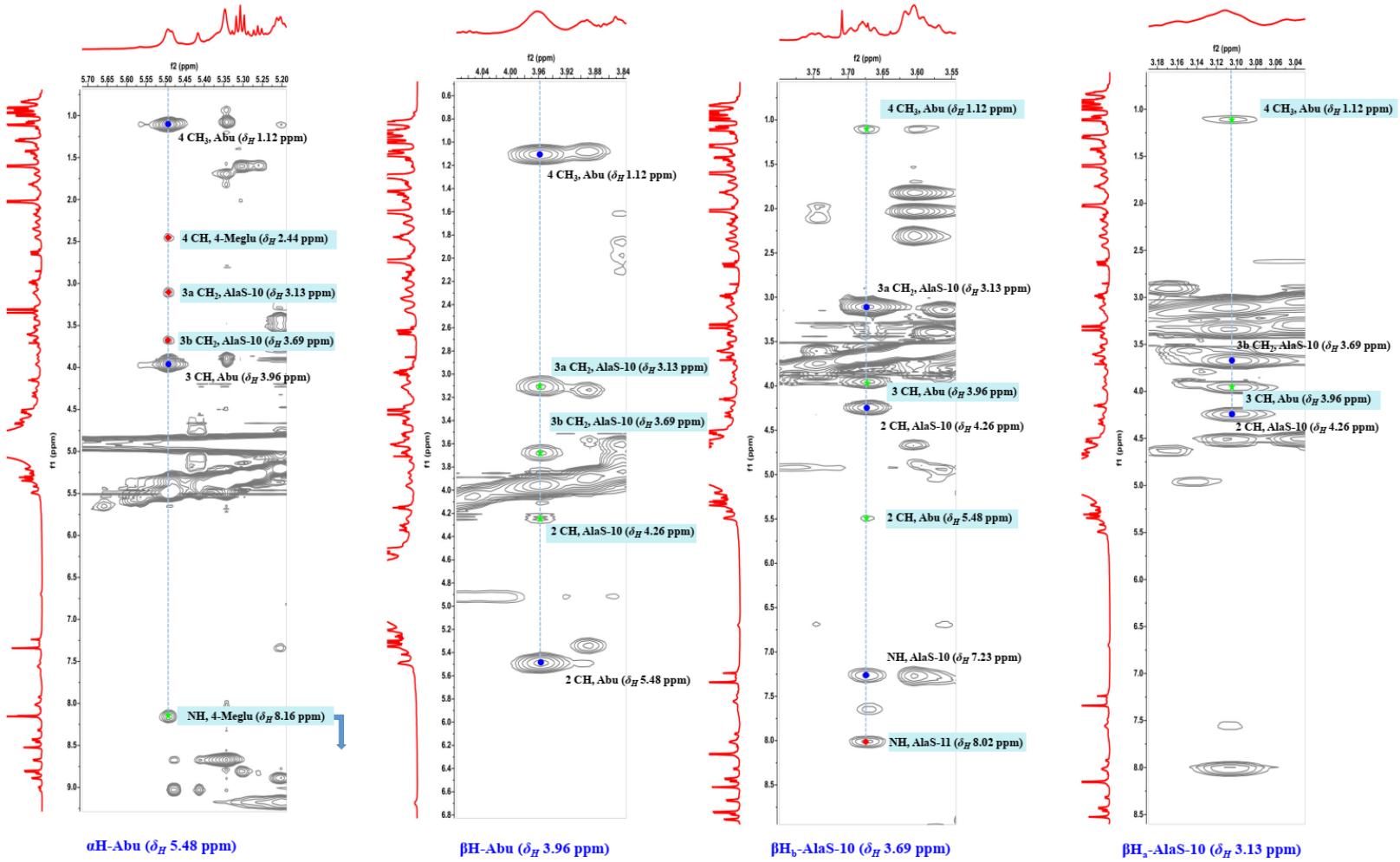

Figure S108A. Annotated ^{1}H-^{1}H NOESY spectrum of the **MeLan** bridge of nocathioamide A (**1**) (d_3-CH_3OH, 700/700 MHz). Cross correlations color code: a blue circle indicates resonances, observed within each amino acid residue; a green asterisk indicates through-space interactions with expected components of **AlaS-10** and **Abu**; a red diamond indicates through-space interactions with distant components of **AlaS-10, AlaS-11**, and **4-Meglu**.

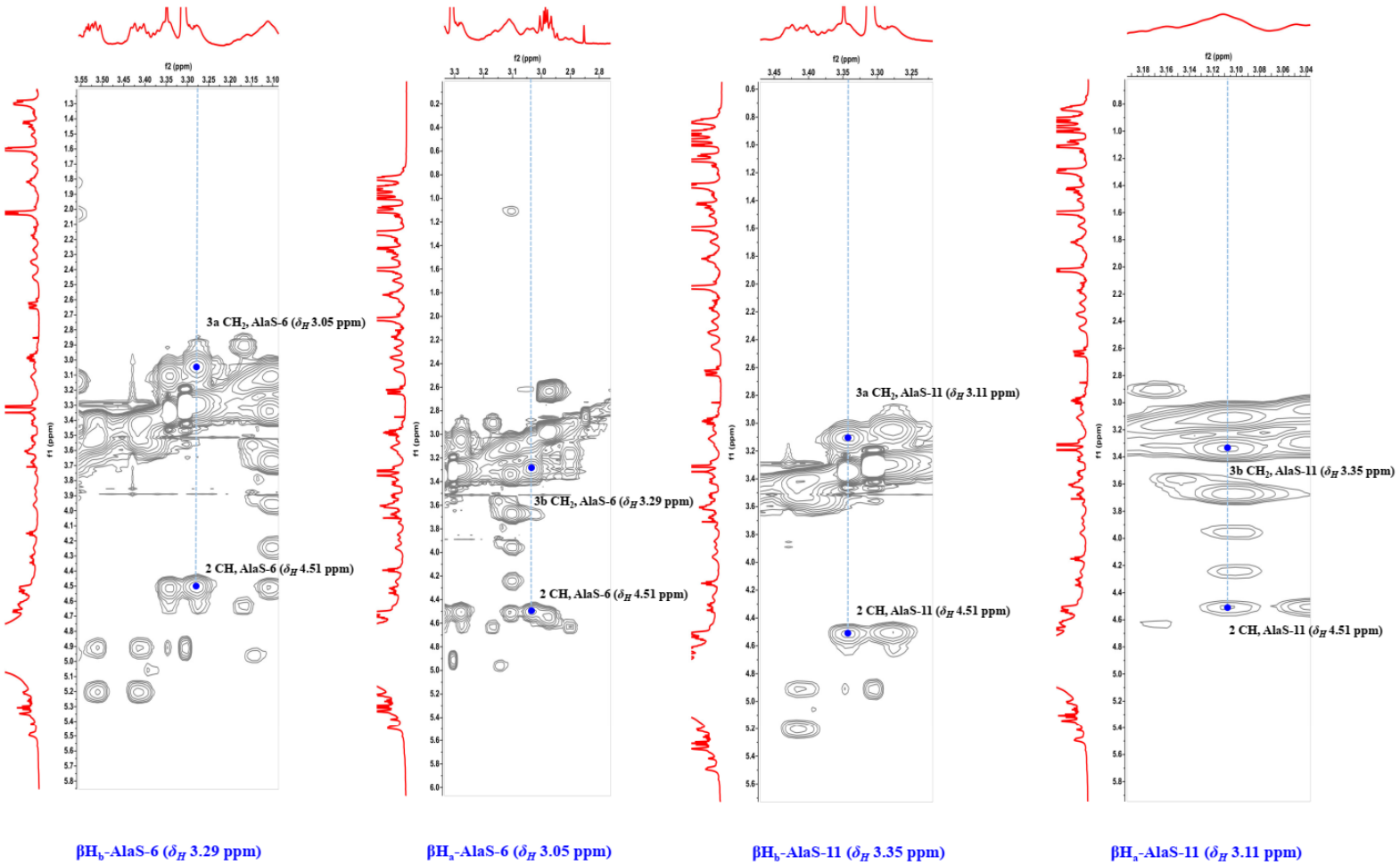

Figure S108B. Annotated ^{1}H-^{1}H NOESY spectrum of the **Lan** bridge of nocathioamide A (**1**) (d_3-CH_3OH, 700/700 MHz). Cross correlations marked with a blue circle indicate resonances, observed within each amino acid residue.

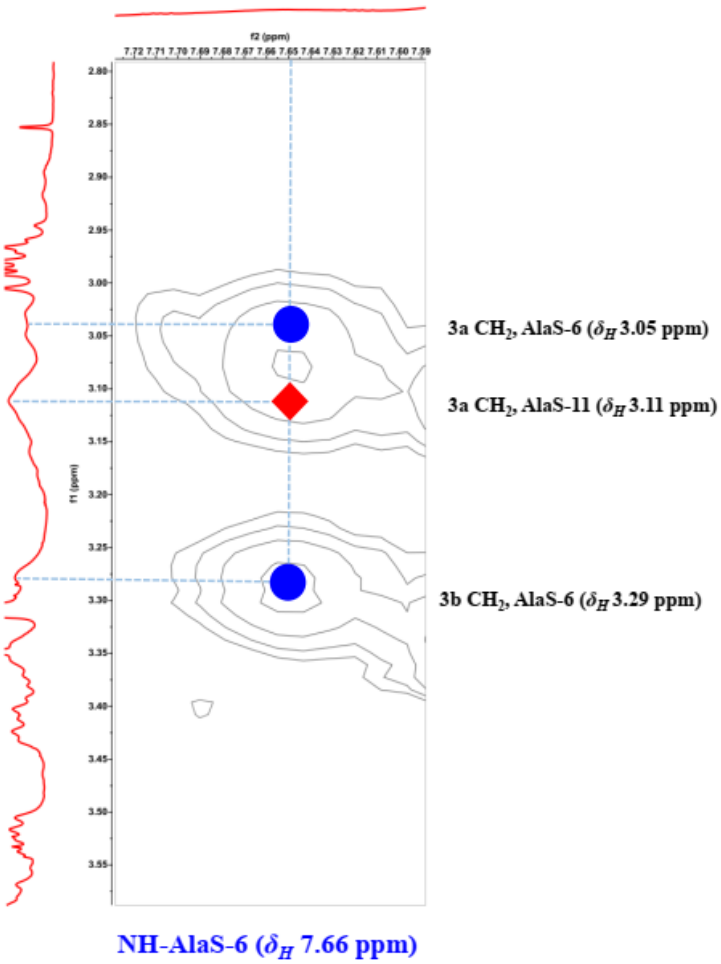

Figure S108C. Annotated ^{1}H-^{1}H NOESY spectrum of the **NH- AlaS-6** of nocathioamide A (**1**) (d_3-CH_3OH, 700/700 MHz). Cross correlations color code: a blue circle indicates resonances, observed within each amino acid residue, while a red diamond indicates through-space interactions with **βHa- AlaS-11**.

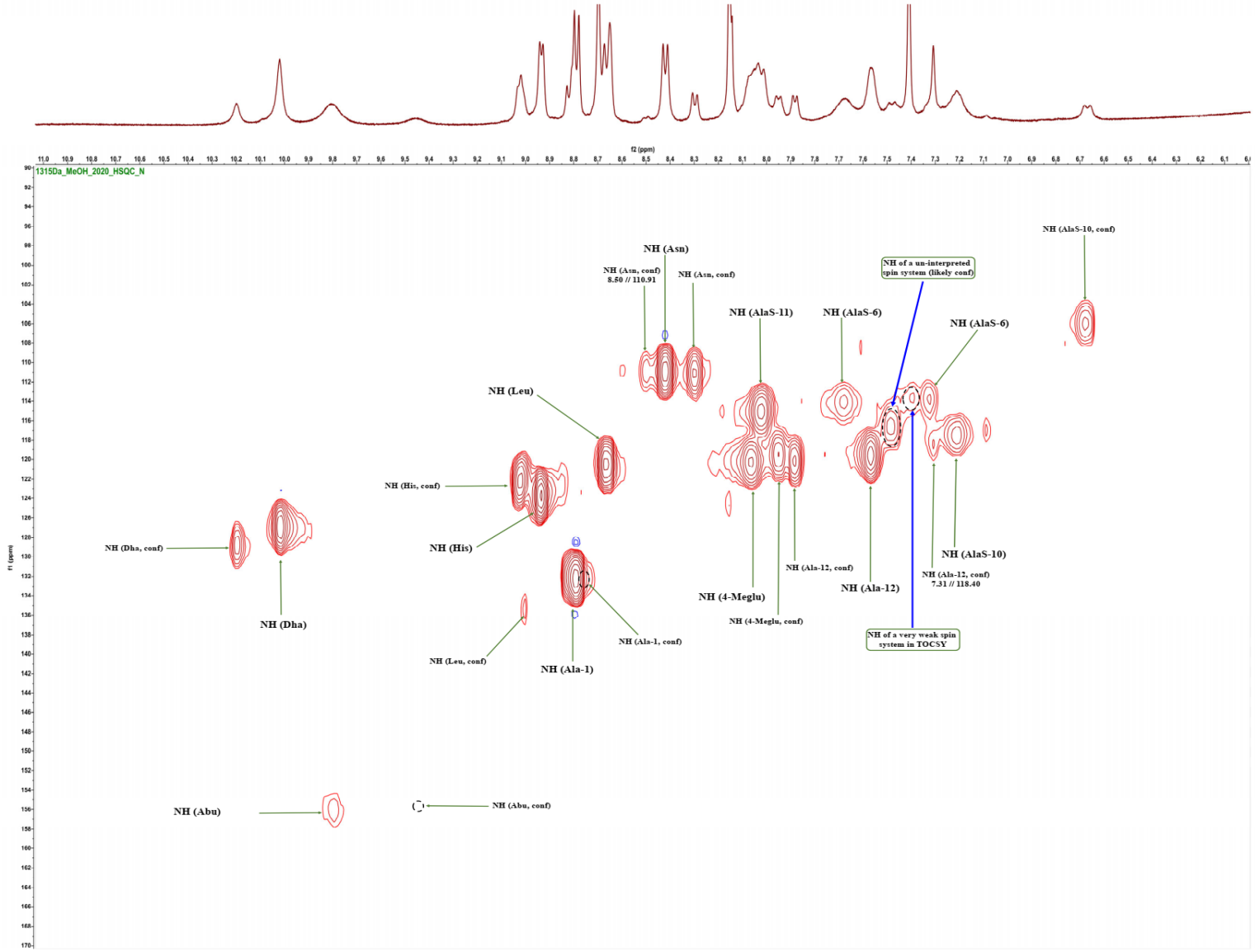

Figure S109. Annotated ^{1}H-^{15}N HSQC spectrum of nocathioamide A (**1**) (d_3-CH_3OH, 400/40.6 MHz)

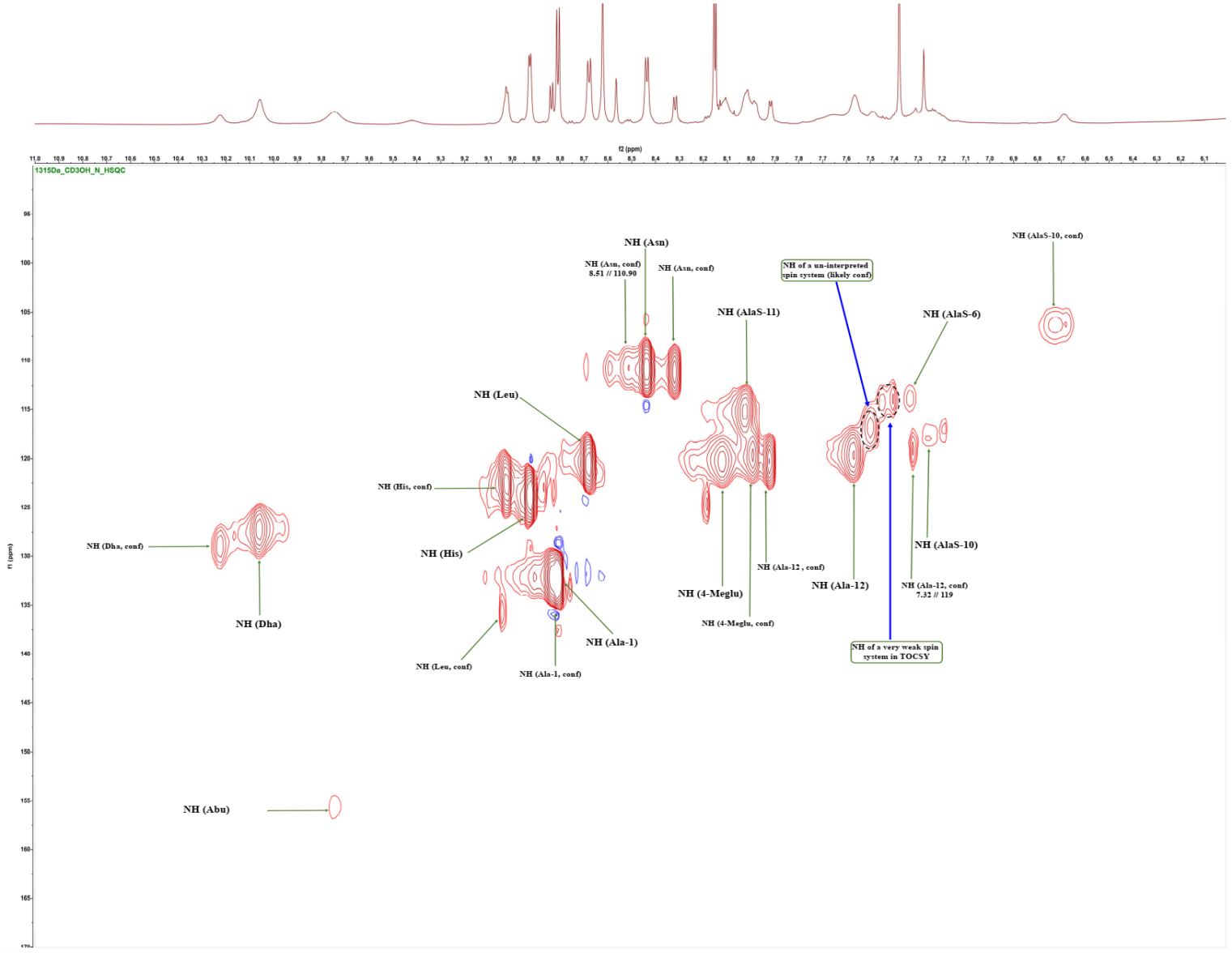

Figure S110. Annotated ^{1}H-^{15}N HSQC spectrum of nocathioamide A (**1**) (d_3-CH_3OH, 700/71 MHz)

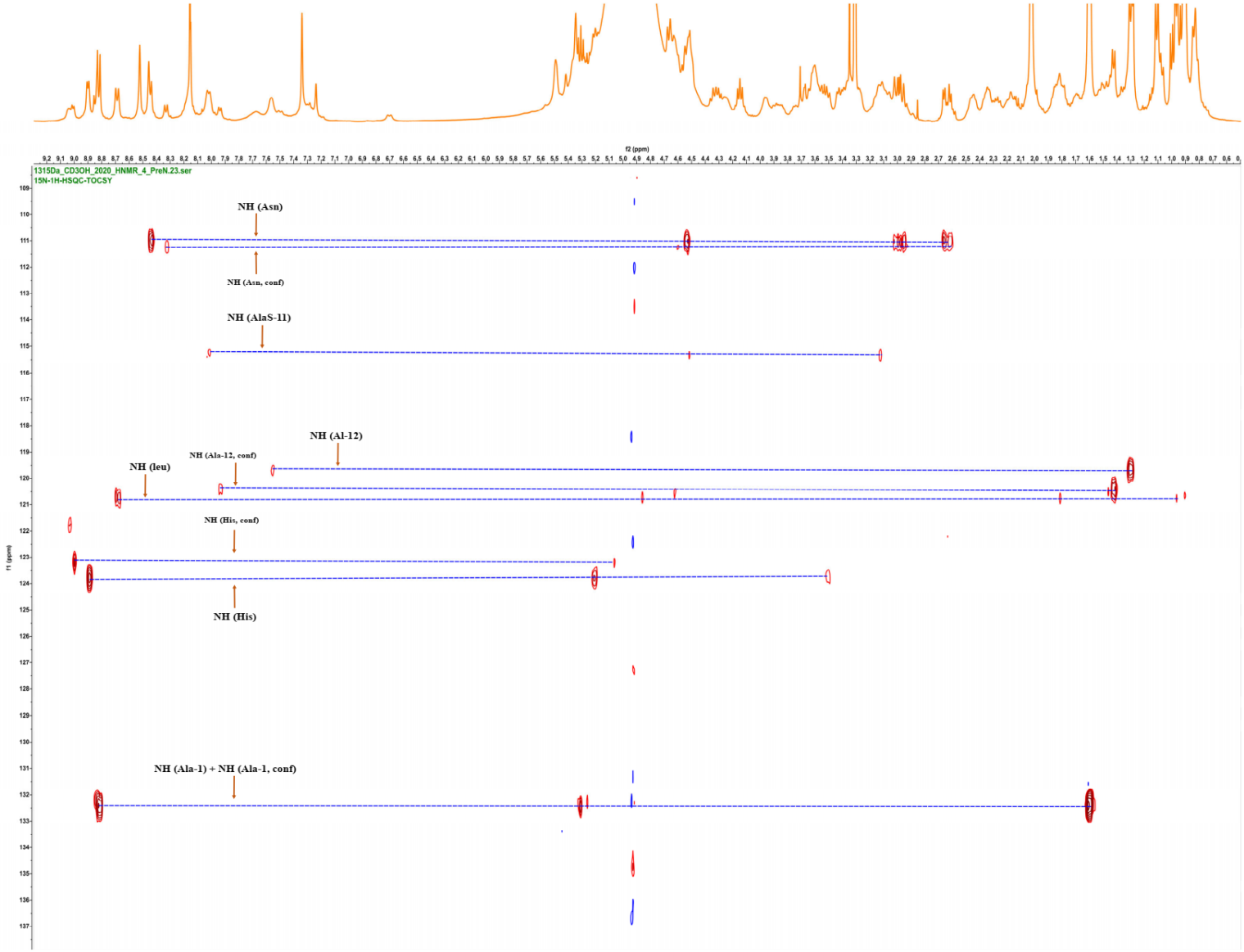

Figure S111. Annotated ^{1}H-^{15}N HSQC-TOCSY spectrum of nocathioamide A (**1**) (d_3-CH_3OH, 400/40.6 MHz)

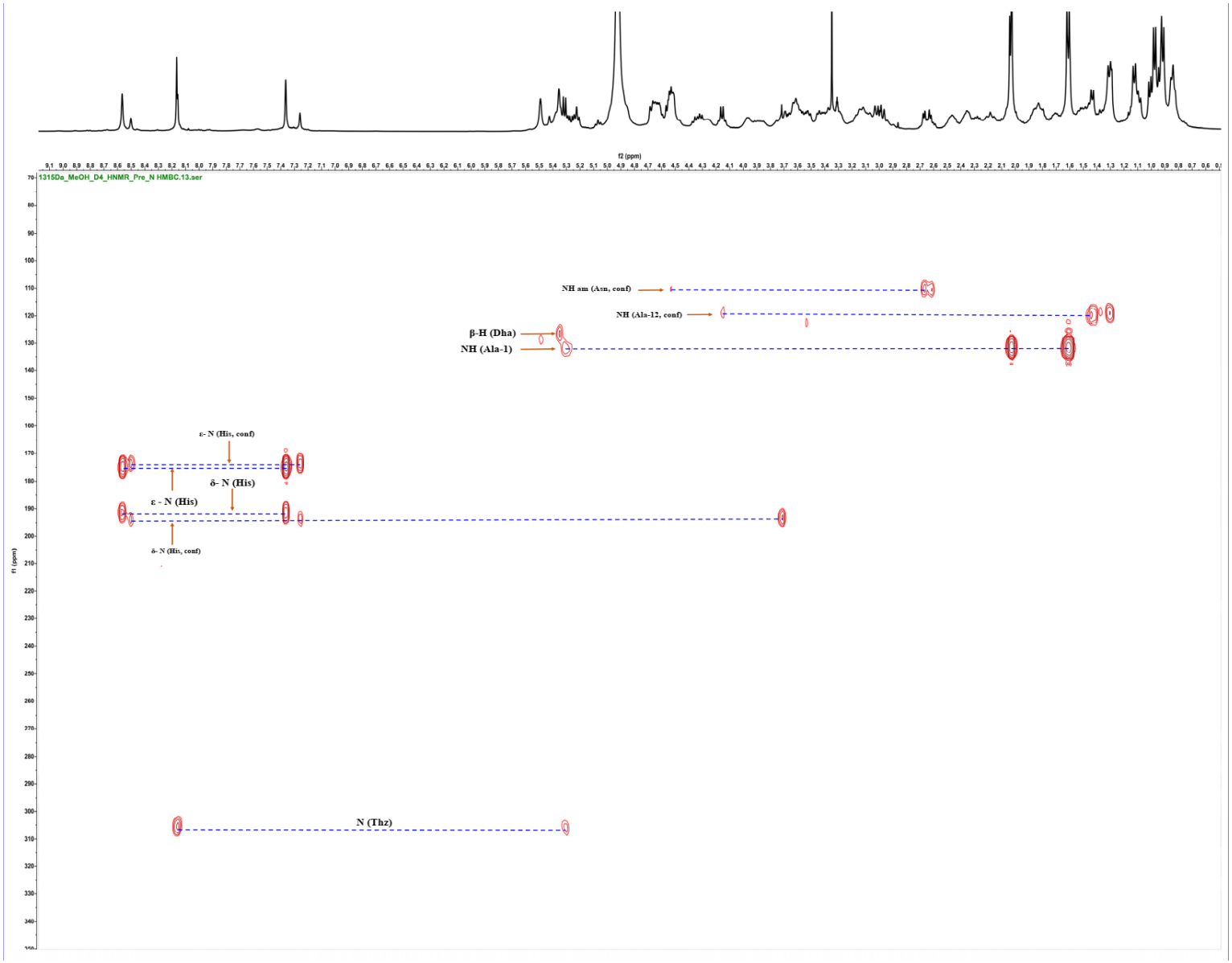

Figure S112. Annotated ^{1}H-^{15}N HMBC spectrum of nocathioamide A (**1**) (d_4-CH_3OH, 400/40.6 MHz)

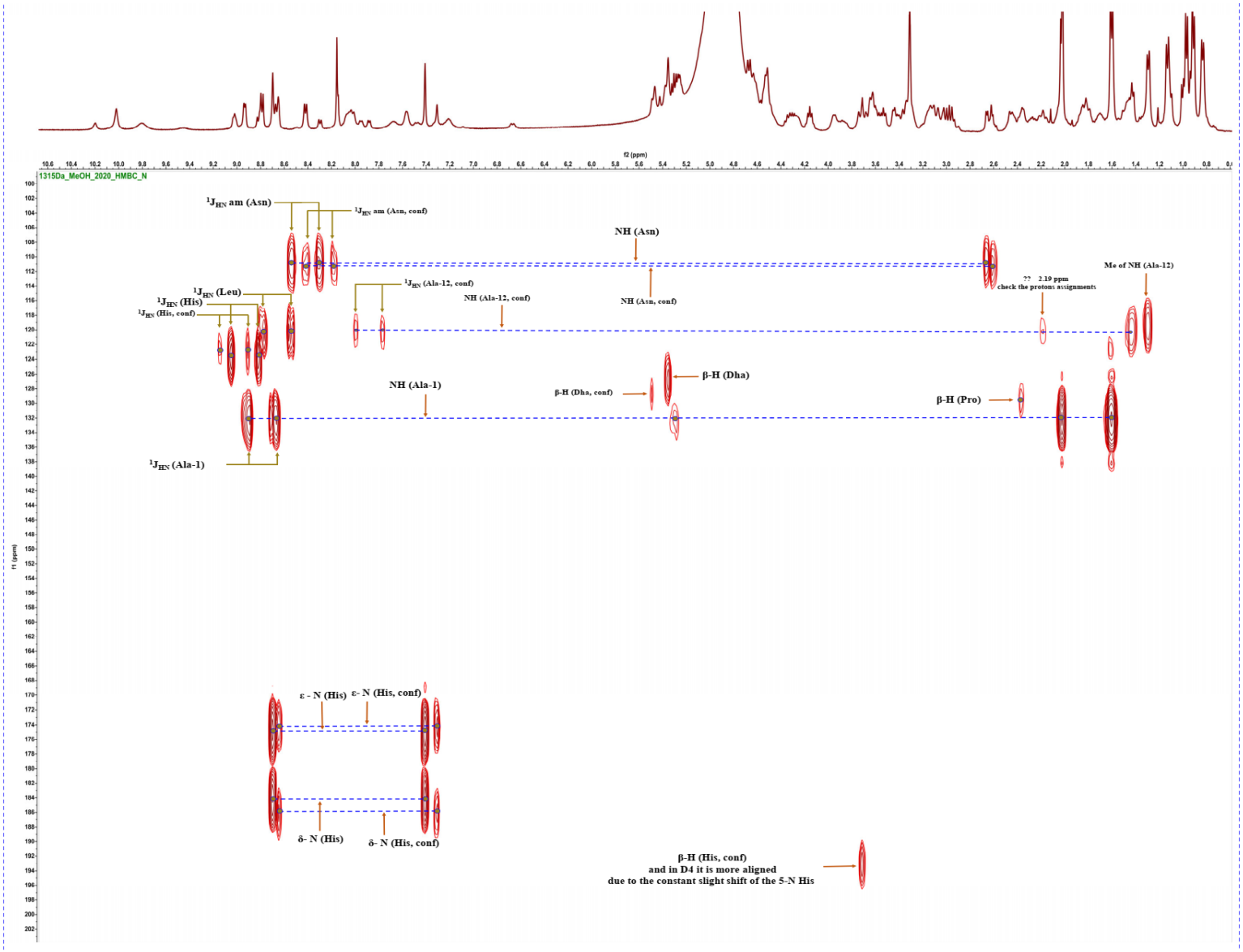

Figure S113. Annotated ^{1}H-^{15}N HMBC spectrum of nocathioamide A (**1**) (d_3-CH_3OH, 400/40.6 MHz)

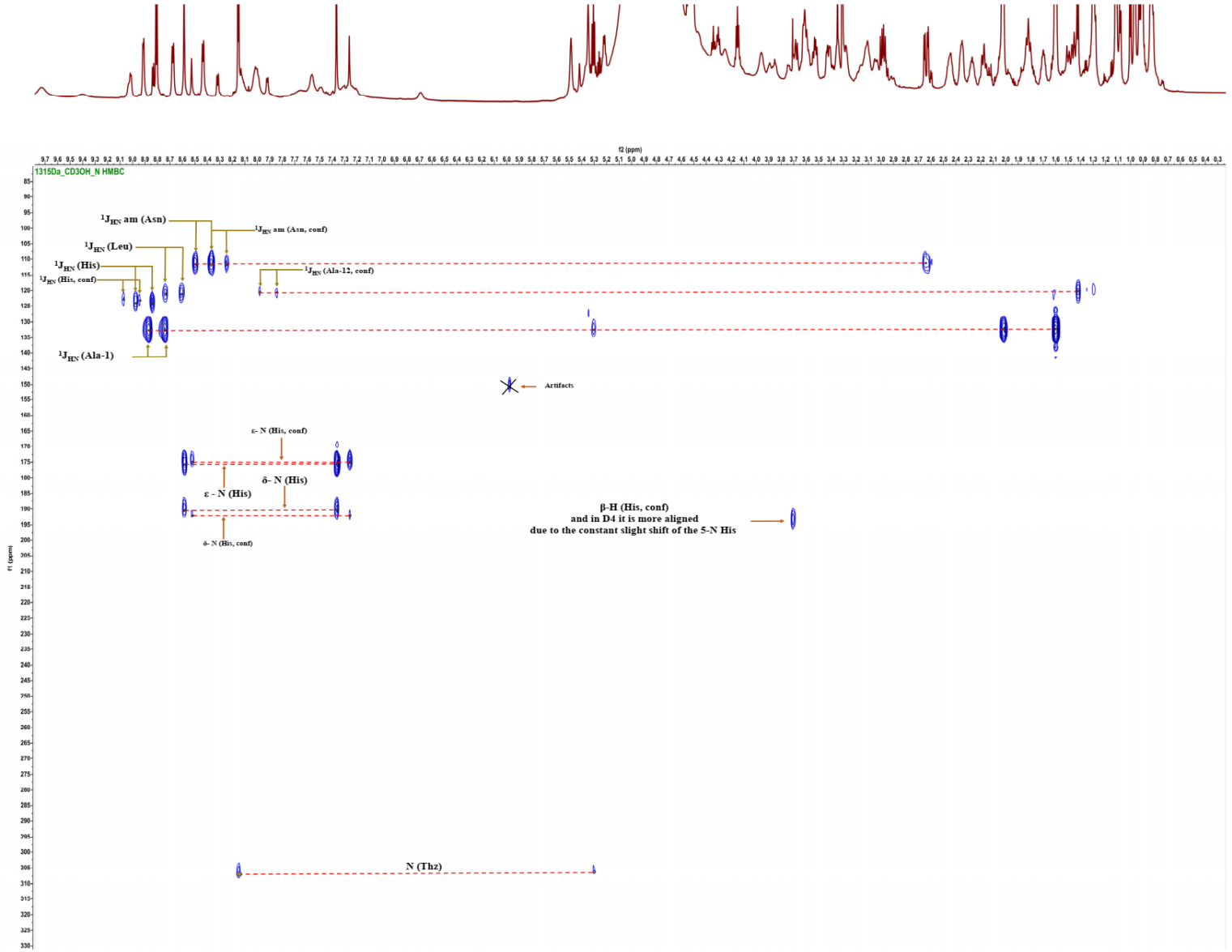

Figure S114. Annotated ^{1}H-^{15}N HMBC spectrum of nocathioamide A (**1**) (d_3-CH_3OH, 700/71 MHz)

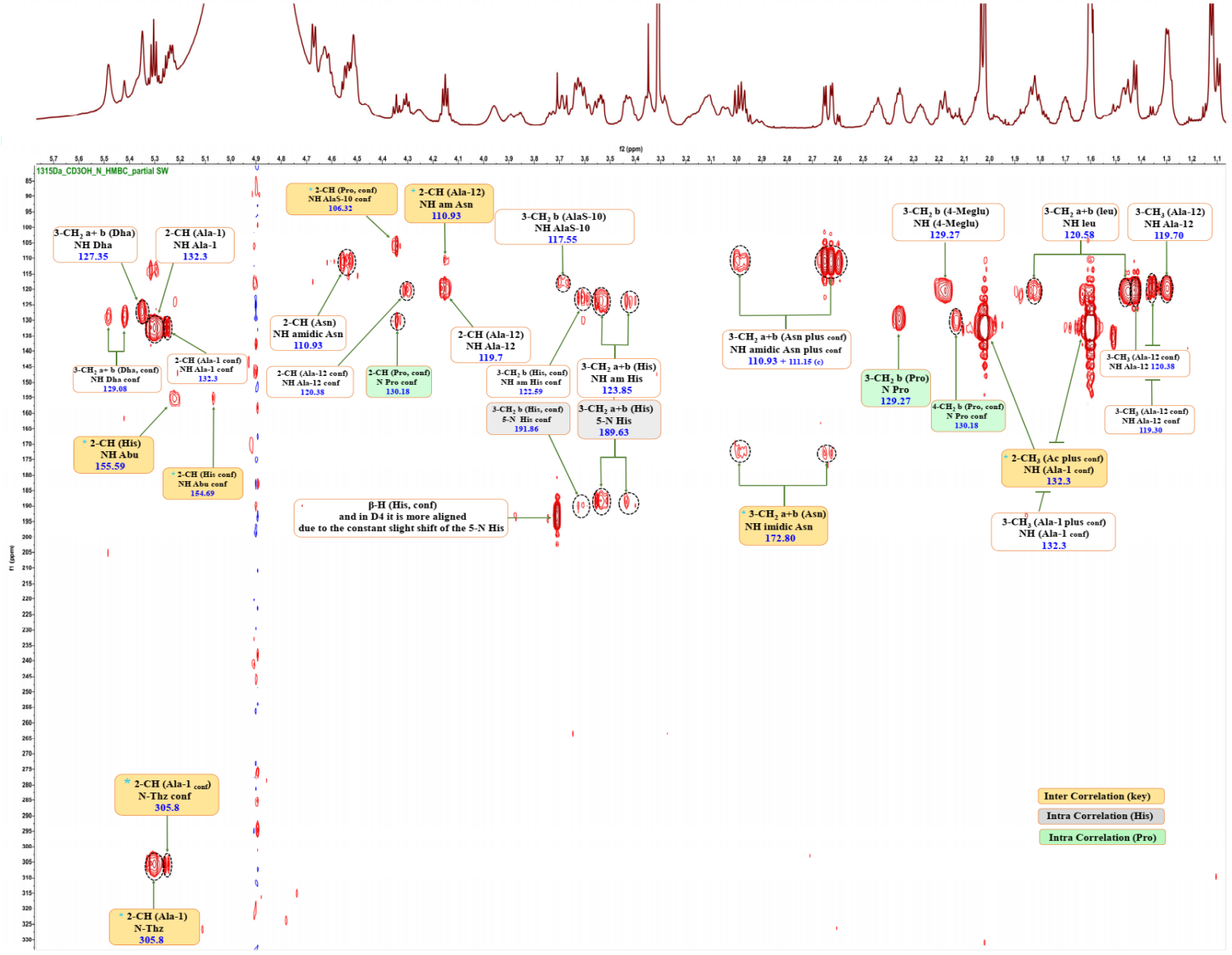

Figure S114A. Annotated ^{1}H-^{15}N HMBC partial SW spectrum of nocathioamide A (**1**) (d_3-CH_3OH, 700/71 MHz)

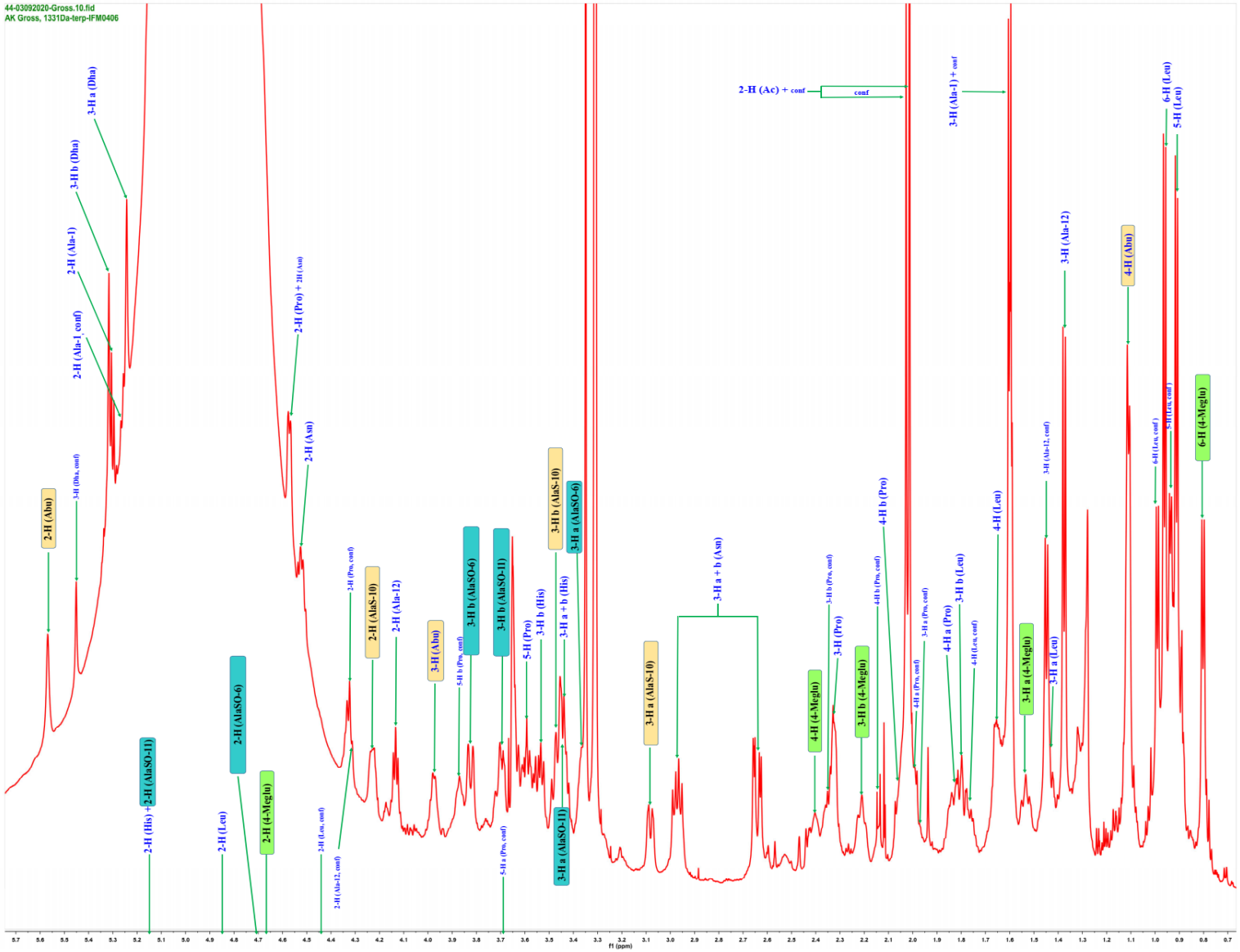

Figure S115. Annotated ^{1}H-NMR spectrum of nocathioamide B (**2**) (d_3-CH_3OH, 700 MHz)

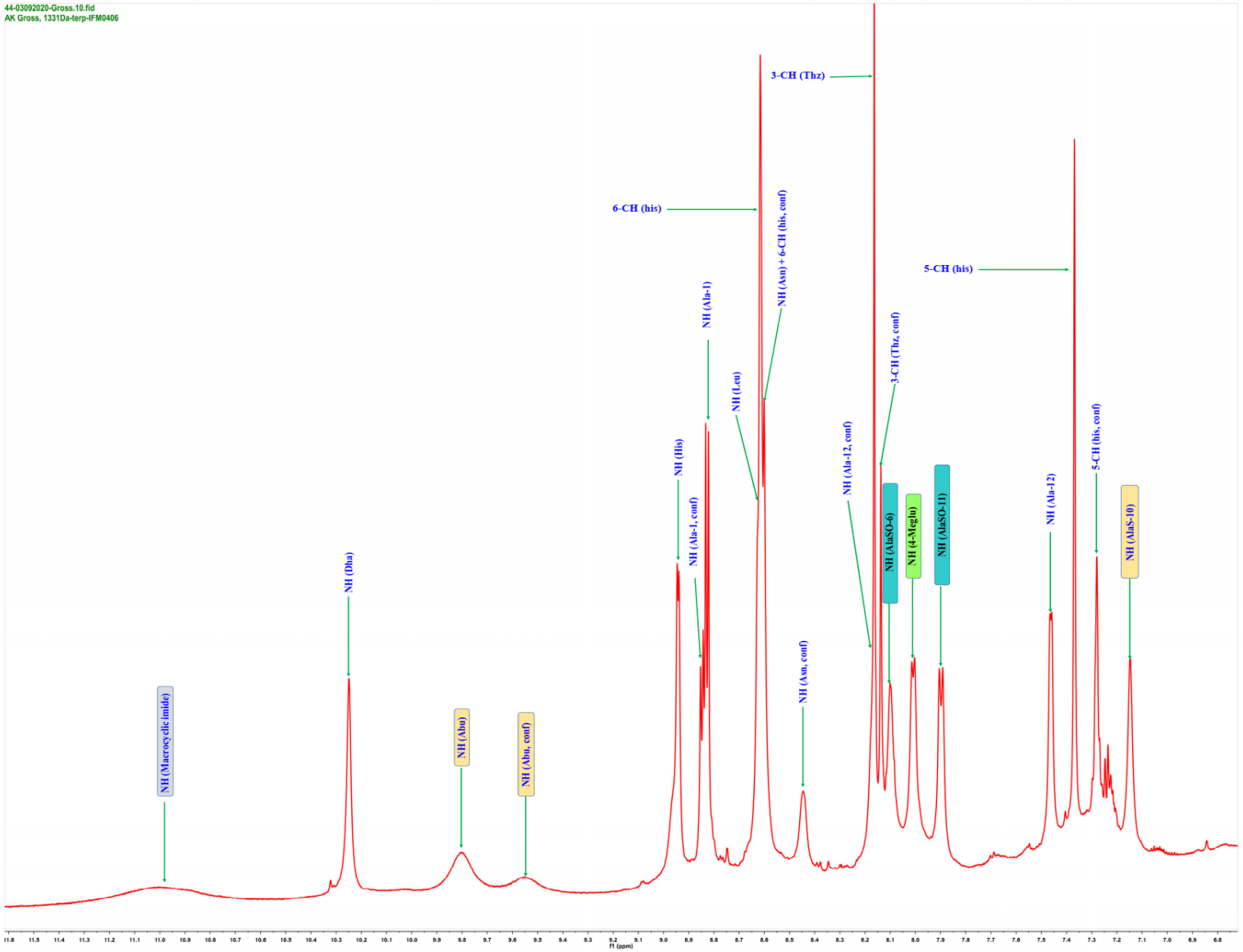

Figure S115A. Annotated ^{1}H-NMR spectrum of nocathioamide B (**2**) (d_3-CH_3OH, 700 MHz)

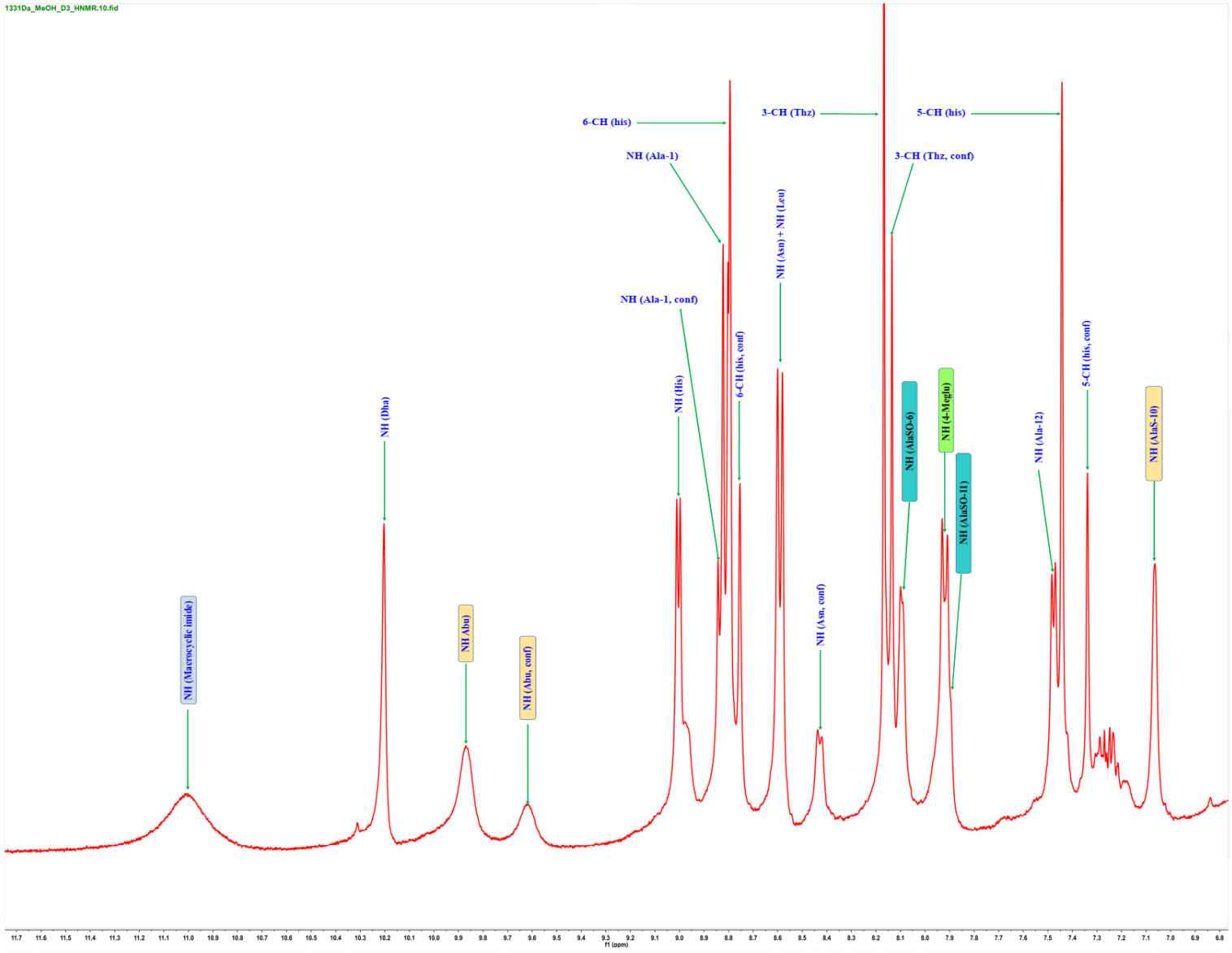

Figure S116. Annotated ^{1}H-NMR spectrum of nocathioamide B (**2**) (d_3-CH_3OH, 400 MHz)

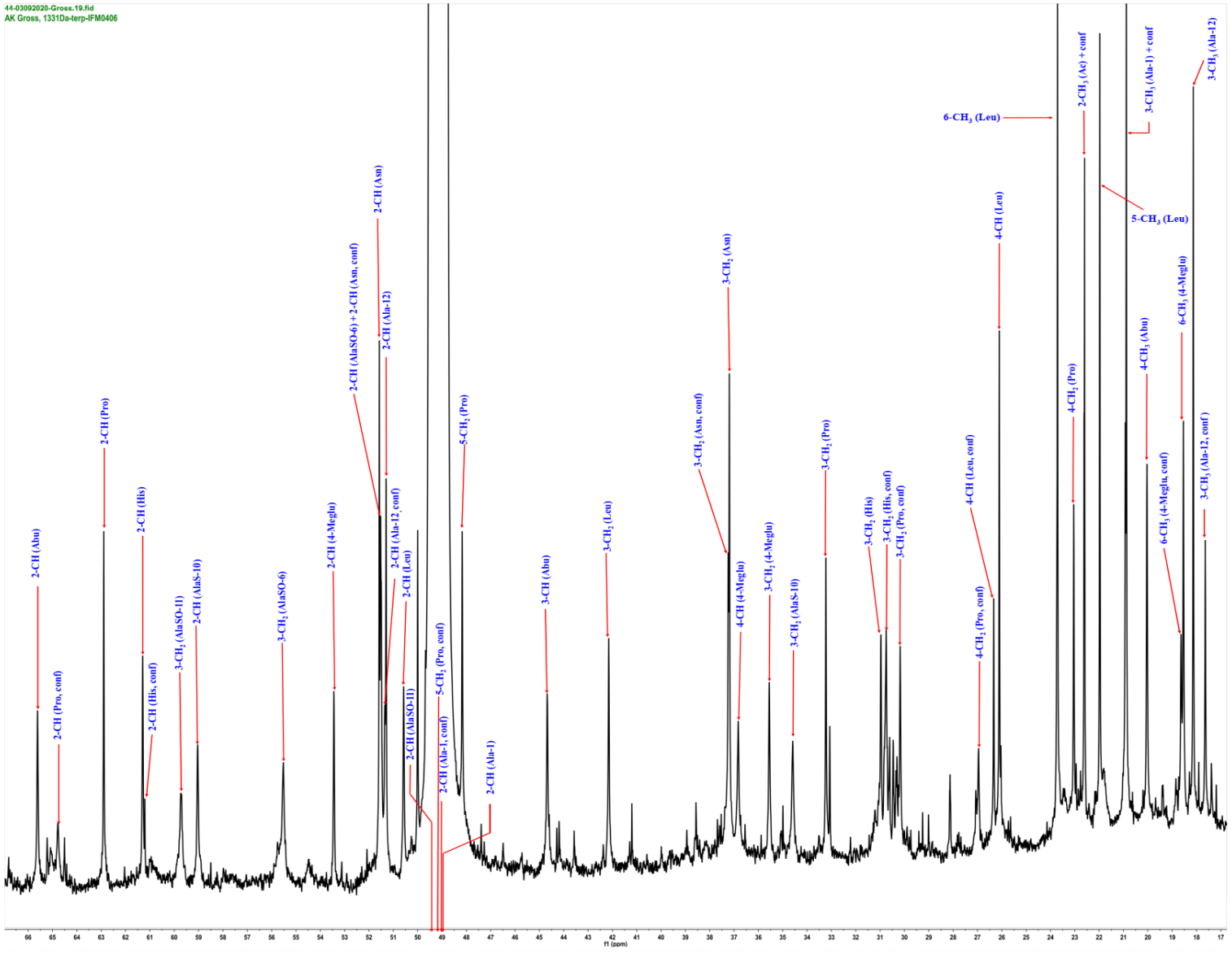

Figure S117. Annotated ^{13}C-NMR spectrum of nocathioamide B (**2**) (d_3-CH_3OH, 176 MHz)

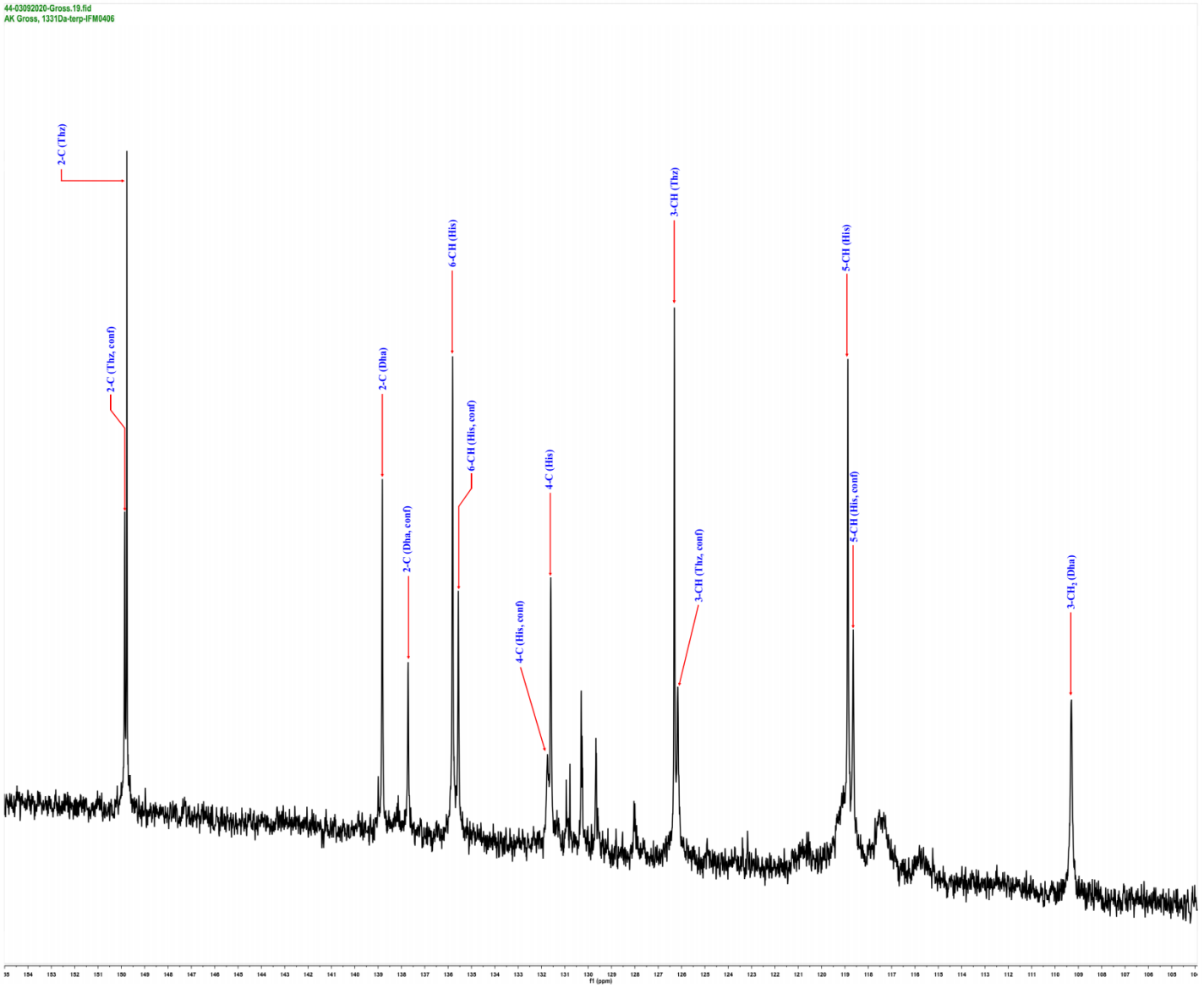

Figure S117A. Annotated ^{13}C-NMR spectrum of nocathioamide B (**2**) (d_3-CH_3OH, 176 MHz)

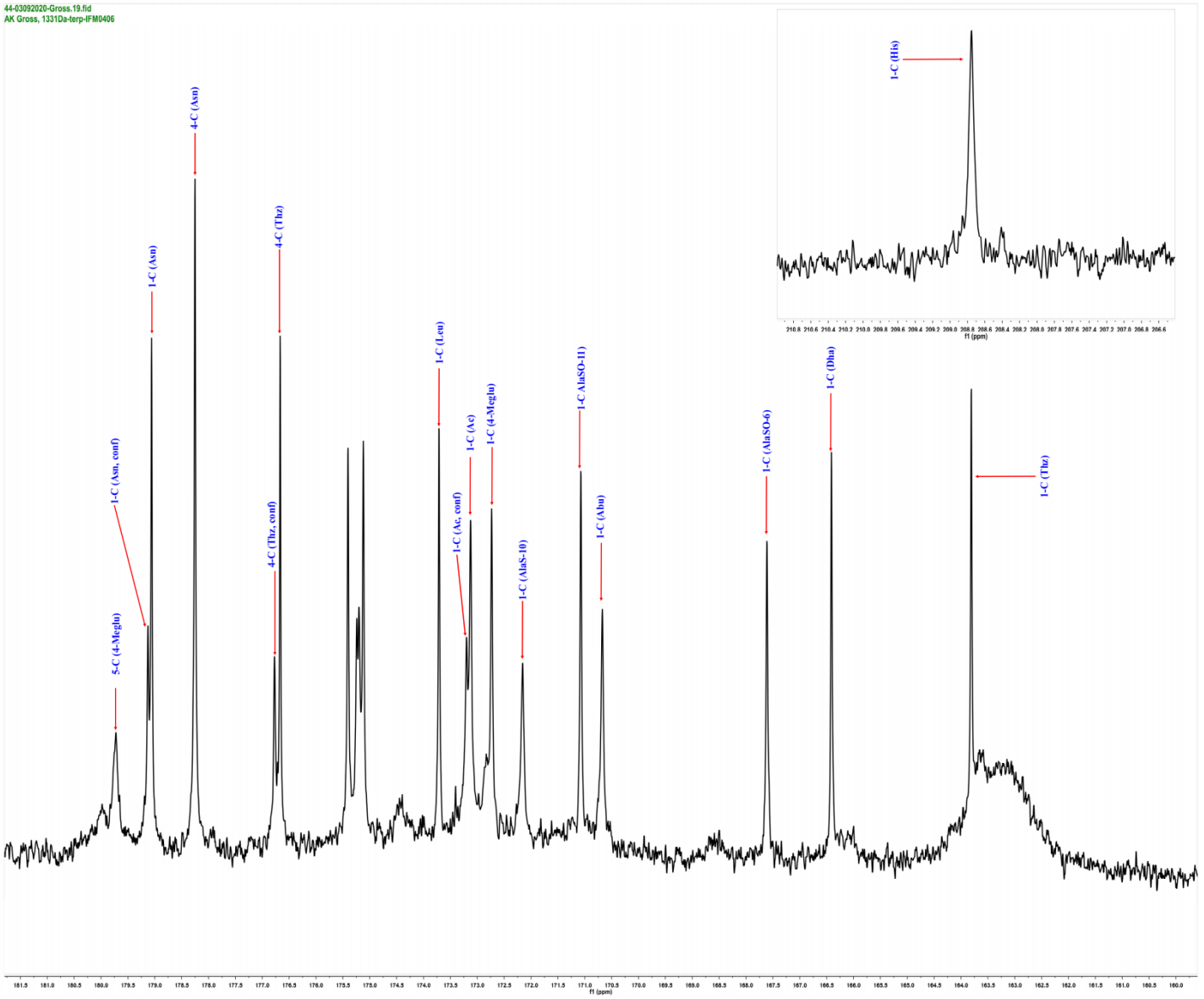

Figure S117B. Annotated ^{13}C-NMR spectrum of nocathioamide B (**2**) (d_3-CH_3OH, 176 MHz)

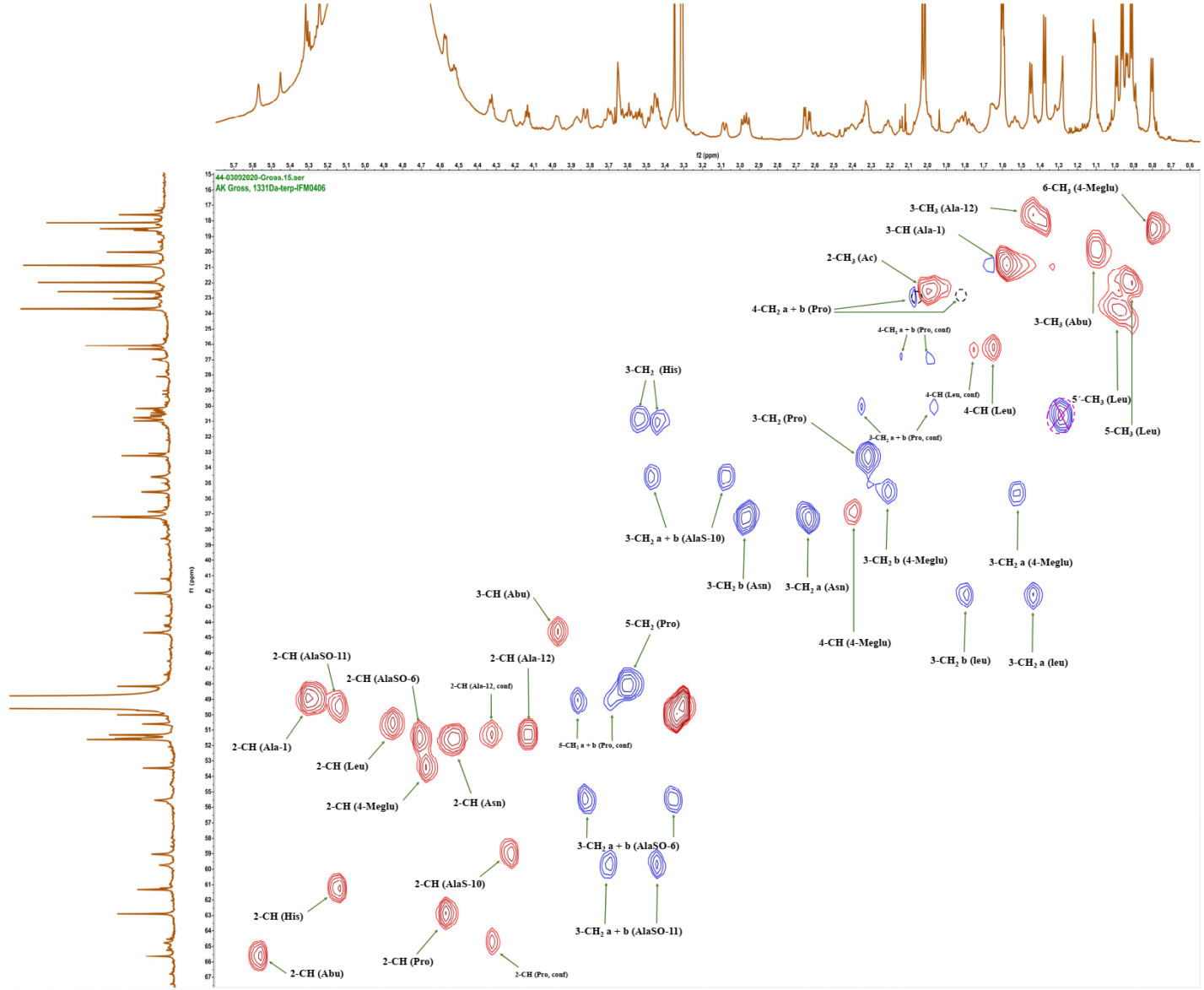

Figure S118. Annotated ^{1}H-^{13}C HSQC spectrum of nocathioamide B (**2**) (d_3-CH_3OH, 700/176 MHz)

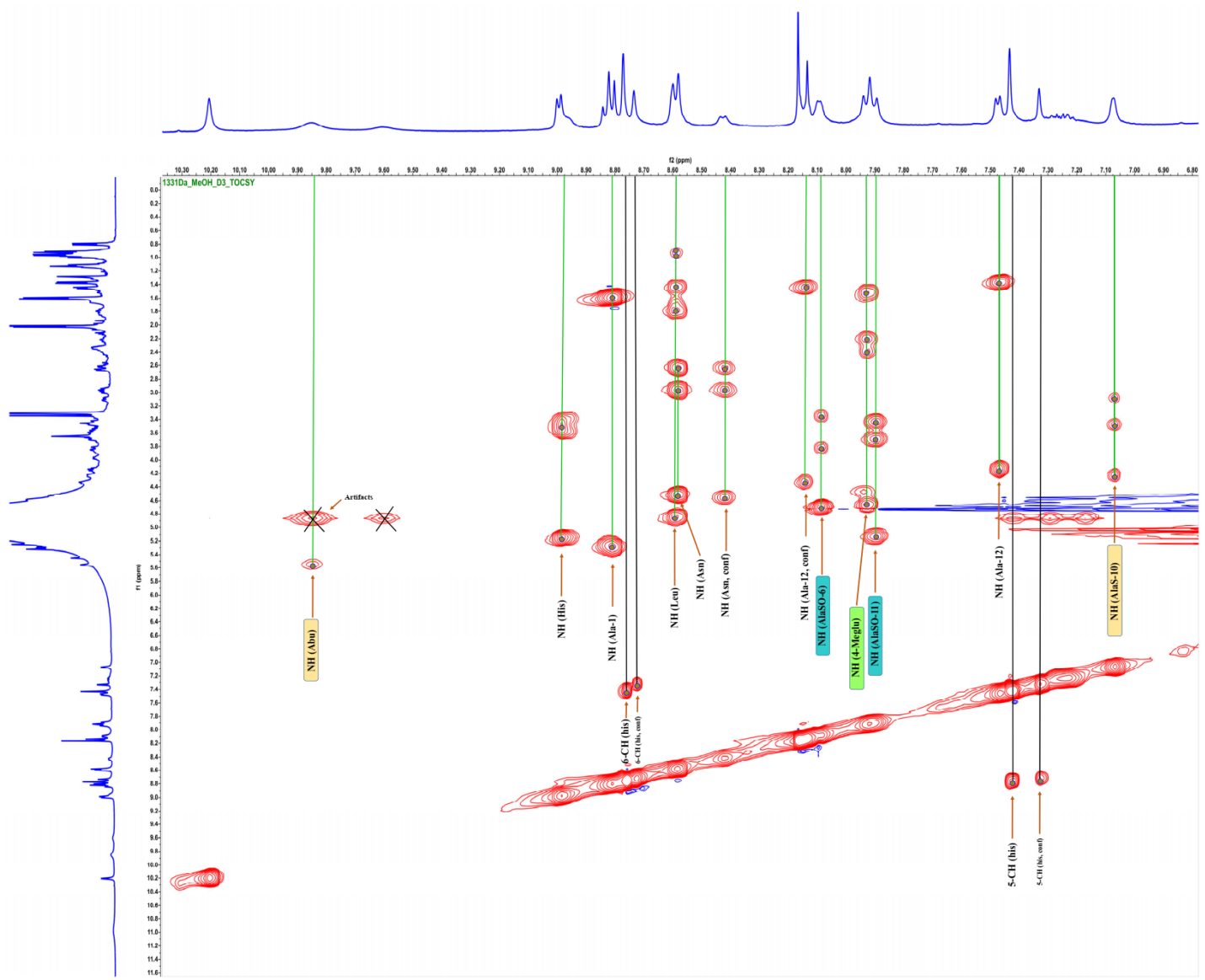

Figure S119. Annotated ^{1}H-^{1}H TOCSY spectrum of nocathioamide B (**2**) (d_3-CH_3OH, 400/400 MHz)

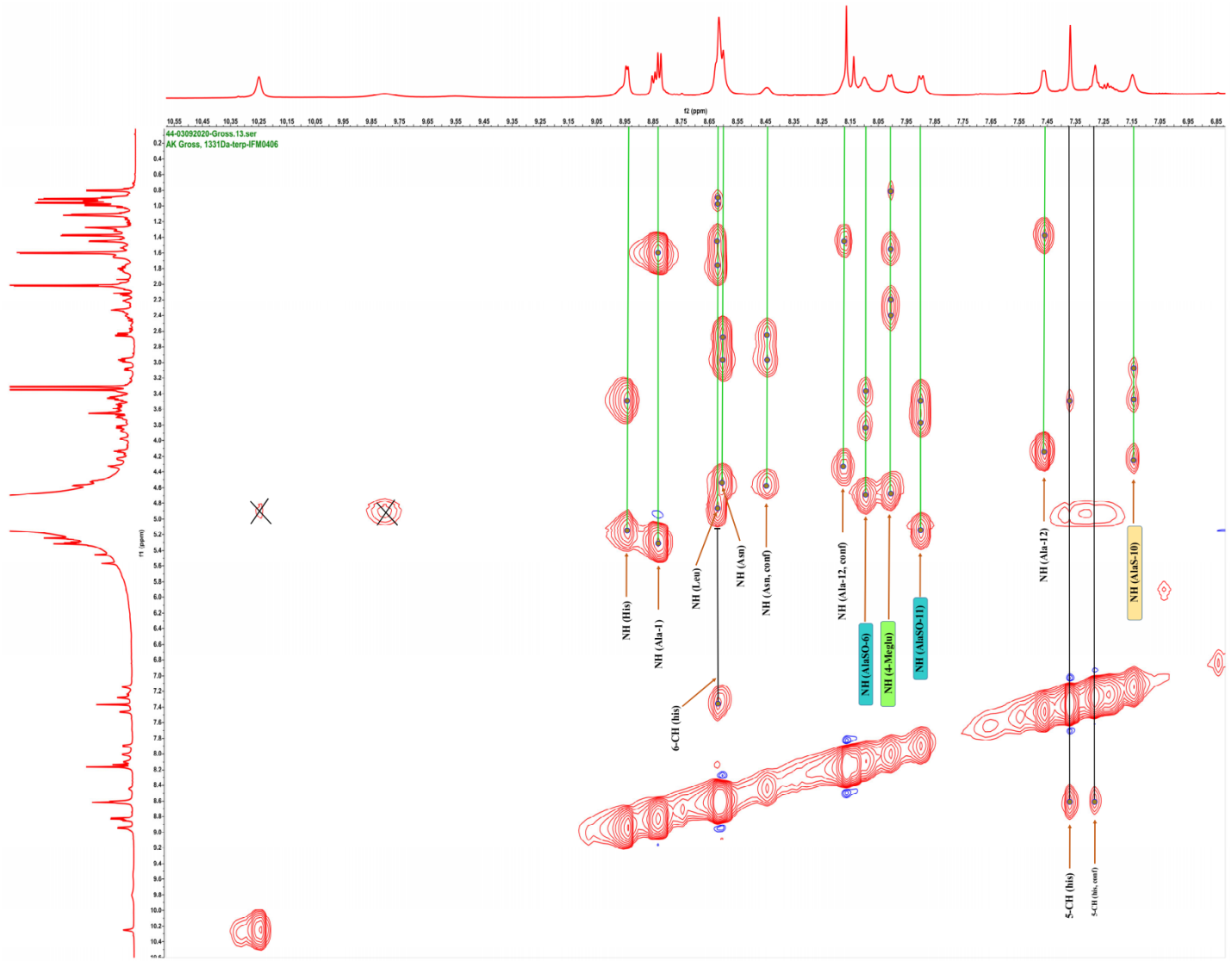

Figure S120. Annotated ^{1}H-^{1}H TOCSY spectrum of nocathioamide B (**2**) (d_3-CH_3OH, 700/700 MHz)

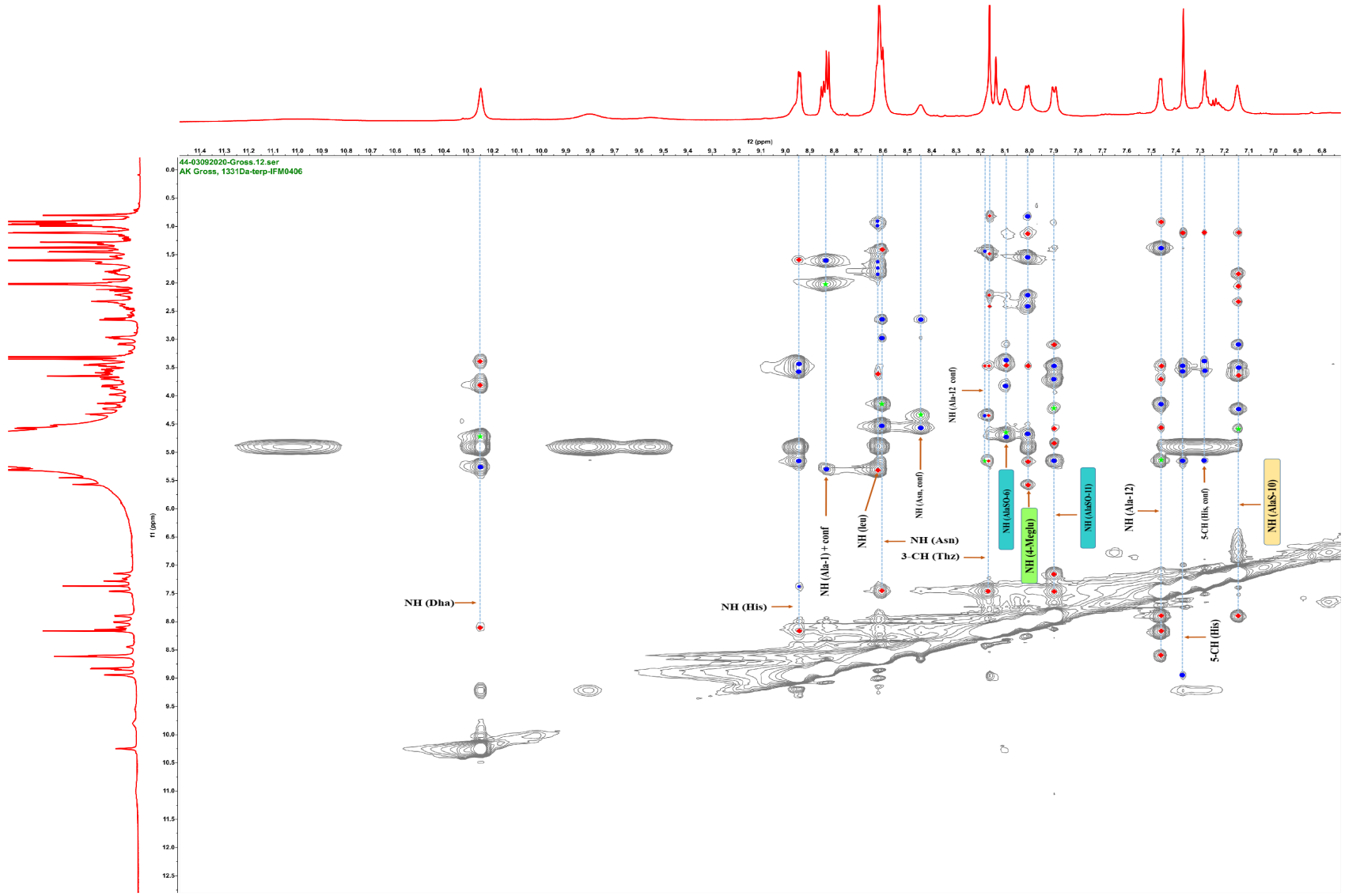

Figure S121. Annotated ^{1}H-^{1}H NOESY spectrum of nocathioamide B (**2**) (d_3-CH_3OH, 700/700 MHz). Cross correlations color code: a blue circle indicates resonances, observed within each amino acid residue; a green asterisk indicates through-space interactions with the adjacent amino acids of the peptidic backbone; a red diamond indicates through-space interactions with distant/unexpected residues.

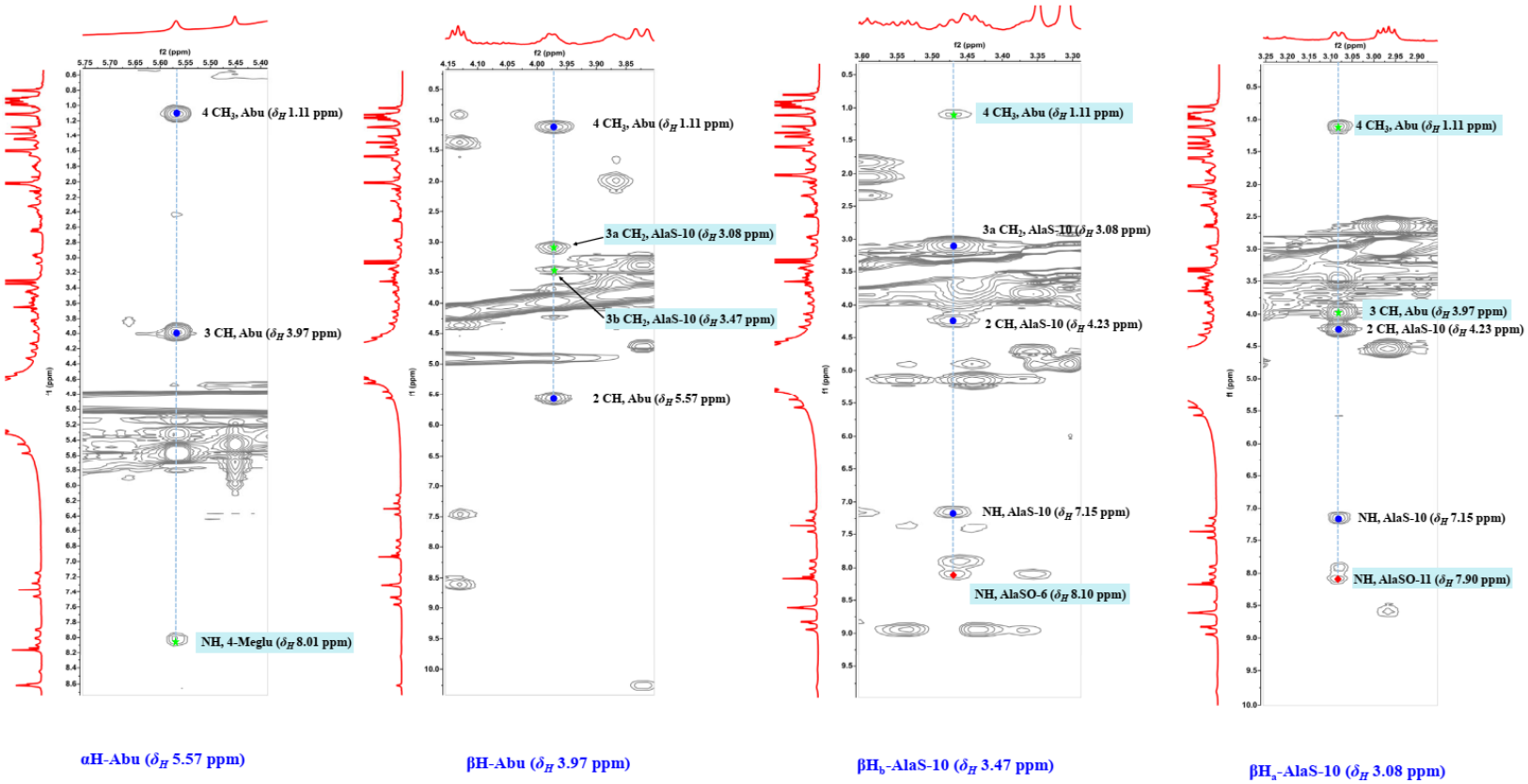

Figure S121A. Annotated ^{1}H-^{1}H NOESY spectrum of the **Melan** bridge of nocathioamide B (**2**) (d_3-CH_3OH, 700/700 MHz). Cross correlations color code: a blue circle indicates resonances, observed within each amino acid residue; a green asterisk indicates through-space interactions with the expected components of **AlaS-10** and **Abu**; a red diamond indicates through-space interactions with unexpected components of **AlaSO-6**, and **AlaSO-11**.

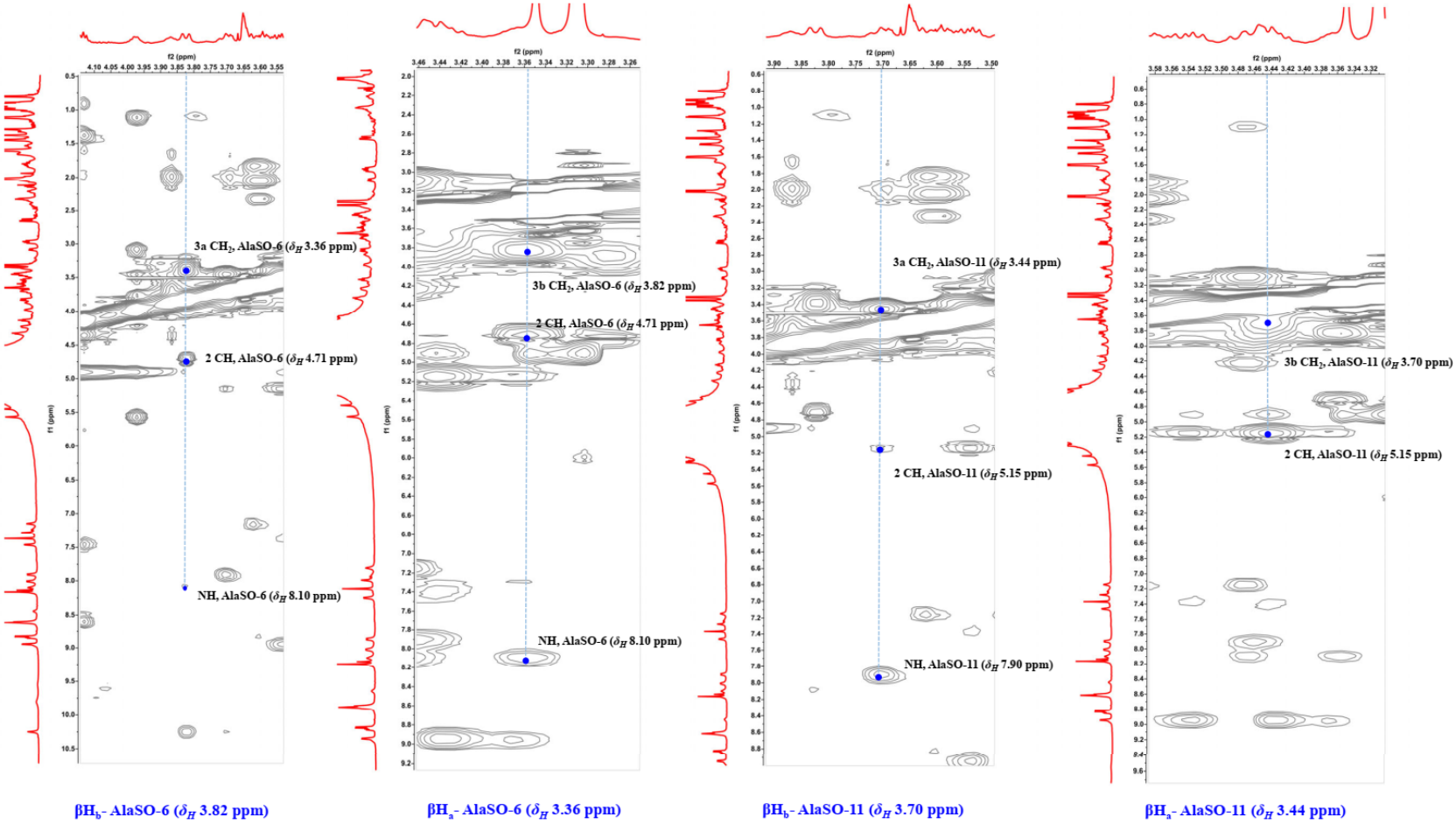

Figure S121B. Annotated ^{1}H-^{1}H NOESY spectrum of the **sulfoxideLan** bridge of nocathioamide B (**2**) (d_3-CH_3OH, 700/700 MHz). A blue circle indicates resonances, observed within each amino acid residue.

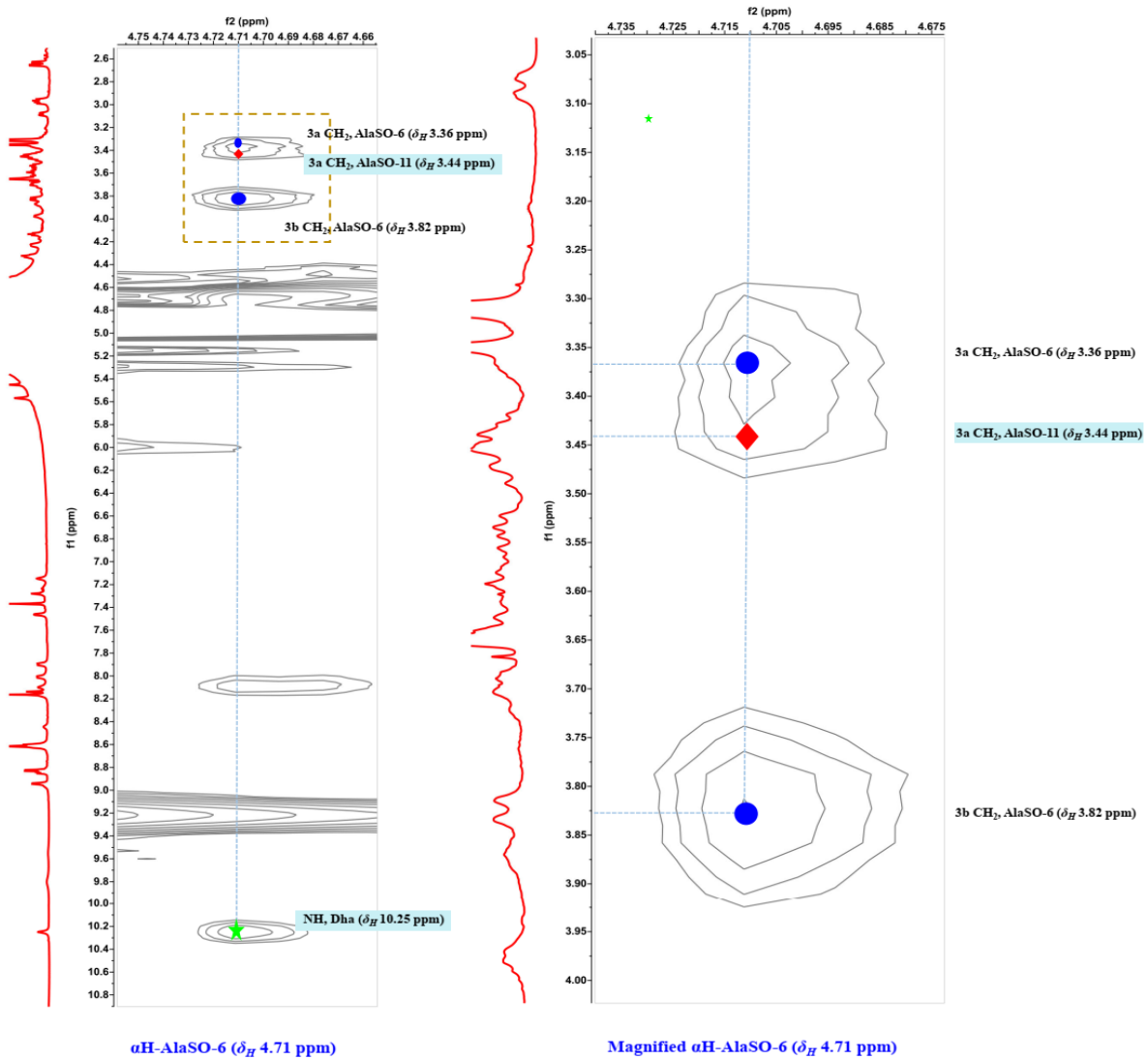

Figure S121C. Annotated ^{1}H-^{1}H NOESY spectrum of the **αH- AlaSO-6** of nocathioamide B (**2**) (d_3-CH_3OH, 700/700 MHz). Cross correlations color code: a blue circle indicates resonances, observed within each amino acid residue; a green asterisk indicates through-space interactions with **Dha**; a red diamond indicates through-space interactions with **βHa- AlaSO-11**.

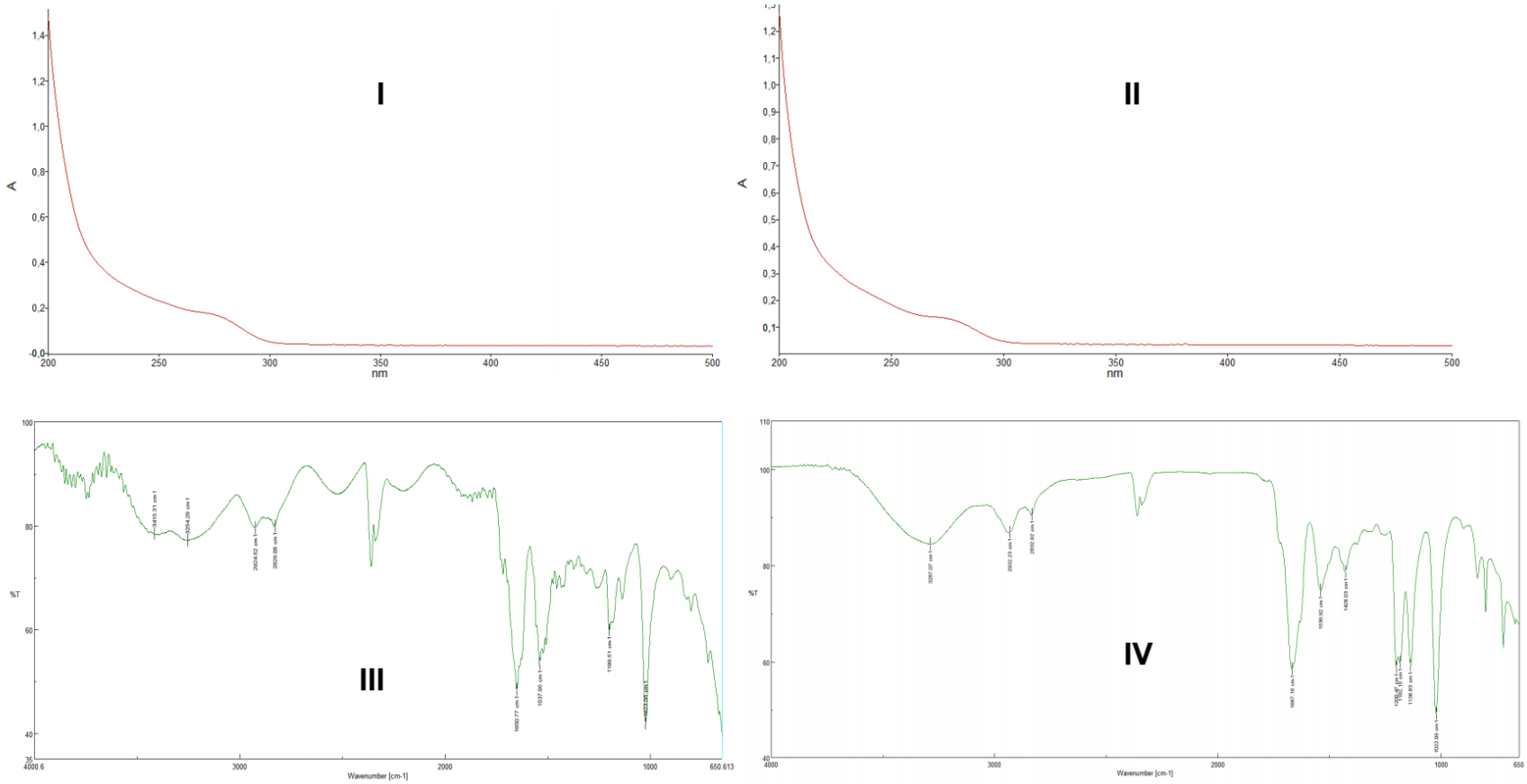

Figure S122. UV spectra of nocathioamide A (**1**) (panel I) and B (**2**) (panel II) & FT-IR spectra of nocathioamide A (**1**) (panel III) and B (**2**) (panel IV).

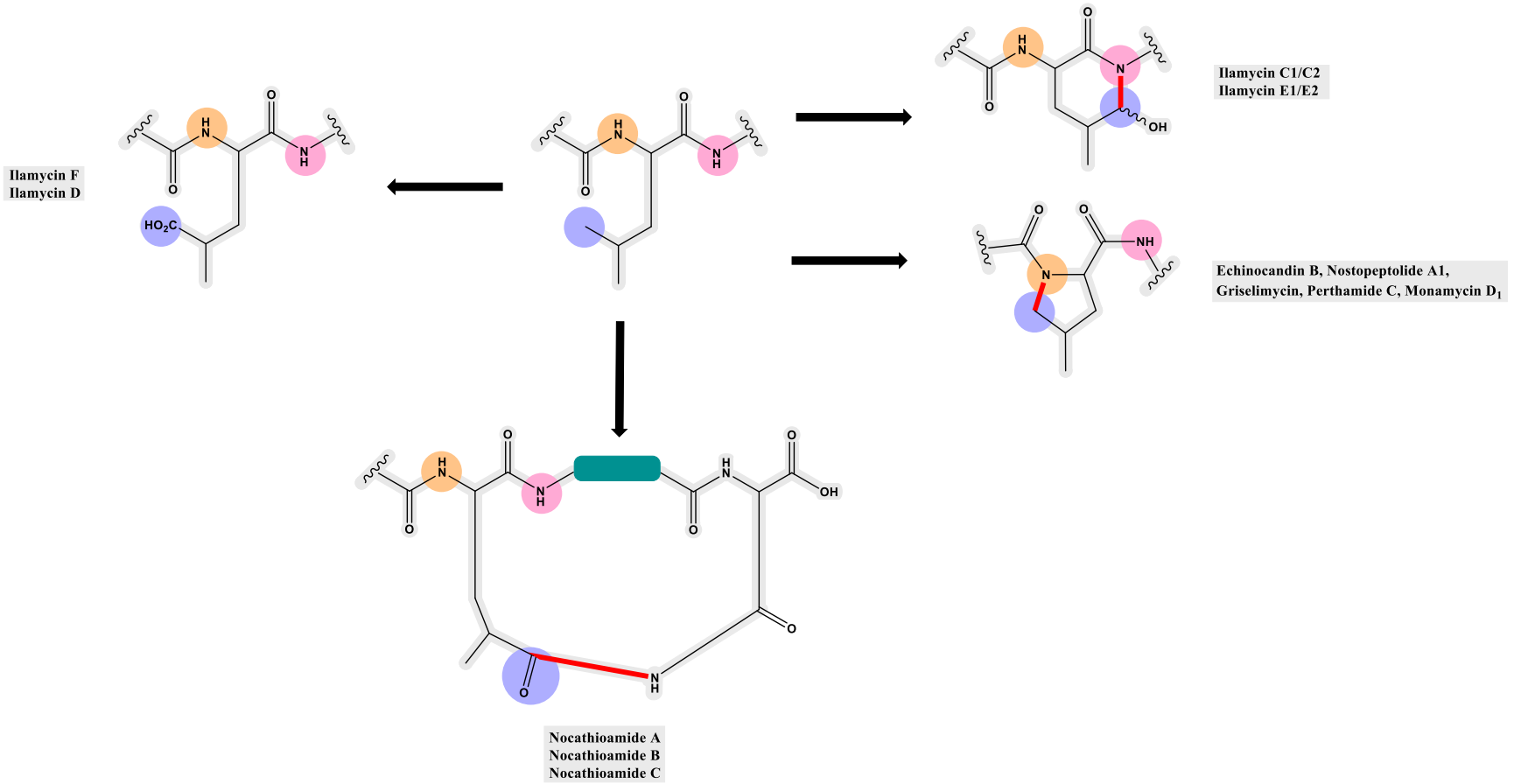

Figure S123. Different fates of oxidized δ-Methyl leucine (4-methylglutamate)

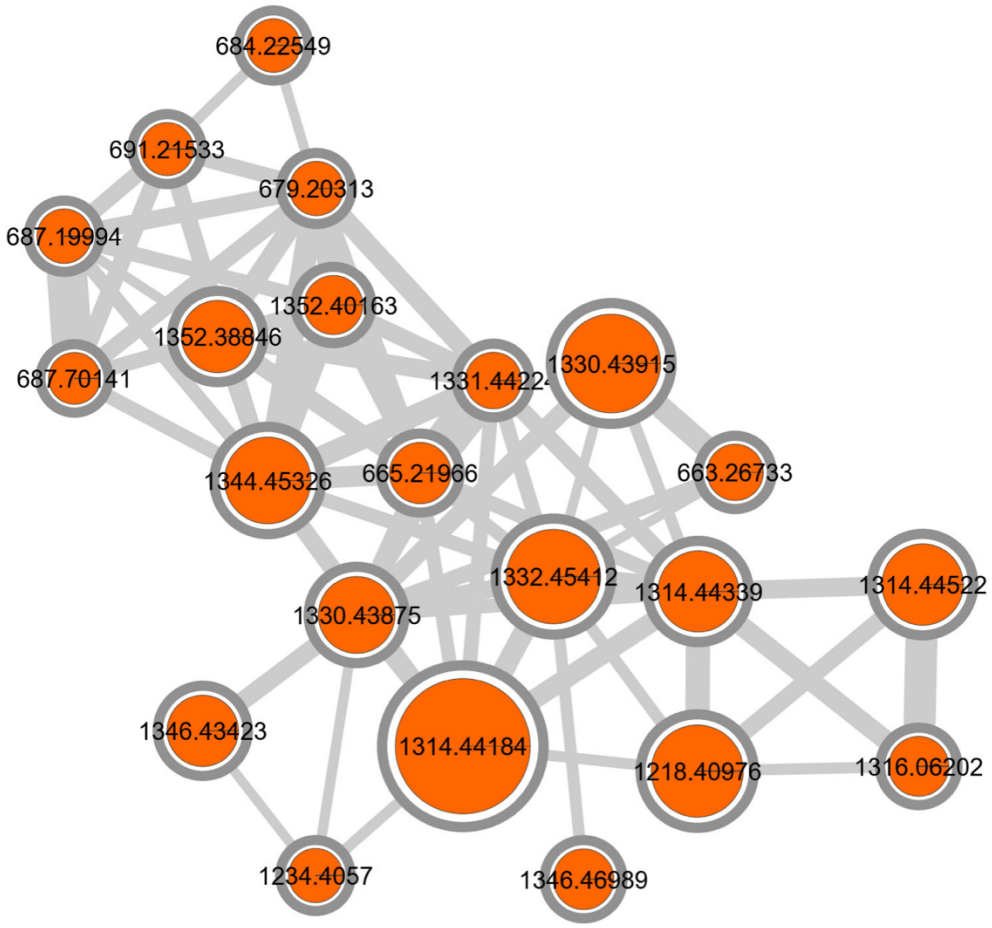

Rt_min	PEPMASS	ADDUCT
24.98133333	1314.44184	ION=[M+2H]2+
21.19366667	1330.43915	ION=[M+2H]2+
23.2775	1332.45412	ION=[M+2H]2+
27.96516667	1218.40976	ION=[M+2H]2+
24.23733333	1344.45326	ION=[M+H+H]2+
19.934	1314.44522	ION=[M+H+H]2+
28.16666667	1314.44339	ION=[M+2H]2+
22.6835	1330.43875	ION=[M+2H]2+
23.92583333	1352.38846	ION=[M+H+H]2+
19.06633333	1346.43423	ION=[M+2H]2+
X 24.72766667	665.21966	ION=[M+H]+
26.34566667	1346.46989	ION=[M+H+H]2+
23.92583333	1316.06202	ION=[M+H+H]2+
24.98133333	1352.40163	ION=[M+H+H]2+
X 24.72766667	1331.44224	ION=[M+H+H]2+
X 19.06633333	663.26733	ION=[M+2H]2+
X 21.7325	687.19994	ION=[M+H]+
X 24.23733333	679.20313	ION=[M+H]+
25.19833333	1234.4057	ION=[M+2H]2+
X 26.34566667	684.22549	ION=[M+H]+
X 22.08016667	691.21533	ION=[M+H]+
X 21.7325	687.70141	ION=[M+H]+

Elucidated by NMR

Envisioned by MS¹, MF, RDB, and few MS² fragments

Difficult to be anticipated

X Non-approached

Figure S124. Molecular network of nocathioamide molecular family

	[M]	Adduct	Rt (min)	Calculated Formula	Error (ppm)	RDB	(Tentative) structural modification(s) to nocathioamide A
🟢	**1314.44118**	$[M+2H]^{2+}$, $[M+H]^{+}$	24.98	$C_{54}H_{74}N_{16}O_{15}S_4$	0.3	26	Nocathioamide A
🟢	**1330.43915**	$[M+2H]^{2+}$, $[M+H]^{+}$	21.19	$C_{54}H_{74}N_{16}O_{16}S_4$	1.7	26	Nocathioamide B (sulfoxidation of Lan)
🟡	**1346.43423**	$[M+2H]^{2+}$, $[M+H]^{+}$	19.06	$C_{54}H_{74}N_{16}O_{17}S_4$	3.2	26	Nocathioamide C (sulfoxidation of Lan , and MeLan)
🟡	**1346.46989**	$[M+2H]^{2+}$, $[M+H]^{+}$	26.34	$C_{55}H_{78}N_{16}O_{16}S_4$	2.6	25	Sulfoxidation of (Me)Lan + 1 less RDB (possibly Dha => Ala)[16] + an extra CH_2
🟡	**1332.45412**	$[M+2H]^{2+}$, $[M+H]^{+}$	23.28	$C_{54}H_{76}N_{16}O_{16}S_4$	2.8	25	Sulfoxidation of (Me)Lan + 1 less RDB (possibly Dha => Ala)[16]
🟡	**1218.40976**	$[M+2H]^{2+}$, $[M+H]^{+}$	27.97	$C_{50}H_{70}N_{14}O_{14}S_4$	2.5	23	C-terminal Asn loss[17] + imide macrocyclisation loss
🟡	**1234.4057**	$[M+2H]^{2+}$, $[M+H]^{+}$	25.19	$C_{50}H_{70}N_{14}O_{15}S_4$	2.3	23	C-terminal Asn loss[17] + imide macrocyclisation loss + Sulfoxidation of Me(Lan)
🔴	**1344.45326**	$[M+2H]^{2+}$, $[M+H+Na]^{2+}$	24.24	$C_{55}H_{76}N_{16}O_{16}S_4$	1.8	26	????
🔴	**1352.38846**	$[M+2H]^{2+}$, $[M+H]^{+}$	23.92	$C_{53}H_{72}N_{14}O_{20}S_4$ $C_{56}H_{68}N_{14}O_{20}S_3$ $C_{55}H_{68}N_{16}O_{17}S_4$	3.4//14.3 1.4//15.0 3.9//18.8	25 30 30	????
🟢	**1314.44522**	$[M+2H]^{2+}$, $[M+H]^{+}$	19.93	$C_{54}H_{74}N_{16}O_{15}S_4$, Conformer 1	3.8	26	Nocathioamide A, conformer 1
🟢	**1314.44339**	$[M+2H]^{2+}$, $[M+H]^{+}$	28.16	$C_{54}H_{74}N_{16}O_{15}S_4$, Conformer 2	2.6	26	Nocathioamide A, conformer 2
🟢	**1330.43875**	$[M+2H]^{2+}$, $[M+H]^{+}$	22.68	$C_{54}H_{74}N_{16}O_{16}S_4$, Conformer	2.9	26	Nocathioamide B, conformer

Table S8. Annotation of some selected features within the nocathioamides positive cluster

Antibacterial Assay			
	MIC in µg/ml		
	Nocathioamide A (1)	**Nocathioamide B (2)**	
***E*nterococcus faecium BM4147-1**	>32	>32	
***S*taphylococcus aureus ATCC 29213**	>32	>32	
***K*lebsiella pneumoniae ATCC 12657**	>32	>32	
***A*cinetobacter baumannii 09987**	>32	>32	
***P*seudomonas aeruginosa ATCC 27853**	>32	>32	
***E*nterobacter aerogenes ATCC 13048**	>32	>32	
***Escherichia coli* ATCC 25922**	>32	>32	
***Bacillus subtilis* 168**	>32	>32	
***Staphylococcus aureus* NCTC 8325**	>32	>32	
***Mycobacterium smegmatis* mc^2 155 ATCC 700084**	>32	>32	
Antifungal Assay			
	MIC in µg/ml		
	Nocathioamide A (1)	**Nocathioamide B (2)**	**Caspofungin**
***Candida albicans* TüC01**	>32	>32	0.125
***Candida albicans* TüC02**	>32	>32	0.06
***Candida albicans* TüC03**	>32	>32	0.06
***Candida glabrata* TüC04**	>32	>32	0.125
***Candida tropicalis* TüC05**	>32	>32	0.25
Cytotoxicity Assay			
	IC_{50} in µg/ml		
	Nocathioamide A (1)	**Nocathioamide B (2)**	
HeLa cell line	>64	>64	

Table S9. Bioassay results. The letters indicated in red refer to the ESKAPE panel, an acronym comprising the scientific names of six highly virulent and resistant bacterial pathogens.

3. Supplemental References

[1] N. Garg, C. A. Kapono, Y. W. Lim, N. Koyama, M. J. A Vermeij, D. Conrad, F. Rohwer, P. C. Dorrestein, *Int. J. Mass Spectrom.* **2015**, *377*, 719 -727.

[2] M. Wang, J. J. Carver, V. V. Phelan, L. M. Sanchez, N. Garg, Y. Peng, D. D. Nguyen, J. Watrous, C. A. Kapono, T. Luzzatto-Knaan, C. Porto, A. Bouslimani, A. V. Melnik, M. J. Meehan, W.-T. Liu, M. Crüsemann, P. D. Boudreau, E. Esquenazi, M. Sandoval-Calderon, R. D. Kersten, L. A. Pace, R. A. Quinn, K. R. Duncan, C.-C. Hsu, D. J. Floros, R. G. Gavilan, K. Kleigrewe, T. Northen, R. J. Dutton, D. Parrot, E. E. Carlson, B. Aigle, C. F. Michelsen, L. Jelsbak, C. Sohlenkamp, P. Pevzner, A. Edlund, J. McLean, J. Piel, B. T. Murphy, L. Gerwick, C.-C. Liaw, Y.-L. Yang, H.-U. Humpf, M. Maansson, R. A. Keyzers, A. C. Sims, A. R. Johnson, A. M. Sidebottom, B. E. Sedio, A. Klitgaard, C. B. Larson, C. A. Boya P, D. Torres-Mendoza, D. J. Gonzalez, D. B. Silva, L. M. Marques, D. P. Demarque, E. Pociute, E. C. O'Neill, E. Briand, E. J. N. Helfrich, E. A. Granatosky, E. Glukhov, F. Ryffel, H. Houson, H. Mohimani, J. J. Kharbush, Y. Zeng, J. A. Vorholt, K. L. Kurita, P. Charusanti, K. L. McPhail, K. F. Nielsen, L. Vuong, M. Elfeki, M. F. Traxler, N. Engene, N. Koyama, O. B. Vining, R. Baric, R. R. Silva, S. J. Mascuch, S. Tomasi, S. Jenkins, V. Macherla, T. Hoffman, V. Agarwal, P. G. Williams, J. Dai, R. Neupane, J. Gurr, A. M. C. Rodriguez, A. Lamsa, C. Zhang, K. Dorrestein, B. M. Duggan, J. Almaliti, P.-M. Allard, P. Phapale, L.-F. Nothias, T. Alexandrov, M. Litaudon, J.-L. Wolfender, J. E. Kyle, T. O. Metz, T. Peryea, D.-T. Nguyen, D. VanLeer, P. Shinn, A. Jadhav, R. Müller, K. M. Waters, W. Shi, X. Liu, L. Zhang, R. Knight, P. R. Jensen, B. O. Palsson, K. Pogliano, R. G. Linington, M. Gutierrez, N. P. Lopes, W. H. Gerwick, B. S. Moore, P. C. Dorrestein, N. Bandeira, *Nat. Biotechnol.* **2016**, *34*, 828–837.

[3] a) A. Buchmann, M. Eitel, P. Koch, P. N. Schwarz, E. Stegmann, W. Wohlleben, M. Wolański, M. Krawiec, J. Zakrzewska-Czerwinska, C. Méndez, A. Botas, L. E. Núñez, F. Morís, J. Cortés, H. Gross, *Genome Announc.* **2016**, *4*, e01391-01316; b) A. Buchmann, H. Gross, *Microbiol. Resour. Announc.* **2020**, *9*, e00689-20.

[4] Y. Ikeda, H. Nonaka, T. Furumai, H. Onaka, Y. Igarashi, *J. Nat. Prod.* **2005**, *68*, 1061– 1065.

[5] J. Chen, A. Frediansyah, D. Maennle, J. Straetener, H. Broetz-Oesterhelt, N. Ziemert, L. Kaysser, H. Gross, *ChemBioChem* **2020**, *21*, 2205-2213.

[6] M. C. Arendrup, J. Meletiadis, J. W. Mouton, K. Lagrou, P. Hamal, J. Guinea and the Subcommittee on Antifungal Susceptibility Testing (AFST) of the ESCMID European Committee for Antimicrobial Susceptibility Testing (EUCAST). Method for the determination of broth dilution minimum inhibitory concentrations of antifungal agents for yeasts. EUCAST DEFINITIVE DOCUMENT E.DEF 7.3.2. April 2020. Accessed under https://www.eucast.org/astoffungi/methodsinantifungalsusceptibilitytesting/susceptibility_testing_of_yeasts/

[7] S. A. Kautsar, K. Blin, S. Shaw, J. C. Navarro-Munoz, B. R. Terlouw, J. J. J. van der Hooft, J. A. van Santen, V. Tracanna, H. G. Suarez Duran, V. P. Andreu, N. Selem-Mojica, M. Alanjary, S. L. Robinson, G. Lund, S. C. Epstein, A. C. Sisto, L. K. Charkoudian, J. Collemare, R. G. Linington, T. Weber, M. H. Medema, *Nucl. Acids Res.* **2020**, *48*, D454-D458.

[8] J. I. Tietz, C. J. Schwalen, P. S. Patel, T. Maxson, P. M. Blair, H.-C. Tai, U. I. Zakai, D. A. Mitchell, *Nat. Chem. Biol.* **2017**, *13*, 470–478.

[9] a) J. E. Leet, W. Li, H. A. Ax, J. A. Matson, S. Huang, R. Huang, J. L. Cantone, D. Drexler, R. A. Dalterio, K. S. Lam, *J. Antibiot.* **2003**, *56*, 232-242; b) X. Bai, H. Guo, D. Chen, Q. Yang, J. Tao, W. Liu *Org. Chem. Front.* **2020**, *7*, 584-589.

[10] a) B. J. Burkhart, C. J. Schwalen, G. Mann, J. H. Naismith, D. A. Mitchell, *Chem. Rev.* **2017**, *117*, 5389-5456; b) L. Kjaerulff, A. Sikandar, N. Zaburannyi, A. Sebastian; J. Herrmann, J. Koehnke, R. Mueller, *ACS Chem. Biol.* **2017**, *12*, 2837-2841; c) L. Frattaruolo, R. Lacret, A. R, Cappello, A. W. Truman, *ACS Chem. Biol.* **2017**, *12*, 2815-2822; d) T. Kawahara, M. Izumikawa, I. Kozone, J. Hashimoto, N. Kagaya, H. Koiwai, M. Komatsu, M. Fujie, N. Sato, H. Ikeda, K. Shin-ya, *J. Nat. Prod.* **2018**, *81*, 264-269; e) C. J. Schwalen, G. A. Hudson, B. Kille, D. A. Mitchell, *J. Am. Chem. Soc.* **2018**, *140*, 9494-9501; f) N. Mahanta, D. M. Szantai-Kis, E. J. Petersson, D. A. Mitchell *ACS Chem. Biol.* **2019**, *14*, 142-163.

[11] a) M. Montalban-Lopez, T. A. Scott, S. Ramesh, I. R. Rahman, A. J.van Heel, J. H.Viel, V. Bandarian, E. Dittmann, O. Genilloud, Y. Goto, M. J. Grande Burgos, C. Hill, S. Kim, J. Koehnke, J. A. Latham, A. J. Link, B. Martinez, S. K. Nair, Y. Nicolet, S. Rebuffat, H-G. Sahl, D. Sareen, E. W. Schmidt, L. Schmitt, K. Severinov, R. D. Sussmuth, A. W. Truman, H. Wang, J-K. Weng, G. P. van Wezel, Q. Zhang, J. Zhong, J. Piel, D. A. Mitchell, O. P. Kuipers, W. A. van der Donk, *Nat. Prod. Rep.* **2021**, *38*, 130-239; b) L. M. Repka, J. R. Chekan, S. K. Nair, W. A. van der Donk, *Chem. Rev.* **2017**, *117*, 5457-5520.

[12] a) J. Ma, H. Huang, Y. Xie, Z. Liu, J. Zhao, C. Zhang, Y. Jia, Y. Zhang, H. Zhang, T. Zhang, J. Ju, *Nat. Commun.* **2017**, *8*, 1-10; b) C. Sun, Z. Liu, X. Zhu, Z. Fan, X. Huang, Q. Wu, X. Zheng, X. Qin, T. Zhang, H. Zhang, J. Ju, J. Ma, *J. Nat. Prod.* **2020**, *83*, 1646-1657.

[13] C. T. Lohans, J. C. Vederas, *J. Antibiot.* **2014**, *67*, 23-30.

[14] a) G. C. Levy, R. L. Lichter in Nitrogen-15 Nuclear Magnetic Resonance Spectroscopy, J. Wiley & Sons, New York, 1979; b) https://wissen.science-and-fun.de/chemistry/spectroscopy/15n-chemical-shifts/; c) https://www.pascal-man.com/pulseprogram/BrukerAlmanac2012.pdf.

[15] a) S. Somma, W. Merati, F. Parenti *Antimicrob. Agents Chemother.* **1977**, *11*, 396−401; b) L. Vertesy, W. Aretz, A. Bonnefoy, E. Ehlers, M. Kurz, A. Markus, M. Schiell, M. Vogel, J. Wink, H. Kogler *J. Antibiot.* **1999**, *52*, 730−741; c) M. Simone, P. Monciardini, E. Gaspari, S. Donadio, S. I. Maffioli, *J. Antibiot.* **2013**, *66*, 73–78.

[16] L. Huo, W. A. van der Donk, *J. Am. Chem. Soc.* **2016**, *138*, 5254 -5257.

[17] K. I. Mohr, C. Volz, R. Jansen, V. Wray, J. Hoffmann, S. Bernecker, J. Wink, K. Gerth, M. Stadler, R. Müller, *Angew. Chem. Int. Ed.* **2015**, *54*, 11254-11258.